

Assessing the regional structural geological setting as fundamental component of the dolomite risk management process

JWP Meintjes
20295235

Dissertation submitted in fulfillment of the requirements for the degree *Magister Scientiae* in Environmental Sciences at the Potchefstroom Campus of the North-West University

Supervisor: Mr PW van Deventer

May 2016

Disclaimer

This report was written with full intention of being accurate and viable, however the Department of Geo-Spatial Science of the North West University, NRF/THRIP, AGES North West (Pty) Ltd and the author of this document cannot be held responsible for any information that might have been influenced by external factors or any other influences leading to misinterpretations of the maps, tables, graphs or portions of text contained herein or referred to.

The author of this document, the Department of Geo-Spatial Sciences of the North West University, AGES North West (Pty) Ltd and/or NRF/THRIP cannot be held liable for any opinion, findings and conclusions or recommendations expressed in this document, or based on the use of any information contained herein, or referred to.

Some of the compiled maps are included as electronic copies for higher quality / scale purposes.

Preface

With the completion of this work, I want to give special thanks and honour to my promoter, Mr. Piet van Deventer, who shared a lifetime of knowledge on dolomite and sinkholes. Your willingness and eagerness to share your life's experience is greatly appreciated.

Thank you to AGES for allowing me to use the information in completing this work – specifically to Mr. Stephan Potgieter and Mr. Fred Calitz for inputs and ideas in frequent discussions, as well as Dr. Stephan Pretorius for initiating the conceptual framework.

I also thank my wife – Nicolene – for being always understanding and supportive.

It is my hope that this work will be of value to the geotechnical fraternity, where the research and concepts presented in this work will lay a steady foundation to build upon.

Abstract

Dolomite stability investigations conducted within the confines of a pre-demarcated project area rarely take the regional structural geological setting into consideration. As such, the site selection process is very often conducted purely from a town planning or economic perspective, with no real consideration of geological aspects, or potentially hazardous dolomitic area.

This study focussed on providing an updated regional geological and hydrogeological setting of the Klerksdorp-Orkney-Stilfontein-Hartebeesfontein (KOSH) area in support of the demarcation of regional indicated dolomite hazard zones for regional dolomite risk management purposes. These zones are aimed at supporting strategic decisions regarding future development planning, spatial development planning, and regional dolomite risk management. It is not intended to replace the detailed site-specific dolomite stability investigation, but rather emphasized the need to first obtain a regional overview of the structural geological- and hydrogeological setting of an area towards effective dolomite risk management.

The findings of this study will serve as a foundation for future planning and detailed hazard determination across the KOSH-area as part of a regional Dolomite Risk Management Strategy.

An initial sinkhole and subsidence database was also compiled as part of this study across the KOSH-area and correlated in terms of structural geological controls. No previous sinkhole and subsidence database or statistical information was available for this area.

A final updated geological map, together with the demarcation of dolomite land and distribution of ground movement events across the area has been compiled. This served as the basis for the demarcation of the *indicated regional dolomite hazard zones*. The performance of the regionally demarcated *indicated dolomite hazard zones* were tested on a local scale by means of a conventional detailed dolomite stability investigation.

Keywords: dolomite stability investigations, dolomite risk management, indicated regional dolomite hazard, sinkholes and subsidences, Klerksdorp-Orkney-Stilfontein-Khuma (KOSH) area, Dr Kenneth Kaunda District Municipality, regional structural geology, hydrothermal quartz veins, dewatering, regional land use planning

Table of Contents

Preface	i
Abstract.....	iii
CHAPTER 1 – Introduction	1
1.1 Karst geology and instability	1
1.2 Problem statement.....	1
1.3 The occurrence of dolomite in South Africa	2
1.4 Focus study areas	2
1.5 Objectives	3
1.6 Methodology	3
1.7 Framework.....	4
CHAPTER 2 – Overview of dolomite and dolomite stability – Literature study.....	7
2.1 Chemical composition, dissolution and weathering of dolomite	7
2.1.1 Chemical composition	7
2.1.2 Weathering and weathering products.....	7
2.2 Karst landscapes.....	10
2.2.1 Definition and development of karst landscapes.....	10
2.2.2 Classification of karst landscapes	14
2.2.3 Karst-related instability features	14
2.3 Record of sinkholes and subsidences in South Africa	19
2.4 Dolomite risk management.....	27
2.5 Overview of dolomite hazard assessment procedures in South Africa	29
2.6 Phases of dolomite stability investigations during development	42
2.6.1 Reconnaissance phase investigation	42
2.6.2 Feasibility level investigation.....	42
2.6.3 Design-level investigation.....	43
2.6.4 Investigations during construction	43
2.7 Current methods and approaches used in South Africa.....	43
2.7.1 The role of the desk study	44
2.7.2 The role of field assessments.....	47
2.7.3 Hazard determining and zoning.....	50
2.7.4 The geotechnical model.....	54

CHAPTER 3 – Geological and structural aspects	58
3.1 Regional geological setting	58
3.2 Origin and deposition of dolomite and chert	59
3.2.1 Origin of dolomite and chert	59
3.2.2 Depositional model.....	60
3.3 Local geological setting.....	62
3.3.1 Stratigraphy	62
3.3.2 Structure	72
3.4 Development of a local geological model in support of dolomite risk management	81
3.4.1 Methodology	81
3.4.2 Geological and geotechnical information from existing maps	83
3.4.3 Aerial photograph investigations and surface mapping.....	83
3.4.4 Incorporation of drilling results	84
3.4.5 Compilation of cross sections	85
3.4.6 Compilation of a sinkhole and subsidence database.....	85
3.5 Local observations and discussions	85
3.5.1 Discussion of the geology of Orkney and surroundings	85
3.5.2 Discussion of the geology of Stilfontein, Khuma and surroundings	88
CHAPTER 4 – Regional hydrogeological setting	135
4.1 Karst and groundwater	135
4.2 Surface water	135
4.2.1 Distribution of surface water.....	135
4.2.2 Precipitation, run-off and evaporation.....	136
4.3 Groundwater.....	136
4.3.1 Aquifer types and associated yield capacity.....	136
4.3.2 Groundwater flow in karst aquifers.....	137
4.3.3 Dewatering of karst aquifers	137
4.4 Groundwater-surface water interaction in karst landscapes	138
4.4.1 Groundwater discharge at springs.....	138
4.4.2 Regional groundwater level distribution	139
4.4.3 Groundwater chemistry.....	140
4.5 Effects of re-watering on dolomite stability.....	142
4.6 Development of a regional hydrogeological model	144
4.6.1 Methodology	144
4.6.2 Results and discussions.....	146

CHAPTER 5 – Case Study 1: Regional dolomite hazard assessment	165
5.1 Background	165
5.2 Hazard assessment criteria and methodology.....	165
5.3 Discussion and regional hazard maps	170
5.3.1 Overview of sinkholes and subsidences across the KOSH-area	170
5.3.2 No hazard areas	173
5.3.3 Low to Medium (and Low to High) hazard areas.....	173
5.3.4 Medium to High hazard areas	174
5.3.5 High hazard areas	175
5.3.6 Very High hazard areas	176
CHAPTER 6 – Case study 2: Detailed dolomite stability investigation on Portions 14 and 21 of the Farm Hartebeesfontein 422 IP	180
6.1 Background of the investigation	180
6.2 Site description	180
6.2.1 Location of the study area	180
6.2.2 Existing infrastructure.....	181
6.2.3 Regional physiographic settings	181
6.3 Investigative methodology	181
6.3.1 Desk study.....	181
6.3.2 Surface mapping	182
6.3.3 Magnetic geophysical surveys	182
6.3.4 Gravimetric geophysical survey	182
6.3.5 Rotary air percussion borehole drilling.....	183
6.4 Regional geological setting	183
6.5 Regional geological structure	187
6.6 Local geological setting.....	187
6.6.1 Local geological structures	188
6.6.2 Summarised key geological factors	190
6.7 Existing karst-related instability features	193
6.8 Hydrogeological setting	193
6.8.1 Aquifer classification.....	193
6.8.2 Groundwater levels	194
6.9 Hazard characterisation and evaluation procedures	196
6.9.1 Nature and mobilisation potential of the blanketing layer	196

6.9.2	Bedrock morphology	198
6.10	Dolomite hazard characterisation of the site	198
6.10.1	Dolomite Hazard Zone A.....	198
6.10.2	Dolomite Hazard Zone B.....	200
6.10.3	Dolomite Hazard Zone C.....	201
6.10.4	Dolomite Hazard Zone D	203
6.10.5	Dolomite Hazard Zone E	204
CHAPTER 7 – Conclusions		208
CHAPTER 8 – Recommendations for further studies		213
Bibliography		215
Annexures		226
Annexure 1: List of technical reports used in geological assessments of the KOSH area		226
Annexure 2: Existing geological maps.....		228
Annexure 3: Sinkhole and subsidence database for the KOSH area		239
Annexure 4: Detailed inherent hazard assessments of key developments and infrastructure across the KOSH area		268
Annexure 5: Rotary air percussion borehole logs drilled on the farm Hartebeesfontein 422 IP		276
Annexure 6: Interpreted magnetic geophysical data.....		297
Annexure 7: Detailed determinations of the various angles of draw for the different lithologies.....		302
Annexure 8: Detailed per-borehole hazard characterization		307

List of Tables

Table 2-1: Summarised results of sinkhole statistics for the West Rand Municipality (summarised and recalculated from Richardson, 2013; and from Oosthuizen, 2013)	22
Table 2-2: Summarised criteria used in the assessment of dolomite land in South Africa – 1975 to 2015 (after Van Rooy, 1996).....	41
Table 2-3: Steps in the application of the method of scenario supposition (after Buttrick, 1992) 44	
Table 2-4: Inherent Hazard Class ratings and susceptibility (after Buttrick et al., 2001 and SANS, 2012) 53	
Table 3-1: Lithostratigraphic units occurring in and around the project area (Eriksson <i>et al.</i> , in Johnson <i>et al.</i> , 2006; Antrobus <i>et al.</i> , 1986).....	64
Table 4-1: Precipitation, runoff and evapotranspiration of various quaternary catchments.....	136
Table 4-2: Aquifer classification (after DWAF, 2006)	137
Table 4-3: Water quality chemical classes (after DWAF, 2006)	141
Table 4-4: Groundwater abstraction rates at various mines across KOSH (after Rosewarne, 1982).....	150
Table 5-1 Initial inherent hazard assessment criteria and considerations	167
Table 5-2: Decision support system to determine indicated inherent hazard of an area for regional planning and risk management purposes.....	169
Table 5-3: Distribution of sinkhole and subsidence dimensions across the various groundwater compartments and geological formations in the KOSH area	172
Table 6-1: Regional stratigraphy of the Karoo-, Transvaal- and Ventersdorp Supergroups ...	183
Table 6-2: Angles of draw for various lithologies (after Buttrick, 1992).....	197
Table 6-3: Detailed list of Technical Reports conducted by other consultants used in the assessment 227	
Table 6-4: Detailed hazard assessment per area across the larger KOSH area dolomite land 269	
Table 6-5: Detailed determination of angles of draw	303
Table 6-6: Detailed determination of angles of draw (cont.).....	305
Table 6-7: Detailed inherent hazard characterisation per drilled borehole	308

List of Figures

Figure 1-1: Regional view of study area	5
Figure 1-2: Local view of the KOSH area and Case Study boundaries	6
Figure 2-1: Typical karst landscape in the Far West Rand (taken from Kleywegt & Pyke, 1982)	8
Figure 2-2: Engineering classification of karst landscapes (from Walhman <i>et al.</i> , 2005).....	15
Figure 2-3: Typical soil profile on dolomite with karst instability features (taken from Wagener, 1982).....	19
Figure 2-4: Distribution of sinkhole and subsidence dimensions across various geological Formations in the West Rand (recalculated from Richardson, 2013)	26
Figure 2-5: Milestones of major contributions and classification systems proposed for dolomite hazard assessments in South Africa	40
Figure 2-6: Example of a geological profile of a borehole drilled for dolomite stability assessment purposes	51
Figure 2-7: Schematic three-dimensional model illustrating various components of dolomite land (from SANS, 2012)	52
Figure 2-8: Geotechnical model and Inherent Hazard Class determination (after SANS 1936 Part 2, 2012).....	54
Figure 3-1: Distribution of the Transvaal Supergroup across the Transvaal Structural Basin (after Eriksson and Reczko, 1995).....	59
Figure 3-2: Carbonate ramp depositional model (from Clendenin, 1989 in Eriksson <i>et al.</i> , 1993)	62
Figure 3-3: Regional geological setting (after Wilkinson, 1986)	63
Figure 3-4: Regional geological structure across the Witwatersrand sedimentary basin (from Wieland, 2006).....	74
Figure 3-5: Stage 1 of deformation and deposition – Witwatersrand Supergroup monocline fold and Klipriviersberg Group (Ventersdorp Supergroup) deposition and folding (from Antrobus <i>et al.</i> , 1986)	77
Figure 3-6: Stage 2 of deformation and deposition – Deformation of the Witwatersrand Supergroup and Klipriviersberg Group and deposition of the Platberg Group (from Antrobus <i>et al.</i> , 1986)	78
Figure 3-7: Stage 3 of deformation and deposition – Erosion of the Platberg Group followed by deposition of the Allanridge Formation and the Transvaal Supergroup (from Antrobus <i>et al.</i> , 1986)	79
Figure 3-8: Stage 4 of deformation and deposition – Re-activation of the Fakawi-, Through- and Jersey Faults causing major deformation of the area (from Antrobus <i>et al.</i> , 1986)	80

Figure 3-9: Stage 5 of deformation and deposition – Final stages of deformation during the Vredefort Impact and subsequent erosion of the geological succession (from Antrobus <i>et al</i> , 1986)	81
Figure 3-10: Key considerations and steps in compiling the first-order geological model of the area	82
Figure 3-11: Colour-code explanation of boreholes used in the geological assessment	84
Figure 3-12: Schematic geologic cross section E-E'	88
Figure 3-13: Schematic geologic cross section A-A'	94
Figure 3-14: Schematic geologic cross section D-D'	94
Figure 3-15: Collated geological information across the KOSH area	95
Figure 3-16: Updated geological and structural model of the KOSH area	96
Figure 4-1: Piper diagram plotting procedure and water origins (unknown source)	140
Figure 4-2: Regional distribution of groundwater and surface water features (adopted after DWAF, 2006; and Holland and Wiegmans, 2009)	143
Figure 4-3: Decision support system for developing a regional conceptual hydrogeological model to determine dolomitic management considerations associated with groundwater	145
Figure 4-4: Groundwater elevation versus topographic elevation across GMAs	147
Figure 4-5: Groundwater elevation versus topographic elevation across Quaternary Catchments	147
Figure 4-6: Groundwater level elevation time series across all compartments	151
Figure 4-7: Depth to groundwater and monthly rainfall in the KOSH groundwater compartment	152
Figure 4-8: Depth to groundwater and monthly rainfall in the Welgegund groundwater compartment	153
Figure 4-9: Piper diagram plot of groundwater chemistry across the regional dolomitic area	155
Figure 4-10: Demarcated dewatered areas in the KOSH region	156
Figure 4-11: Regional groundwater assessment results – KOSH depth to groundwater	157
Figure 4-12: Regional groundwater assessment results – KOSH groundwater recharge values	158
Figure 4-13: Regional groundwater assessment results – KOSH registered groundwater usage	159
Figure 4-14: Regional groundwater assessment results – KOSH groundwater chemistry classes	160

Figure 4-15: Regional groundwater assessment results – Welgegund depth to groundwater	161
Figure 4-16: Regional groundwater assessment results – Welgegund groundwater recharge values.....	162
Figure 4-17: Regional groundwater assessment results – Welgegund registered groundwater usage.....	163
Figure 4-18: Regional groundwater assessment results – Welgegund groundwater chemistry classes	164
Figure 5-1: Sinkhole and subsidence size distributions across the various geological formations in the KOSH-area.....	172
Figure 5-2: Distribution of sinkholes and subsidences across demarcated dolomite land in the KOSH-area.....	177
Figure 5-3: Inherent Dolomite Hazard – Orkney Area.....	178
Figure 5-4: Inherent Dolomite Hazard - Stilfontein - Khuma – Hartebeesfontein Area	179
Figure 6-1: Case Study 2 project area boundaries and locality	184
Figure 6-2: Previously investigated areas surrounding the Case Study 2 site.....	185
Figure 6-3: Geotechnical Investigation	186
Figure 6-4: Project area in relation to the regional 1:250 000 scale geological map (after Wilkinson, 1986).....	191
Figure 6-5: Compiled local geological setting based on previous mapping, geological information and new field investigations	192
Figure 6-6: Local hydrogeological setting of the project area	195
Figure 6-7: Inherent Hazard Class zones determined across the project area.....	207
Figure 6-8: Isopach map of the base of the Transvaal Sequence (Anthrobus et al., 1986)	229
Figure 6-9: Structural mapping of the Klerksdorp-Ventersdorp-Carletonville-Fochville-Parys-Potchefstroom area – Map 1 (Brink, 1996).....	230
Figure 6-10: Structural mapping of the Klerksdorp-Ventersdorp-Carletonville-Fochville-Parys-Potchefstroom area – Map 2 (Brink, 1996).....	231
Figure 6-11: Structural mapping of the Klerksdorp-Ventersdorp-Carletonville-Fochville-Parys-Potchefstroom area – Map 3 (Brink, 1996).....	232
Figure 6-12: Structural mapping of the Klerksdorp-Ventersdorp-Carletonville-Fochville-Parys-Potchefstroom area – Map 4 (Brink, 1996).....	233
Figure 6-13: 1:50 000 scale Potchefstroom gap geological map – selection of map 1 of 3	234
Figure 6-14: 1:50 000 scale Potchefstroom gap geological map – selection of map 2 of 3	235
Figure 6-15: 1:50 000 scale Potchefstroom gap geological map – selection of map 3 of 3	236

Figure 6-16: Old Black reef isopach map (Antrobus <i>et al</i> , 1986).....	237
Figure 6-17: Surface geological map of the Buffelsdoorm mine lease area (Brink, 1986)	238
Figure 6-18: Magnetic geophysical traverse line 1	298
Figure 6-19: Magnetic geophysical traverse line 2.....	298
Figure 6-20: Magnetic geophysical traverse line 3.....	299
Figure 6-21: Magnetic geophysical traverse line 4.....	299
Figure 6-22: Magnetic geophysical traverse line 5.....	300
Figure 6-23: Magnetic geophysical traverse line 6.....	300
Figure 6-24: Magnetic geophysical traverse line 7.....	301

CHAPTER 1 – Introduction

1.1 Karst geology and instability

Areas underlain by water-soluble rock types, such as limestone and dolomite, pose a serious threat to the formation of subsidences and catastrophic sinkholes (Waltham *et al.*, 2005, Ford & Williams, 2004), frequently resulting in property damage and the loss of life. Such areas are described as karst landscapes or areas exhibiting karst topography, due to its diagnostic underground drainage characteristics and associated subsurface dissolution of rock to form caves, valleys and caverns (Collins Dictionary of Geology, 1990; Waltham *et al.*, 2005). According to both Brink (1979) and Wagener (1982), damages to structures on dolomite land far exceeds that of other geological formations in Southern Africa, and to date 39 people died due to dolomite-related incidents (Buttrick and Roux, 1993; Buttrick, 2014). Instability associated with dolomite has since recent times not only been regarded in areas where dolomite forms outcrops at surface, but also in areas covered by non-dolomitic rocks that are underlain by dolomite in depth. Dolomite land is currently defined as areas underlain by dolomite up to depths of between 60 and 100 m, depending on the current status of groundwater management and control in the area in question (SANS, 2012).

1.2 Problem statement

A clear-cut contextual understanding of the regional geological setting and groundwater regime of an area is required prior to assessing any form of development of dolomite land. This is required to In order to accurately define the extent of dolomite land and to ascribe permissible land-uses to an area that is representative to the context of the geological setting. As such, a basic understanding of the structural geological setting will allow for the more accurate demarcation of high-risk areas in dolomitic strata. Such areas frequently pose a higher inherent hazard for the formation of sinkholes and subsidences, due to preferred dissolution and erosion along zones of weakness. It is furthermore essential to have a regional understanding of the groundwater status of an area with respect to dewatering – and possible later re-watering – as well as current and future groundwater usage of the area, which could impact on the stability of an area.

Dolomite stability investigations currently conducted by industry are for the most part carried out strictly within the confines of a pre-determined project area considered for development. The site selection process rarely takes the regional geological setting into consideration and is predominantly driven from a town-planning- or economic standpoint, often with stringent availability of funding to conduct extensive investigations. This is especially true in highly

urbanised areas where vast amounts of previous work has been carried out by various consultants and organisations, and information got lost, misplaced or forgotten about over time. The effective regional management of the dolomitic risk of an area is frequently misguided due to a lack of understanding of the larger geological context and the fragmentation of historical information. On the contrary, development of open land is often condemned after costly investigations have been carried out, which could have been avoided by means of sound regional planning and the considering of available information. This need for considering the regional geological setting and context in dolomite stability investigations was underlined during the annual Dolomite Seminar held in June 2014 (Van Rooy, 2014).

1.3 The occurrence of dolomite in South Africa

Much work has been done regarding the distribution, structure, and the various lithostratigraphic sub-divisions of dolomite in South Africa, and is well documented in most areas. Up to 98 % of all dolomite occurs predominantly in two basins in South Africa (Van Schalkwyk, 1981), namely the Transvaal basin in the northeastern parts of the country, and the Griqualand West basin located towards the eastern parts of South Africa (Eriksson *et al.*, 2001; Eriksson *et al.*, in Johnson *et al.*, 2006). This accounts for 3% of the total surface area of South Africa being classified as dolomite land (Wagener, 1982) and up to 25% of the Gauteng Province (Council for Geoscience, 2003).

Stratigraphically, dolomite from both basins is of Transvaal age (i.e.: belonging to the Transvaal Supergroup), which is regarded as one of the earliest carbonate platforms in the world (Beukes, 1987; Alterman & Wotherspoon, 1995). The Transvaal Supergroup is dated *circa (c.)* 2 714 to 2 050 Ma (Alterman and Wotherspoon, 1995; Beukes, 1987), and occurs as two prominent basins in South Africa, namely the Transvaal basin, consisting of the Chuniespoort Group which contains two outliers; the Marble Hall outlier and the Crocodilebridge outlier, and the Griqualand West basin, which is classified into two sub-areas, namely the Prieska sub-basin and the Ghaap Plateau sub-basin, both forming part of the Ghaap Group (Eriksson *et al.*, 2001).

1.4 Focus study areas

The study area is located across the Klerksdorp-Orkney-Stilfontein-Hertebeesfontein (KOSH)-region in the southwestern parts of the Dr. Kenneth Kaunda District Municipality (KKDM) in the North West Province of South Africa. Dolomite outcrops across the Dr. Kenneth Kaunda District Municipality are associated with the Malmani Subgroup, Chuniespoort Group, which are situated at the basal parts of the Transvaal Supergroup (Wilkinson, 1986). These deposits are located in the southwestern-most parts of the Transvaal basin.

The primary focus across the study area is assessing the regional geological setting with respect to dolomite hazard in support of regional risk management (case study 1), which is assessed on a local scale to determine the accuracy of regional information (remaining extent of Portions 14 and 21 of the Farm Hartebeesfontein 422 IP, east of Stilfontein – case study 2).

1.5 Objectives

This study has the following primary objectives:

- To describe the regional geological setting and structure of dolomite of the Transvaal Supergroup occurring in the KOSH-area.
- To determine the indicated effects of structural deformation (e.g.: fault zones, fracturing, folding etc.) caused by major geological events on the Black Reef Formation and Malmani Subgroup occurring in the KOSH-area.
- To determine the current groundwater status of the KOSH area with regards to dewatering status of the dolomite compartment(s).
- To determine the inferred extent of dolomite land in the greater KOSH area based on the regional geological setting and related structures to an inferred level of confidence.
- To compile a record of sinkholes and subsidences (known and inferred features) for the KOSH area.
- To demarcate regional *indicated dolomite hazard zones* for the KOSH area.

1.6 Methodology

Available literature and published information on the extent and structure of the regional geological- and structural geological setting, published geological maps, academic literature, and available dolomite stability investigations (in the form of technical reports obtained via the databank held by the Council for Geoscience) were collated and evaluated as basis for this study. Factual and geo-scientific information of importance were extracted and compiled into an ArcGIS® database for evaluation. More detailed site assessments were conducted at selected areas using conventional dolomite stability investigative methods. This was done in order to obtain an indication of subsurface dolomitic conditions that could be extrapolated and applied in similar structural settings throughout the remainder of the study area. More detailed investigations included:

- aerial photograph investigations

- regional surface geological mapping
- conducting of geophysical surveys, using magnetic and gravimetric methods
- the drilling of rotary-air percussion boreholes, and
- the evaluation and interpretation of all geo-scientific data

Available data and published information was considered in the demarcation of the regional *indicated dolomite hazard zones* for the KOSH-area. These broadly delineated *hazard zones* are intended to assist in dolomite risk management and development planning of a regional basis.

1.7 Framework

This paper will provide – as an introductory foundation – a brief literature overview (Chapter 2) of the main concepts relating to dolomite, sinkhole formation, sinkhole statistics in South Africa, current best-practise guidelines and industry requirements for hazard assessments, and various levels of geotechnical investigations on dolomite land with a description of the main phases and investigative techniques commonly used for each.

Chapters 3 and 4 will describe the structural geological and hydrogeological aspects of the study area, and provide a structural geological model for the KOSH-area. It should be noted that the intention of this research is not aimed at conducting an in-depth sedimentological and lithological analysis of the various dolomitic Formations, but rather to delineate regional *indicated dolomite hazard zones* based on the inferred extent of the various stratigraphic subdivisions of the various dolomitic Formations in conjunction with the regional structural geological setting.

The development of regional dolomite land assessment model is discussed in Chapter 5, which is applied to the KOSH-region to demarcate the extent of dolomite land and classify it into inferred dolomite hazard zones (case study 1). Demarcated regional zones are evaluated on a local scale in Chapter 6 by means of a conventional detailed dolomite stability investigation, conducted within the extent of site boundaries (case study 2). Chapter 7 concludes the research, with recommendations for further research regarding regional geological assessments as foundation to dolomite stability investigations listed in Chapter 8.

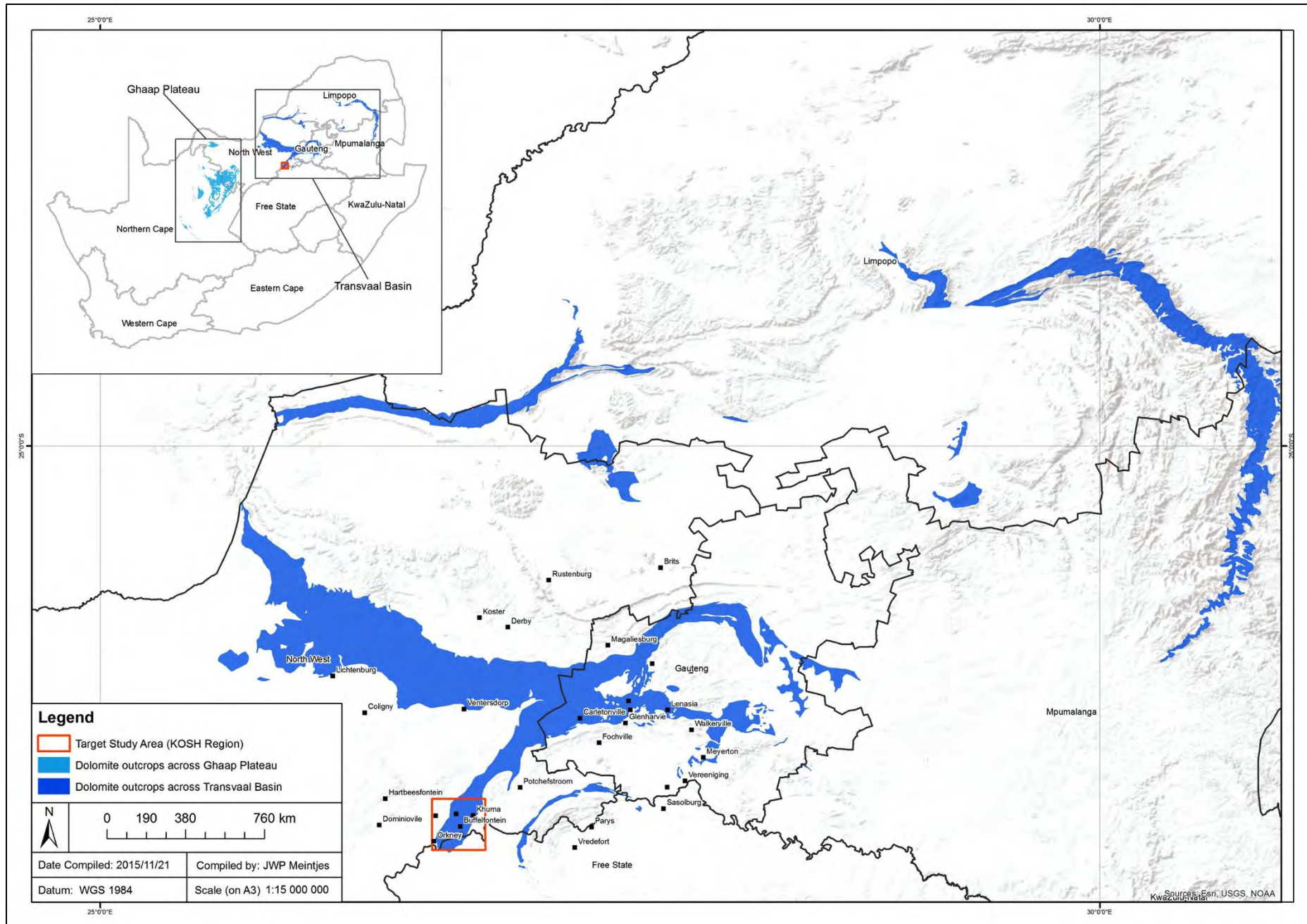


Figure 1-1: Regional view of study area

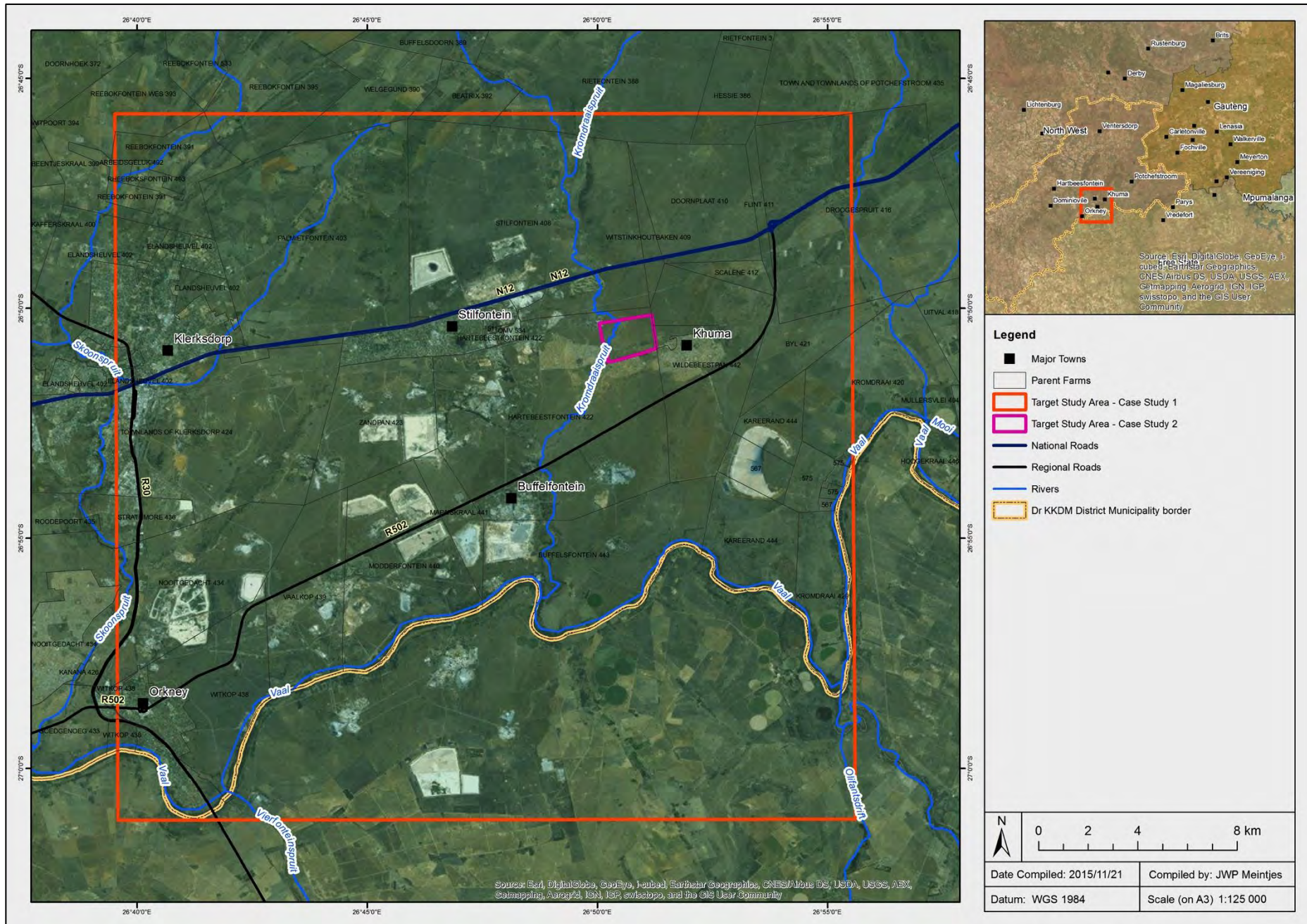


Figure 1-2: Local view of the KOSH area and Case Study boundaries

CHAPTER 2 – Overview of dolomite and dolomite stability – Literature study

2.1 Chemical composition, dissolution and weathering of dolomite

Dolomite and the weathering thereof have been well researched over the years (Buttrick, 1986; Ford and Williams, 2007; Waltham *et al.*, 2005). However, it still remains a fundamental component in understanding the inherent nature of dolomite and the related hazard it poses (Brink, 1981; Wagener, 1982). Due to the focus of this paper not being on the detailed dissolution kinetics, chemical compositions and petrographic elements of dolomite and its weathering products, only an overview will be provided in this regard. A more focussed discussion on the relationship between structural deformation, various lithological aspects and preferred weathering of dolomite is also briefly discussed.

2.1.1 Chemical composition

Dolomite is a bio-chemical sedimentary rock type, composed predominantly of calcium magnesium carbonate (e.g.: $\text{CaMg}(\text{CO}_3)_2$). In the research conducted by Bradley *et al.* (1953), it was stated that the Ca:Mg ratios in dolomite rocks could vary between 1:1 to 1:5. Buttrick (1986) furthermore substantiated the occurrence of manganese (Mn) and iron (Fe) in dolomite (e.g.: $\text{Ca}(\text{Mg}, \text{Mn}, \text{Fe})(\text{CO}_3)_2$), causing the dolomite structure to be diadochic. Theories regarding the origin of dolomite and chert are elaborated in Chapter 3.

2.1.2 Weathering and weathering products

The dissolution process of dolomite can be illustrated by the following chemical reaction: $\text{CaMg}(\text{CO}_3)_2 + 2\text{HCO}_3 \approx \text{Ca}(\text{HCO}_3)_2 + \text{Mg}(\text{HCO}_3)_2$ (Buttrick, 1986). This indicates that dolomite is soluble in an acidic medium. Freely occurring carbon-dioxide (CO_2) from the earth's atmosphere and in the soil profile is dissolved by rainwater to form weak carbonic acid (e.g.: HCO_3) (Waltham *et al.*, 2005). As this acidic rainwater infiltrates the dolomitic profile, it is capable of dissolving the carbonaceous strata. Crystalline dolomite has a very low porosity – as low as 0.3 % – resulting in very limited infiltration and dissolution (Brink, 1979). In order for widespread dissolution of the dolomite rock to occur, a large effective weathering surface is required. This is generally attained along joints, faults, tension fractures and fissures in the dolomite rock (Brink 1979). Wide-spread dissolution of dolomite to form suitable sub-surface respeticles in the form of caves and voids, occurs over thousands- to hundred-of-thousands of years.

The resulting weathering products of dolomite, commonly referred to as residuum, typically include residual soils derived from pedogenesis of dolomite bedrock, chert gravel and boulders, detached remnants of un-weathered dolomite boulders (or floaters), ferroan soils, and insoluble residuum such as wad (weathered after dolomite). Chert, being practically insoluble, remains undissolved and intact as part of the dolomite residuum and between dolomite bedrock pinnacles (Buttrick, 1986).

Such a typical weathered profile is well illustrated by Kleywegt & Pyke (1982; Figure 2-1), as well as Trollip (2006) based on the conceptual diagrammatic illustration of a typical karst landscape in South Africa (after Waltham and Fookes, 2003).

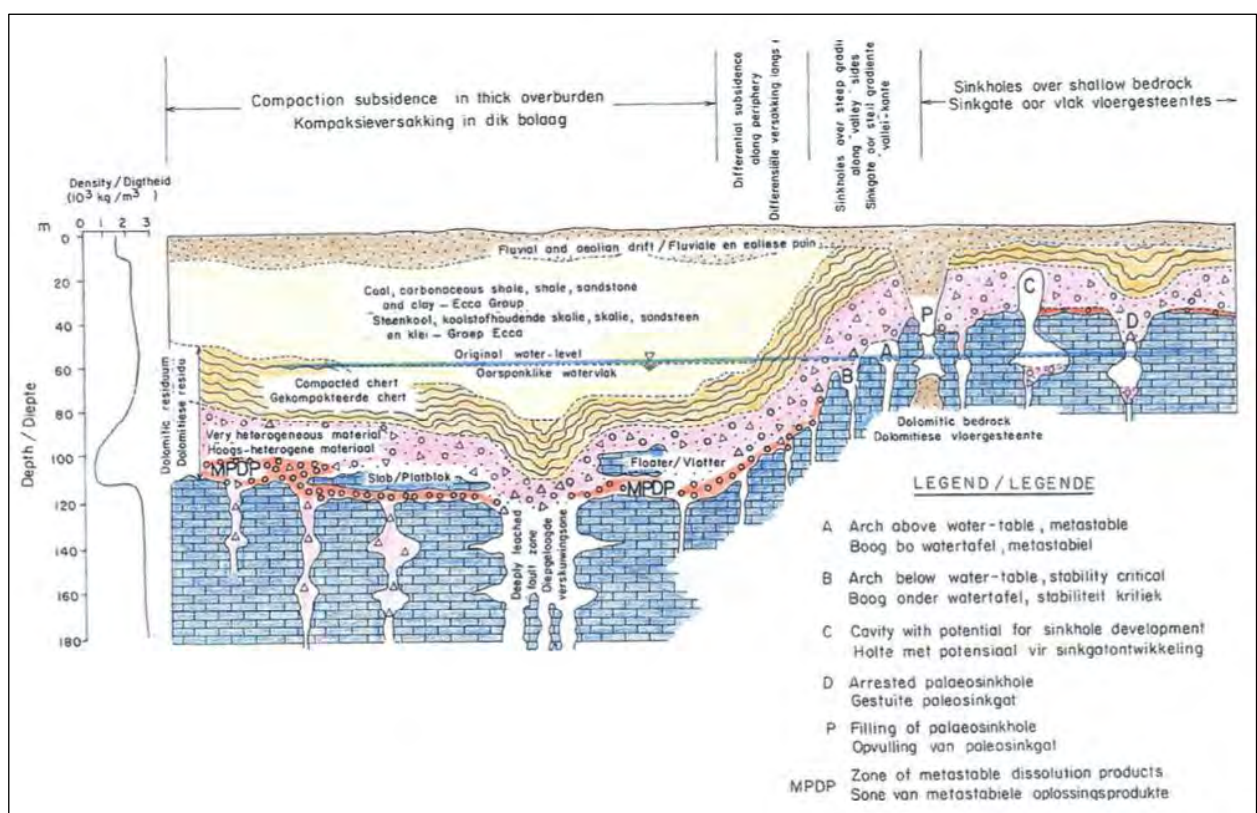


Figure 2-1: Typical karst landscape in the Far West Rand (taken from Kleywegt & Pyke, 1982)

An increase in strength and associated decrease in permeability and porosity of dolomite residuum is ascribed to prolonged and progressive deepening of the weathering profile of the dolomitic strata. This eventually results in the compaction and densification of low strength materials due to an increase in overburden pressures and loads (e.g.: consolidation). However, this is not the case in all instances. (Trollip, 2006).

Where dolomite residuum is situated close to surface, or has not undergone sufficiently deep burial over geological time, it could exhibit low strength characteristics and be highly porous and permeable, depending on the degree of weathering. Dolomite residuum is generally underlain

by bedrock that has been subjected to intense jointing, fracturing, faulting and tension deformation, in which case will exhibit cave formation, disseminated voids and the development of dissolution channels (or grykes) along preferred dissolution pathways. Such bedrock may exhibit various degrees of weathering, depending on the frequency and intensity of fracturing. In most cases, the rock head of the less weathered dolomite is not smooth, but is characterised by a rugged topography that could vary with great depths over short distances. Detached boulders (or dolomite floaters) are also common in the profile. Dolomite bedrock that has not been subjected to intense fracturing and deformation is generally preserved as hard unweathered dolomite bedrock.

The same observations were made by Wagener (1982) who stated that from the compacted chert gravel horizons, the overall consistency of the profile drastically decreases unto the slightly weathered rock head, which is contrary to profiles of other geological successions (except for calcrete). Disseminated voids and cavities may exist in the dolomite bedrock as well as the residual and transported overburden. The various commonly encountered weathering products derived from dolomite strata can be summarised as follows:

2.1.2.1 Chert gravel and boulders

Chert gravel and boulders – also referred to as chert rubble, or in the case of faulted areas as chert breccia – are derived from the *in situ* weathering of a dolomitic succession that is rich in chert. According to Wagener (1982), chert in the profile may vary from generally angular gravel-sized fragments with a diameter of 2 mm up to tabular boulders with diameters of up to (and possibly in excess of) 1 m. The upper parts of the residual chert horizon is frequently unsorted and randomly orientated, and become more orientated and closely packed with depth. Finer materials such as silts and clays derived from insoluble weathering products of dolomite, or sandy material from overburden, sometimes accumulates between chert gravel and boulders. The consistency of chert may vary greatly from friable powdery gravel to rock with a very hard to medium-hard rock consistency. Wagener (1982) also described instances where parallel chert bands (or orientated boulders) are slumped over bedrock pinnacles and boulders. Slumping of chert bands is often an indication of paleo sinkholes and subsidences. Chert bands are characterised as having high shear strength parameters, especially where they are long and continuous, and deformation occurs as brittle deformation, resulting in the sudden failure of chert bands (Wolmarans, 1996).

2.1.2.2 Wad and ferroan soils

The research done by Buttrick (1986) and Beck & Sinclair (1986) in conjunction with prior work done by Brink (1979) and Wagener (1982), described WAD – also referred to as manganiferous earth – as a black, blue-grey or purple, clayey silt or silty clay that is rich in manganese oxides and silica, as well as lesser constituents of various oxides (AlO and FeO, among other). This is derived from the decomposition of magnesium-rich carbonate rock that remains as insoluble material. Eriksson (1972) compiled the percentage distribution of Mn for dolomite strata occurring in the West Rand and concluded that the Oaktree- and Lyttleton Formations contain the highest Mn-concentrations compared to the other dolomitic Formations of the Chuniespoort Group. WAD is frequently associated with very low bulk densities, a highly compressible character and very low shear strength parameters (Roux, 1981), although these parameters could vary greatly.

According to Buttrick (1986), ferroan soils are similar to wad, with the exception of slight colour variations and increased silica and iron oxide contents, in contrast to high quantities of manganese oxides encountered in wad.

2.1.2.3 Post-karst overburden material

Roux (1984) stated that the overall thickness and characteristics of non-dolomitic overburden plays an important role when determining an area's susceptibility to the formation of instability features. Typical post-karst overburden can include Pretoria Group sedimentary and volcanic rock types, Karoo-age sediments, intrusives, and transported materials of mixed origins (e.g.: alluvium, aeolian sand, colluvium etc.). The degree of consolidation of these stratigraphically younger materials must also be considered during detailed hazard assessments.

2.2 Karst landscapes

2.2.1 Definition and development of karst landscapes

Based on the detailed study conducted by Brink and Partridge (1965), karst features occurring in the former Transvaal Province (currently the Gauteng and North West Provinces of South Africa) were described as “*topographies developed upon soluble rocks, during the formation of which fluvial processes of erosion and corrosion have marked subterranean component*” where “*the water table tends to be fairly flat and the flow of carbon dioxide charged water near the phreatic surface results in the development of a network of interconnecting caverns in the zone immediately below the water table*”. Jennings (1966) also described the area of maximum dissolution to be directly beneath the water table, due to an increase rate of movement, causing

progressive dissolution through jointed rock, provided groundwater is acidic. Swart (1991) stated that the material overlying the newly established water level was subsequently exposed to the phreatic and vadose zones, causing subterranean erosion and weathering adjacent to these zones.

Deep karst valleys are common in areas associated with faults or fault zones, where deep leaching of dolomite bedrock occurs (Swart, 1991). The development of such unusually deep fault-related valleys, as described by Brink (1979), can be summarised as follows:

- A fault (or faulted zone) that is younger than the dolomite rock it intersects is widened due to chemical degradation of the carbonate bedrock by the unrestricted percolation of acidic surface water. Such a widened fault plane is termed a slot or gryke.
- As slots are progressively widened, the overall increased permeability of the bedrock allows for the occurrence of more dissolution, especially along insoluble material such as chert.
- Lateral corrosion along bedding planes in the dolomite (and along chert bands and ledges) progressively dissolved the carbonate bedrock. In the instances where chert bands and ledges are brittle and thin, the delicate framework collapses, resulting in poorly compacted chert residuum (e.g.: chert rubble).
- Wad is generally encountered in the lower portions of the weathered profile due to subterranean erosion. This insoluble material is often encountered as a poorly consolidated horizon directly above the unweathered dolomite bedrock.
- Areas associated with deeply weathered faulted valleys are often characterised by numerous karst-related instability features – such as depressions, sinkholes and subsidences – and chert breccia that was later in filled with transported material. Over time, substantial amounts of material might have accumulated along these valleys.
- Due to the generally unconsolidated nature of such valleys in relation to the surrounding bedrock, increased permeability often results in easy erosion of material to form instability features.

Swart (1991) derived five prominent karst features (referred to as “*dolomite conditions*”) based on the inspection of various sinkholes and the drilling of boreholes during its rehabilitation process. These conditions include (i) throats, (ii) basins, (iii) through, (iv) horizontal cavities, and (v) naturally stabilised surficial material. In addition, Trollip *et al.* (2008) described slot development in shallow dolomite areas, referred to as grykes.

2.2.1.1 Grykes

Grykes refer to the vertical, or sub-vertical, weathering of faults, faulted zones, and joint sets in the carbonaceous bedrock. Grykes can vary in width and cause significant changes in depth to bedrock over a very short distance (e.g.: within meters), depending on the extent of dissolution along joints and fracture zones. Grykes can be up to tens of metres deep, and is generally filled with unconsolidated transported materials. Sinkholes associated with grykes are usually small at surface, but can be up to tens to hundreds of meters deep.

2.2.1.2 Throats

A throat is a sub-vertical pipe that can be up to 10 m in diameter as assessed by Swart (1991) in the Far West Rand. This feature formed due to dissolution and erosion along intersecting vertical planes (e.g.: joints and faults). It was found by Swart (1991) that throats are filled with unconsolidated residuum and/or contains cavities.

2.2.1.3 Basins

Basins are formed where throats undergo lateral dissolution. It can either represent the enlargement of a single throat, or the interconnection of closely spaced throats that merged after prolonged weathering. The geometry of basins are oval-shaped and frequently situated on faults or faulted zones, with the long axis orientated along strike with the major principal stress of the region. Basins are weathered deeper towards the centre, hence the depth to bedrock in the centre exceeds the depth to bedrock at the sides. Swart (1991) measured the average basin in the Far West Rand to be in the order of 25 by 40 m at surface, with an average depth of 40 m. He ascribed the average basin depth to correlate well with the depth to the original water table.

It was determined that basins are filled with *in situ* weathered dolomite and associated residuum that is sometimes in-filled and capped with stratigraphically younger strata and transported material. Disseminated voids and small cavities present within the weathered profile of a basin are in some instances capped with stratigraphically younger rock types, such as Karoo-aged sedimentary rocks. This provides sufficient strength to prevent total, or localised smaller, collapse of the basin due to exceeding overburden pressures, provided that the capping layer spans the width of the disseminated void or cavity. Where no large enough receptacle is present below a basin (e.g.: a cave or void), easily erodible residuum, such as wad, gets transported towards the lower parts of the basin where it accumulates and becomes consolidated over time. Strata derived from the *in situ* weathering along basins are generally unconsolidated, due to insufficient overburden weight to naturally compact the underlying strata.

2.2.1.4 Troughs

Troughs are elongated valleys with relatively steep sides that are filled with dolomite residuum. Stratigraphically younger materials are also often deposited within troughs, especially where the weathered residuum has been eroded or compacted. As with basins, troughs are frequently located on faults or faulted zones, with the long axis orientated along strike with the major principal stress of the region. This type feature is developed by the lateral weathering of sub-vertical regionally prominent faults- or joint planes. Laterally connected throats and basins could converge where they are located along strike of a larger fault plane or a regionally prominent joint set, to form a through.

Geometrically, troughs can be up to 1 km wide, several kilometres long and up to 200 m deep. Troughs in the Far West Rand were measured to be up to 1 km long, 150 m wide and 100 m deep. Due to the large lateral extent of troughs, sufficient overburden weight could result in the natural consolidation of the subsurface materials, particularly in the central parts of the trough. However, this is not always the case, seeing as differential consolidation could occur across the extent of a trough. Residual and infill material occurring at the sides of the trough generally remains unconsolidated, and are more prone to subsurface erosion along steep sidewalls of the adjacent bedrock pinnacles. For this reason, karst-related instability features are known to form along the steep sides of trough.

2.2.1.5 Horizontal cavities

Horizontal cavities – as the name implies – are features, which are formed due to the horizontal dissolution of the dolomite strata (throats, basins and troughs can be ascribed to vertical dissolution). These horizontally orientated features formed in the upper portions (e.g.: couple of meters) of the phreatic zone (Brink and Partridge, 1965). The formation of horizontal cavities are dependent on the chemical composition of the dolomite strata, the duration of weathering along the phreatic water level, and the porosity of the strata to allow horizontal flow of acidic groundwater.

Swart (1991) described horizontal cavities to be either horizontally continuous unfilled voids frequently occurring below insoluble chert bands or ledges, or to be horizontally porous zones, that are voids still containing insoluble dolomite residuum such as wad.

2.2.1.6 Naturally stabilised surficial material

Naturally stabilised surficial materials are karst features associated with areas where the dolomite rock head forms an uniform plateau and has been covered by well consolidated strata,

also usually of uniform thickness. Such material can comprise dolomite residuum, stratigraphically younger sediments and transported soils. Areas covered by naturally stabilized surficial material are generally associated with limited development of cavernous conditions, primarily due to the continued deposition and consolidation of strata across the dolomite bedrock.

2.2.2 Classification of karst landscapes

Waltham and Fookes (2003) conducted a global assessment of karst landscapes and proposed a classification system in support of engineering construction on karst terrain. As part of this classification system they evaluated sinkhole frequency, rock head variability (or bedrock topography), and the size of underground caves. Based on the evaluation of these features, they proposed a classification system defining five levels of extremity, namely: (1) juvenile karst, (2) youthful karst, (3) mature karst, (4), complex karst, and (5) extreme karst. However, the application of this proposed classification system is for the most part challenging in the South African context, because almost all karst landscapes are blanketed by transported soil horizons (Trollip, 2006). The different levels of karst maturity are illustrated in Figure 2-2.

2.2.3 Karst-related instability features

Instability features related to karst landscapes have been well established (Jennings *et al.*, 1965; Wagener, 1982; Buttrick, 1986; Swart 1991), and primarily include sinkholes and subsidences (previously termed dolines). The major difference between sinkholes and subsidences are related to the speed of onset and the geometry of the feature. Sinkholes usually occur suddenly, whereas subsidences tend to develop over longer periods. Wagener (1982) illustrated the typical differences between a sinkhole and a subsidence (Figure 2-3).

The mechanisms and conditions for the formation of the above-mentioned karst instability features are mainly associated with two primary scenarios: non-dewatering type (in a water ingress scenario) and dewatering type (in a groundwater level drawdown scenario) (Buttrick *et al.* 2001; SANS, 2012). Karst-related instability features do occur as a natural phenomenon provided favourable conditions prevail. However, its formation is drastically enhanced due to man's activities and insufficient management practises, as proven by the study conducted by Buttrick *et al.*, (2011).

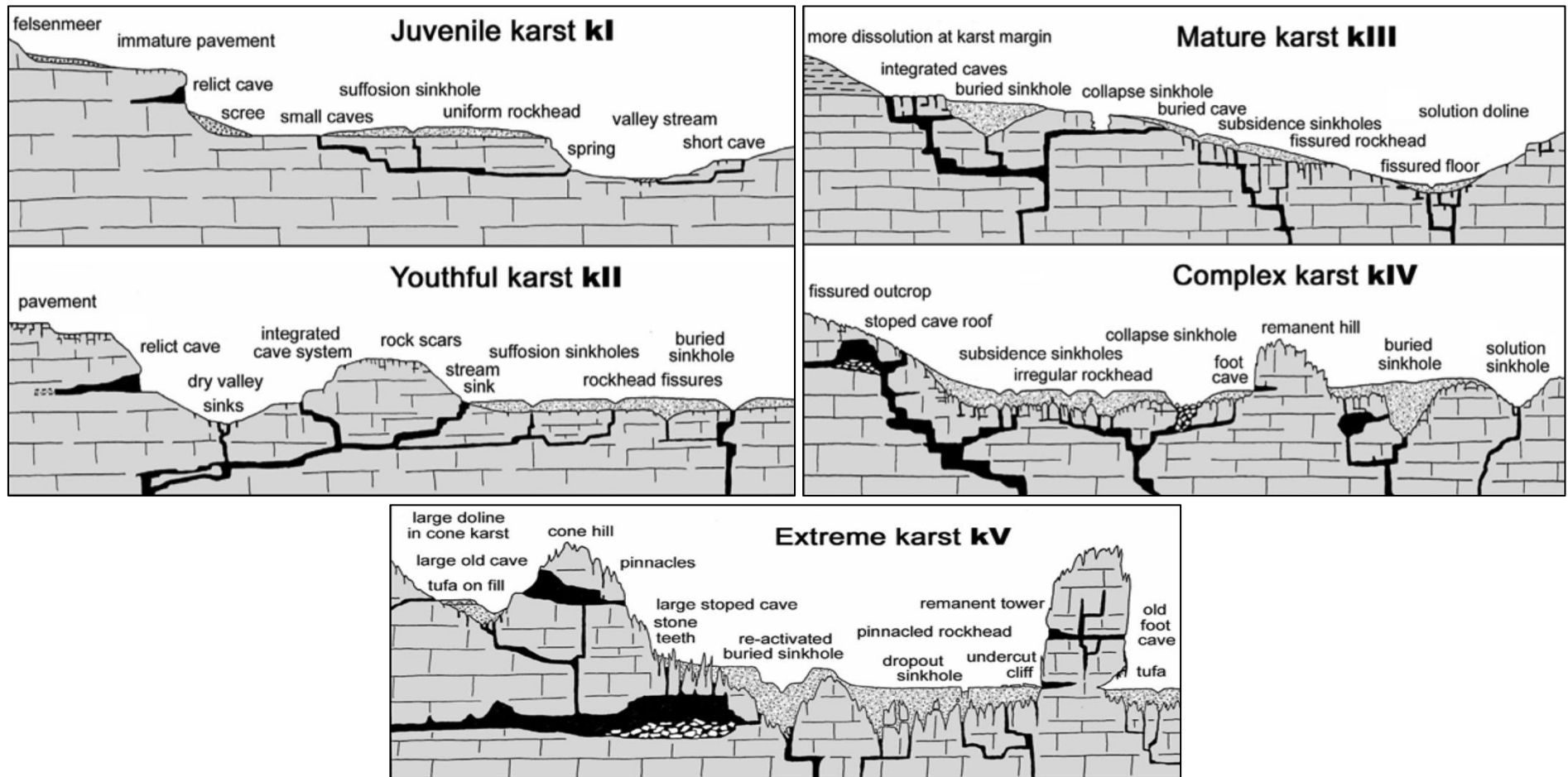


Figure 2-2: Engineering classification of karst landscapes (from Walhman *et al.*, 2005)

2.2.3.1 Sinkholes

Prevailing subsurface conditions:

Based on compelling evidence gathered and presented by Jennings *et al.* (1966), the following independent (but related) conditions are required prior to the formation of a sinkhole:

- (i) There must be adjacent rigid abutments for the roof of the cavity. The span must be appropriate to the strength of the bridging material. Should the span be too large, no arch can form.
- (ii) A condition of arching must develop below the arch in the residuum (i.e.: the self-weight must be carried by arching thrusts to the abutments).
- (iii) A cavity must develop below the arch in the residuum. This cavity may be small (e.g.: a horizontal crack) which may not be disclosed during investigations by means of drilling.
- (iv) A reservoir must exist to accept material, which is removed to enlarge the cavity. Some means of transportation such as water, is also essential.
- (v) A disturbing agency is then required to cause the roof to collapse. Water can be such an agency, leading to loss of strength or washing out of the critical binding material.

Jennings *et al.*, (1965) stated that it is required for all of the mentioned conditions to exist in order for a sinkhole to form. It was later stated by Buttrick (1986) that the conditions mentioned by Jennings *et al.*, (1965) should also include the careful consideration of the nature and composition of the residual and transported materials occurring between the mentioned abutments.

Water ingress as triggering mechanism:

In the case of a dewatered scenario, the ingress of surface water is considered to be the principal triggering mechanism leading to the formation of a sinkhole, provided the above-mentioned conditions prevails. Jennings *et al.*, 1966 described water ingress as triggering mechanism for the formation of sinkholes as follows:

- (i) Cavernous conditions are prevalent within dolomite residuum, dolomite residuum, transported materials, and/or weathered dolomite bedrock.

- (ii) The concentrated ingress of surface water (either due to poor surface drainage or leaking liquid-bearing infrastructure) causes a reduction in shear strength of materials, resulting in subsurface erosion into existing cavernous areas.
- (iii) An arch starts to develop in the dolomite residuum (or in-filled material – or both) over the cavity, resulting in collapse due to a loss of strength, causing progressive head ward erosion and collapse. This finally manifests at surface as a sinkhole when the final layer of overburden is breached.

Groundwater abstraction as triggering mechanism:

Buttrick & Van Schalkwyk (1995), as well as Brink (1996), described the current water level (prior to dewatering) as the base level of subterranean erosion. The artificial lowering of the natural groundwater level represents a two-folded issue relating to sinkhole formation, provided the five conditions as set out by Jennings *et al.* (1966) prevails:

- (i) During the process of excessive groundwater abstraction, the state of equilibrium of the subsurface material prior to dewatering is disturbed; causing a drastic reduction in strength of the overlying material as groundwater abstraction takes place (Jennings *et al.*, 1966; Wagener, 1982). Overburden (including dolomite residuum and in-filled- or transported material) also undergoes a reduction in strength due to loss of buoyant support from groundwater.
- (ii) On the other hand, an increased depth to the groundwater results in a larger exposed erosional profile, causing more material to be subjected to erosion, as surface water infiltrates the dolomitic profile.

Current industry guidelines (SANS 1936, 2012) define natural groundwater fluctuations in dolomitic environments to be ± 6 m from the original water level. As such, the historic original water level of the area has to be determined and correlated with the current water level.

2.2.3.2 Subsidence

Prevailing subsurface conditions:

Subsidence is generally defined as an enclosed depression. Its formation is conditional to the occurrence of highly compressible unconsolidated material (such as chert rubble and wad) within the dolomite profile. The formation of subsidence is – as in the case of sinkholes – also related to water ingress or dewatering. Partially developed sinkholes, defined as suffosion sinkholes by Waltham *et al.*, 2005, are commonly observed as a subsidence at surface.

Water ingress as triggering mechanism:

In order for a typical surface saturation-type (water ingress) subsidence to develop, the following triggering mechanisms should prevail (Council for Geoscience, 2003):

- (i) Highly compressible dolomite residuum (such as unconsolidated chert rubble, transported material or wad) needs to be present within the dolomite profile at relatively shallow depths.
- (ii) It is required that the current water table be within or directly below the highly compressible overburden.
- (iii) As the compressible overburden is saturated as a result of concentrated ingress of surface water that infiltrates the dolomite profile, the low density highly compressible material becomes more consolidated, causing the gradual formation of a surface depression.

Groundwater abstraction as triggering mechanism:

In the instance where groundwater level drawdown serves as triggering mechanism for the formation of a subsidence, the feature is termed a dewatering-type subsidence. In order for a dewatering-type subsidence to form, the following conditions needs to be prevalent:

- (i) Weathered zones within the dolomite profile (generally deeper) should be filled with highly compressible overburden (e.g.: unconsolidated chert rubble, wad and transported materials).
- (ii) As the groundwater level is rapidly drawn down, a reduction in hydrostatic support provided by water to the highly compressible material causes consolidation of material.
- (iii) The consolidation of highly compressible material causes a subsidence to manifest at surface, which may be accompanied by surface tension cracks.

Classification and identification

The size of both types of subsidences is largely dependent on the nature of the underlying materials, the degree of consolidation, and the degree of saturation. In instances where the unconsolidated- and highly compressible material is thick, with a large depth to bedrock, larger subsidences may occur. This is provided that saturation was suitably prolonged to allow

adequate consolidation of highly compressible materials. The same classification is currently applied to subsidences and sinkholes in South Africa (Buttrick and Van Schalkwyk, 1995).

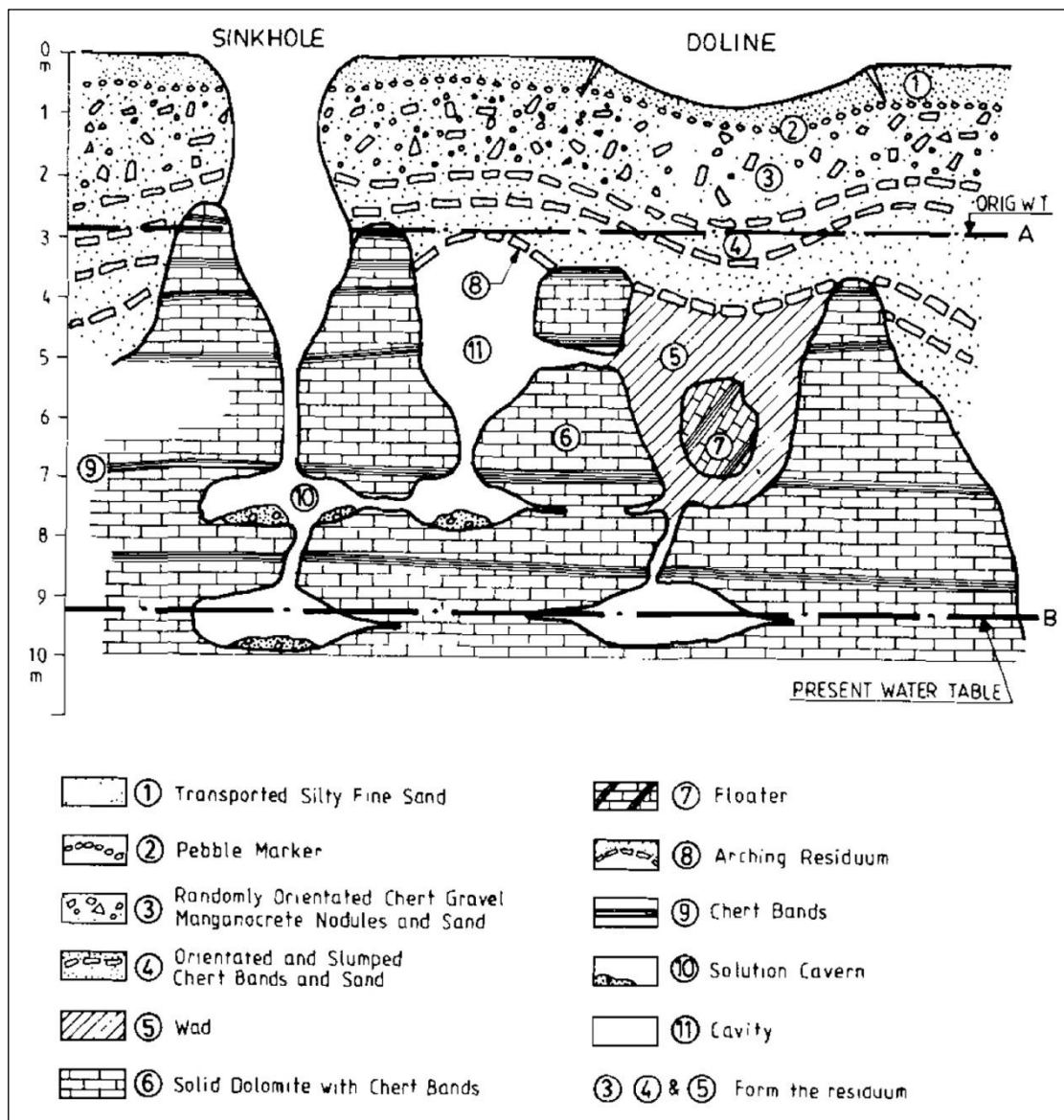


Figure 2-3: Typical soil profile on dolomite with karst instability features (taken from Wagener, 1982)

2.3 Record of sinkholes and subsidences in South Africa

Richardson (2013) and Oosthuizen (2013) recently conducted comprehensive studies on the record of sinkholes and subsidences in South Africa. Both authors focussed solely on data from the Gauteng province. In the mentioned research conducted by Richardson (2013), published information of 3 048 karst related instability events that occurred over a time period of 60 years (up until 31 December 2011) were compiled into a databank and evaluated in terms of: (i) type of event, (ii) occurrence in terms of geological Formation, (iii) triggering mechanism, and (iv)

size and depth distribution. Collated information was evaluated on a statistical basis, and correlated in terms of the mentioned criteria.

Wolmarans (1984) first made the observation that not all the lithostratigraphic Formations of the Malmani Subgroup exhibit the same frequency of sinkhole and subsidence formation, by assessing 691 sinkholes that manifested in the Far West Rand. He found that more sinkholes are associated with the chert-rich dolomitic Formations than those containing little to no chert. Wolmarans ascribed this due to selective and extensive weathering of the carbonate bedrock along chert bands and ledges, related to the uniformly weathered chert-poor strata. A number of sinkholes have been indicated by Wolmarans (1996) to occur through the overlaying non-dolomitic strata of the Pretoria Group sedimentary rocks.

The work done by Schöning (1990 and 1996) using statistical analysis to correlate sinkhole causes based on the geological Formation in which it occurs, as well as other external factors such as rainfall, generally indicated the following:

- A linear correlation exists between sinkhole formation and rainfall where up to 79% of the sinkholes, evaluated during his work, formed where annual rainfall exceeded 70 days in total.
- Formations that are chert-rich aren't always more prone to forming sinkhole and subsidence.
- The relative exposed surface areas between the chert-poor and chert-rich formations differ, and therefore the total number of sinkholes cannot be directly correlated, but must be viewed in terms of events per area size.

Oosthuizen (2013) concluded on similar findings than that of Wolmarans (1984), and stated that the largest majority of sinkholes and subsidences occurred within the chert-rich dolomitic formations (i.e.: the Monte-Christo Formation followed by the Eccles Formation) in the Centurion-area, Pretoria. Oosthuizen ascribed the relatively higher-than-expected number of sinkholes having formed on the Lyttleton Formation to a larger concentration of people and wet services located on this Formation in the applicable study area.

The focus of the work presented in this research paper is not aimed at the same in-depth statistical correlation as compiled by Wolmarans (1984), Schöning (1990), Richardson (2013) and Oosthuizen (2013), but rather to compare these findings in terms of the same geological Formations occurring in the focus study area, in support of regional dolomite risk management. The information presented by Richardson (2013) for the West Rand Municipal area is of specific interest, as it is inferred to more closely relate to the regional structural geological setting of the

KOSH-area. Therefore, only the findings from the West Rand Municipal area, as presented by Richardson, are summarised (Table 2-1). It should be noted that Richardson states some limitation, ascribed to incomplete historical documentation of features, and must be taken into consideration, these include:

- (i) Sinkhole and subsidence diameter and depth data was not available for a majority of the dataset (60 % and 67 % unavailable respectively).
- (ii) 16 % of the formed events do not indicate a triggering mechanism.
- (iii) 4 % of the formed features are not described in terms of type of feature (e.g.: sinkhole or subsidence).
- (iv) Large gaps exist regarding recorded date of occurrence (59 to 61 % of the dataset).
- (v) 48 % of the described sinkholes (e.g.: 1 473 of the 3 048) occur in the West Rand Municipal area.
- (vi) The occurrence of features in terms of geological Formation was determined based on available 1:250 000 and 1:50 000 scale geological maps of each respective area.

The summarised data represented by Richardson (2013) regarding feature distribution per geological Formation has been recalculated in terms of feature type, as well as size and depth distributions, which are included in Table 2-1 and summarized in Figure 2-4. By incorporating the structural geological setting, in conjunction with land use and historical information of engineering services, a much clearer understanding of the distribution of these analysed sinkholes and subsidences could have been obtained. The distribution and rate of new occurrence was taken as concluded on separately by Richardson (2013) and by Oosthuizen (2013) for the West Rand area. The Chamber of Mines (1966) described the biggest known sinkhole at the time to be 370 m across and 55 m deep, located in the Gatsrand near Doornfontein (West Rand, South Africa), and ascribed the relative age of this sinkhole having formed in prehistoric times (*in Wagener, 1982*).

Table 2-1: Summarised results of sinkhole statistics for the West Rand Municipality (summarised and recalculated from Richardson, 2013; and from Oosthuizen, 2013)

Feature type	Number of recorded events	Geological Formation ¹	Size distribution ²	Depth distribution ³	Triggering mechanism ⁴	Distribution and rate of occurrence (all event types) ⁵
Sinkholes	1 195 events (81% of tot West Rand dataset)	Vmo: 179 events (12% of Shs)	S = 10% M = 13% L = 40% VL = 38% n = 28	Sh = 17% In = 45% D = 30% VD = 7% n = 18	47 % WI 53 % GWLD	DA = #0.035 or 0.19 NDA = #0.041 or 0.22 Overall = #0.036 or 0.19
		Vmm: 461 events (31% of Shs)	S = 16% M = 22% L = 34% VL = 29% n = 197	Sh = 20% In = 55% D = 22% VD = 3% n = 174		DA = #0.046 or 0.25 NDA = #0.054 or 0.29 Overall = #0.048 or 0.26
		VI: 95 events (6% of Shs)	S = 13% M = 22% L = 39% VL = 26% n = 67	Sh = 14% In = 61% D = 19% VD = 6% n = 51		DA = #0.017 or 0.09 NDA = #0.020 or 0.11 Overall = #0.018 or 0.10
		Ve: 320 events (22% of tot)	S = 11% M = 22% L = 34% VL = 33% n = 165	Sh = 17% In = 52% D = 25% VD = 6% n = 143		DA = #0.069 or 0.37 NDA = #0.081 or 0.44 Overall = #0.072 or 0.39
		Other: 140 events (10% of tot)	S = 10% M = 16% L = 27% VL = 47% n = 52	Sh = 20% In = 30% D = 39% VD = 11% n = 41		Excluded

Table 2-1: Continues

Feature type	Number of recorded events	Geological Formation ¹	Size distribution ²	Depth distribution ³	
Subsidences	110 events (7.5% of tot West Rand dataset)	Vmo: 17 events (1.1% of tot)	S = 50% M = 0% L = 0% VL = 50% n = 2	Sh = Incl. In = Incl. D = Incl. VD = Incl. n = 1	<u>Rate of formation*</u> : Richardson (2013): DA = #0.05 NDA = #0.06 Overall (DA & NDA) = #0.055 or 25.5 events / annum across 493 km ² Oosthuizen (2013): DW = #0.03 WI = #0.01
		Vmm: 42 events (2.9% of tot)	S = 29% M = 14% L = 30% VL = 27% n = 24	Sh = 86% In = 11% D = 3% VD = 0% n = 26	
		VI: 9 events (0.6% of tot)	S = 13% M = 21% L = 28% VL = 38% n = 13	Sh = 65% In = 24% D = 10% VD = 0% n = 7	
		Ve: 29 events (2.0% of tot)	S = 23% M = 3% L = 28% VL = 47% n = 30	Sh = 91% In = 5% D = 4% VD = 0% n = 20	
		Other: 13 events (0.9% of tot)	S = 28% M = 2% L = 31% VL = 39% n = 10	Sh = 75% In = 21% D = 4% VD = 0% n = 10	

Table 2-1: Continues

Feature type	Number of recorded events	Geological Formation ¹	Size distribution ²	Depth distribution ³		
<p>Surface cracks</p>	<p>106 events (7.2% of tot West Rand dataset)</p>	<p>Vmo: 16 events (1.1% of tot)</p>	<p>N/A</p>	<p>N/A</p>		<p><u>Events / km²:</u></p> <p>Richardson (2013): DA = 0.4 to 7.3 events per km² (average 2.8/km²) NDA = 0.4 to 4.17 events per km² (average 2.5/km²)</p> <p>Oosthuizen (2013): DA = 2.2 events per km² NDA = 0.3 events per km²</p>
		<p>Vmm: 41 events (2.8% of tot)</p>				
		<p>VI: 8 events (0.6% of tot)</p>				
		<p>Ve: 28 events (1.9% of tot)</p>				
		<p>Other: 12 events (0.8% of tot)</p>				
<p>Undefined event type</p>	<p>62 events (4.2% of tot West Rand dataset)</p>	<p>Undiff.</p>	<p>Undiff.</p>	<p>Undiff.</p>		

1 Vmo = Oaktree Formation. Vmm = Monte Christo Formation. VI = Lyttleton Formation. Ve = Eccles Formation. Other is inferred to represent the Black Reef Formation, Karoo Supergroup and Pretoria Group. Undiff. = Undifferentiated.

2 S = Small < 2 m diameter. M = Medium = 2 to 5 m diameter. L = Large = 5 to 15 m diameter. VL = Very Large > 15 m diameter.

3 Sh = Shallow = depth of less than 1 m. In = Intermediate = depths of between 1 and 5 m. D = Deep = depths of between 5 and 15 m. VD = Very deep = depths in excess of 15 m. (*Definitions proposed by author*). Incl. = Inconclusive.

4 WI = Water Ingress. GWLD = Groundwater level drawdown (e.g. artificial lowering of the water level). It should be noted that where dewatering was the triggering mechanism, the relevant groundwater compartment in which the feature is situated should also be taken into consideration (this is discussed in Chapter 4)

5 All types of events are included as a total, and sinkholes, subsidences, cracks and “other” are not recalculated separately. # represents the number of events / km² / annum (i.e.: #NSH), and is defined as the rate of formation. The inherent hazard – as defined by SANS 1936-2 – has also been recalculated from Richardson, 2013 (where low = less than 0.1 events per hectare per 20 year, medium = between 0.1 and 1.0 events per hectare per 20 years, and high = more than 0.1 events per hectare per 20 years). DA = Dewatered areas and NDA = non-dewatered areas. DW = Formation of sinkholes and subsidences due to groundwater level drawdown (dewatering). WI = Formation of sinkholes & subsidences due to water ingress.

NOTE: Features recorded as “other” in Richardson (2013) remains undifferentiated in terms of geological Formation, size, and depth.

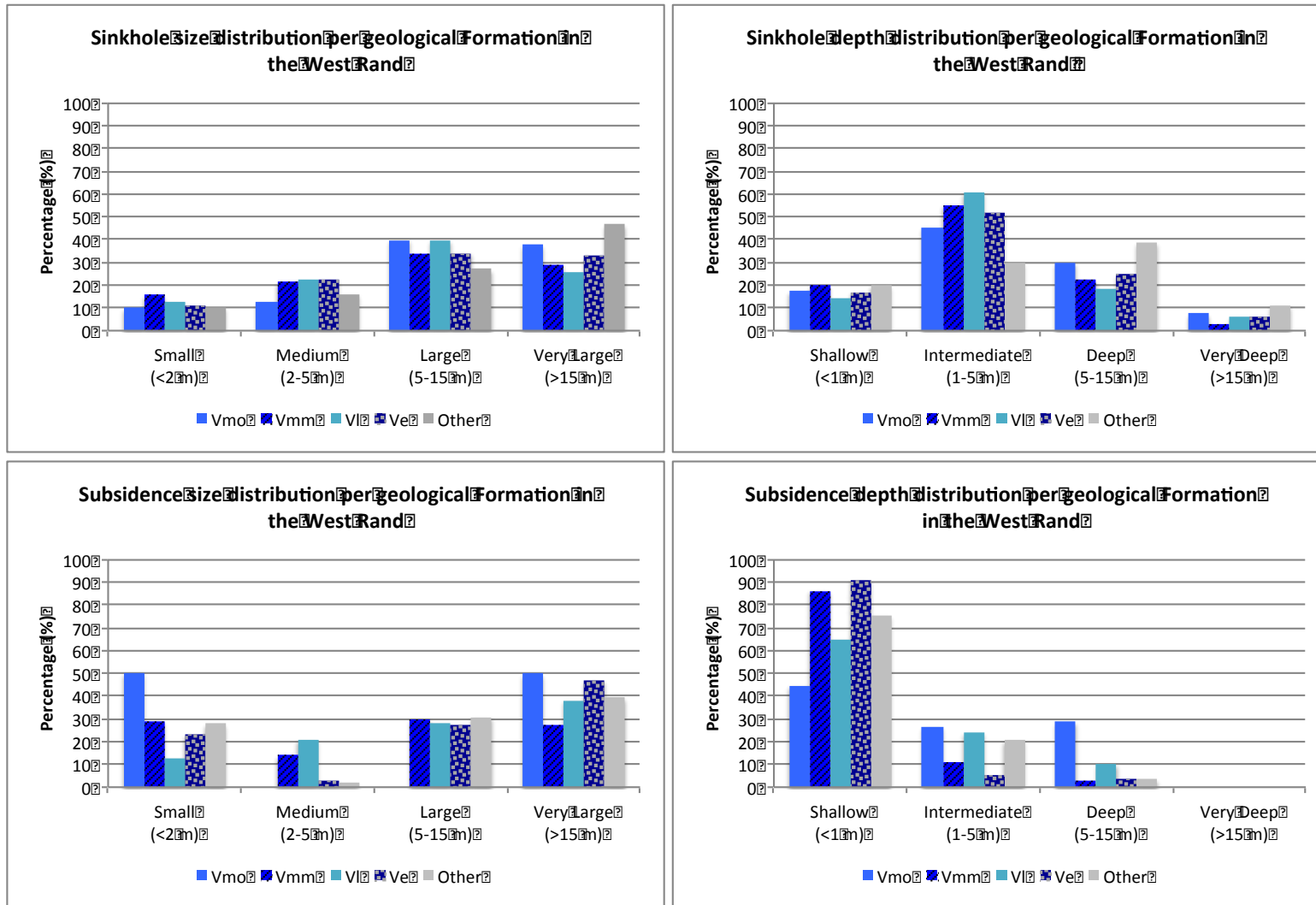


Figure 2-4: Distribution of sinkhole and subsidence dimensions across various geological Formations in the West Rand (recalculated from Richardson, 2013)

2.4 Dolomite risk management

The concept of risk management currently forms the basis for development on dolomite land in South Africa. This is defined in detail in the National Standard: SANS 1936 Part 4 (SANS, 2012). The work conducted by Buttrick *et al.* (2011) revealed that up to 98% of all causes of sinkholes and subsidences in South Africa could be attributed to anthropogenic influences, such as leaking infrastructure, poor storm water management, and insufficient (or no) groundwater management. In this light, it was concluded that effective risk management could significantly reduce the likelihood of an event occurring. Dolomite risk management is defined by SANS 1936 Part 4 (SANS, 2012) as the “*scientific, planning, engineering and social processes, procedures and measures to manage an environmental hazard, and encompasses policies and procedures set in place to reduce the likelihood of events (sinkholes and subsidences) occurring on dolomite land*”. Risk management is implemented by Dolomite Risk Management Strategies and –Plans, which is underpinned by Dolomite Stability Investigations that attempts to define the inherent hazard of the area.

In order to effectively understand the concept of dolomite risk management, the different definitions related to this concept – as defined by Buttrick & van Schalkwyk (1995), Buttrick *et al.* (2001) and later adopted by SANS 1936 (SANS, 2012) – must be clearly understood:

Likelihood and probability

Likelihood refers to the description of the probability or frequency of occurrence. Vick (1994) stated that it considered as generally acceptable and reasonable to estimate probability using three different methods:

- (i) Mathematical modeling.
- (ii) Frequency of observations from historical data.
- (iii) Quantification of specialist judgment.

Hazard

In broad terms a hazard refers to a “*source of potential harm*” (SANS, 2012). In the context of dolomite, it specifically refers to the occurrence of a karst-related instability event of a certain size (i.e.: formation of a sinkhole or subsidence) that can cause damage to the built environment or cause loss of life.

Inherent Hazard

Inherent hazard is the potential for a karst-related instability event to develop in a particular dolomite profile on dolomite land. The likelihood of the formation of a sinkhole or subsidence is classified in terms of Inherent Hazard Classes (1 to 8), where IHC 1 represents the lowest inherent hazard and IHC 8 represents the higher inherent hazard, based on the respective susceptibility of a certain size feature to develop.

Inherent Susceptibility

Inherent susceptibility is defined as the likelihood of a sinkhole or subsidence forming in a specific dolomite profile (Buttrick, 2014).

Anthropogenic Susceptibility

Anthropogenic susceptibility is defined as the likelihood of a sinkhole or subsidence forming when a triggering mechanism is introduced by human actions (proposed by Buttrick, 2014).

Vulnerability

According to Alcantara-Ayala (2002), vulnerability encapsulates the status assessment of the physical, social, environmental and economical aspects that increase the susceptibility of a community's exposure to a hazard.

Risk

Risk is the effect of uncertainty on objectives, and can be defined by the following equation (Buttrick, 2014):

$$\text{Risk} = fn (\text{hazard} \times \text{vulnerability} \times \text{damage})$$

Buttrick (2014) suggested that hazard includes both the inherent susceptibility as well as the anthropogenic susceptibility. In other words, hazard is the “*function of the inherent susceptibility of an area to the occurrence of an event (sinkhole or subsidence) of a certain magnitude (small to very large) and the frequency (return period) thereof, in the context of a specific scenario (i.e.: anthropogenic susceptibility)*”.

Development risk

This term is defined by Buttrick *et al.* (2001) as the likelihood of property damage and related financial losses, as well as loss of life. Development risk is either regarded as acceptable or unacceptable. Development risk is based on the inherent hazard and susceptibility of a specific site, and specific land uses or development types are generally selected based on these two factors.

As such, the work presented as part of this study will focus on estimating the probability (using the quantification of specialist judgement and frequency of observations from historical data) of a hazard occurring as part of the *inherent susceptibility* of the area being investigated in support of regional risk management. The requirements for alternative approaches and appropriate methods of assessing the overall dolomitic risk of an area were proposed by Buttrick (2014). In order to determine the full extent of risk in the area, other factors that are included as a function of risk must be evaluated (e.g.: anthropogenic susceptibility, vulnerability and damage).

2.5 Overview of dolomite hazard assessment procedures in South Africa

The investigative hazard assessment procedures of dolomite land in South Africa (i.e.: assessment of the inherent susceptibility of dolomite landscapes) has changed over recent times, since the early 1970's – when a large number of sinkholes started to develop in the West Rand due to dewatering associated with mining activities – to more recent times (2001 and 2011). The assessment of the inherent hazard is commonly referred to as the Dolomite Stability Investigation component of dolomite risk management, and underpins the entire risk assessment and subsequent compilation of a Dolomite Risk Management Strategy of an area. The various approaches and evaluation methods up until 1992 have been well documented by Van Rooy (1984) and Buttrick (1992) as summarised by Van Rooy (1996), of which some are very briefly discussed and summarised in Table 2-2 and chronologically represented in Figure 2-5:

1955 to 1980:

The initial approach for demarcating dolomite land that was generally widely accepted, narrated that no sinkholes should develop where the average depth to the dolomitic bedrock exceeds 15 m (Enslin & Smit, 1955; Kleywegt, 1980). The use of gravimetric surveys supplemented by a limited number rotary air-percussion drilling was considered the most effective means of determining sub-surface conditions in dolomitic areas.

1973:

The work done by Kleywegt & Enslin (1973) focussed on the application of the gravity method in the Far West Rand during the dewatering of groundwater compartments in the dolomite, and found the following:

- Instances where the original water table prior to dewatering was between 0 and 30 m below ground level (mbgl) in topographic low-lying areas indicated the highest number of

occurrences of instability features. Sinkholes in these areas developed along transition zones into gravity lows, in gravity high areas, and across “*narrow features*”.

- Few sinkholes formed in areas where the original water table was in close proximity of the dolomite bedrock (i.e.: slightly weathered rock head) and occurs at between depths of 30 to 60 mbgl. The authors ascribed this phenomenon generally to extensive capping of stratigraphic younger geological Formations (i.e.: Karoo-aged sedimentary rocks) that hindered the formation of sinkholes, and served as an aquitard. It could be that this condition as ascribed by the authors is closely related to the local geological setting of the area that was investigated.
- Isolated large sinkholes formed in areas associated with topographic high areas, where the original water table was deeper than 90 mbgl. The authors ascribed the primary triggering mechanism causing the formation of these sinkholes as ingress of surface water.
- Gradual settlement (i.e.: the formation of subsidences) was generally encountered in gravity low areas accompanied by the presence of compressible material (wad) and where the original water level was situated above the dolomite bedrock.
- Steep gravity gradients between gravity high and gravity low areas – representing a steeply sloping bedrock rock head – were associated with differential settlement, causing surface tension cracks to form, which allows for the increased concentrated ingress of surface water, later resulting in the formation of sinkholes.
- Sinkholes are associated with altered/weakened zones along dyke intrusions. The area of influence of one such a dyke – the Bank dyke in particular – is up to 1 km adjacent the intrusion, based on the extent of ground movement in the area surrounding the intrusion (Van Deventer, 2013).
- Groundwater level drawdown resulted in the re-activation of paleo sinkholes and subsidences.

1975:

Stephan (1975) proposed to assign a numerical value to each lithological unit encountered in the geological profile, as determined by the drilling of boreholes. The assigned number is multiplied by the thickness of the specific lithological horizon in order to obtain a final total numerical rating per borehole. A 10 % reduction value is applied for every 5 m depth increment.

The final total numerical ratings are divided into three broad classes to determine the areas suitability for development:

- Values < 0 = area is suitable for development.
- Values of 0 to 40 = area is suitable for development provided the application of water precautionary measures.
- Values > 40 = area is unsuitable for development.

1979:

Weaver (1979) proposed the so-called "*X-factor*" empirical classification system. This system relied on the evaluation of borehole information, generally not exceeding a depth of 30 m, and is primarily focussed on the Lytleton Formation in a non-dewatered area south of Pretoria. The stability ratings derived from each borehole, ranging from 1 (unsuitable / highest risk) to 4 (suitable / lowest risk) is contoured into three development suitability zones to produce a development potential map, where:

- $x < 1$ = highly unsuitable for development.
- $1 < x < 4$ = doubtful with respect to development.
- $x > 4$ = suitable for development.

1979:

Brink (1979) indicated the importance of groundwater in relation to sinkhole formation, and stated that the current groundwater level is considered as the base level of sub-surface erosion in dolomite areas. As such, voids and cavernous conditions located below the groundwater level cannot serve as receptacle for mobilised material. The profile and geomechanical properties of the overburden are therefore regarded as having a significant contribution to the eventual probability for the formation and size of a sinkhole. Brink furthermore stated the use of gravimetric information to delineate non-dewatered areas into initial hazard zones, which were classified:

- Steep gravity gradient anomalies: high risk.
- Gravity high anomalies: High risk for small sinkhole formation.

- Gravity low anomalies: Low risk for sinkhole formation, provided the water table is deep and the overburden is up to and in excess of 15 m thick.

1980:

The methods used as part of geotechnical investigations did not progress much over the timespan of 25 years since approximately 1955 to 1980 (Wagener, 1982).

Martinelli and Hubert (1980) illustrated that the use of the electrical resistivity geophysical method in combination with limited rotary air-percussion drilling can be successfully implemented to define geological contacts between dolomitic and non-dolomitic rocks (specifically dolomite/shale contacts) to a depth accuracy of better than 10 m and proves to be economic.

1981:

More formalised evaluation systems were proposed in 1981 by Venter and by De Beer (Venter, 1981; De Beer, 1981). These methods relied on the grouping together of influencing factors that is considered to contribute to the formation of instability features, and assigned a numerical value to derive areas regarded as low to high-risk areas. Venter (1981) emphasized the difficulty of using analytical methods that are based on soil-mechanical principals to characterise dolomitic risk, due to the many aspects that influence the stability of the dolomite profile. Venter (1981) indicated that the most widely-used approach for evaluating dolomitic terrains are empirical methods aimed at determining the factors that may impact on the stability of an area, which includes:

- Surface topography and site drainage.
- Thickness, strength, and erodability of the overburden material.
- Topography of the bedrock.
- Cavities in the dolomite bedrock and overburden.
- Level and fluctuation in the water table.
- Structural geological features such as the occurrence of faults and dykes.
- The proposed future development and land use.

Buttrick (1992) stated that prior to 1992, the classification system proposed by Venter (1981) reflects the most comprehensive classification system produced at the time that takes into consideration numerous complex interdependent factors. The more formal classification system proposed by Venter is one of the very few that pertinently considered structural geological factors in the evaluation process.

1981:

Kleywegt (1981) proposed a geological approach to the evaluation of dolomitic terrains, and stated that a strong understanding of the sub-surface geological profile is required in combination with an empirical understanding that the current meta-stable conditions will be affected during dewatering and water infiltrating the profile. Aspects such as the depth of the original water table, the nature and thickness of the overburden, and the depth to bedrock in relation to the original water table were all considered, especially in dewatered areas.

1982:

During the early 1980's, the initial understanding of dolomite land was altered based on observations made by Wagener (1982), who found that sinkhole depths in the Vaal Reefs Shaft 8 area exceeded the 15 m depth margin that was widely accepted at the time. At that time a total of 5 m of competent bedrock encountered during the drilling process was considered as sufficient evidence to rule out dolomite floaters. Based on the understanding of the behaviour of dolomite at the specific time, Wagener stated that it is not possible to "*lay down fixed rules for the evaluation of different site conditions*" and that "*all available information should be considered together rather than concentrating on one set of results in isolation*". Wagener argues that where the original water table has not been drawn down, areas associated with steep gravity gradients or areas associated with fault or fracture zones must be avoided when considering development (Wagener, 1985). It was proposed to classify dolomitic sites broadly based on the average overburden thickness that blankets the dolomite bedrock and pinnacles:

- Class A: Where dolomite pinnacles and boulders are at surface or covered by less than 3 m of overburden.
- Class B: Where dolomite pinnacles and boulders are overlain by overburden of moderate thickness (e.g.: 3 to 15 m deep).
- Class C: Where dolomite pinnacles and boulders are overlain by thick overburden (e.g.: in excess of 15 m deep).

The use of other geophysical methods (e.g.: ground penetrating radar, seismic methods, magnetic methods, electrical methods, and resistivity methods) have been considered by a number of authors in the past, but either proved unsuccessful in South African conditions, or was too costly to implement in assessing larger portions of land.

1984:

Jones (1984) considered dolomite instability along Karoo outliers. It was proposed that dolomite stability in this very specific geological setting could be evaluated by:

- Ranking of all physical engineering characteristics of the various lithologies encountered in the geological profile according to their respective susceptibility for instability.
- Weighing of all physical engineering characteristics of the various lithologies according to their apparent thickness to express its instability potential.
- Prediction of the impact that the groundwater level elevation will have on the specific geological profile.
- Consideration of the character of the dolomite bedrock, including cavernous conditions.
- Potential for instability of various lithologies as a function of compressibility, erodability, and inverse of tensile strength (or cohesion) for rock and subsoil materials.
- Risk evaluation criteria includes the consideration of:
 - Lithological sequence.
 - Subsurface water.
 - Configuration of the dolomite bedrock and paleo-karst surface: As stated by Jennings *et al.* (1965; *in* Jones, 1984), paleo-karst topographies with steep-sided and closely spaced dolomite pinnacles enhances the risk for the formation of sinkholes, provided the material possess poor tensile strength and is highly erodible. On the contrary, in-filled paleo-karst topographies representing a gentle undulating dolomite rock head will favour the development of subsidences or differential surface settlement, due to a too great span between shallow sloped abutments to allow for the formation of an arch and subsequent head ward erosion.
 - Extent and occurrence of cavities and voids in the profile.

1984:

Van Rooy (1984) proposed a method of evaluating dolomitic terrains using the so-called “*MF classification system*”, which followed the normal approach of site investigations conducted on dolomitic terrains at the time. This approach was primarily implemented in a non-dewatered area, with the approach divided into three main stages:

- Stage 1: This initial stage aims to satisfy the macro-classification of the site in order to ensure that all significant areas across the terrain are investigated. The demarcation of the initial macro zones are based on collation of the following geo-scientific information:
 - Inputs from surface features, including: outcrop areas, chert-gravel horizons, areas with similar vegetation cover, existing and rehabilitated sinkholes and subsidences, scattered outcrop areas, different stratigraphic horizons and intrusive bodies. These are generally obtained by means of geological maps, aerial photograph investigations, stratigraphic information, surface geological mapping, and field verifications.
 - The use of thermal infrared line-scanned images to obtain an overview of the surface drainage of the site. Care must be given to the accurate defining of anomalies, seeing as variations in colour shading could indicate changes in vegetation, surface topography, urbanisation and variations in geology. This method proves little to no use across small sites or urbanised areas. Van Rooy designated five risk classes based on the variations in shading representing changes in surface topography: (i) black = very high risk, (ii) dark grey = high risk, (iii) grey = medium risk, (iv) light grey = low risk, (v) white grey = very low risk.
 - Macro-classification using gravimetric data is based on the zonation of the produced residual gravity contours. General anomalous features that can be distinguished include (i) gravity high anomalies, (ii) gravity low anomalies, (iii) steep gravity gradient zones, and (iv) shallow gravity gradient zones. The risk classification of the gravimetric survey is based on the guidelines set out by Brink (1979).
- Stage 2: The macro-classification zones are investigated by the drilling of rotary air percussion boreholes (up to a maximum depth of 30 m at the time), which are divided into five severity classes (i.e.: 0,24 to 4 representing very poor to very good) by the

evaluation of five factors in order to calculate various risk classes for each borehole.

The five evaluation factors include:

- Depth of erodible soil (including wad).
 - Thickness of erodible soil.
 - Properties of erodible soil.
 - Material type above first occurrence of erodible soil.
 - Material type beneath last occurrence of erodible soil.
- The calculated boreholes stability values relate to the various levels of risk is as follows: (i) 0.0 to 0.0024 = very high risk, (ii) 0.0025 to 0.124 = high risk, (iii) 0.125 to 0.5624 = medium risk, (iv) 0.5625 to 15.0 = low risk, (v) 16 to 256 = very low risk.
 - Stage 3: The *FM system* is concluded by incorporating all available information into a final dolomite risk zonation map. This is based on collating (a) the initial macro-zonation of the site using surface geology, surficial information, drainage and gravimetric information, (b) confirmation of the initial zonation using borehole data including the quantification of variability and risk, and (c) final correlation of the above with the current and historic damage to structures and infrastructure across the site.

1984:

Roux (1984) also considered a strong geological-based approach to hazard assessment with the specific emphasis on residential development of the area south of Pretoria, and stated the following:

- The chert-poor and relatively Mn-rich Oaktree Formation contained no sinkholes in the dolomitic area south of Pretoria.
- Sinkholes occurring in the chert-free and Mn-rich Lyttleton Formation are controlled by structural geological features where deep weathering of the dolomite bedrock occurred along fractures zones and faults, and are generally smaller than 3 m in diameter.
- The chert-rich dolomitic formation (e.g.: the Monte-Christo- and Eccles Formations) indicated the most sinkholes. Sinkholes in the Monte-Christo Formation are generally up to 30 m in diameter, and in the Eccles Formation up to 100 m in diameter and up to 20 m deep.

- Paleo sinkholes are re-activated where the current groundwater table is more than 30 m below the original surface elevation (in the investigated non-dewatered area).

Roux (1984) stated that all available information must be considered in determining the stability characteristics of a dolomitic site. This includes considering aspects such as the availability of existing information, remote sensing techniques, the stratigraphic position of the site in terms of the various lithostratigraphic sub-divisions determined by means of available geological information and surface mapping, conducting of geophysical surveys, invasive geotechnical exploration including drilling of boreholes and excavation of test pits, evaluation of the nature, thickness and extent of the overburden, and the occurrence of collapsible/compressible materials. With respect to the thickness of overburden, it was considered that overburden that is less than 15 m thick is considered as thin, and coverage up to and in excess of 15 m is considered as thick. Where the overburden is thicker than 15 m and does not represent a paleo sinkhole, the area was considered as stable. Where Karoo-aged sedimentary deposits and its associated residual material cover a dolomitic area, a thickness of up to 20 m was regarded as stable conditions.

Early 1990's:

The widely applied understanding of 30 m depth to dolomite was drastically challenged during the early 1990's when a 100 m deep sinkhole developed near the military base at Waterkloof (Pretoria, South Africa), which gave rise to the current depths to dolomite bedrock regarded as dolomite land. Similar events were reported elsewhere. One such event that occurrence was a sinkhole at the Strathmore Primary School in Stilfontein during 1981 that spanned 1.3 m at surface and was reportedly 300 m deep.

1992, 1995, 2001 (2011):

The hazard assessment procedure and methodology adopted in SANS (2012) is largely based on the method of scenario supposition as detailed in the work done by Buttrick (1992) and Buttrick & van Schalkwyk (1995), which was later revised by Buttrick *et al.* (2001) and tested using the performance of selected study areas across Gauteng (Buttrick *et al.*, 2011). This is discussed in more detail in Section 2.7.

- The method of scenario supposition was widely applied by the Department of Public Works (DPW) in 2006, and focussed on the eventual appropriate development of infrastructure on dolomite land, as well as the risk management of infrastructure situated over dolomite land (DWP, 2006). Risk characterisation in this regard was more

focussed on large-scale risk management, and defined the grouping of zones into areas of low susceptibility (i.e.: Inherent Hazard Class (IHC) 1), medium susceptibility (i.e.: IHC 2 to 4), and high susceptibility (i.e.: IHC 5 to 8).

1999:

During this time the National Home Builders Registration Council (NHBRC) promulgated guidelines and requirements for geotechnical investigation (both foundation investigations as well as dolomite stability investigations) for housing developments, and subsidence-linked developments.

2002:

During 2002, the National Department of Housing published the Generic Specifications for greenfields subsidy-linked housing developments (GFSH-2) guidelines. These guidelines also made specific mention of the norms and requirements for geotechnical investigations and dolomite stability investigations for greenfields housing developments.

2003 to 2007:

In the interim after the proposed method of scenario supposition (Buttrick & van Schalkwyk, 1995) and prior to the promulgation of SANS 1936 (SANS, 2012), the Council for Geoscience published a consultant's guide on how to approach the investigation of sites situated on dolomite (Council for Geoscience, 2003). This document aimed to provide a more formalised approach to the investigation of dolomite land, risk characterisation, and some generalised precautionary measures, all based on the work done by Buttrick and Van Schalkwyk (1995).

2012:

During 2012 the national standard SANS 1936 was promulgated. This current best-practice guidelines dictates that areas should be investigated to a minimum depth of 60 m where no prior dewatering has occurred and where groundwater monitoring and control measures are in place, and to a depth of up to 100 m where prior dewatering has occurred, where the dolomite compartment is currently dewatered, or where no groundwater monitoring and control measures are in place. A thickness of at least 6 m of competent dolomite bedrock encountered during drilling is deemed sufficient to prove intact dolomite bedrock (and not floaters) (SANS, 2012).

2014:

Buttrick (2014) stated that very little progress has been made over the past 20 years (i.e.: ± 1992 – 2014) with respect to dolomite hazard assessments, with the exception of the work conducted by Kirsten *et al.* (2009).

More recently, various analytical methods have been proposed to understand the geo-mechanical drives behind sinkhole formation and propagation, as well as material properties, as highlighted by Venter (2014). These methods focus on probability-based quantitative risk assessments, centrifuge modelling, and finite element stress analysis (e.g.: Avutia & Kalumba, 2014; Jakobz, 2014; Venter, 2014; Kleinhans & van Rooy, 2014; Parrock, 2014).

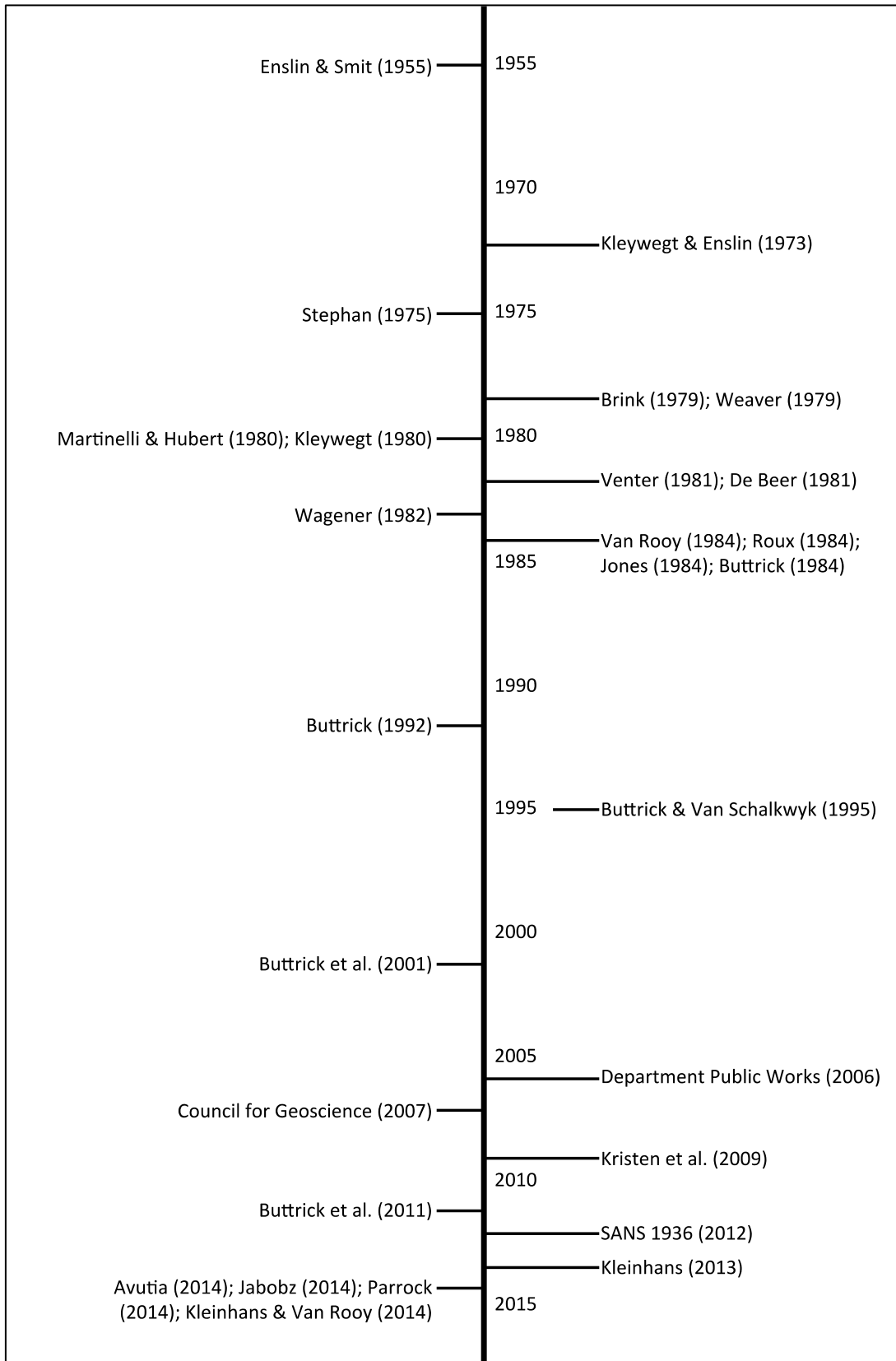


Figure 2-5: Milestones of major contributions and classification systems proposed for dolomite hazard assessments in South Africa

Table 2-2: Summarised criteria used in the assessment of dolomite land in South Africa – 1975 to 2015 (after Van Rooy, 1996)

Parameter included as part of evaluation criteria	Stephan (1975)	Weaver (1979)	Venter (1981)	De Beer (1981)	Wagener (1982)	Roux (1984)	Van Rooy (1984)	Jones (1984)	Buttrick (1992)	Buttrick & v.Schalkwyk (1995)
Surface topography and terrain morphology				x		x	x			
Site history (prior land uses, previous instability)				x		x	x			
Overburden:										
Soil / rock type	x		x	x		x	x		x	x
Strength			x	x			x	x		
Erodability			x					x	x	x
Thickness	x	x	x	x	x	x	x	x	x	x
Permeability*										
Dolomite residuum:										
Type	x	x	x	x		x	x		x	x
Strength	x		x	x			x	x		
Erodability			x			x		x	x	x
Thickness	x	x	x	x	x	x	x	x	x	x
Karst topography (rock head variability)			x			x	x		x	x
Structural features (faults, shear zones, fractures, geological contacts, lithostratigraphic sub-divisions)			x			x				
Groundwater regime:										
Depth to groundwater				x		x		x	x	x
Groundwater movement								x	x	x
Dewatering status and original water level									x	x
Other triggering mechanisms						x			x	x
Feature size (sinkholes & subsidences)									x	x
Risk indication / determination			x						x	x
Appropriate land use			x	x	x	x			x	x

2.6 Phases of dolomite stability investigations during development

Various authors discussed the consecutive stages of dolomite land investigations in the past (e.g.: Roux, 1984; Wagener, 1982; Trollip, 2006 – among other). The culmination of this work was collated to a large extent in SANS 1936 Part 2 (SANS, 2012), which defines three primary stages of investigations when considering construction works of dolomite land. These stages include a (i) feasibility level investigation, (ii) design-level investigation (including footprint investigations), and (iii) investigations during the installation of services and construction. Previous authors relied strongly on the information obtained during the reconnaissance phase of an investigation. The latter is not pertinently stated in SANS 1936 (2012) as a stand-alone phase and is included as part of the feasibility-level investigation. For the sake of this paper, it is separated as a stand-alone investigation phase.

2.6.1 Reconnaissance phase investigation

This initial phase of the investigation is predominantly focussed on the collation and evaluation of all available information regarding the site being investigated. After considering all available information, a surface walkover survey of the terrain is essential. During this phase of the investigation it is critical to determine – at least in broad terms – the intended use of the land being investigated, and to obtain an initial indication on the overall development potential of the site.

2.6.2 Feasibility level investigation

The primary aim of the feasibility level investigation is to characterise the geotechnical and dolomite stability hazard zones of the site in broad terms. This is carried out primarily to determine the suitability of the proposed land use of the site and to provide guidance on the required precautionary and remedial measures to be employed on site, all forming part of a Dolomite Risk Management Plan (DRMP) for the specific site. The complexity and conclusiveness of the retrieved information (or the variability of the information) usually determines the requirements of consecutive investigations as part of the feasibility-level investigation in order to reduce uncertainty, or in some instances the requirements to abandon a site due to prevailing poor subsurface conditions.

Geo-scientific data is collected during this level of investigation by means of geophysical surveys, the drilling of exploration boreholes, excavation of test pits and drilling of auger boreholes (and the subsequent profiling of the above), penetrometer testing, *in situ* material testing, and laboratory analysis of retrieved material samples.

2.6.3 Design-level investigation

The broadly delineated dolomite stability hazard zones that allows for certain types of development to continue is further investigated as part of the design-level investigation. This usually follows the same methods of investigation as set out in the feasibility-level investigations.

2.6.4 Investigations during construction

The main objectives of the investigations conducted during the construction phase of a project, is to confirm the initial anticipated prevailing conditions in each of the demarcated geotechnical zones. During the inspection of service and foundation trenches, it will be possible to obtain confirmation that the required precautionary measures to be implemented on a specific site are adhered to, and that no paleo sinkholes or other problematic dolomitic conditions (that could have been missed in the prior phases of the project) occur on the site.

2.7 Current methods and approaches used in South Africa

Day (2011) stated that during the drafting of the SANS 1936 (part 2) national standard, it was advocated to use the method of scenario supposition (as proposed by Buttrick (1992), and later adapted by Buttrick *et al.* (2001), termed “*method for dolomite hazard and risk assessment in South Africa*”) in the assessment of dolomite land. However, the interpretations associated with this empirical method are to some extent subjective and closely associated with the experience of the investigator, and relies on a number of assumptions. This method is currently regarded as a “*deemed-to-satisfy*” hazard assessment process, while provision is made in the SANS 1936 standard to allow for alternative assessment procedures and methods, based on rational assessments. The application of the method of scenario supposition requires the meticulous application of nine (9) pertinent steps (Buttrick, 1992) as set out in Table 2-3.

The application of the various investigative techniques that were incorporated by Buttrick (1992) as part of the method of scenario supposition to eventually characterise a specific project area in terms of inherent susceptibility (e.g.: Inherent Hazard Classes), have been considered by a number of authors, as outlined in section 2.5 of this chapter. The applications and general principles underlying these techniques were well summarised by Wagener (1982 & 1985), Venter (1981) and Roux (1984) among others, with the major components requiring consideration when conducting dolomite land assessments – regarded as the current industry minimum requirements – being incorporated in SANS 1936 Part 2 (SANS, 2012; Figure 2-8). Due to the focus of this paper being on the regional assessment of terrains in support of regional dolomite risk management (i.e.: generally steps 1 and 2 of the method of scenario

supposition), only limited focus will be given to the discussion of the various investigative methods associated with steps 3 and 4 (i.e.: drilling techniques, the gravimetric geophysical method, test pit excavations, and laboratory analysis and testing methods). The focus of this study is outlined in the green blocks (e.g.: hazard determination as part of research) on a regional scale as indicated in Figure 2-8.

Table 2-3: Steps in the application of the method of scenario supposition (after Buttrick, 1992)

Step	Evaluation criteria and requirements	
Step 1	Desk study and field reconnaissance of the site	
Step 2	Preliminary zoning using Aerial Photograph Investigations and geophysical methods (generally gravity geophysical method)	
Step 3	Drilling of boreholes to characterise preliminary zoning	
Step 4	Characterisation process using the method of scenario supposition by means of application to individual borehole profiles, in the context of the selected scenario (dewatering / non-dewatering)	
	<p><i>Evaluating factors for assessing sinkhole formation:</i></p> <ul style="list-style-type: none"> ▪ Mobilising agencies ▪ Receptacle development ▪ Potential development space ▪ Nature of blanketing layer(s) ▪ Mobilising potential of blanketing layer(s) 	<p><i>Evaluating factors for assessing subsidence formation:</i></p> <ul style="list-style-type: none"> ▪ Mobilising agencies ▪ Nature of blanketing layer(s) ▪ Mobilising potential ▪ Lateral extent
Step 5	Grouping of individual borehole characterisation and amending of preliminary zonation, considering all available historical information	
Step 6	Finalized zonation characterised in terms of a certain risk of a certain sized feature forming	
Step 7	Selection of appropriate development types and precautionary measures	
Step 8	Implementation of appropriate development types and precautionary measures	
Step 9	Vigilance and maintenance	

2.7.1 The role of the desk study

Swart (1991) stressed the requirements of a thorough desk study prior to any fieldwork, especially in dolomitic areas. The desk study serves the initial assessment of an area, and a thorough desk study could eliminate potentially hazardous areas from the proposed development, prior to costly invasive field-testing. Wagener (1982) also argued the essence of obtaining an overall impression of the area to be investigated prior to conducting detailed field assessments. The main objectives and key points to consider during the reconnaissance phase of the investigation can be summarised as follows (Roux, 1984):

- (i) All information of the terrain being investigated (farm name and number, district, subdivisions of the farm, jurisdiction of the local authority etc.) must be obtained.
- (ii) Well-established terms of reference and scope of work should be established.

- (iii) Obtain terrain locality and morphological information (extent of the site boundaries, surface contour and primary natural drainage features and -patterns, survey beacons etc.).
- (iv) Assess meteorological information (primarily rainfall data).
- (v) Determine the occurrence and extent of existing infrastructure on the terrain.
- (vi) Any available published information or previous investigations in the area (e.g.: site geology and soils distribution, history of flooding, erosion, previous instability events, previous geotechnical investigations etc.) must be considered.
- (vii) Previous land uses of the terrain with specific emphasis on dumping sites, inundated and marshy areas, waste pits etc. should be established.
- (viii) Determine the availability of construction materials in the vicinity of the project area.
- (ix) Existing surface water management and drainage measures, as well as sewerage system, employed on site – if any – must be determined.
- (x) Envisaged future land use of the site being investigated must be clearly established.

Roux (1984) furthermore discussed the various imagery that can be used during remote sensing, with detailed discussions on the pros and cons of each that was primarily based on the detailed work conducted by Minnett (1979). It was stated that the use of colour infrared imagery was found to be the most useful in dolomite hazard assessments, followed by thermal infrared imagery, and black-white infrared imagery proved to be least successful. The application of all these methods proved to be the most useful in areas where dolomite and chert forms outcrops and shallow sub-outcrops. Minnett (1979) also stated that care should be given to the season and time that infrared imagery is obtained, where the best results can be obtained before sunrise in the middle of winter, provided at least a 60 % overlap in images. White (1977) made the very important statement regarding the use of remote sensing – specifically aerial photographs – and said that it must be used to determine variations and patterns in surface coverage, and not to identify rock and soil types across an area. Such information regarding variations in patterns may include aspects such as surface texture, lineations, colour variations, relief and topography, and vegetation cover and densities (or sparseness). Conducting a proper stereo photograph investigation across a project area can reduce the overall intensity (and subsequent cost) related to field-testing (Wagener, 1982). Van Rooy (1984) also argued this point, and stated that preliminary zones, based on variations, inferred boundaries between soil

cover, rock outcrops etc., should be derived as part of the desk study, in order to establish the primary zones across the site, and to ensure that all areas are investigated during the field assessments. The significant contribution of a detailed and properly conducted desk study on dolomite areas couldn't be ignored, especially in the detection of paleo sinkholes (Brink *et al*, 1982). Some of the main contributions of such a desk study on dolomite areas (as listed by Wagener, 1982) include:

- (i) The delineation of linear features that normally represents slot developments (or grykes) in the dolomite bedrock, or faults (and fault zones).
- (ii) The detection of Paleo sinkholes.
- (iii) Delineation of boundaries between shallow dolomite pinnacles, boulders and chert gravel cover.

Another remote sensing method that is often used in assessments of dolomite areas is thermal infrared line-scanning of an area. This method is well summarized by White (1977), Viljoen (1980) and Wagener (1982). These authors stated that optimal results are acquired when the area that is scanned is dry and vegetation cover is sparse. As such, surveys in the winter months just before sunrise yields optimal results. The output of the thermal imagery represents variations in surface temperature, where dark areas represents thermal cool areas, and light colors warm areas. High thermal contrasts across a site can produce very useful additional information to the area. Hartopp (1978) made mention of some aspects that must be taken into consideration when interpreting thermal line-scanned imagery of an area, such as:

- (i) Occurrence of broad-leafed vegetation types that could skew the thermal readings.
- (ii) Areas where urbanization occurred, as well as cultivated land.
- (iii) The occurrence of surface water features.
- (iv) The thickness of overburden in the area.

The thermal infrared line-scanning method was used by Cooper (1979) with a fair amount of success, in order to attempt to detect cavernous areas in the West Rand. It was concluded that this method provides very useful additional information to sites underlain by shallow or pinnacle dolomite outcrops and sub-outcrops, but thick overburden could mask any thermal contrasts. Thermal imagery is optimally used in combination with aerial photographs (Wagener, 1982).

When considering all available published information, remote sensing methods, and basic geological principles, a significant amount of information can be gathered of most areas, and some preliminary indication can be obtained whether a site is totally undevelopable, or possible plausible for additional investigations.

2.7.2 The role of field assessments

The importance of field observations is emphasized by Roux (1984); Van Rooy (1984) and Wagener (1982), where information obtained as part of the desk study must be verified in the field. Current industry standards and guidelines (SANS, 2012 – Part 2) state the minimum requirements for field assessments include a walkover assessment of the site, conducting of a gravimetric geophysical survey accompanied by the drilling of rotary air percussion boreholes, near surface geotechnical investigations and recording and determining of the current groundwater regime and usage of the area. Good foundational geomorphological and surface outcrop mapping of the area that is investigated will play a very important role during the final interpretations of the gravimetric results as well as the siting of air percussion boreholes to characterise the dolomitic hazard of an area.

During the mapping and walkover stages of the field investigation, the various geomorphological features and bedrock lithologies covering the project area should be determined, due to the strong connotation it poses to specific dolomite conditions. It is furthermore of the utmost importance to determine if any existing ground movement have occurred on the area that is investigated. The field identification of the various geomorphological features and bedrock outcrops of the KOSH-area are discussed in Chapter 3.

It has been well established by Enslin & Smit (1955), Jennings (1966), Roux (1984) and Wagener (1982) that the use of rotary air percussion drilling on the basis of gravimetric surveys proves to be most effective in characterising the geological profile of a dolomitic area. The use of other drilling methods was used with varying levels of success, as discussed by Wagener (1982). Various geophysical methods have also been tested over the years to determine the extent of sub-surface cavities. This was conducted as part of a research program, initiated during the 1960's by the "State Technical Committee on underground cavities and subsidences" (Wagener, 1982). Due to the importance of the gravimetric geophysical method and the testing of the gravimetric anomalies by means of rotary air percussion drilling, these two methods are briefly discussed (largely based on the work done by Roux (1984) and Wagener (1982), and the requirements of the current industry standards (SANS, 2012).

2.7.2.1 Gravimetric geophysical survey

Roux (1984) compiled a very detailed description of the rationale and methodology behind the gravimetric geophysical technique. This method relies on Newton's gravity theory to determine the attractive forces between two spheroidal bodies. As a result, the gravity acceleration value (g) is the primary parameter of concern. Once the gravity acceleration of an area is determined, a number of corrections must be accounted for, including: longitude corrections, elevation corrections, Bouguer free air corrections, topographic and terrain corrections, and accounting of instrumental- and tidal drift.

Reference is made to Roux (1984) regarding the detailed mathematical calculations behind these corrections, and the considerations in conducting and interpreting gravimetric survey. The conducting of a gravimetric survey can subsequently be summarised in five primary steps (Roux, 1984):

Step 1: The gravimetric survey must be conducted at a minimum station spacing of 30 m, set out on a grid across the study area, and should include as a minimum an area of up to 150 m surrounding the project area boundaries. The elevation heights of the various stations must be to a minimum accuracy of 0.005 m, and the gravity readings must have an accuracy of at least 0.03 mgal, after correction of instrumental drift has been made.

Step 2: Based on field observations and calculations, a gravity anomaly map must be compiled and presented together with the locations of the survey points. Gravity contours must be constructed on an isopach map representing gravity readings at 0.1 mgal intervals.

Step 3: A residual gravity map must be produced, by removing the regional gravity field as determined using depths to dolomite bedrock (established during the reconnaissance drilling of a few initial boreholes), as well as the positions of shallow bedrock outcrops.

Step 4: After the completion of the gravimetric survey, taking into consideration the regional gravity field, all the necessary corrections, and incorporating of initial drilling results, a number of boreholes must be drilled into the various gravity anomalies to characterise the underlying strata, and to determine the correlation of depth to bedrock, as depicted in the gravity contour map. According to Wagener (1982), 0.1 mgal gravimetric contours represent 3 to 4.5 m depth to bedrock. However, care must be given to the final interpretation of the produced gravity anomaly map, because gravity low anomalies could represent both thick unconsolidated material, or relatively shallow cavernous conditions or slots, thus emphasizing the need to verify anomalies by means of drilling.

Step 5: After drilling results confirmed the actual depths to bedrock in combination with the produced gravity anomaly map and the depth to groundwater, a depth to bedrock isopach map should ideally be constructed.

2.7.2.2 Rotary air percussion drilling

The use of rotary air percussion drilling is the preferred method of drilling to characterise the gravimetric anomalies across a site that is investigated. As part of assessing the underlying geological succession, it is required to state the diameter of the drill bit used, the compressor air capacity as well as the air pressure. Wagener (1982) stated why this is a requirements: smaller diameter drill bits, higher air pressures, and a more powerful drill rig will all contribute to quicker penetration rates per meter drilled. Additionally, the material that is being drilled into also plays a significant role in establishing penetration times, where slightly weathered hard rock will be easier to drill than clay with a stiff consistency. Wagener also described the difficulty associated with sample contamination, where the lower lying material that is returned becomes contaminated with the upper horizons drilled through, and can often be overcome by the insertion of casing through the upper unconsolidated horizons to prevent contamination. Soft layers encountered during drilling must also be considered with great care, seeing as soft unconsolidated clayey silts and silty clays (wad) often results in very low penetration rates, but aren't readily blown to the surface by return air. Wagener described this issue as being related to the wad getting blown further in between chert bands and disseminated voids.

Current national standards (SANS, 2012) dictate that all the major gravimetric anomalies across the area that is investigated should be assessed, and where dolomite bedrock occurs deeper than 60 m below ground level, a deep borehole should be drilled on a gravity high anomaly to intersect the rock head. The guidelines requires a minimum of 6 m of competent dolomite bedrock to be intersected, and boreholes must be drilled to a depth of 60 m in non-dewatered groundwater compartments, and to a depth of 100 m in dewatered compartments (or where no groundwater management and control measures are in place). The minimum number of boreholes to be drilled across a project area of a certain size is also stated for the feasibility phase of the investigation. Thereafter, additional drilling is based on the area size of the various IHC's determined during the initial zoning.

It was found during previous experience using the same drill rig (e.g. Super Rock 1000 using a 27.6 m³/s air capacity, delivering 19 bar air pressure with a 165 mm drill bit) that competent hard rock dolomite generally exhibits penetration tempos of between 2 and 3 minutes per meter. Material with penetration rates of less than 20 seconds per meter is regarded as very soft / unconsolidated. The minimum information to be collected during drilling include (SANS, 2012):

- (i) Diameter of drill bit, compressor capacity and air pressure.
- (ii) Penetration tempo of every meter drilled into – determined using an electronic stopwatch.
- (iii) Description of the various lithostratigraphic horizons according to the current industry standard as set out by Brink and Bruin (2002).
- (iv) Collecting of a material sample for every 1 meter drilled.
- (v) Recording of air loss, poor sample return and irregular hammer tempos encountered during the drilling process.
- (vi) Description of water strikes and blow yields.
- (vii) Measurement of the static groundwater level at least 24 hours after drilling.
- (viii) All of this information is collated onto a driller's log and geological profiles. One such an example is included in Figure 2-6.

2.7.3 Hazard determining and zoning

The determining of the IHC of each respective borehole depends on the consideration of the criteria as set out in Step 4 of Table 2-3. This includes the empirical evaluation of the mentioned criteria to conclude on an expected qualitative angle of draw (α_x – generally between 45 and 90° from the horizontal) for each respective lithological unit encountered in the geological succession. As such, the maximum possible sinkhole size (MPS – small to very large) at surface (1a and 1b) can be estimated based on the thicknesses of the various lithological units (Figure 2-7). Buttrick (1992) defined broad angle of draw ranges for different material types:

- Chert: 90°
- Alternating chert and silty clay (wad): 80 – 90°
- Shale: 90°
- Clayey silt (wad): 45 – 60° and silty clay (wad): 45 – 75°
- Chert rubble with clayey silt: 45 – 90°

The IHC – ranging from 1 to 8 – is based on the inherent susceptibility of a certain size feature occurring (Table 2-4).

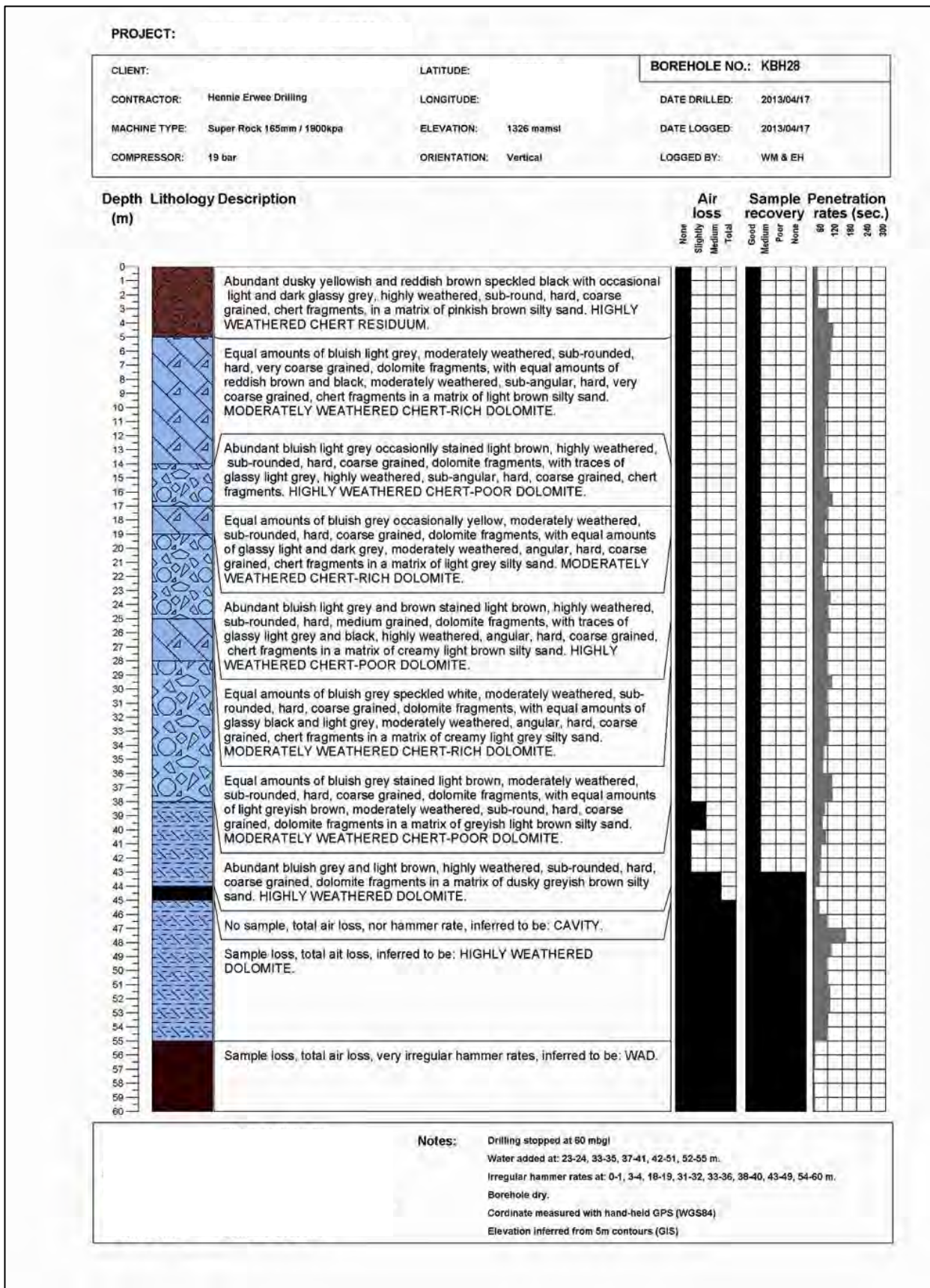


Figure 2-6: Example of a geological profile of a borehole drilled for dolomite stability assessment purposes

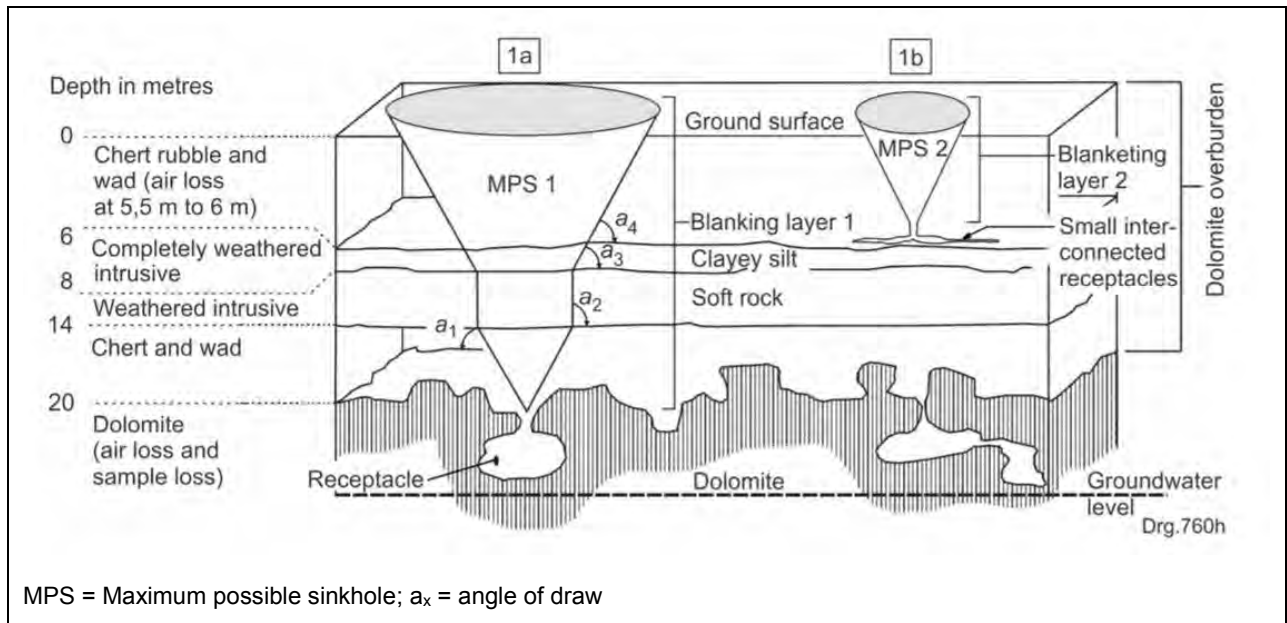


Figure 2-7: Schematic three-dimensional model illustrating various components of dolomite land (from SANS, 2012)

Venter (2014) gave a qualitative illustration of the relationship between hazard and uncertainty across the various IHC zones. This gives some idea whether or not the specified hazard condition (e.g.: IHC) indeed does occur at a specific point within a demarcated hazard zone. Venter stated that, for instance, in IHC 7 and 8 situations, the associated hazard is high and the uncertainty is small with respect to the probability of that condition occurring. In the same light, areas demarcated as IHC 5 are characterised by a relatively small hazard rating, but uncertainty regarding the accuracy of that condition occurring within the demarcated boundaries of the zone is high. As such the total number of data points required to accurately determine the probability of that condition occurring (i.e.: a high risk for the formation of small-sized sinkholes) will be substantially higher in order to reduce the level of uncertainty to an acceptable level.

Table 2-4: Inherent Hazard Class ratings and susceptibility (after Buttrick et al., 2001 and SANS, 2012)

IHC Rating	Small Sinkhole ($\varnothing < 2$ m)	Medium Sinkhole ($\varnothing 2 - 5$ m)	Large Sinkhole ($\varnothing 5 - 15$ m)	Very Large Sinkhole ($\varnothing > 15$ m)	Subsidence
1	Low ¹	Low	Low	Low	Low
2	Medium	Low	Low	Low	Medium
3	Medium	Medium	Low	Low	Medium
4	Medium	Medium	Medium ²	Low	Medium
5	High	Low	Low	Low	High
6	High	High	Low	Low	High
7	High	High	High	Low	High
8	High	High	High	High	High ³
IH Category	Anticipated number of events per hectare per 20 years				
Low	Typically less than 0,1 events, but occurrence of events cannot be excluded. Return period of an event occurring in an area of 1 ha is greater than 200 years.				
Medium	Typically between 0,1 and 1,0 events. Return period of an event occurring in an area of 1 ha is between 200 years and 20 years.				
High	Typically greater than 1,0 events. Return period of an event occurring in an area of 1 ha is less than 20 years.				
Inh. Susceptibility	Description				
Low	The profile displays no voids. No air loss or sample loss is recorded during drilling operations. Either a very shallow groundwater level or a substantial horizon of materials with a low potential susceptibility to mobilization might be present within the blanketing layer (e.g. continuous intrusive features or shale material). Depth to potential receptacle is typically great and the nature of the blanketing layer is not conducive to mobilization.				
Medium	This type of profile is characterized by the absence of a substantial protective horizon and has a blanketing layer of materials potentially susceptible to mobilization by extraneous mobilization agents. The groundwater level might be below the blanketing layer. Certain geological settings of shallow, continuous outcropping and sub-outcropping dolomite bedrock, with limited weathering and fissure development, might be characterized by favorable inherent hazard conditions.				
High	The blanketing layer reflects a great susceptibility to mobilization. A void might be present and is interpreted to be very likely, within the potential development space, indicating that the process of sinkhole formation might have already started. Boreholes might register large cavities, sample loss, air loss, etc. Convincing evidence exists of cavernous subsurface conditions, which might act as receptacles. The groundwater level might be below or within the blanketing layer. In a de-watering scenario, the lowering of a shallow groundwater level might not only generate sinkholes or subsidences due to dissipation of pore pressure and increase in effective stress in the then exposed soils, but also exposes a deeper profile to the action of ingress water.				

Examples of final characterisation:

- 1: Area is characterised as reflecting a low inherent susceptibility for the formation of all sized features
- 2: Area is characterised as reflecting a medium inherent susceptibility for the formation of up to large-sized features
- 3: Area is characterised as reflecting a high inherent susceptibility for the formation of up to very large-sized features

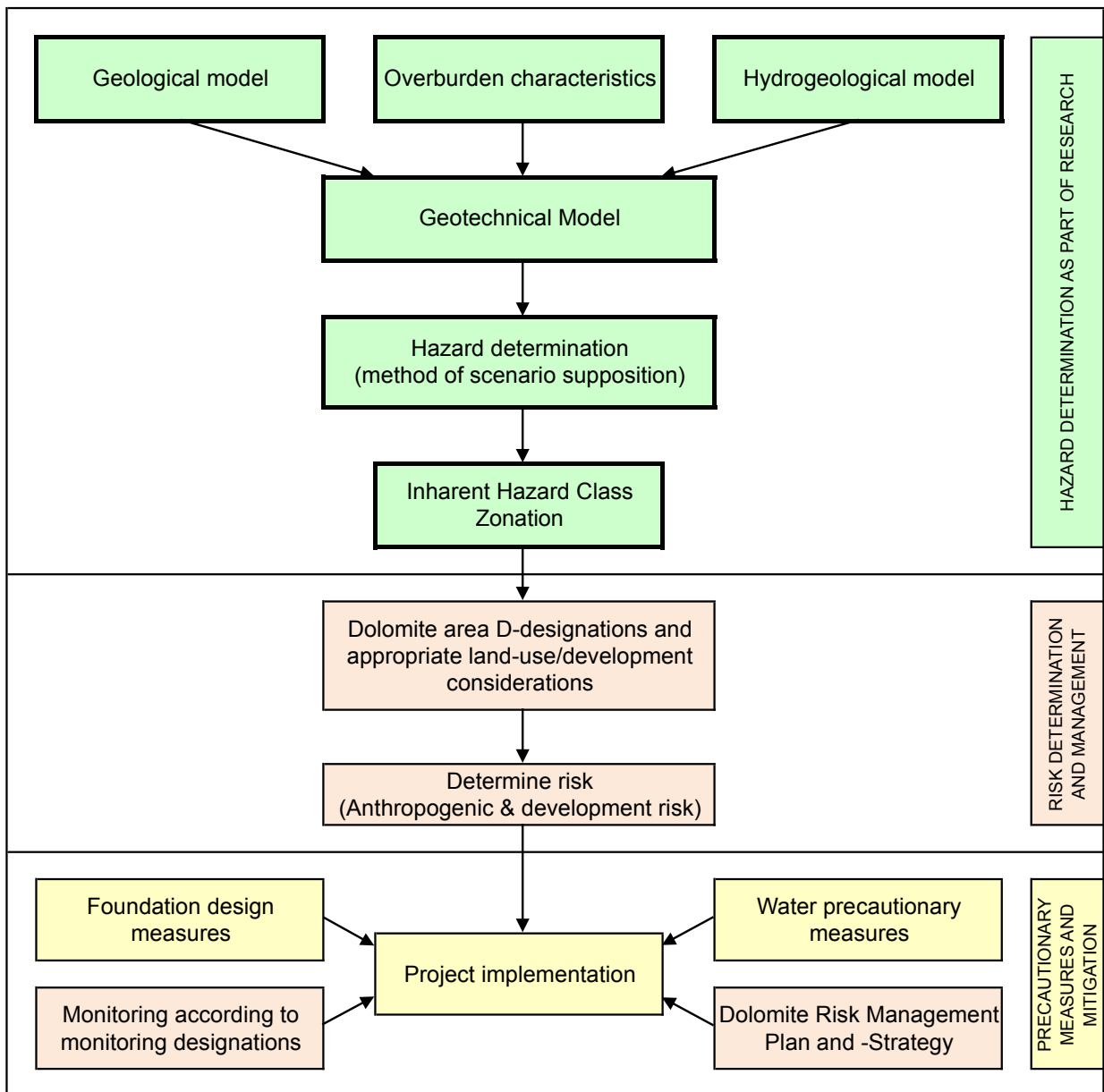


Figure 2-8: Geotechnical model and Inherent Hazard Class determination (after SANS 1936 Part 2, 2012)

2.7.4 The geotechnical model

The geotechnical model forms the geo-scientific basis for the determining and zonation of the inherent susceptibility of a specific area with respect to the formation of sinkholes and subsidences. As described by SANS 1936 (2012), the geotechnical model comprises the following components, including: the geological model, the overburden model, and the hydrogeological model (Figure 2-8). These are henceforth discussed based on this current best-practise industry standard:

2.7.4.1 Geological model

SANS defines the geological model required for a dolomitic terrain as a three dimensional representation of the lithostratigraphic materials that occurs in, and in close proximity, of the project area that is considered for development. This model is based on the acquisition of all geological information – both from existing sources as well as more detailed on-site investigations – that is represented in the form of a geological map with representative cross sections to illustrate the regional structure of the area. The minimum requirements needed to compile the geological model of a project area that is investigated include:

- (i) Site geology, geological setting, and dynamics.
- (ii) Terrain geomorphology.
- (iii) Bedrock lithologies and karst features.
- (iv) Occurrence of intrusions (e.g.: dykes and sills).
- (v) Presence and occurrence of existing (or historic) karst features, including: sinkholes, subsidences, shallow holes etc.).
- (vi) Presence and extent of voids in the overburden and bedrock.
- (vii) Overburden thickness and composition.
- (viii) Weathering and weathering products.
- (ix) Site drainage.

It should be noted that no specific reference is made to the occurrence of prominent geological structures (e.g.: faults, fault zones, jointing in the bedrock, joint orientations, and shear zones) that is known to be closely associated with the occurrence of sinkholes (Calitz, 2015; Swart, 1991). This was pointed out by Bosch (2007), who emphasized the need for geotechnical practitioners in South Africa to take the regional geological setting much more into account when conducting site-specific assessments of dolomite land.

2.7.4.2 Overburden model

The overburden model of a project area is closely associated with the geological model of a site. This includes a detailed discussion of the geo-mecahnical properties of the overburden (generally soil- and pedogenetic material) overlying the bedrock in the area. The overburden

covering the dolomitic bedrock of an area is one of the primary parameters that needs to be well established in order to accurately determine the inherent susceptibility of material to be mobilised. This will also impact on the subsequent IHC of the area. As such, the geotechnical properties of such materials will contribute in deciding on the material's erodability, permeability and the effect of saturation on the material, and the angle of repose. SANS 1936 Part 2 (SANS, 2012) states the following geotechnical properties of the overburden to be essential in determining the above-mentioned:

- (i) Grading analysis and Atterberg Limits of disturbed soil samples collected during fieldwork.
- (ii) Shear strength parameters of the material occurring on site with specific reference to cohesion.
- (iii) Consolidation characteristics of material.
- (iv) Erodability and dispersion potential (both physical and chemical).
- (v) Permeability of various materials, by means of *in situ* testing or laboratory testing.
- (vi) Mineralogical composition of the materials occurring on site. This could provide some indication on ferroan soils, wad, and indications on possible origins of transported materials.
- (vii) The micro-structure of the overburden can be determined by means detailed profiling of profiles exposed by means of test pit excavations of the drilling or auger holes.

Recognition is given to the highly variable nature of overburden across dolomitic terrains. This could warrant recommending a combination of geotechnical testing methods in order to attempt to determine the lateral and vertical distribution of such materials.

2.7.4.3 Hydrogeological model

As with the overburden model, the hydrogeological model is also closely associated with the geological setting. This component of the geotechnical model includes the hydrogeological properties of the various materials occurring in the vicinity of the project area. SANS 1936 Part 2 (SANS, 2012) makes reference to the following primary considerations in the hydrogeological model:

- (i) Current and historic depth to groundwater in the region.

- (ii) The position of the groundwater level (both static or perched) in relation to the unweathered bedrock.
- (iii) Time-series information and groundwater fluctuations over time in order to determine the probability of dewatering of the dolomite aquifer.
- (iv) Groundwater abstraction and recharge in the area.

SANS 1936 Part 2 (SANS, 2012) does not make any specific mention of current registered groundwater use in the area, or the groundwater quality of the area. It is argued that available water chemistry information could also provide valuable information to the regional groundwater regime of an area. This information can be freely obtained from the National Groundwater Archive (NGA), or determined on a regional scale by means of selected groundwater sampling and testing (including isotope studies). Additionally, the current groundwater usage in the area must be closely considered, seeing as this could indicate any “red flags” to the potential for dewatering of non-dewatered dolomite aquifers, even on a regional scale, which can have an impact on development.

CHAPTER 3 – Geological and structural aspects

3.1 Regional geological setting

According to Van Schalkwyk (1981), up to 98% of carbonate rocks in South Africa are associated with the Transvaal Supergroup. These are preserved in two structural basins, namely the Transvaal Basin in the north-eastern sector of the country, and the Griqualand West Basin in the central parts (Figure 3-1, Eriksson & Reczko, 1995; Eriksson *et al.*, 2001). As discussed by (Eriksson *et al.*, in Johnson *et al.*, 2006) and by Eriksson and Reczko (1995), the carbonate platform of the Transvaal Supergroup associated with the Transvaal Basin represents five primary lithostratigraphic subdivisions. These include protobasinal rocks representing the oldest rocks associated with the Transvaal Supergroup, namely the sedimentary Black Reef Formation, the Chuniespoort Group carbonate platform unit and banded ironstone formations (BIF) towards the upper portions. Overlying the carbonate platform of the Transvaal basin is the Pretoria Group volcano-sedimentary unit, and the Rooiberg Felsite Group, situated in the upper parts of the Transvaal Supergroup. According to Beukes (1987) and Altermann & Wotherspoon (1995), the Transvaal Supergroup contains what is considered one of the world's earliest carbonate platforms, which is dated *circa* (c.) 2 714 to 2 050 Ma, representing a geological timeframe of approximately 640 Ma (i.e. Neo-Archaeon to Paleoproterozoic). Obbes (2000) argued that the carbonate sequence must have been deposited between c. 2 643 and 2 520 Ma, which represents a geological timeframe of approximately 120 Ma. The study area is located along the south-western rim of the Transvaal Basin.

The Transvaal Supergroup is directly underlain by the Ventersdorp Supergroup in the study area, which is predominantly composed of igneous and sedimentary rocks derived from the Ventersdorp-age volcanism (c. 2 714 to 2 709 Ma; Eriksson *et al.*, in Johnson *et al.*, 2006). Outcrops of the Witwatersrand Supergroup (c. 3 074 to 2 714 Ma; Eriksson *et al.*, in Johnson *et al.*, 2006) occur on a more regional scale towards the western parts of the study area. The Witwatersrand Supergroup represents a tectonic-sedimentary sequence, and is the primary host for gold, silver and uranium (Brink, 1979). Isolated exposed outcrops of the basement rocks that are associated with the pre-Dominium-age granitic crust forms outcrops towards the north and west of the study area. These outcrops are closely associated with tectonic events such as upliftment and faulting (Brink *et al.*, 1999). Sedimentary units of the Pretoria Group and Karoo Supergroup unconformably overlie the Transvaal Supergroup dolomite.

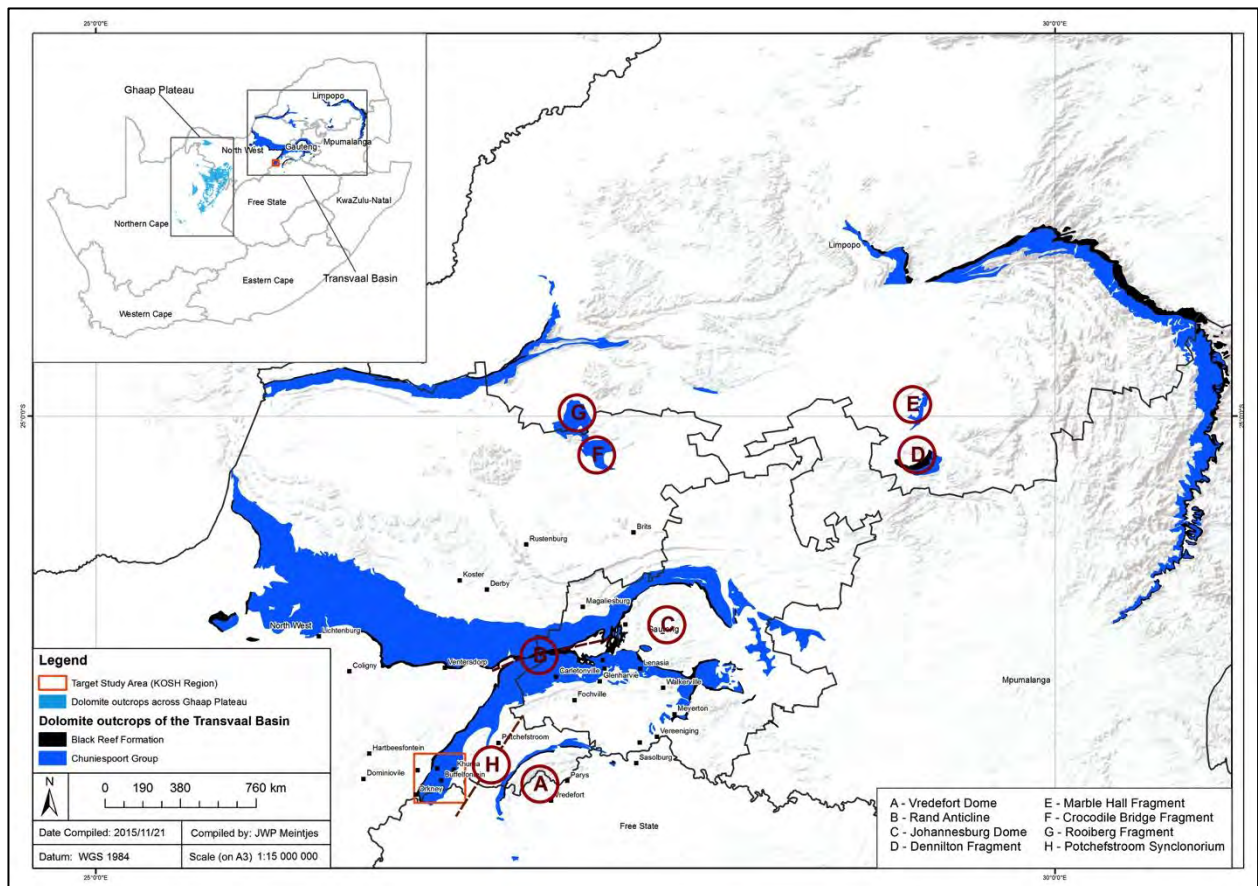


Figure 3-1: Distribution of the Transvaal Supergroup across the Transvaal Structural Basin (after Eriksson and Reczko, 1995)

3.2 Origin and deposition of dolomite and chert

3.2.1 Origin of dolomite and chert

Buttrick (1986) made reference to problems regarding the origin of dolomite, because the predominant mineralogical constituents of dolomite does not directly originate from shell material excreted by organisms. The direct precipitation of dolomite from solution seems unreasonable, due to the thickness of the succession in the South African geological profile.

A number of researchers (Button, 1973; Beukes, 1978; Clendenin, 1989) are like-minded that dolomite of the Malmani Subgroup is related to the deposition and subsequent dolomitization of primary limestone. This depositional model is referred to as the Dorag – or mixing zone – model. Limestone, a calcium carbonate (e.g.: CaCO_3), originated from ormicrite and calcite cement derived from the accumulation of the shells from marine-dwelling creatures associated with warm, shallow water (Beukes, 1987). After the deposition of primary limestone an environment was formed in which dolomitization can occur whereby saline water mixed with meteoric water (Eriksson and Warren, 1983). This left a fluid mixture that was under-saturated

with calcite and supersaturated with silica and magnesium, allowing for favourable conditions for dolomitization and chertification (Eriksson *et al.*, 1975; Eriksson and Warren, 1983). Eriksson and Warren (1983) and Beukes (1978) concluded that the deposition of dolomite and chert are closely related. Limestone is therefore regarded as being the first precipitation (or depositional) product, where after dolomite formation (via the process of dolomitization) and secondary replacement of chert (e.g.: chertification) followed.

Eriksson *et al.* (1975) discussed the depositional model of chert and indicated that the occurrence of chert is associated with oolites and domical stromatolites in the dolomite, which can be traced back to a cyclical distribution across the Chuniespoort Group. He ascribed the origin of chert to be secondary, where the depositional environment is closely associated with the identified cyclical distributions. Favourable conditions for chertification to occur were controlled by the pH of the solution and saturation with respect to silica. As such, in order for chertification – and the subsequent dissolution of silica – to occur, high temperature alkaline water is required. The exact period of certification of the chert-containing succession of the Chuniespoort Group is uncertain, and could either be associated with a penecontemporaneous diagenetic- or post-consolidational replacement of carbonate by chert (Eriksson *et al.*, 1975). Eriksson *et al.* (1975) argues that the infiltration of a siliceous solution through the thick carbonate succession seems improbable, when related to his observation, which favours a penecontemporaneous diagenetic origin of chert.

3.2.2 Depositional model

After the Ventersdorp volcano-sedimentary event, a major period of erosion occurred, which resulted in the formation of the north-east/ south-west orientated Transvaal Basin (Eriksson *et al.*, in Johnson *et al.*, 2006). Subsequently, the depositional surface of the Transvaal Supergroup is largely controlled by the prevailing Ventersdorp Supergroup topography (or the pre-Transvaal Paleosurface) at the time of initial deposition (Coetzee, 1996). The Transvaal basin became filled with water that was super-saturated in bicarbonate and silica derived for the weathering of the basement complex in the region (Brink, 1979). This led to the deposition of the Transvaal Supergroup sediments across the approximately 500 km² epeiric sea (Button, 1973).

The depositional onset of the Transvaal Supergroup is associated with the Black Reef Formation. The Black Reef Formation is characterised as a fluvial and shallow marine depositional environment (Button, 1973). This was followed by the deposition of primary limestone across the basin. Walraven and Martini (1995) estimate the onset of limestone deposition across the Transvaal Basin at c. 2 550 ±3 Ma, which is initially deposited as

unconsolidated deposits, and became consolidated as diagenesis proceeded. Alteration of primary limestone to dolomite (i.e.: dolomitization) took place shortly after deposition (Eriksson *et al.*, 1975), followed by secondary certification.

Eriksson and Truswell (1974) initially sub-divided the Chuniespoort Group into four Formations based on their proposed three distinctive environments of deposition, which was based on the model proposed by Irwin (1965). These three environments include an intertidal zone, a high-energy agitated regime, and a shallow sub-tidal environment. Eriksson and Truswell's tidal flat paleoenvironmental model was later revised by Clendenin (1989) whom derived sub-divisions based on genetically related successions that are separated by low-angle unconformities. As such, he proposed an inclined ramp depositional environment, rather than a tidal flat.

Clendenin (1989) described the carbonate ramp depositional environment as representing a shallow marine environment that is less than 40 to 80 m deep, in which strata was deposited in a sheet-like manner with approximately uniform thickness. Clendenin (1989) described the depositional model based on the various facies that were observed, which is illustrated in Figure 3-2 and summarised as follows:

- (i) Shallow siliclastic fluvial facies marking the deposition of the Black Reef Formation across the Transvaal Basin.
- (ii) Submerged shelf sub-facies associated with a periplatform shelf, marking the deposition of the Oaktree Formation.
- (iii) Shoaled flats sub-facies associated with a periplatform shelf, marking the deposition of the lower Monte Christo Formation.
- (iv) Disrupting of carbonate sedimentation that resulted in a sub-regional unconformity after the deposition of the Lower Monte Christo Formation, marking the Middle Monte Christo Formation.
- (v) North-north-eastward transgression resulted in rapid deepening of the marine environment which re-introduced carbonate sedimentation, marking the depositional onset of the upper Monte Christo Formation as a shoaled flats sub facies associated with a periplatform shelf.
- (vi) After the deposition of the Monte Christo Formation, the Lyttleton-Eccles depositional system commenced. The onset is marked by a period where no deposition occurred between the upper Monte Christo Formation and the Lyttleton Formation, resulting in a

sub-regional unconformity. The deposition of the basal parts of the Lyttleton Formation is associated with a shoaled flats sub-facies associated with a periplatform shelf.

- (vii) The upper parts of the Lyttleton Formation and the Eccles Formation are associated with a submerged shelf.
- (viii) After the deposition of the Eccles Formation, the marine facies retreated into the Northern Cape. Resulting in a second sub-regional unconformity.
- (ix) After the retreat of the marine facies, the Frisco-Penge depositional system commenced.
- (x) The deposition of the Chuniespoort Carbonate platform ceased after rapid regression, which resulted in a third sub-regional unconformity.

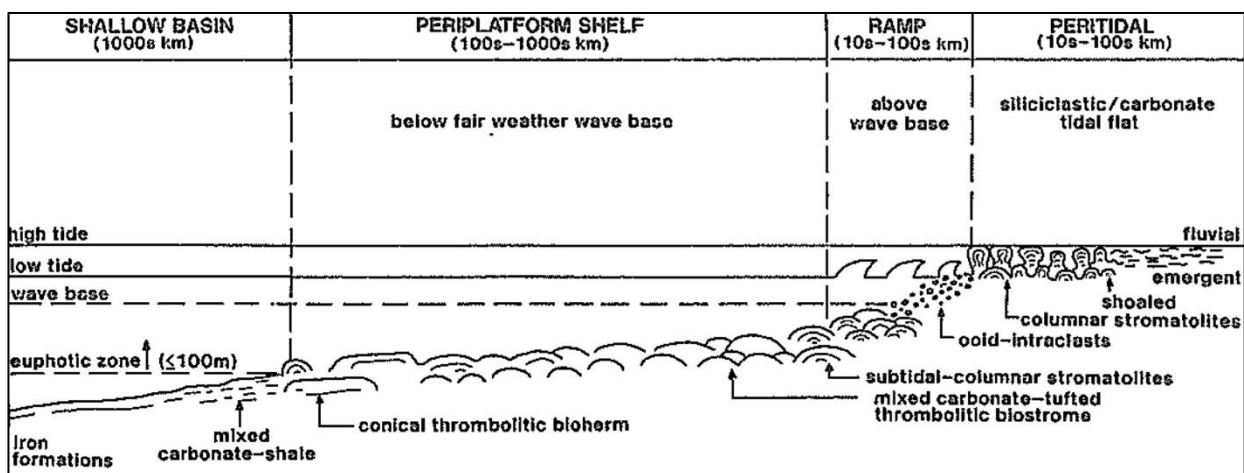


Figure 3-2: Carbonate ramp depositional model (from Clendenin, 1989 in Eriksson *et al*, 1993)

3.3 Local geological setting

3.3.1 Stratigraphy

According to the published 1:250 000 scale geological maps (2626 West Rand and 2726 Kroonstad), the study area is underlain by a wide array of geological Formations (Figure 3-3). These published regional geological maps represents the culmination of a number of authors' work, and are most often the only geological information that is considered by the industry when conducting dolomite assessments of an area. No published 1:125 000 or 1:50 000 scale geological maps exist for the area. The contacts of the different lithostratigraphic sub-divisions of the Malmani Subgroup have not been differentiated in the KOSH-area. The regional stratigraphy is indicated in Table 3-1, and the prominent lithostratigraphic successions across the project area (marked with an asterisk) are henceforth briefly discussed or referred to.

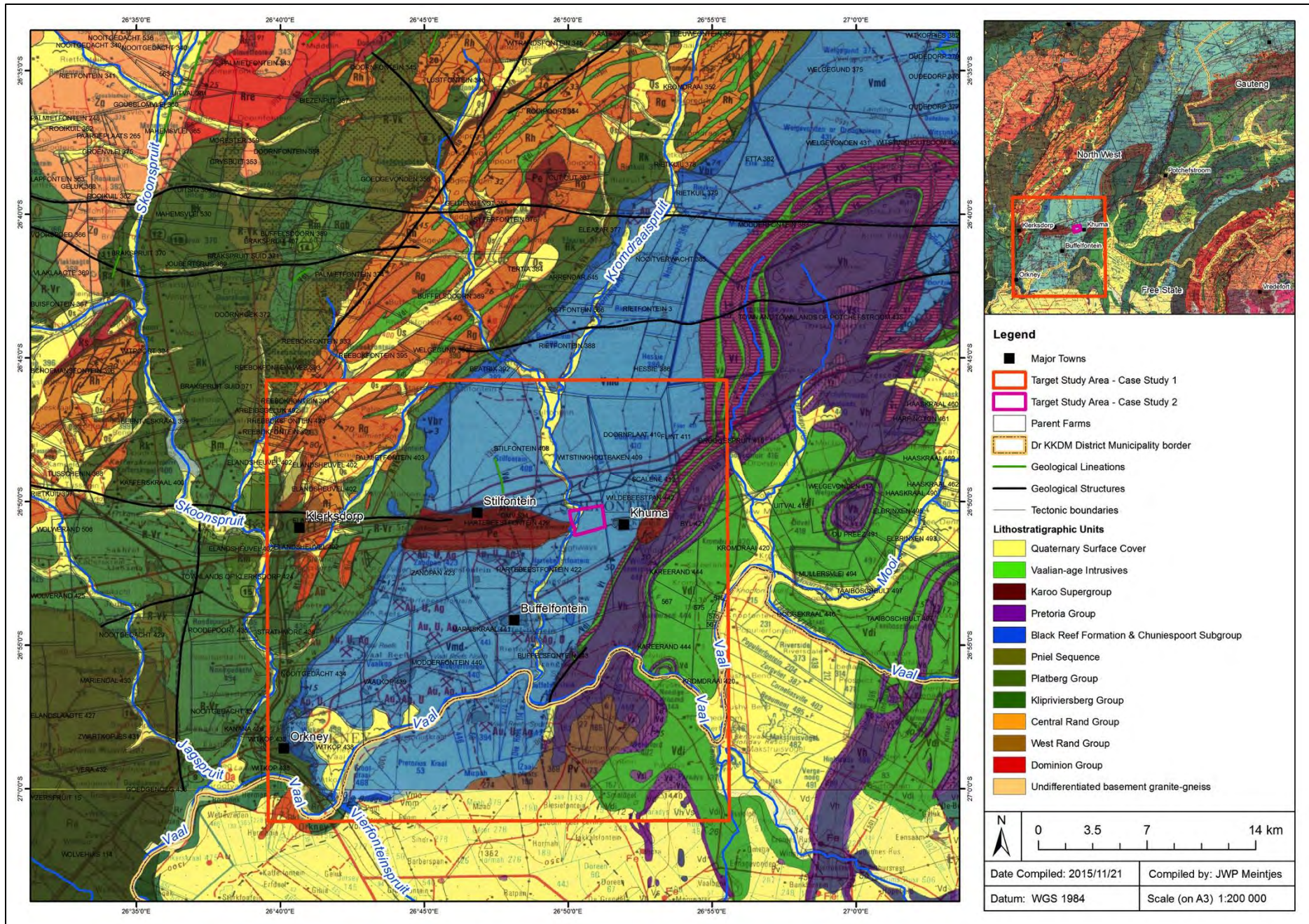


Figure 3-3: Regional geological setting (after Wilkinson, 1986)

Table 3-1: Lithostratigraphic units occurring in and around the project area (Eriksson et al., in Johnson et al., 2006; Antrobus et al., 1986)

Super-group	Group	Formation	Dominant rock type	Stratigraphic thickness in area (m)	Marker beds		
Karoo	Ecca	Volksrust*	Grey to black silty shale, thin siltstone and sandstone lenses and beds	Varying (few meters to ±190)			
		Vryheid*	Mudstone, siltstone and fine- to coarse-grained sandstone (pebbly in places)				
	Dwyka	Dwyka*	Diamictite and tillite	< few meters			
	Unconformity						
Transvaal	Pretoria Group	Magaliesberg	Sandstone, mudstone lenses	150 to 430			
		Silverton	Carbonate rocks Shale and various volcanic members	500 to 1 328	Upper carbonates		
		Daspoort	Sandstone, mudstone	65 to 120			
		Strubenkop	Mudstone, subordinate sandstone	50 to 360			
		Dwaalheuwel	Sandstone, conglomerate, subordinate mudstone	15 to 70			
		Hekpoort	Basaltic andesite, pyroclastic rocks	190 to 890			
		Boshoek	Sandstone, conglomerate, diamictite	35 to 70	Significant conglomerate		
		Timeball Hill*	Ferruginous shale, hornfels and ferruginous quartzite Interlayered diabase	17 to 232	Basal conglomerate		
		Rooihoogte*	<u>Pologrounds</u> Sandstone, mudstone, shale, siltstone (interbedded)	2 to 30 6 to 30			
	<u>Bevets</u> Ferruginous chert conglomerate Shale and siltstone		0.5 to 4 11.5 to 30				
	Unconformity (paleokarst topography)						
	Chuniespoort Group	Penge, Duitschland*		Limestone and dolomite, carbonaceous mudstone with subordinate diamictite, conglomerate and lava	Up to 700		
							Frisco*
		Sub-regional facies unconformity					
		Eccles*		Chert-rich light grey dolomite Giant Chert breccia in upper parts	477 (5 to 10)	120 m thick oolitic dolomite at base	
Lyttleton*							Chert-poor dark grey stromatolitic dolomite, minor shale and quartzite
		Sub-regional facies unconformity between <i>Lower-</i> and <i>Middle</i> Monte Christo, and after <i>Upper</i> Monte-Christo					

Table 3-1 continued

Super-group	Group	Formation	Dominant rock type	Stratigraphic thickness in area (m)	Marker beds	
		Monte Christo*	Chert-rich grey-brown dolomite Chert-rich and colour-banded dolomite Chert-rich light grey dolomite Chert-free light grey dolomite (stromatolitic and oolitic dolomite)	300 to 500	Black carbonaceous shale markers near base	
		Oaktree*	Chert-free dark brown stromatolitic dolomite, quartzite, carbonaceous shale	10 to 200	Pyrite stringers near base	
		Black Reef*	Quartzite, conglomerate, shale, minor dolomite (all interbedded)	11 to 31	-	
	Unconformity					
Ventersdorp	Pniel Sequence	Allanridge*	Crystalline lavas	Up to 275	-	
		Bothaville*	Conglomerate, quartzite, shale	40	-	
	<i>Pniel</i> unconformity					
	Platberg Group	Rietgat	Amygdaloidal lava, agglomerate, tuff	Unknown	-	
		Makwassie	Quartz feldspar-porphry	Unknown	-	
		Goedgenoeg	Crystalline lavas with numerous feldspar and ferromagnesian phenocrysts	300	-	
		Kameeldoorns*	Volcanic conglomerate	185	-	
	Unconformity					
	Klipriviersberg Group	Edenville	Dense to fine-grained lavas	1 000	Dense, mottled, welded tuff	
		Loraine	Fine- to medium-grained lavas, "Altered Zone" marking top	300	"Altered Zone:	
		Jeanette	Not specifically distinguishable	-	High proportions of agglomerate	
		Orkney	Medium-grained, amygdaloidal lavas, with zones of purple-tinted lava	150	Upper Purple Zone Lower Purple Zone	
		Alberton	Medium-grained, amygdaloidal lavas, with clusters of cruciform aggregates of feldspar phenocrysts	300	Upper porphoritic Zone Porphoritic Marker	
		Venterspost*	Quartzite and conglomerate	7	VCR	
	Unconformity					
Witwaters-rand	Central Rand Group*	Shale, quartzite, conglomerate up to 7 500 m thick				
	West Rand Group*					
Unconformity						
Basement crust		Granite and gneiss				

3.3.1.1 Pre-Witwatersrand Supergroup outcrops

Exposures of the pre-Witwatersrand Supergroup-age granitic basement crust outcrops south of Ventersdorp (Wilkinson, 1986) and as an isolated outcrop on the Farm Katdoornbosch 138 (Brink *et al.*, 1999). These exposures are associated with tectonic movement, which uplifted the strata through the much younger geological Formations, where after erosion occurred. Nel (1924) and Brink *et al.* (1999) initially discussed this by observing the granitic crust situated in the Malmani Subgroup dolomites on the Farm Katdoornbosch 138.

3.3.1.2 Witwatersrand Supergroup

Based on regional published geological mapping (2626 West Rand), the Witwatersrand Supergroup outcrops towards the western regions of the KOSH-area. Rock belonging to this Supergroup serves as the primary host of gold, silver and uranium deposits in South Africa, which are mined. The Witwatersrand Supergroup (c. 2700 Ma) represents a tectonic-sedimentary sequence of shale, quartzite, and conglomerate that attains a maximum thickness in the order of 7 500 m. Ferruginous shale and banded ironstone occurs in the Hospital Hill Subgroup, which is situated at the base of the West Rand Group. Large-scale outcrops of conglomerate, quartzite and shale belonging to the West Rand Group occur to the north and west of Klerksdorp. Outcrops from the Central Rand Group (underlying the West Rand Group) outcrop to the east of Klerksdorp.

3.3.1.3 Ventersdorp Supergroup

The Ventersdorp Supergroup is predominantly composed of igneous and sedimentary rocks, with a total thickness of up to 1 800 m. Outcrops of the Ventersdorp Supergroup cover a large area towards the west of the KOSH-area. At the base of the Ventersdorp Supergroup is the Klipriviersberg Group, starting off with the gold-bearing Venterspost Formation (also referred to as the Ventersdorp Contact Reef) that in turn is overlain by several igneous Formations (Eriksson *et al.*, in Johnson *et al.*, 2006).

The Platberg Group is composed of an interlayered succession of clastic sedimentary and igneous rock types, and unconformably overlies the Klipriviersberg Group. The Kameeldoorns Formation, which is composed of clastic sedimentary rocks, forms the basal parts of the Platberg Group and the Bothaville- (composed of conglomerate, quartzite and shale) and the Allanridge Formations (composed of mafic igneous rocks) the upper-most succession (Eriksson *et al.*, in Johnson *et al.*, 2006).

3.3.1.4 Transvaal Supergroup

Overlying the Ventersdorp Supergroup is the Transvaal Supergroup. At the base of the Transvaal Supergroup is the Black Reef Formation, which in turn is overlain by the Chuniespoort- and the Pretoria Groups. The Chuniespoort Group comprises of the primary carbonate platform. The Transvaal Supergroup represents a sequence of rocks with a maximum thickness of up to 15 000 m across the larger Transvaal Basin (Eriksson *et al.*, 2001), but was measured in the Potchefstroom–Fochville area to a total thickness of only 3 900 m (Jansen, 1967). The dolomitic Malmani Subgroup reaches a maximum thickness of up to 2 000 m across the Transvaal Basin (Eriksson *et al.*, in Johnson *et al.*, 2006), but was measured to attain a maximum thickness of only 1 500 m in the south-eastern sector of the KOSH mining area (Antrobus *et al.*, 1986).

3.3.1.4.1 Black Reef Formation

The Black Reef Formation predominantly consists of upwards-fining clastic-sedimentary rocks (i.e. quartzite, conglomerate and shale) and is generally only a few meters thick and seldom exceeds 31 m (Eriksson *et al.*, in Johnson *et al.*, 2006; Venter, 2015). In the Klerksdorp-area, the Black Reef Formation is generally between 6 and 15 m thick (Antrobus *et al.*, 1986). The economically important Black Reef, a gold-bearing reef, is associated with the basal parts of the Black Reef Formation, which has a dark-grey to bluish-grey colour, and consists of siliceous quartzite with thin layers of conglomerates, grits or scattered pebbles, especially at or close to the base (Venter, 2015). Alternating layers of fine- to medium-grained quartzite and carbonaceous shale overlie the Black Reef. The base of the Black Reef Formation is well defined, whilst the upper contact is transitional into the Oaktree Formation, where this contact is usually defined as the base of the first layer of dolomite (Antrobus *et al.*, 1986; Obbes, 2000). According to Wagener (1982) and Brink (1979), and as observed in the KOSH-area, WAD is known to occur in the Black Reef Formation, and must as such be regarded as the first dolomitic formation from a dolomite stability perspective. The Oaktree Formation conformably overlies the Black Reef Formation (Antrobus *et al.*, 1986; Obbes, 2000).

3.3.1.4.2 Oaktree Formation

Martini *et al.*, (2006) and Eriksson *et al.*, (2001) describe the Oaktree Formation as a transitional succession consisting of siliclastic sediments (localised developed quartzite, carbonaceous shale and shale marker beds) to platform carbonates (chert-free dark chocolate-brown stromatolitic dolomite with localised pyrite stringers near the basal regions). The Formation has a stratigraphic thickness of between 10 and 200 m (Eriksson *et al.*, in Johnson *et al.* 2006).

The Oaktree Formation is associated with Mn concentrations in excess of 1 % as determined by Roux (1984), which are regarded as high concentration. The weathering product of this Formation is generally WAD-rich dolomite residuum. Day (1981) stated that the overall consistency of the WAD occurring at the basal parts of the Oaktree Formation is “*surprisingly stiff*”. This could be associated with accumulation and later consolidation of WAD in the basal parts.

The Monte Christo Formation conformably overlies the Oaktree Formation. Obbes (2000) described the contact between the Oaktree- and Monte-Christo Formations as gradational. This contact is generally taken at the area of increased chert content and a where change in colour from dark brown dolomite to light grey dolomite occur.

3.3.1.4.3 Monte Christo Formation

Chert-rich light grey dolomite from the Monte-Christo Formation represents the deposition of carbonates from bicarbonate and silica rich water through chemical and organic (algal) precipitation. This is recognised by the presence of stromatolitic structures within the dolomite as seen in the study area. Eriksson *et al.* (2001) describes the Monte Christo Formation as an oolitic and stromatolitic platform in the basal parts that grades into an erosive breccia towards the upper parts of the succession. The Monte Christo Formation contains various sedimentary structures, such as ripple marks, climbing ripple marks, interference ripple marks and oolites (Button, 1972), and has a stratigraphic thickness of between 300 and 500 m (Eriksson *et al. in* Johnson *et al.*, 2006). Button (1972) states that the thickness of the various chert layers throughout the Monte Christo Formation varies from thin laminae up to 2 m.

According to Eriksson and Truswell (1974) and Obbes (2000), and described in the study area by Fletcher (2006), the Monte Christo Formation can be divided into four zones (unofficially as this is not recognised by SACS), based on the occurrence of stromatolites, chert-in-shale breccia, and chertified stromatolites, which include the Rietfontein Member at the base, followed by the Mooiplaats- and Rietspruit Members, and the Crocodile Bridge Member in the upper parts. Fletcher (2006) also described four zones occurring throughout the Monte Christo Formation in the regions of the West Rand. This was presented in an in-house unpublished report from AngloGold Ashanti (Venter, 2015), and includes the “*Lower Monte Christo*”, the “*Middle Monte Christo*”, the “*Recrystallized Zone*” and the “*Upper Monte Christo*”:

- The “*Lower Monte Christo Formation*” represents intertidal sediments associated with closely-spaced oolitic horizons across the succession. The basal portions are characterised

by a number of black carbonaceous shale marker beds. This succession is approximately 160 m thick.

- The “*Middle Monte Christo Formation*” is characterised by pale grey (often stromatolitic) dolomite with intercalated intertidal sediments and chert. The basal parts is characterised by a very dark grey stromatolitic marker bed. This succession is approximately 250 m thick.
- The succession between the “*Middle Monte Christo Formation*” and the “*Upper Monte Christo Formation*” is characterised by an approximately 75 m thick re-crystallised zone. Despite some form of re-crystallisation observable throughout the Monte Christo Formation, this zone is distinguishable by intense re-crystallisation. The remainder of this succession is similar to the “*Upper Monte Christo Formation*”.
- The “*Upper Monte Christo Formation*” is characterised by pale grey (often stromatolitic) chert-rich dolomite. This succession is approximately 220 m thick.

The Lyttleton Formation conformably overlies the Monte Christo Formation.

3.3.1.4.4 Lyttleton Formation

The Lyttleton Formation is characterised by shale, quartzite and dark grey chert-poor stromatolitic dolomite (Eriksson *et al.*, 2001). Localised discontinuous thin chert lenses occur in this Formation. Weathering of the Lyttleton Formation is characterised by a subdued topography and dark chocolate-brown colour, ascribed to the increased wad content. Roux (1984) determine the wad content of the Lyttleton Formation is higher than the chert-rich Formations, and contains up to 1.5 wt.% Fe and Mn. The Lyttleton Formation has a stratigraphic thickness of between 100 and 200 m (Eriksson *et al.*, 2001).

The Eccles Formation conformably overlies the Lyttleton Formation.

3.3.1.4.5 Eccles Formation

The Eccles Formation consists of cherty dolomite with a light grey colour and is characterised by sedimentary stratification. This stratification is often characterized as horizontal to wavy laminated, rippled and cross-stratified layers. The occurrences of chert bands, lenses and breccia of varying thicknesses (millimeters up to meters) and densities, are furthermore characteristic of the Eccles Formation. Due to intense heat that remobilised the fluids, the upper parts includes a series of erosion breccia that may be gold bearing in areas where it was affected by the Bushveld Igneous Complex (Eriksson *et al.*, 2001). The Eccles Formation is 600

m thick and a few narrow oolitic horizons are present approximately 120 metres above the base of the Eccles Formation (Eriksson *et al.*, 2001).

The Frisco Formation overlies the Eccles Formation, and is separated by an erosional breccia (termed the Giant Chert Breccia by De Kock (1964) and the Leeuwenkloof Member by Obbes (2000)). However, the Giant Chert Breccia – also referred to as the Leeuwenkloof Member – is not regarded as a stratigraphic succession, but represents a tectonic connotation within the upper-most regions of the Eccles Formation.

3.3.1.4.6 Frisco-, Penge- and Duitschland Formations

The Frisco Formation is characterised by a succession composed predominantly of dark grey stromatolitic dolomite that weathers to dark brown sandy silt in the basal parts and shale towards the upper parts. Chert occurs throughout the succession as poorly developed bands and lenses. The Frisco Formation has a stratigraphic thickness of up to 400 m. (Eriksson *et al.*, 2001).

The Penge- and Duitschland Formations has a combined stratigraphic thickness of up to 700 m, and consists of limestone, dolomite, banded ironstone and carbonaceous mudstone with subordinate occurrences of diamictite, conglomerate and lava (Eriksson *et al.*, 2001).

The Frisco-, Penge- and Duitschland Formations only occur in certain geographic areas of the Transvaal basin. Its absence is often ascribed to loss of ground due to thrust faulting, the specific depositional environment in across the Transvaal Basin, and erosion prior to the deposition of the Pretoria Group.

3.3.1.5 The Pretoria Group

Regionally the Chuniespoort Group is unconformably overlain by Pretoria Group rocks, which can reach a thickness of up to 1 535 m across the regional area (SACS, 1980). The Pretoria Group predominantly consists of clastic sedimentary rocks (i.e.: siltstone, mudstone and quartzitic sandstone) that are significantly interbedded with basaltic-andesitic lava, conglomerate, diamictite and subordinate carbonate rocks (Eriksson *et al.*, in Johnson *et al.*, 2006).

The Rooihogte Formation marks the base of the Pretoria Group, and is the first succession after the prominent carbonate platform. The Rooihogte Formation is composed of clastic sedimentary rocks and chert breccia, which overlies the Malmani Subgroup Paleosurface (Eriksson *et al.*, in Johnson *et al.*, 2006). The base of the Rooihogte Formation is classified as

the Bevet's Member, which is often composed of a reworked chert conglomerate. The upper parts of the Rooihogte formation is characterised as mudstone and sandstone. This succession has a stratigraphic thickness of between 10 and 150 m. (Eriksson *et al.*, in Johnson *et al.*, 2006)

The Rooihogte Formation is overlain by the Timeball Hill Formation that is characterised by a sedimentary succession of ferruginous shale and ferruginous quartzite with local interbedded layers of sedimentary rocks, as well as hornfels – ascribed to local metamorphism of fine-grained clastic sedimentary rocks. The Timeball Hill Formation attains a thickness of between 17 and 232 m in the KOSH area. Three prominent diabase sills have intruded the Timeball Hill Formation throughout the succession. These sills are ascribed to Bushveld-age. The Timeball Hill Formation is overlain by a succession of various sedimentary and volcanic Formations (i.e.: Boshok-, Hekpoort-, Dwaalheuwel-, and Strubenkop etc. Formations). (Eriksson *et al.*, in Johnson *et al.*, 2006)

3.3.1.6 Karoo Supergroup

The Karoo Supergroup in the study area is subdivided into the Dwyka- and Eccca Groups, and most commonly occurs as erosional remnants of paleo valley-fill deposits in the study area, which are situated within the Malmani Subgroup, described as inliers.

The Dwyka Group (Dwyka Formation) – where preserved – is generally less than a few meters thick, and represents a glacial deposit that comprises of diamictite and tillite. The Eccca Group overlies the Dwyka Group.

The Eccca Group comprise of a total of 16 Formations across the entire Karoo sedimentary basin, of which only two are preserved in the vicinity of the project area, namely the Vryheid and Volksrust Formations. The Vryheid Formation comprises of mudstone, siltstone and fine- to coarse-grained sandstone (pebbly in places). The occurrence of upward-fining fluvial cycles is typically sheet-like in geometry and commonly form valley-fill deposits (Eriksson *et al.*, in Johnson, et al., 2006). The Volksrust Formation is predominantly argillaceous and is composed of grey to black silty shale with thin siltstone and sandstone lenses and beds.

3.3.1.7 Intrusives

A number of dyke and sill intrusions with varying age relations are common in the investigation area and varies in age from post-Klipriviersberg (Ventersdorp Supergroup-age) to post Karoo Supergroup-age. Six types of intrusives were recognized in the area by Antrobus *et al* (1986) and are briefly summarised:

3.3.1.7.1 Quartz-diabase dykes and sills

These intrusives are of Post-Klipriviersberg (Ventersdorp Supergroup) / Pre-Transvaal-age and are the most commonly encountered intrusive across the area. Evidence exist that these intrusives were affected by faulting. The quartz-diabase intrusives are composed of grey-green fine-grained aphanitic rocks, which are entirely altered, and generally strike north-west with a dip towards the east at steep angles.

3.3.1.7.2 Ilmenite diabase dykes and sills

These dykes and sills are of the Post-Ventersdorp / Pre-Karoo-age. In hand specimen the rocks are dark green, fine grained and fresh looking with leucoxene speckling visible to the naked eye. The dykes are variable in strike and dip and are not significantly affected by faulting. The ilmenite diabase dykes are thicker than other dykes occurring in the area, with thicknesses ranging from 5 to 75 m.

3.3.1.7.3 Carbonatite dykes and sills

Carbonatite dykes and sills in the area are of the Post-Transvaal / Pre-Karoo-age. In hand specimen the rock has a breccia appearance, ascribed to the variety of xenolithic inclusions set in a greyish-brown, carbonate matrix. These dykes strike north-south and dip at approximately 60° to the east.

3.3.1.7.4 Post-Karoo-age dykes

Two prominent Post-Karoo age dykes are recognised in the area:

- Olivine lamprophyre dykes that are dark-grey in colour with numerous black olivine phenocrysts (up to 1cm long). Dykes are usually thin (1 – 2m), strike north-south, and are highly altered.
- Pilanesberg-age dolerite dykes have similar strikes as the olivine lamprophyre dykes, but often strike east-west in the Stilfontein area. Karoo-age dolerite dykes are coarse, grey-green in hand specimens and distinctly magnetic.

3.3.2 Structure

Authors such as Winters (1987), Brink *et al* (1999), Brink *et al* (2000), Brink (1996), Brink *et al* (2005), Wieland (2006), and Antrobus *et al* (1986) extensively researched the regional structural geological setting of the greater Far West Rand area. The work presented by these authors include the culmination of geological interpretations to better understand the deformation

caused by the Vredefort impact structure and pre-Vredefort deformation of the Witwatersrand- and Ventersdorp Supergroups, to determine the extent of gold-bearing ore-bodies in the region. Although the various geological structures related to deformation have a significant impact on the modelling and mining practices of the underlying ore bodies that generally occur depths well in excess of 100 m, the sphere of influence of these structures play an immensely important role on surface and near-surface development from a geotechnical perspective, especially across dolomite land. A regional overview of the geological structure across the Witwatersrand sedimentary basin (from north of Klerksdorp towards Parys in the south-east) is indicated in Figure 3-4 as extracted from the work conducted by Wieland (2006).

Antrobus *et al* (1986) and Brink (1996) described the major stages of deformation of the strata in the greater KOSH-area, and the following section on the structure of the region is largely based on the work conducted by these authors. Winters (1987) termed three regionally prominent orogenic periods, namely the (i) Witwatersrand basining (termed the Sotho orogeny), the (ii) Post-Makwassie Formation – Pre-Rietgat Formation deposition (termed the Ndebele orogeny), and the (iii) Post-Transvaal-age deformation and deposition (termed the Tswana orogeny). The unconformable surface of the underlying Ventersdorp Supergroup on which the Black Reef Formation has been deposited, determined the structure of the base of the Transvaal Supergroup to a large extent. As such, only brief attention is given to the structure of the Witwatersrand- and Ventersdorp Supergroup, with more focussed attention given to the Transvaal-age and Post-Transvaal-age deformation of the area.

3.3.2.1 Pre-Transvaal-age structure

The regional Pre-Transvaal-age structure across the KOSH-area (Figure 3-3) is characterised as a basin-shaped body, forming part of the Witwatersrand sedimentary basin, and is associated with horst-and-graben structures across the area. The basin-shaped body is disrupted towards the northeast of the area by means of block faulting, whereas the northern half is characterised as a graben between the so-called Kromdraai- and Buffelsdoorn Faults. The central parts of the area is characterised by a horst-and-graben-structure. In the upper-central regions, a horst is distinguishable that is structurally bound between the Kromdraai Fault and the Fakawi-/Eastern Shaft Faults. Towards the lower-central parts, a graben is structurally bound between the Fakawi-/Eastern Shaft Faults and the BU4-/Through Faults. The southern-most parts of the basin-shaped body are structurally defined as a horst between the BU4-/Through Faults and the Jersey Fault. A number of the mentioned faults represent Pre-Transvaal time periods, and as such not considered of significant importance from a

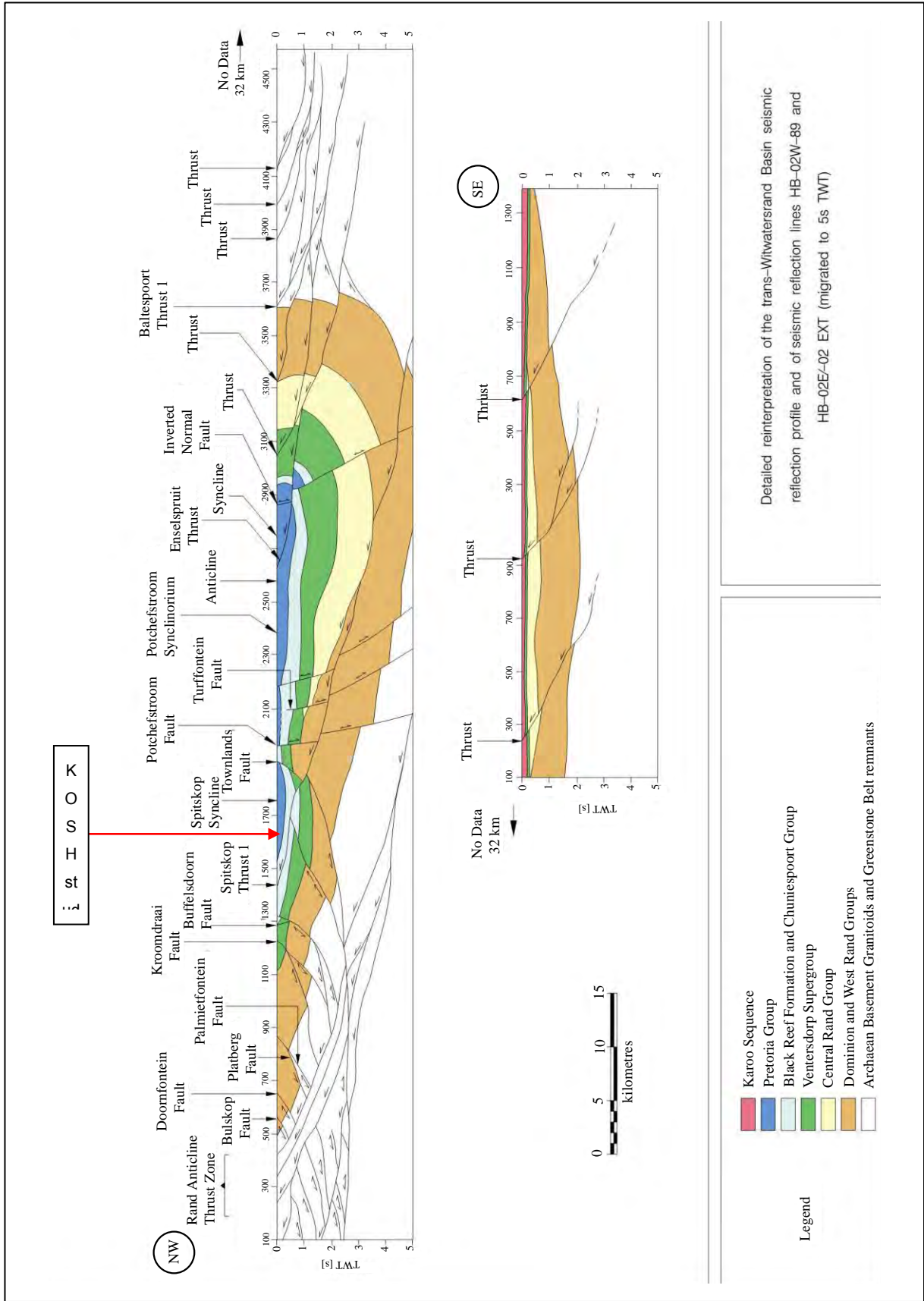


Figure 3-4: Regional geological structure across the Witwatersrand sedimentary basin (from Wieland, 2006)

Transvaal-age (or dolomite) perspective. However, the lateral extent of some major Ventersdorp-age faults impacted on the Transvaal Supergroup, where these faults were re-activated during later stages of crustal deformation and tectonic events of the region. Antrobus *et al* (1986) describes various smaller normal faults in the area, but states that these faults are generally small in throw and deemed insignificant from a regional structural and mining-perspective. It could be argued that these smaller faults (or other Post-Transvaal-age faults) where re-activated to intersect the Transvaal Supergroup at a sufficiently shallow depth, could have a significant contribution to dolomite instability at surface.

Deformation of the Ventersdorp Supergroup is characterised by localised small-scale folding, with significant faulting having occurred during this time period. Folding is generally characterised by a steepening in the dip of the succession in close proximity of major faults, such as observed with the Pre-Transvaal age Kromdraai- and Pioneer Shaft Faults, as well as Ventersdorp-age associations with the Jersey Fault.

3.3.2.2 Transvaal-age and Post-Transvaal-age structure

Deformation of the Transvaal Supergroup in the KOSH-area can be ascribed to three prominent stages, including (i) the re-activation of Ventersdorp-age tectonism where residual stress was relieved along existing Ventersdorp-age fault planes, (ii) Transvaal-age deformation, and (iii) the Vredefort meteor impact event. Antrobus *et al.*, states that deformation (folding, tilting and faulting) of the Black Reef Formation is evident in the area. However, the difficulty associated with identifying deformation that can be correlated solely to Transvaal-age tectonism is apparent, due to the absence of a pertinent pre-Ventersdorp age – post-Transvaal age datum plane. The major principal stress of the Transvaal-age structures indicates similar orientations to those known to be of Ventersdorp-age. One such an example of a re-activated Ventersdorp-age structure is the so-called Kromdraai Fault, which displaces the Black Reef Formation. Transvaal-age intrusives in the KOSH-area are associated with north-west/south-east striking faults, ascribed to the similar orientation of these structures. North-west/south-east orientated faults are generally small in throw, and could have facilitated post-Ventersdorp-age tectonic stress relief. Localised folding and faulting is closely associated with Transvaal-age structures, as can be observed in close proximity of such structures. Some of these regionally prominent structures in the KOSH-area, known to be of late- to post-Transvaal-age, is the so-called Fakawi Fault in the east, which is traceable at surface, as well as the sub-surface Jersey- and Zuiping Faults towards the south of the area.

The regional strike of the strata in the area is generally uniform in a north-east/south-west direction. The overall dip direction of the Transvaal Supergroup is generally towards the south-

east. An increase in dip angles towards the south and the east is unmistakable, and is associated with Vredefort-age folding of the Transvaal Supergroup succession. This localised folding towards the south-east of the area is unofficially termed the Loopspruit Syncline. Post-Transvaal deformation of the area is largely associated with thrust faulting, as observable by the Katdoornbosch Thrust Fault and Potch-Foch Thrust Fault located along the eastern border of the dolomitic outcrops in the KOSH-area, the Spitskop Thrust Fault located towards the north of the KOSH-area at Spitskop, and the regionally prominent Enslin Thrust Fault towards the east between Potchefstroom and Parys, traceable along the north-east/south-west striking Potchefstroom Synclynorium (Brink *et al.*, 1999 and Brink *et al.*, 2000).

Vredefort-age deformation could have resulted in the single most significant stage of deformation on the Transvaal Supergroup in the KOSH-area. The Vredefort Impact structure is characterised as a concentrically orientated set of parallel structures around the exposed granitic crust south-east of Parys, rippling outwards towards the north, north-west and west (Brink, 1992). The Loopspruit Syncline in the KOSH-area exhibits the same concentric orientation to that of the larger Vredefort Impact structure. Antrobus *et al* (1986) describes the KOSH-area to be situated on the western limb of the Loopspruit Syncline, which forms a structurally complicated regional depression. It could be that the Loopspruit Syncline is associated, or structurally genetic, to the Spitskop Syncline located along strike towards the north of the area (west of Potchefstroom), and the Frederikstad Syncline towards the far north (southwest of Welverdiend). Brink (1996) states that these synclines might be footwall synclines associated with the Potch-Foch Thrust Fault (and possibly the KDB thrust fault). The subsidence-associated tilt of the Loopspruit Syncline is closely associated with the overall sum-total of tilting, measurable across the Black Reef in the KOSH-area (Antrobus *et al*, 1986). Various bedding plane faulting is also associated with Vredefort-age deformation of the area and were most likely established from the Post-Transvaal – Pre-Karoo-age (Brink (1982)).

Prior to the deposition of the clastic sedimentary succession of the Pretoria Group of the Transvaal Supergroup, a large period of erosion took place, where today extensive cavernous conditions are associated with the unconformable contact (Martini *et al*, 1995). After the deposition of the Karoo Supergroup, the Post-Transvaal sedimentary strata remained unaltered across the majority of the area. This can be argued due to the still-horizontal orientation of the Karoo Supergroup. As such, it is evident that the Karoo Supergroup was deposited after the regionally prominent Vredefort Meteor Impact event.

After the deposition of the Karoo Supergroup, the initial onset of karst development took place. This primarily occurred during two time periods, namely during Jurassic period and during the

Tertiary Period (Brink and Partridge, 1965). During these two main periods of karst development, the base water table was established, possibly due to the melting of glacial drift across the area. Brink (1979) describes unusually deep valleys (up to 200 m deep in some cases) within the leached dolomite that are known to be associated with faults in the Carletonville area. These valleys are almost all orientated along the major principal stress of the area, namely 10° east of north. Despite this prominent period of karst development (i.e.: approximately during the last 250 Ma), Eriksson and Alterman (1998) describe some much older karst events that are preserved across the Transvaal Basin.

3.3.2.3 Summary of structural evolution across the KOSH area

The various stages of deposition, structural evolution and tectonic deformation across the Buffelsfontein mine lease area has been reconstructed and discussed by Antrobus *et al* (1986), and were summarised and illustrated (Figure 3-5 to Figure 3-9) by these authors as follows:

Stage 1:

During the initial stages of the crustal evolution of the KOSH-area, the Witwatersrand Supergroup was subjected to monoclonal folding, where after andesite of the Klipriviersberg Group (Ventersdorp Supergroup) was deposited. After deposition, the Witwatersrand- and Ventersdorp Supergroups were affected by gentle folding. This stage of deformation is illustrated in Figure 3-5, and represents a north-west/south-east section (i.e.: section B-A – south looking) across the Buffelsfontein mine area.

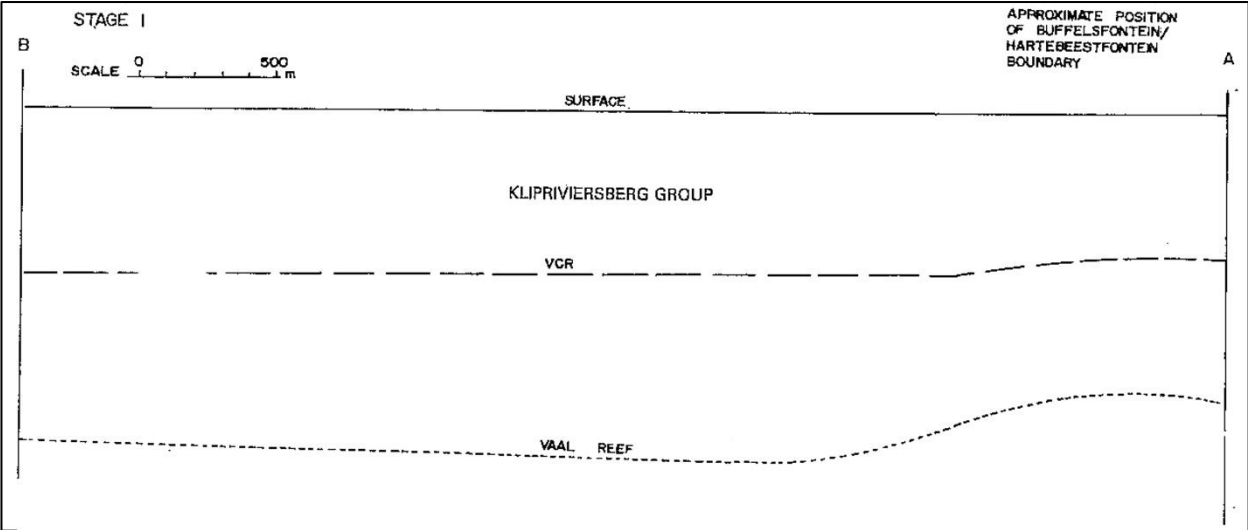


Figure 3-5: Stage 1 of deformation and deposition – Witwatersrand Supergroup monocline fold and Klipriviersberg Group (Ventersdorp Supergroup) deposition and folding (from Antrobus *et al*, 1986)

Stage 2:

The second stage of deformation is characterised by the initial formation of horst-and-graben structures, by block faulting along the Pioneer Shaft Fault (blue line) and the Eastern Shaft Fault (red line). Localized folding of the adjacent rock is inferred with movement along these faults. After the block-faulting phase, the Platberg Group (Ventersdorp Supergroup) was deposited as immature clastic sediments across the graben portions of the block faults (e.g. on the down throw side of fault scarps). An association of the Jersey Fault (purple line) is inferred as part of this phase of deformation, displacing strata of the Ventersdorp Supergroup. This stage of deformation is illustrated in Figure 3-6.

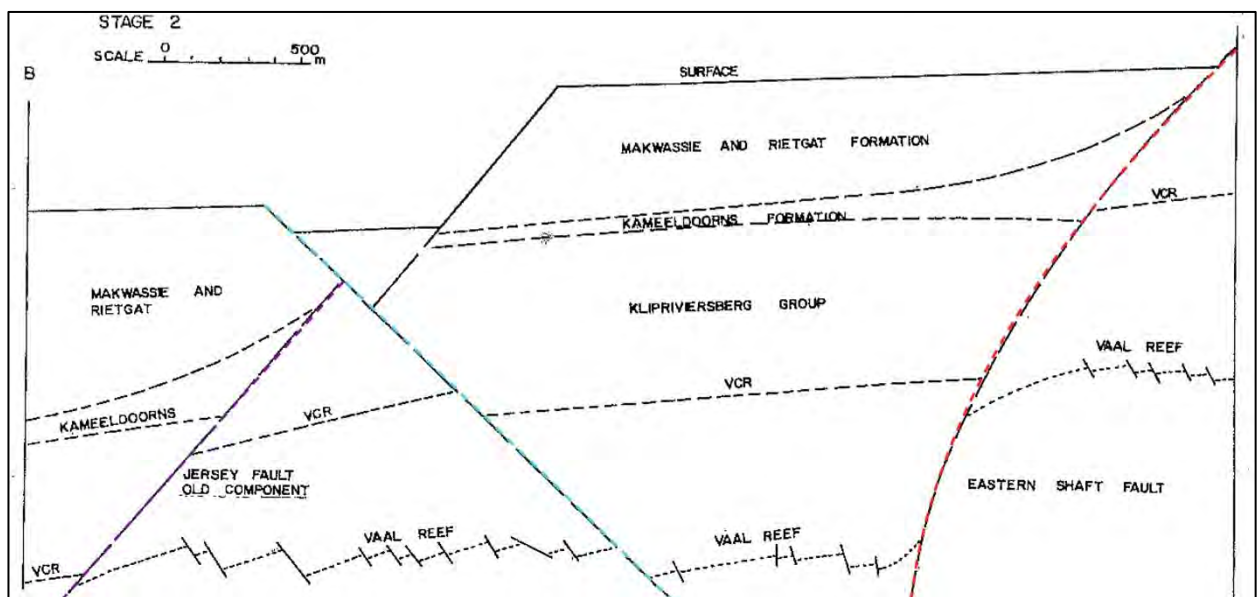


Figure 3-6: Stage 2 of deformation and deposition – Deformation of the Witwatersrand Supergroup and Klipriviersberg Group and deposition of the Platberg Group (from Antrobus *et al*, 1986)

Stage 3:

The third stage of crustal deformation and deposition is characterised by an initial period of erosion (observable by the Pniel Unconformity), which was succeeded by the conformable deposition of the near horizontal and uniform extrusion of andesite of the Allanridge Formation (upper Ventersdorp Supergroup). This was followed by the conformable deposition of the lower-most parts of the Transvaal Supergroup (i.e.: the Black Reef Formation). Although the Ventersdorp Supergroup does not underlie the Black Reef Formation conformably in all instances across the regional area, this is the case across the Buffelsfontein mine area. This stage of deformation and deposition is illustrated by Figure 3-7.

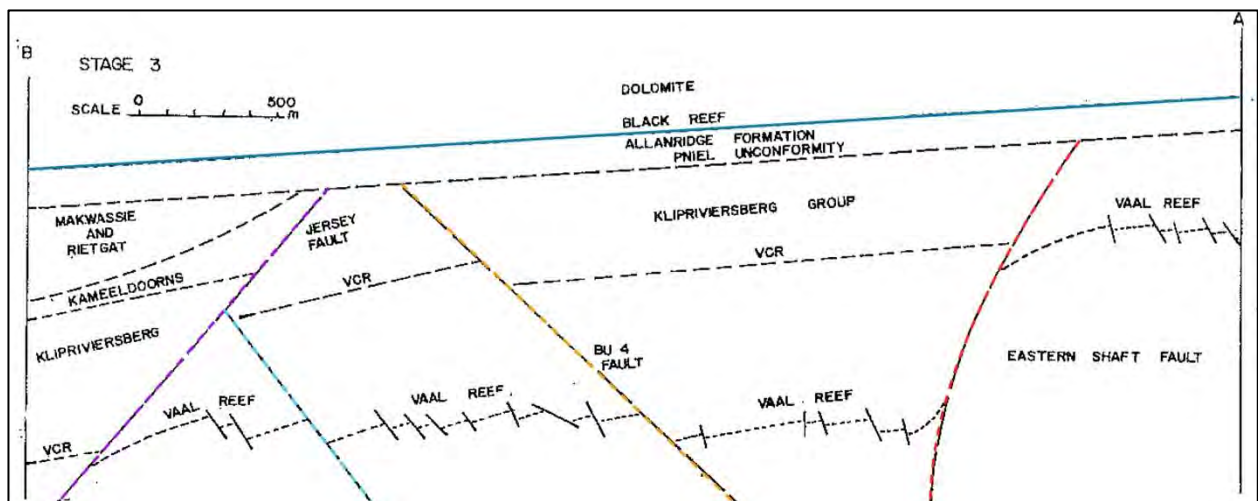


Figure 3-7: Stage 3 of deformation and deposition – Erosion of the Platberg Group followed by deposition of the Allanridge Formation and the Transvaal Supergroup (from Antrobus et al, 1986)

Stage 4:

After the deposition of the Transvaal Supergroup, the Fakawi- (dark blue lines), Through- (green lines) and Jersey Faults (purple line) were re-activated, resulting in large-scale deformation of the lithostratigraphic succession. The strata towards the east of the Jersey fault were substantially tilted towards the south-east, resulting in an increased dip angle of the succession. A small portion of the geological succession was uplifted between the Through- and Jersey Faults. The Fakawi Fault displaced the Eastern Shaft-, Through- and BU4 Faults (the Fakawi Fault is therefore the younger fault). This stage of deformation is inferred as having occurred prior the Vredefort Meteor Impact, and is illustrated in Figure 3-8.

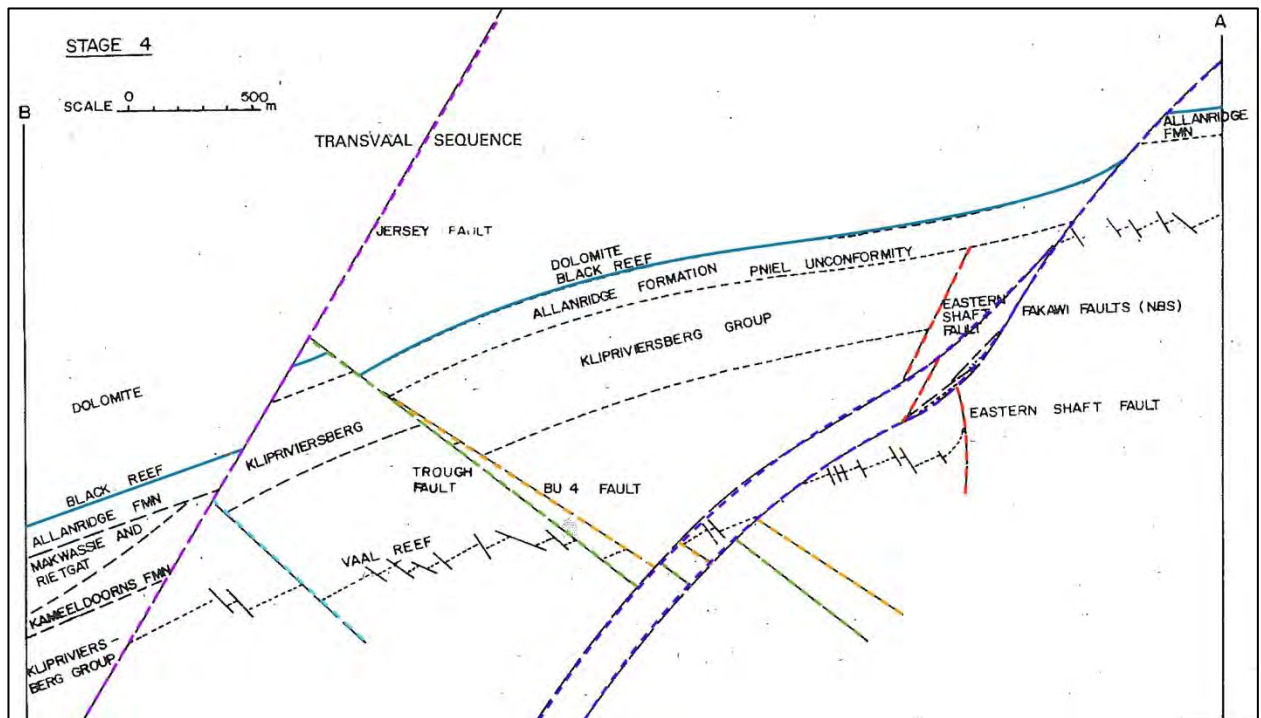


Figure 3-8: Stage 4 of deformation and deposition – Re-activation of the Fakawi-, Through- and Jersey Faults causing major deformation of the area (from Antrobus et al, 1986)

Stage 5:

The final stage of deformation is characterised by the re-activation of the Fakawi Fault, and possibly also the Jersey Fault, during folding and subsidence of the Loopspruit Syncline, caused by the Vredefort Meteor Impact. This caused gravity sliding of the bedding plane of the Witwatersrand Supergroup at depth. As such the so-called bedding plane faults in the Witwatersrand Supergroup formed at depth. Due to the occurrence of large horst-and-graben blocks of the Ventersdorp Supergroup, the bedding-plane faults in the Witwatersrand Supergroup terminated against the Ventersdorp Supergroup, due to the higher resistance of these blocks that acted as a buffer to deformation, preventing extension of the bedding plane faults into the overlying Transvaal Supergroup. After deformation, a period of erosion occurred, that was followed by the deposition of the Karoo Supergroup in the area, and subsequent erosion of the entire geological succession to the current-day surface. This stage of deformation is illustrated by Figure 3-9.

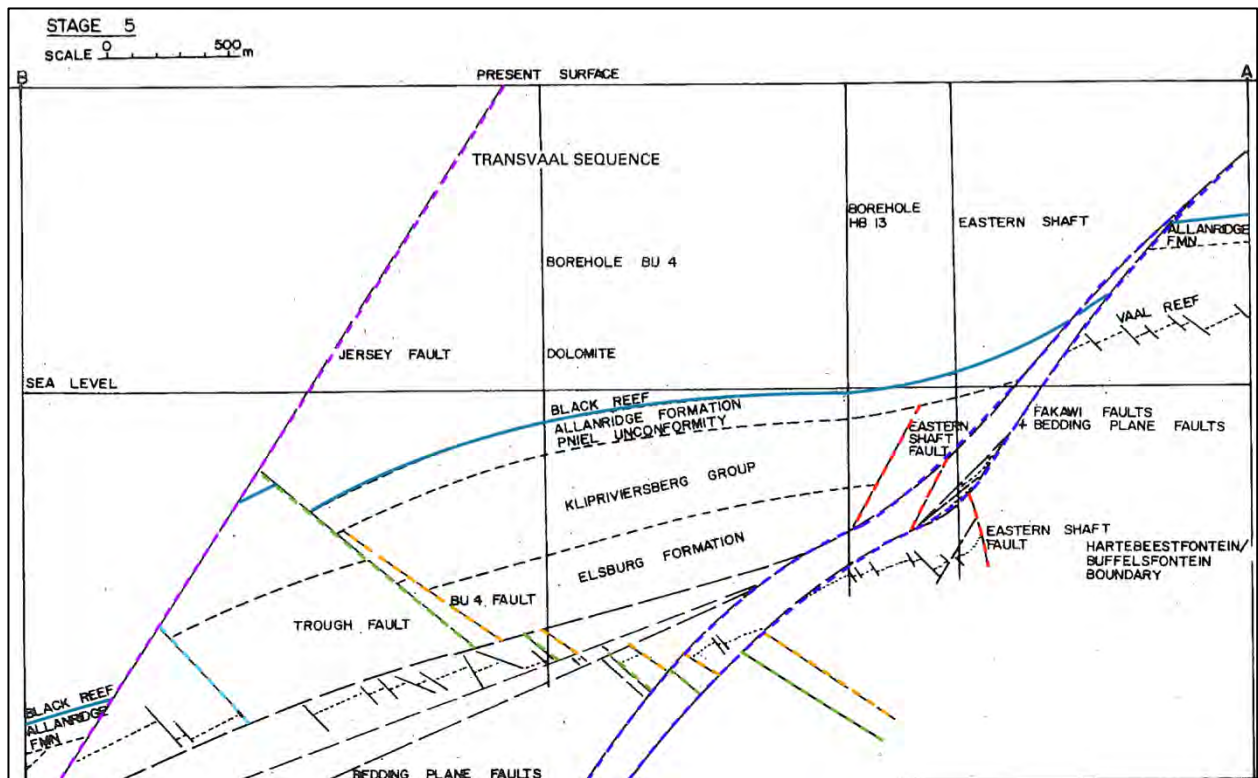


Figure 3-9: Stage 5 of deformation and deposition – Final stages of deformation during the Vredefort Impact and subsequent erosion of the geological succession (from Antrobus *et al*, 1986)

3.4 Development of a local geological model in support of dolomite risk management

3.4.1 Methodology

Available geological information, including background research, remote sensing, mapping and descriptions, and borehole information, was used as basis from which the geological model was developed. The published 1:250 000 scale geological map of the West Rand (2626) is referred to as the “*base map*”, seeing as this is the map that is most commonly referred to when conducting geotechnical investigations. Various regions across the KOSH-area were attended to on a local scale. Assessments in these regions included considering the following available information: structural geological research, stereography, map interpretations, assessments and interpretations of previously drilled boreholes, assessments of *Google Earth™* and rectified satellite imagery, focussed field observations, verifications and mapping. The various areas that are attended to on a local scale and the steps that were considered to compile the first-order geological model of the area are illustrated in Figure 3-10.

It is reiterated that this first-order geological model is aimed at characterising the general character of the dolomitic strata and adjacent rock types in the vicinity of the area, which is intended to serve as basis on which to demarcate the extent of dolomite land (i.e. dolomite up to a depth of 100 m) across the region, and to determine as a first-order any significant gaps in geological information across the area.

All observed stratigraphic discrepancies in relation to the *base map* are discussed in Section 3.5 towards the compilation of a first-order local geological model of the area. The updated geological and structure map of the area is included as Figure 3-16.

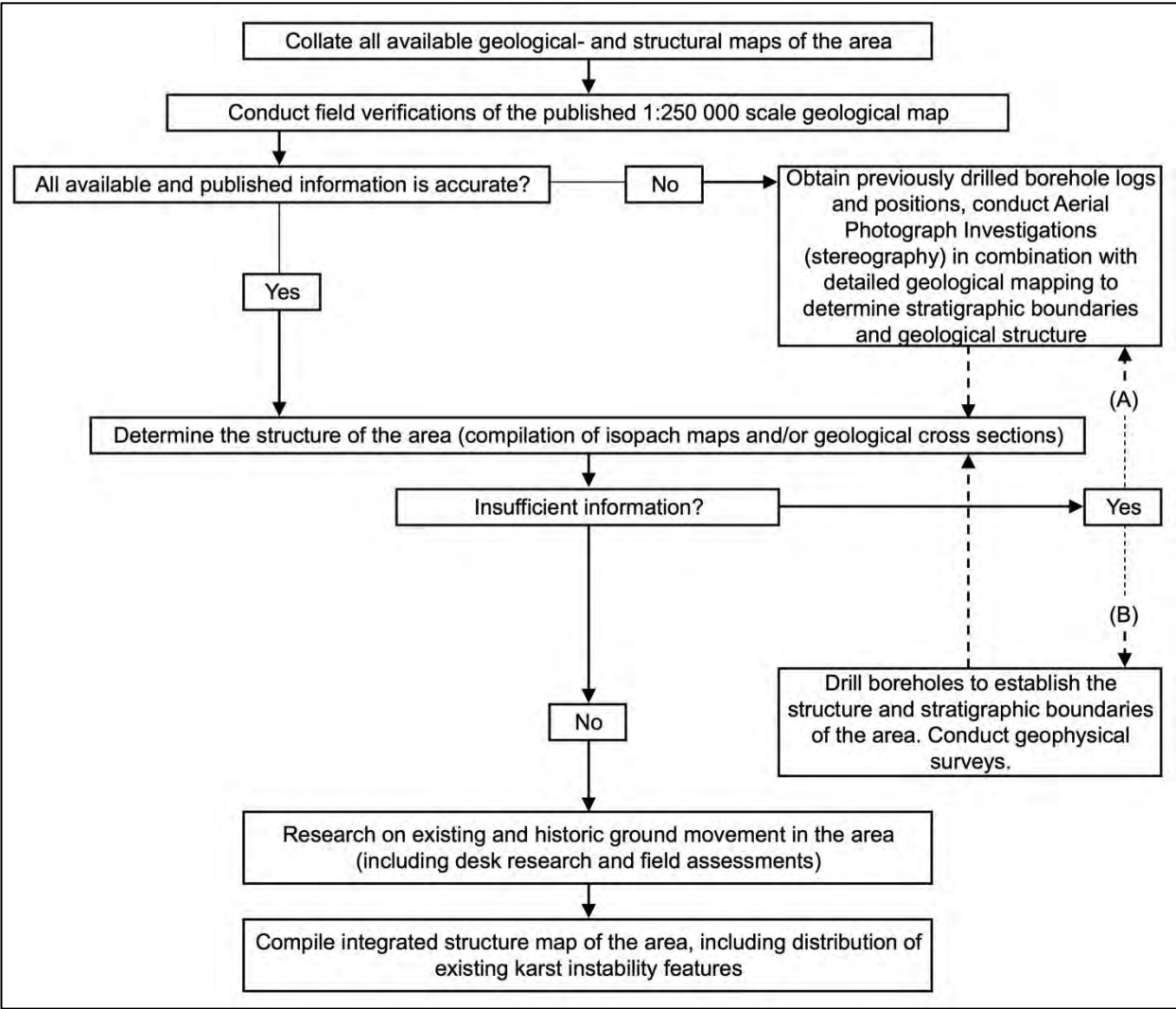


Figure 3-10: Key considerations and steps in compiling the first-order geological model of the area

3.4.2 Geological and geotechnical information from existing maps

The existing baseline geological maps were identified in- and around the study area, and were studied and used to develop an updated geological outcrop and structure map prior to the incorporation of all drilling and geotechnical information (refer to Annexure 1 for a detailed list of technical reports considered). Previous mapping and structural plans (Annexure 2) that were considered as part of the development of the local geological model include:

- (a) 1:250 000 scale geological map 2626 West Rand (Wilkinson, 1986; **base map**)
- (b) 1:250 000 scale geological map 2726 Kroonstad
- (c) Mapping of the Klerksdorp-Ventersdorp area conducted by L.T. Nel (1934)
- (d) Isopach map of the base of the Transvaal Supergroup (Antrobus *et al*, 1986)
- (e) Map of Potchefstroom showing fifteen mile radius, Council of Geoscience no. KF 589 (Mellor, 1934)
- (f) 1:35 000 scale regional map of the geology of Potchefstroom, Council of Geoscience no. KF 588 (Lombaard, 1935)
- (g) The Potchefstroom Town-and Townsland Geological map. 1:50 000 (Bischoff, 1992)
- (h) Regional discussion (and accompanying maps) of the structural geological setting of the regions surrounding Klerksdorp, Ventersdorp, Carletonville, Fochville, Potchefstroom and Parys conducted by Brink (1996)
- (i) Published 1:50 000 scale Potchefstroom Gap Geological map (Government Printer, unknown date)
- (j) Published 1:50 000 scale geological map of the area surrounding Ventersdorp (Government Printer, 1920)
- (k) Mapping of the Buffelsdoorn mine lease area conducted by Brink (in Antrobus *et al*, 1986)

3.4.3 Aerial photograph investigations and surface mapping

Upon collation and interpretations of the above maps, an aerial photograph investigation (API) was conducted across the region using stereo-pair photographs. As part of the aerial photograph investigation, lineations, dykes, geological structures and possible geological contacts, positions of sinkholes and subsidences, as well as other possible karst-related

features were identified and mapped out. This was followed by field verifications and assessments conducted across selected focus areas to:

- test the accuracy of the published information,
- broadly differentiate the various lithostratigraphic subdivisions of the various dolomitic formations on a regional scale, seeing as the Malmani Subgroup in the area is undifferentiated, and
- verify potential sinkholes and subsidences identified on aerial photographs and satellite imagery.

3.4.4 Incorporation of drilling results

The existing geological and geotechnical maps were re-interpreted, or verified, in the light of the available drilling results. Rotary core boreholes (approximately 614) and rotary air percussion geotechnical boreholes (approximately 165) drilled across the area, as well as excavated test pits (approximately 40) have been assessed in detail. Only lithologies of the upper parts of the Ventersdorp Supergroup, the Transvaal Supergroup, Pretoria Group and Karoo Supergroup were available from the exploration borehole databank that was used to assess the depth to dolomite and the non-dolomitic overburden thickness across the KOSH-area, and to determine the general structure of the geological succession. Borehole collars were plotted and colour-coded (legend included in Figure 3-11) for analysis and testing of the geological model for dolomitic ground.

Available geotechnical borehole information (specifically for the KOSH-area) was re-interpreted in order to more accurately determine the extent of the inferred Karoo Supergroup Inlier in the Stilfontein area, which could have an associated lower dolomitic risk. Some of the previous drilled boreholes across the entire study area indicate a highly variable profile, and indications of dis-homogeneity and extensive karst formation of the underlying dolomitic formations.

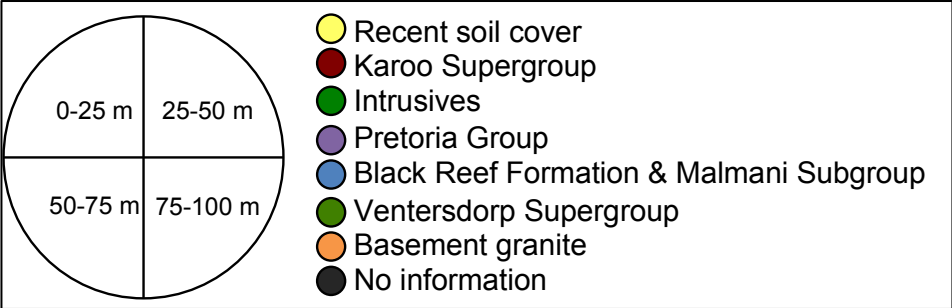


Figure 3-11: Colour-code explanation of boreholes used in the geological assessment

3.4.5 Compilation of cross sections

Upon collation of all available geological and geotechnical information, three cross sections were generated across the KOSH-area (sections A-A', D-D' and E-E') to illustrate the structure of the region. The published base of the Transvaal Supergroup isopach map was used as basis for the generated cross sections, and was supplemented by additional borehole information and surface mapping. The constructed cross sections are discussed in section 3.5 and their locations indicated in Figure 3-16, together with the determined extent of dolomite land across the KOSH-area (i.e.: depth to dolomite up to 100 m).

3.4.6 Compilation of a sinkhole and subsidence database

As part of the construction of the geological model of the area, research was conducted to collate all existing information on previous ground movement events in the area. This was supplemented by aerial photograph investigations and the assessment of satellite imagery to determine the extent of karst features. At the time of this study, no available records of sinkholes and subsidences were available from the national databank managed by the Council for Geoscience for reference. As such, all available information and records making mention of historic ground movements events in the study area were researched and collated into a database, together with newly identified and previously undocumented events. Aspects that are considered as part of the compiled database include:

- (i) Geological formation in which the feature is located.
- (ii) Brief description of the feature locality and notes of specific interest.
- (iii) Feature type and size.
- (iv) Level of confidence allocated to the identification of the feature.

3.5 Local observations and discussions

3.5.1 Discussion of the geology of Orkney and surroundings

This area mainly involves the discussion of the geology in and around the town of Orkney up towards the south of Stilfontein and the Vaal Reefs Mineworkers Village in the east. The regional extent of this area includes the coverage of Figure 3-15.

The base map (i.e.: published 1:250 000 scale geological map of the West Rand 2626) indicates that the Rietgat Formation of the Ventersdorp Supergroup directly underlies the Malmani Subgroup dolomite, which can be interpreted as a major unconformity. Scattered

outcrops of the Central Rand Group of the Witwatersrand Supergroup occurs as uplifted lenses along a north-eastwardly trending fault zone, deemed to represent the Buffelsdoorn Fault (the Buffelsdoorn fault, as interpreted from the satellite image and mapping by Brink (1999), follows generally the same path as the fault on the base map). The Black Reef Formation varies in thickness across the area and dips at shallow angles (5 to 15°) towards the east. The different lithostratigraphic sub-divisions of the Malmani Subgroup dolomite have not been differentiated on the base map in the area.

The observed correlations and discrepancies in this area can be summarised as follows:

- The upper and lower contacts of the Black Reef Formation are arbitrary mapped across the area, where the lower contact (with the Ventersdorp Supergroup) is mainly concealed and the upper contact with the Oaktree Formation is transitional and sometimes concealed with scree.
- The overall structure and position of the Black Reef Formation as mapped in the field was found to correlate fairly well with the base map with dips towards the east at shallow angles and a strike of approximately north-east/south-west between Orkney and Stilfontein, and approximately north-south in Orkney.
- Some of the mapped contacts of the Black Reef Formation on the base map was updated to reflect recent field and stereographic observations, as well as surface borehole information, and include:
 - The Black Reef Formation mapped in the north-eastern parts of Orkney was found to represent dolomitic strata of the Oaktree- and Monte Christo Formation and the lower contact of the Black Reef Formation was adjusted approximately 600 m west.
 - The Black Reef Formation contacts across the built-up areas of Orkney are concealed. Scattered quartzite outcrops in town, in combination with drilled boreholes (e.g.: KK584, KK580, KK578, KK577, KK388 and KK353), enable the broad demarcation of the extent of the Black Reef Formation. The Black Reef Formation contact appears to be located more towards the west, in contradiction with the base map, and was subsequently amended based on field observations and stereographic interpretations. However, due to the concealed nature of the contact, the drilling of a number of boreholes in combination with geophysical surveys (possibly magnetic, resistivity and gravimetric) will be required to accurately map out the contact.

- The Black Reef Formation lens indicated on the base map towards the north-east and north-west of Orkney is inferred to be mapped based on the information represented in boreholes KK468 and KK470. The exact tectonic mechanisms that led to the inlier is not known, and can be described as complicated, but seems to be associated with the north-northeast/south-southwestwardly strike of the Buffelsdoorn Fault.
- Another Black Reef Formation lens as mapped in the Potchefstroom Gap Map, but not mapped on the base map, was confirmed by borehole KK368, also towards the north-west of Orkney.
- The contacts of the Black Reef Formation with the Ventersdorp Supergroup and Oaktree Formation in the areas north of Orkney was mapped broader than what can be observed on stereographic photos and field mapping, and was adjusted accordingly. This is confirmed by surface boreholes collared in the Ventersdorp Supergroup (e.g.: KK476) where the base map indicates outcrops of the Black Reef Formation at surface.
- The soil covered area (mapped as alluvium) directly east of Orkney was confirmed to be underlain by dolomite based on the drilled boreholes in the area. All these boreholes have been collared in dolomite, and do not include transported strata of recent origin in the borehole logs.
- The lithostratigraphic contact between the chert-poor Oaktree Formation (along the western parts of the area) and the chert-rich Monte Christo Formation are not indicated on the published base map, and were subsequently mapped across the Orkney-Stilfontein area.
- No significant number of sinkholes is associated with this portion of the KOSH-area, and could be related to large areas being covered by the chert-poor Oaktree formation, as well as a lower concentration of faulting of the succession. The Black Reef Formation and Malmani Subgroup in this part of the regional area are inferred to having been more subjected to folding. A number of sinkholes are recorded towards the south of the Vaal River and at the Mineworker's village towards the east of Orkney (Figure 5-2). Both of these areas are situated across the chert-rich Monte Christo Formation.
- A cross section was constructed in the Orkney area along section line E-E' (Figure 3-12), using the available isopach map of the base of the Black Reef Formation, which was updated and verified using field observations and all available geological drilling results. The section line has a north-west-west/south-east-east orientation, and is discussed:

- The isopach map correlates well with the available borehole information, with the exception of localised discrepancies that were updated with supplementary borehole information and refined in the area directly north-east and south-east of Orkney.
- The geological succession dips at relatively shallow angles towards the south-east, and dip angles tend to be steeper along structural controls.
- The concealed Ventersdorp Supergroup / Black Reef Formation contact towards the western parts of Orkney was confirmed to be between boreholes KK580 and KK598.
- Localised small-scale folding of the Black Reef Formation and the Malmani Subgroup is evident in the area, as derived from the isopach map.
- The Kromdraai Fault (and faults sympathetic to the Kromdraai Fault) uplifted a portion of the dolomitic succession in the areas south-east of Orkney, and tectonic movement along the Jersey fault resulted in a significant downthrow of the succession and steepening in dip angle towards the south-east.
- The different lithostratigraphic contacts as indicated on the cross section are based on surface mapping and projections of contacts from adjacent boreholes (where the Malmani Subgroup was differentiated in logging).

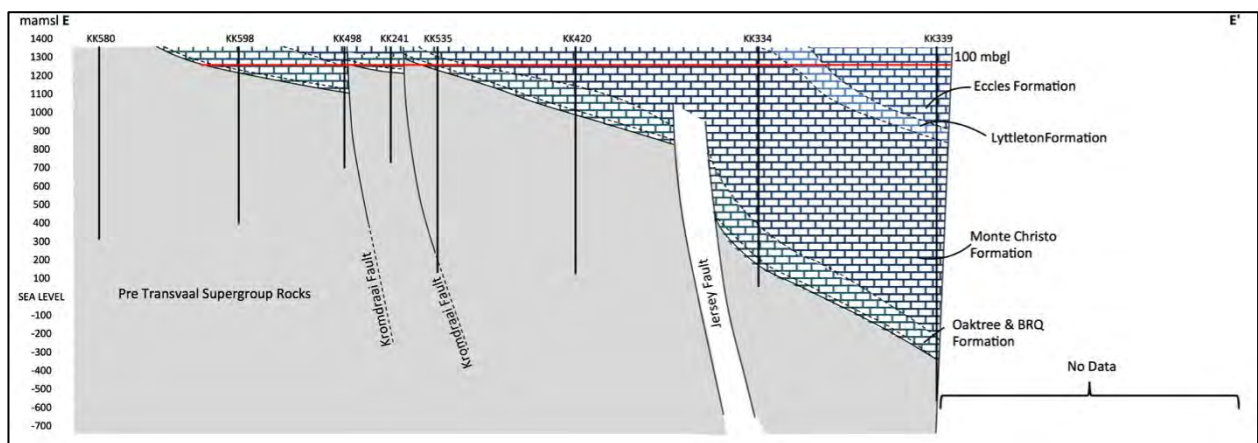


Figure 3-12: Schematic geologic cross section E-E'

3.5.2 Discussion of the geology of Stilfontein, Khuma and surroundings

This area involves the discussion of the geology in the area around Stilfontein in the west, Khuma in the east and the Vaal River in the south. The regional extent of the area is covered by Figure 3-15.

The base map (i.e.: published 1:250 000 scale geological map of the West Rand 2626) indicates that the area is predominantly covered by chert and dolomite outcrops of the Malmani Subgroup in the central and eastern regions, and by sedimentary- and volcanic rock outcrops of the Pretoria Group towards the far-east. A local east-west trending Karoo Supergroup outlier is indicated across the central regions of the area, which stops abruptly at the point of intersection with the Kromdraaispruit. A second highly localized oblong-shaped Karoo Supergroup Inlier is indicated directly east of Khuma. The two outliers are not indicated to be laterally continuous. The geological succession is indicated to dip at steep angles (50°) towards the south-east. No prominent faults are indicated across the Malmani Subgroup dolomite. A regionally prominent north-eastwardly trending fault is indicated along the bedding plane between the Timeball Hill Formation and the Hekpoort Formation, which represents an unconformity (i.e.: the upper parts of the Timeball Hill Formation and the total Boshhoek Formations were removed, with a maximum possible loss in stratigraphy of 300 m. This fault is terminated at the point of intersection with the eastern oblong-shaped Karoo Supergroup Outlier. Only one dyke with a north-south strike is indicated to outcrop towards the north of Stilfontein for approximately 2.3 km. No other structural features are indicated on the published base map, and the different lithostratigraphic sub-divisions of the Malmani Subgroup dolomite have not been differentiated.

The observed correlations and discrepancies in this area can be summarised as follows:

- The general strike direction of the geological succession correlates with the published base map.
- The overall impression of the geological succession correlates well with the published base map, with some disparities that were observed across the area with respect to bedrock outcrops:
 - The various lithostratigraphic sub-divisions of the Malmani Subgroup was confirmed and amended in some areas, largely based on the prior surface mapping conducted by Brink (2000) across the Buffelsfontein mine lease area. The eastern-most extent of the dolomitic succession is covered by outcrops of the Eccles Formation, and is underlain by the Lyttleton Formation towards the west. Both these successions are comparatively thin in the area, due to faulting that removed large parts of the succession. The majority of the central regions of the dolomitic area is characterised as outcrops of the Monte Christo Formation. The Oaktree- and Black Reef Formations underlie the areas towards the far west.

- A pronounced joint structure is observable in the strata directly north-east of the old Khuma area, however, bedrock outcrops in the area are sparse. The soil cover over the bedrock in this area is not deemed to be very thick.
- Outcrops of the Pretoria Group towards the south of the area near the Vaal River seems to be accurately mapped, as confirmed by a number of boreholes drilled in the area. Of specific interest are boreholes KK52 and 53. These two boreholes were both collared in Pretoria Group rocks, which corresponds with the base map. It is evident that these boreholes were drilled in a structurally disturbed area, which is displayed in the borehole profiles. Dolomite was intersected well below 100 m in these boreholes (e.g.: 254 m and 461 m respectively). It is inferred that the Katdoornbosch Thrust Fault is positioned between these two boreholes, the Fakawi Fault west of borehole KK52 and the Potch-Foch Thrust Fault south of borehole KK53. The geological succession towards the south-east of these two boreholes were found to be displaced by up to 600 m, which corresponds well with Brink *et al's* (2000) interpretation of the Potch-Foch Thrust system that has downthrows towards the south-east. Boreholes drilled east of borehole KK53 suggest that the geological succession was duplicated by imbricates of the Potch-Foch Thrust Fault, but could not be verified by field mapping.
- The mapping conducted by Brink of the area revealed the occurrence of the Giant Chert Breccia directly overlying the Eccles Formation, which is considered to be associated with the Potch-Foch Thrust System and Katdoornbosch Thrust Systems in the area. The Giant Chert Breccia is overlain by the Rooihogte Formation in the area, as mapped by Brink. Field mapping and verifications is in agreement with the findings of Brink with respect to the occurrence of the Giant Chert Breccia towards the upper parts of the Eccles Formation. The occurrence of the Rooihogte Formation (shale and quartzite) could not be correlated with certainty, however, a quarry towards the east of the Orkney Bridge (intersection of the R502 with the N12) revealed siltstone outcrops, which could be associated with the Rooihogte Formation. According to Brink *et al* (2000) the Giant Chert Breccia is associated with the sole of the Potch-Foch Thrust- and Katdoornbosch Thrust Fault's ramp zone.
- The east-west striking Karoo Supergroup outlier on which large parts of Stilfontein were built was found to be laterally continuous across the area, and not separate pockets as indicated on the published base map. This was determined using the drilled boreholes in the area, seeing as the outlier does not form outcrops in all instances. A quarry directly south of Stilfontein also verified the southern-most extent of the outlier in the

Stilfontein area. The extent of the Karoo Supergroup outlier towards the south of Khuma along the R502 road (as mapped by Brink, 2000) was verified by boreholes KK 574, 365, 490, 492 etc. The outlier is inferred to represent a paleo-karst valley-fill deposit formed by an east-west trending regionally prominent fault zone, where the remainder of the Karoo Supergroup was eroded to the present day surface, and the underlying dolomite bedrock exposed. A number of similarly oriented east-west lineations are observable on the 2626 West Rand aeromagnetic survey in the KOSH-area. The possibility exists that the Karoo Supergroup outlier could have been a glacial deposit of sedimentary strata and glacial till (in the basal parts). The thickness of the Karoo Supergroup outlier varies significantly and is generally between 5 and 190 m thick.

- Numerous structural features intersect the eastern parts of the area and exhibit a north-east/south-west trend, bearing more towards the east in the northern parts of the area. These structural features are traceable at surface across long distances where it is associated with breccia and hydrothermal quartz vein intrusions that structurally deformed the upper 100 m (and deeper) of the dolomitic succession. The same observation was made by Trollip (2006) who drew the correlation between hydrothermal quartz vein intrusions and shear zones in an area south of Pretoria. The regionally prominent faults intersecting the area are described:
 - The Kromdraai Fault seems to be laterally semi-continuous from the Orkney area, and trends more towards the north-east in the Khuma area. As in the Orkney area, the Kromdraai Fault uplifted the geological succession between sympathetic faulting, with downthrows of approximately 100 m towards the south-east.
 - The Katdoornbosch Thrust Fault and the Fakawi Fault (an east-south-east dipping normal fault) runs approximately parallel to each other across the area from the Vaal River in the south towards the N12 in the north. The Katdoornbosch Thrust represents a significant regionally prominent thrust fault that is laterally continuous from the Vaal River, all the way towards Carletonville where it is termed the Witpoortjie Thrust Fault. The same applies to the Potch-Foch Thrust fault.
 - The Potch-Foch Thrust Fault intersects the southern parts of the dolomite succession in the regions of the Vaal River, and bends towards the north-east in the direction of Potchefstroom.
 - The Katdoornbosch Thrust Fault and the Fakawi Fault have been displaced by an east-west striking thrust fault towards the east by up to 1 000 m. This was confirmed by

means of aerial photograph investigations of the area, where the fault is easily identifiable.

- The structural features represent the regionally prominent structures of the area, and it is inferred that sympathetic faulting occurred parallel to these structures. This can also be observed in the stratigraphy of boreholes drilled adjacent to these regionally prominent faults.
- The surface outcrop of the north-east striking diabase dyke directly north of Stilfontein is accurate. However, this structure was mapped across the various mining properties in the KOSH area and separates the groundwater flow in the area into various compartments (discussed in Chapter 4), but does not form outcrops in all instances. The dyke is of Post-Transvaal (Pilansberg) age, and has a known thickness of up to 12 m, with varying degrees of permeability. The dyke stretches from the indicated outcrop north of Stilfontein in a south-south-eastwardly direction where it intersects the Vaal River. The dyke is indicated by the mapping conducted by MC Brink to have been displaced by the Fakawi Fault south of the Vaal River.
- Two cross sections were constructed in the Stilfontein-Khuma-Hartebeesfontein area along section lines A-A' (Figure 3-13) and D-D' (Figure 3-14), using the available isopach map of the base of the Black Reef Formation, which was updated using field observations and all available geological drilling results. Section A-A' has a north-west/south-east orientation and section D-D' an east-west orientation, and are discussed:
 - The isopach map correlates very well with the available borehole information, and no significant discrepancies were observed.
 - Both cross sections indicate the same structural trend across the area, with a relatively shallow-dipping succession towards the western parts that drastically steepens in dip adjacent to the Fakawi- and Jersey Faults in the south-east.
 - The succession was uplifted in the vicinity of the Kromdraai Fault, and folding of the Black Reef Formation (and possibly the Malmani Subgroup) is evident in the vicinity of Stilfontein.
 - The different lithostratigraphic contacts as indicated on the cross sections are based on surface mapping and projections of contacts from adjacent boreholes where the Malmani Subgroup was differentiated in logging.

- A significant number of sinkhole and subsidence occurrences were observed in the eastern regions of the KOSH-area. It is argued that these features are closely associated to the larger concentration of faults and shear zones in the area due to tectonic deformation caused by the Vredefort Meteor Impact. Based on field observations and stereography carried out in the area, it was found that ground movement events are situated along strike (and parallel to) fault zones and hydrothermal quartz vein intrusions. The same observations were made by Wagener (1982), who described the occurrence of 28 sinkholes along north-south trending lineaments (inferred to be faults) in the Vaal Reef no.8 shaft south of the Vaal River. It must be noted that the majority of sinkholes in the KOSH-area have south-eastwardly dipping throats (Van Deventer, 2013).
- Reference is made to the occurrence of Paleo sinkholes and -subsidence towards the north of the old Khuma township area. These features generally occur across the Eccles Formation, however some Paleo-sinkholes occurring on the Monte-Christo Formation are known in the KOSH-area and directly north of the Stilfontein along the N12. The Paleo-sinkholes north of Khuma are closely associated with structural geological controls, and the same were observed during prior field visits in the Carletonville area. Specific reference is made to a combination of three Paleo-sinkholes in the Carletonville area that have a combined diameter of approximately 300 m (an aerial photograph of this feature is included at the end of the Chapter). Paleo-sinkholes in the KOSH-area are generally associated with the occurrence of *Acacia erioloba* (Camel Thorn) trees that are known to favour deep, loose, well-drained soil, that is typical of in-filled Paleo-sinkholes, but are not as large in diameters as those found in the Carletonville area.

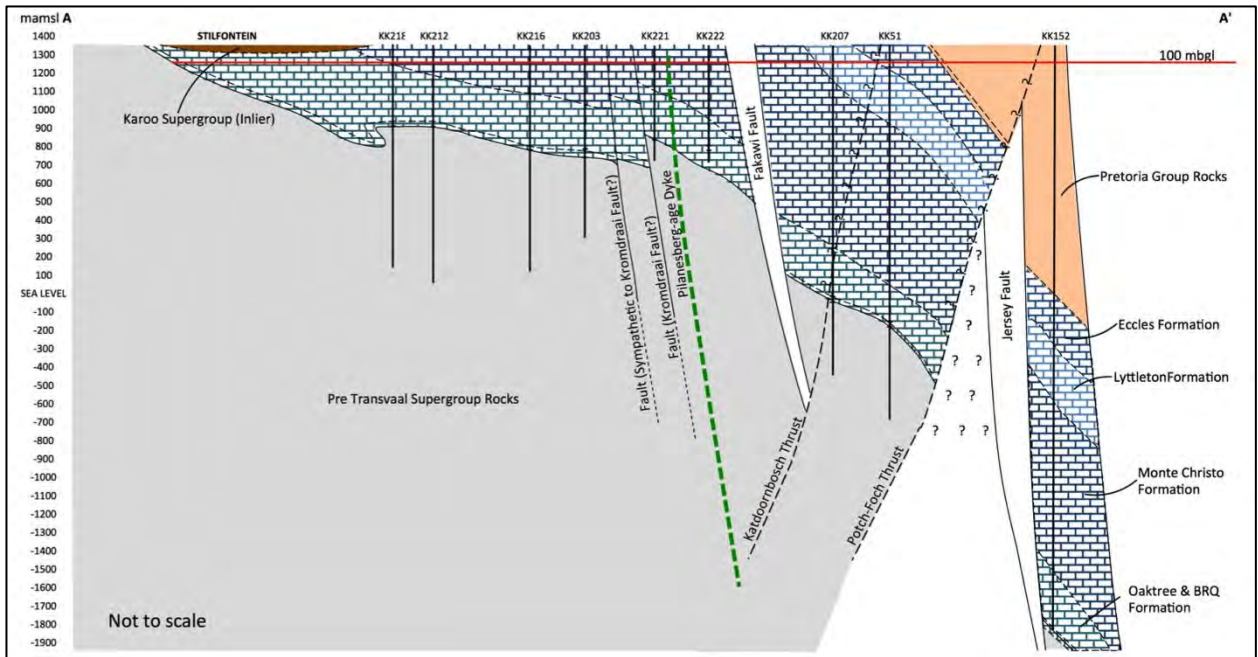


Figure 3-13: Schematic geologic cross section A-A'

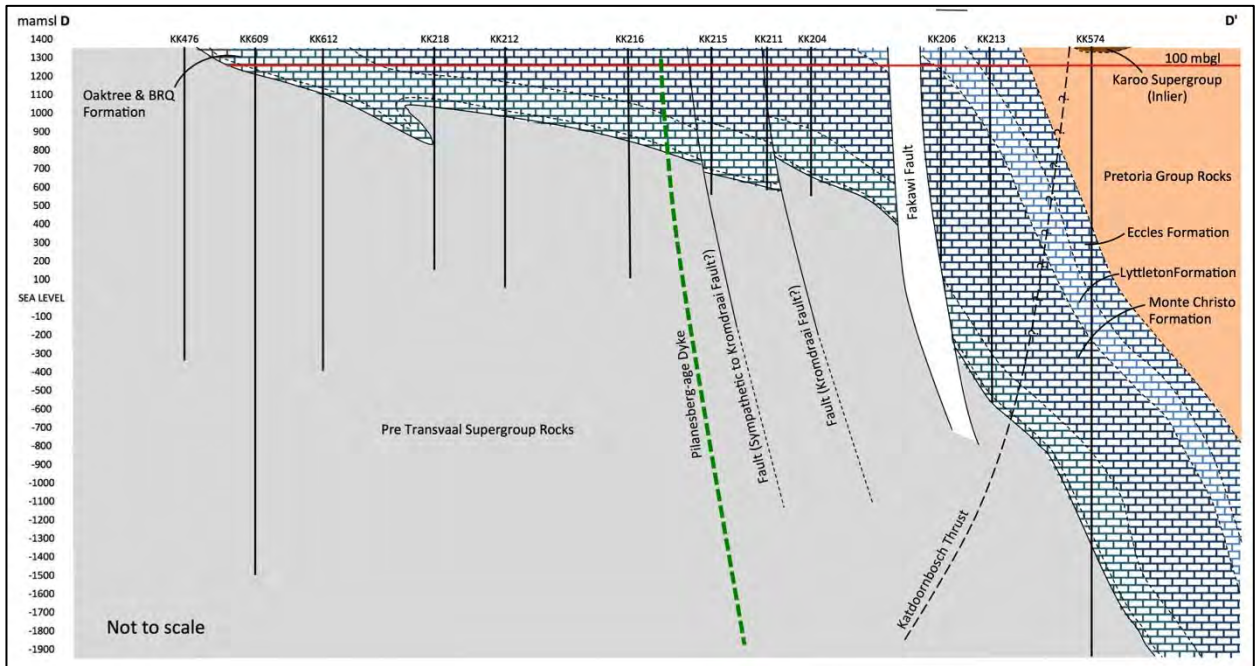


Figure 3-14: Schematic geologic cross section D-D'

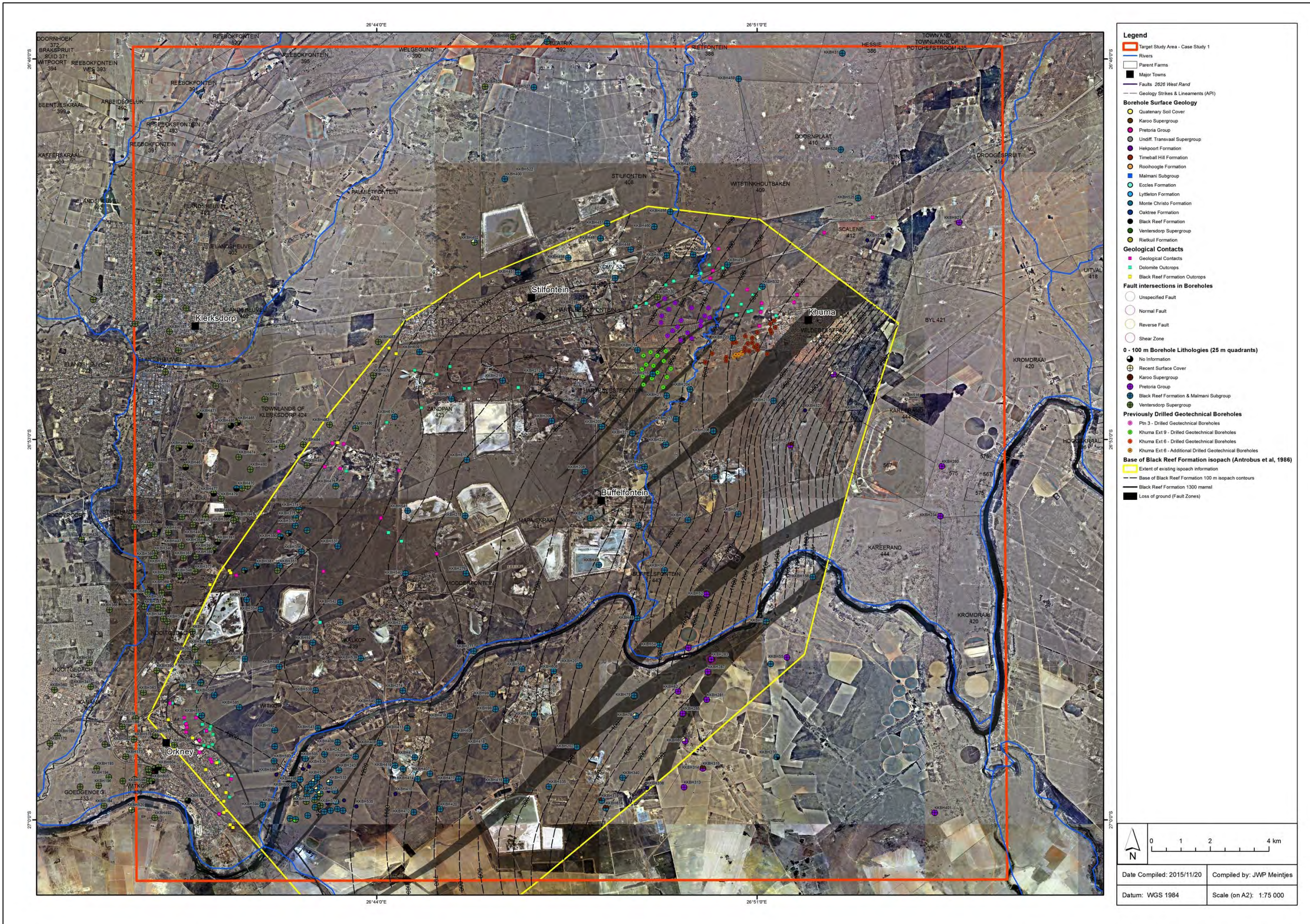


Figure 3-15: Collated geological information across the KOSH area

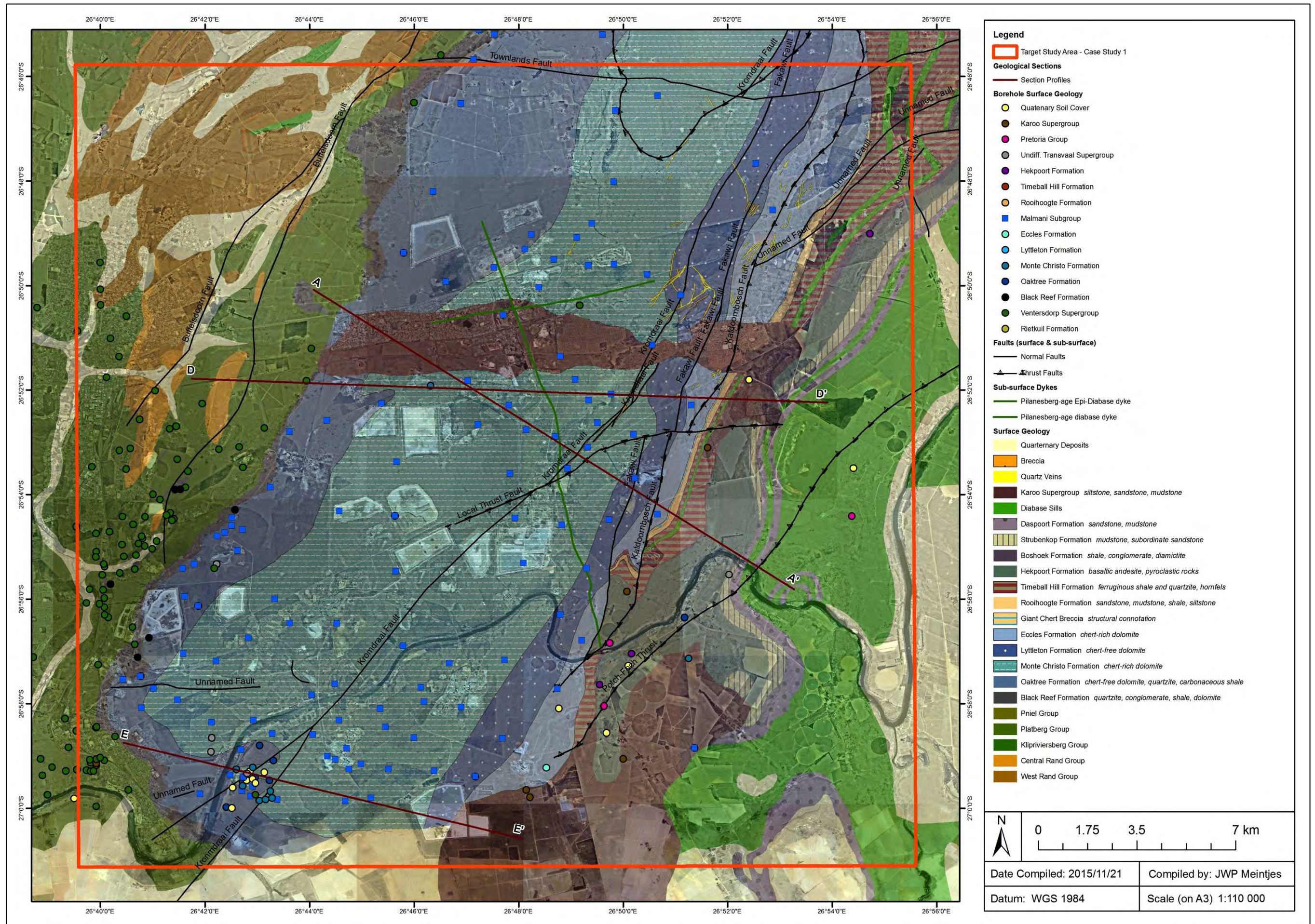


Figure 3-16: Updated geological and structural model of the KOSH area



Photo 3-1

Panoramic view of the KOSH area from on top of the prominent ridge formed by the Black Reef Formation in the western parts of the study area (north of Orkney) looking east. Topographic depression in the foreground (recognizable by the increase in vegetation) is characteristic of the contact between the quartzitic Black Reef Formation and the dolomitic Oaktree Formation.



Photo 3-2

Panorama view of the KOSH area standing in the east (near the Eccles- and Lyttleton Formation contact north of Khuma), looking west. The Eccles – Lyttleton contact is characterised in the field by a slight surface depression due to the chert of the Eccles Formation being less prone to weathering, and the Lyttleton Formation weathering as a negative relief. The contact between the Lyttleton – Eccles Formation was found to be associated with sinkholes and subsidences in the field.



Photo 3-3

Scattered quartzite scree and outcrops of the Black Reef Formation north of Orkney and south of Stilfontein. The Black Reef Formation is characterised as having a pinkish-brown colour in hand specimen and is associated with an easily traceable prominent topographic ridge between Orkney and Stilfontein. The basal parts of the Black Reef Formation gradually flatten in slope (towards the bottom of the photo) as it starts to transition into the dolomitic Oaktree Formation.



Photo 3-4

Prominent pinkish-brown quartzite of the Black Reef Formation in the south-eastern parts of Orkney (far back of photo).



Photo 3-5

Evidence of karstification in the light grey quartzite of the Black Reef Formation in the vicinity of Orkney. Note the weathering of a dolomite band in the quartzite, leaving an un-filled cavity with traces of wad at the sides of the void. The left hand part is characterised as manganiferous residue. Pen for scale.



Photo 3-6

Sparse and highly scattered quartzite outcrops and sub-outcrops in the south-western parts of Orkney (bottom-middle of photo). Bedrock outcrops in these areas are generally covered with transported overburden or not observable due to urbanisation that inhibits mapping of the area. The basal contact between the Black Reef Formation and the Ventersdorp Supergroup in the vicinity of Orkney is generally covered by transported overburden.



Photo 3-7

Light grey quartzite and meta-quartzite outcrops of the Black Reef Formation directly adjacent the transition into the dolomitic Oaktree Formation (towards the left of the photo), north of Orkney.



Photo 3-8

Conglomerate hand specimen of the Black Reef (situated at the basal parts of the Black Reef Formation) north of Orkney. Photo by Leon Venter, 2015.



Photo 3-9

Quarry profile of the Karoo Inlier directly south of Stilfontein: light yellowish-brown horizontally bedded siltstone, with approximately 1 to 2 m thick light orange-brown to reddish-brown transported overburden capping the bedrock outcrops.



Photo 3-10

Panorama view of the mined-out Karoo Inlier directly south of Stilfontein. It is evident that the Karoo Inlier strata is horizontally bedded, and does not show significant signs of major deformation or displacement.



Photo 3-11

Panorama view looking north, standing south of Stilfontein, indicating the homogenous extent of surficial cover and vegetation across the Karoo Inlier. No bedrock outcrops are associated with the Karoo Inlier.



Photo 3-12

Panorama view standing in the east looking west across the old Khuma Township. The area is characterised by extensive surficial cover of unknown thickness, with not observable bedrock outcrops. The surficial cover is very similar to that encountered in the vicinity of Stilfontein, and is inferred to represent the same Paleo-karst valley infill deposit of Karoo age (i.e. Karoo Supergroup).



Photo 3-13

Scattered light brown shallow dolomite outcrops of the Oaktree Formation towards the south-west of Stilfontein, exhibiting typical “elephant-skin” weathering. The numerous dissolved joints or slots (found to be orientated in three directions) can be observed in the photograph. Slots vary and are spaced between a few feet to more than a couple of meters in width.



Photo 3-14

Highly weathered grey dolomite of the Oaktree Formation in the vicinity of Orkney indicating karstification and a small-scale in-filled Paleo-sinkhole (on the right) and a small slot (on the left). The upper parts of the Oaktree Formation outcrops around Orkney is characterised as being covered with a thin near horizontal dark-grey to black siliceous scree (visible in the upper parts of the dolomite outcrop on the photo).



Photo 3-15

Oolites in the Oaktree Formation near Orkney. Pen for scale.



Photo 3-16

Scattered dolomite outcrops of the Oaktree Formation east of Orkney. The highly scattered and irregular nature of bedrock outcrops in this area is evident, and is blanketed with alluvium, possibly a Paleo drainage regime of the regionally prominent Vaal River, in some areas.



Photo 3-17

Quartz vein hydrothermal inclusion within the dolomite of the Oaktree Formation east of Orkney. Pen for scale.



Photo 3-18

Highly weathered dolomite of the Oaktree Formation that is capped with a dark grey siliceous scree. Note in the central parts of the photo the vertically developed fissure in the dolomite bedrock that is capped with the horizontal siliceous scree. This siliceous layer – where horizontally continuous and sufficiently thick (75 m) – could provide some form of stability from a dolomite stability perspective, but must be verified by means of drilling. Pen for scale.



Photo 3-19

Geological contact revealed along an excavated service trench at the old Hartebeesfontein gold mine north-west of Stilfontein. Outcrops of the Monte Christo Formation are exposed in the trench towards the left of the photo (east) and the Oaktree Formation towards the right of the photo (west).



Photo 3-20

Panorama view of the regional contact between the Monte Christo Formation and the Oaktree Formation standing south of the old Hartebeesfontein gold mine looking west. The contact in the field is characterised as a topographic depression, as can be seen in the photograph along the left-right orientation of trees. The photograph's horizon represents the prominent quartzite ridge of the Black Reef Formation in the far west.



Photo 3-21

Chert-rich dolomite of the Monte Christo Formation near the Oaktree Formation contact. Karstification can be seen in the hand specimen as visible in the upper parts of the photo. Outcrops are highly fractured and show signs of significant tensional deformation. These outcrops are deemed to represent the Monte Christo Formation. Pen for scale.



Photo 3-22

Chertified stromatolites in the Monte Christo Formation near Orkney. Pen for scale.



Photo 3-23

Scattered chert scree of the Monte Christo Formation encountered north of Khuma. The southern parts of this area is characterised by loose chert-rich scree and surficial cover, whereas the northern parts comprise of prominent shallow bedrock outcrops. The drilling rig used during the detailed dolomite stability assessment is visible in the photograph.



Photo 3-24

Stromatolitic chert-rich dolomite of the Monte Christo Formation encountered north of Khuma. This outcrops is deemed to represent the unofficially termed "*Upper Monte Christo Formation*", but has not been differentiated across the region.



Photo 3-25

Chert-poor light grey and coarse-grained dolomite mapped at the Vaal Reefs mineworkers village north-east of Orkney. These outcrops are deemed to represent the unofficially termed “*Recrystallized Zone / Middle Monte Christo Formation*” of the Monte Christo Formation.



Photo 3-26

Close-up photo of the coarse-grained light grey chert-poor dolomite of the unofficially termed “*Recrystallized Zone / Middle Monte Christo Formation*” of the Monte Christo Formation. Geological pick for scale.



Photo 3-27

Typical “elephant skin weathering” of dolomite outcrops of the Lyttleton Formation mapped towards the west of Khuma. Outcrops in the area have been subjected to intense fracturing, as can be seen in the photo.



Photo 3-28

Panoramic view of outcrops of the Lyttleton Formation east of Khuma. From the photo it can be observed that bedrock outcrops are generally widely spaced. Areas between adjacent outcrops are covered by overburden, and follow the same strike as the geological succession of the area as well as the regional trend of prominent faults. It is inferred that these overburden-filled areas in between adjacent bedrock outcrops could be interpreted as slots within the dolomite associated with faulting and fracturing of the bedrock.



Photo 3-29

Lithified manganiferous concretions between adjacent light-brown dolomite outcrops of the Lyttleton Formation north of Khuma. This is deemed to represent a highly weathered dolomite profile. Geological pick for scale.



Photo 3-30

Horizontal flow structures visible in the light-brown dolomite of the Lyttleton Formation north of Khuma. This structure that is observable in bedrock outcrops are characteristic of the regional dolomite signature on aerial photographs. Geological pick for scale.



Photo 3-31

Scattered light-brown chert-free dolomite outcrops of the Lyttleton Formation directly west of the old Khuma Township. A surface depression is observable on the left-hand side of the photo.



Photo 3-32

Highly decomposed and weathered chert-free dolomite outcrops of the Lyttleton Formation exposed along the railway cutting north of Khuma. Localised – and small scale – tufa-type sedimentation, and cave-fill deposits (containing skeletal fragments) was observed at this outcrop.



Photo 3-33

Typical contact between the chert-free dolomite of the Lyttleton Formation (in the foreground of the photo) and the chert-rich dolomite of the Monte Christo Formation (in the background of the photo) as observed in the field.



Photo 3-34

Panoramic view (looking towards the west) of scattered chert-free dolomite outcrops of the Lyttleton Formation exposed along a surface drainage feature directly west of the old Khuma Township. This photo illustrates the thin surficial cover across the dolomite in the area.



Photo 3-35

Panoramic view across the chert-rich reddish-brown and white outcrops of the Eccles Formation north-east of Khuma in the vicinity of the existing railway line. Photograph was taken looking towards the south.



Photo 3-36

Reddish-brown and white chert-rich outcrops of the Eccles Formation directly north of the old Khuma Township. Photograph taken looking towards the south-west.



Photo 3-37

Hand specimen illustrating the sharp contact between the Lyttleton Formation (the upper light brownish-grey chert-free dolomite) and the Eccles Formation (white and black chert). The effect of regional deformation and folding can be seen in the chert beds of the Eccles Formation in the hand specimen (lower parts of the hand specimen). Deformed areas of the hand specimen are associated with a higher concentration of cavernous conditions, as can be observed on a small scale.



Photo 3-38

Panorama view across the KOSH area looking west, standing on the Eccles Formation in the far east. The contact between the Lyttleton Formation and the Eccles Formation can be seen in the central parts of the photo and is characterised in the field by a prominent surface depression, associated with the Lyttleton Formation.



Photo 3-39

Photograph illustrating the highly deformed and brecciated chert and siliceous matrix of the Giant Chert Breccia.



Photo 3-40

Close-up view of a hand specimen of the Giant Chert Breccia illustrating the intense fracturing that occurred in the chert beds.



Photo 3-41

Panoramic view of typical Giant Chert Breccia boulders encountered towards the north-eastern parts of Khuma close to the existing railway line. Photo was taken looking towards the south-west.



Photo 3-42

Bedrock outcrops of the Rooihoogte Formation siltstone exposed in a quarry towards the north-east of Khuma adjacent the existing railway line. Geological pick for scale, positioned along strike of the outcrop (i.e.: north-east/south-west).



Photo 3-43

Photo of the exposed railway cutting at the Vaal Reef mineworkers' village indicating sagging chert bands of the Monte Christo Formation (in the central parts of the exposed profile) representing a Paleo sinkhole / subsidence.



Photo 3-44

Plate 1 of 3 indicating sagging chert bands of the Monte Christo Formation adjacent a dolomite pinnacle exposed along the railway cutting directly east of Stilfontein. The water tower at the so-called Camper Lands (Khuma extensions) is exposed in the background.



Photo 3-45

Plate 2 of 3 indicating sagging chert bands along the existing railway cutting east of Khuma. From the photograph it can be observed that the chert bands seems to be undulating, which could be a result of sagging (i.e.: historic ground movement) or ascribed to structural deformation (i.e.: folding).



Photo 3-46

Plate 3 of 3 indicating sagging chert bands adjacent two dolomite pinnacles at the existing railway cutting east of Stilfontein.



Photo 3-47

Backfilled sinkhole in which trees established north of the Vaal Reef Mineworker's village on the Monte Christo Formation. From the field observations, it seems that the sinkhole was either not properly backfilled, or consolidation occurred after backfilling, resulting in a slight surface depression.



Photo 3-48

Typical photo of a scattered tree encountered across the undisturbed parts of the Monte Christo Formation deemed to be associated with in-filled Paleo karst structures that enable the establishment of trees.



Photo 3-49

Photograph of two poorly expressed subsidences visible in the foreground and central parts of the photo (traceable along the darker patches of grass). These features developed on the Monte Christo Formation.



Photo 3-50

Re-activated backfilled sinkhole along the railway line adjacent existing ESKOM power lines north of Khuma. This sinkhole seems to have been backfilled with mine tailings and dump rock, and was approximately 2 m deep with a diameter of 8 m at the time. This feature developed in close proximity of the contact between the Lyttleton- and Eccles Formation.



Photo 3-51

Typical “suspect” irregularly spaced circular cluster of trees visible across the undisturbed dolomite land of the larger KOSH area, especially across the Eccles Formation north of Khuma. These features do not indicate any pronounced surface expression in the field and seems to be in-filled with reddish-brown transported soil. It is inferred that these features represent in-filled Paleo sinkholes or subsidences, with favourable conditions for the establishment of trees.



Photo 3-52

Shallow backfilled sinkhole along the power lines north of Khuma. This sinkhole formed in the Eccles Formation and is approximately 1 m deep with a diameter of 4 m.



Photo 3-53

Photograph of a subsidence (or partially-activated Paleo sinkhole) located across the Eccles Formation north of Khuma. As seen in the photograph, *Acacia erioloba* (Camel Thorn) trees – known to favour deep, loose, well-drained soil – established in this surface depression. The surface depression is traceable along the burnt velt in the foreground to the far back of the photograph.



Photo 3-54

Surface depressions in close proximity of the contact between the Monte Christo- and Lyttleton Formations north of Khuma Extension 6. The subsidence is approximately 40 m in diameter and is less than 1 m deep.



Photo 3-55

Partially activated sinkhole directly north of Khuma along the Lyttleton- Eccles Formation contact. The sinkhole is less than 1 m deep and has a diameter of approximately 10 m.



Photo 3-56

Photo of a surface depression situated across the Lyttleton Formation north of Khuma. The depression has a north-east-south-west orientation, as can be seen in the photograph (central-bottom of photo towards the middle). The depression developed adjacent shallow bedrock pinnacle outcrops.



Photo 3-57

Partially backfilled sinkhole directly east of the Eagles Creek Golf Club (Stilfontein) situated across the Monte Christo Formation. The sinkhole was less than 1 m deep with a diameter of approximately 15 m at the time.



Photo 3-58

Backfilled sinkhole situated across the Monte Christo Formation directly east of the Eagles Creek Golf Club (Stilfontein). The sinkhole has been backfilled with dump rock, and has a diameter of approximately 5 m.



Photo 3-59

Two shallow sinkholes with diameters of up to 2 m situated across the Eccles Formation north of Khuma.



Photo 3-60

Shallow sinkhole (approximately 2 m deep) with a diameter of approximately 15 m directly north of Khuma situated across the Monte Christo Formation. As can be seen in the photograph, this sinkhole is deemed to represent the activation of a typical “suspect” feature that is associated with scattered trees and shrubs that is not stereotypic across the entire dolomitic area in the region.



Photo 3-61

Plate 1 of 4 of a large sinkhole that formed across the Monte Christo Formation north-east of Khuma Extension 6 adjacent the Kromdraaispruit. The dolomite pinnacles can be seen in the photograph, with unconsolidated and highly weathered material between the pinnacles being eroded away. Khuma Extension 6 can be seen towards the far back (south) of the photo.



Photo 3-62

Plate 2 of 4 of the sinkhole that developed north of Khuma. Toni shaft can be seen in the background. The sinkhole is approximately 10 m deep with a diameter of up to 50 m at surface.



Photo 3-63

Plate 3 of 4: Photograph of the approximately south-eastwardly dipping throat of the sinkhole. From the photograph the shallow overburden covering the sinkhole's throat can be seen



Photo 3-64

Plate 4 of 4: Photograph of the sinkhole throat from the inside of the sinkhole. The sub-vertical slot, along which dissolution occurred, can be seen as it widens towards the lower parts to form a throat.



Photo 3-65

View of a backfilled sinkhole directly north of Khuma Extension 6 across the Monte Christo Formation, visible in the centre of the photo.



Photo 3-66

Panoramic view of a large subsidence with a diameter of approximately 400 x 150 m, north-east of Khuma Extension 6, identifiable by a gentle surface depression and seasonal inundation after heavy precipitation events. This subsidence is associated with an east-west striking fault zone that was identified during the aerial photograph investigation of the area.



Photo 3-67

Panorama view of a series of 8 sinkholes that developed directly adjacent the N12 at Stilfontein (November 2015). Concentric surface cracks are visible in the foreground, and connects the partially developed sinkhole and 8 smaller sinkholes. The larger feature has a diameter of ± 25 m, and leaking infrastructure and disruption of the ground surface during construction works is inferred to be the triggering mechanism.



Photo 3-68

Aerial view of the KOSH area looking south-east towards Khuma. Quartz vein outcrops are clearly visible in the foreground, with localized high concentrations of trees associated with paeleo sinkholes and karst features (bottom-centre of photograph).



Photo 3-69

Panorama aerial view looking east across a major east-west trending tectonic disrupted area (marked in photo – 200 x 70 m partially developed sinkhole) directly north of the old Khuma. Shear-zone associated quartz veins intrusions and breccia outcrops visible in bottom of photo.



Photo 3-70

Panorama aerial view of a combination of three Paleo-sinkholes (marked on the photograph) in the Carletonville area, inserted for reference to the occurrence of such features in the KOSH area. The features are arguably closely associated with structural deformation in the area. The sinkholes have a combined diameter of approximately 600 m and are commonly referred to as “ring structures”.

CHAPTER 4 – Regional hydrogeological setting

4.1 Karst and groundwater

Most karst areas throughout South Africa have been studied in great detail, mainly due to the associated high groundwater potential, and the risk for sinkhole and subsidence formation during artificial lowering of groundwater levels (Martini, 2006). These studies brought to bear the demarcation of various compartments within the dolomite of the Chuniespoort Group across the Transvaal Basin (Holland and Wiegmans, 2009).

Accurate conceptualization of groundwater and surface water interactions are vital for resource management, especially in a dolomite terrain as dolomitic aquifers are associated with large openings such as sinkholes, fractures and sub-vertical joints (or grykes), and interconnected underground cave systems. These secondary openings are responsible for high transmissivity values within the dolomitic succession, and as such, water movement through the dolomite is generally unhindered. The high transmissivity of secondary openings result in high borehole yields and recharge values, but also leaves the aquifer more vulnerable for abstraction impacts and pollution, as contaminants in the recharging water can rapidly enter the profile and spread throughout the aquifer. According to DWAF (2006), dolomite of the Malmani Subgroup forms the most important aquifer in South Africa. Recharge values for different portions of a dolomitic aquifer can vary between 9 and 14 % of the mean annual precipitation, and at least half of the boreholes used for groundwater abstraction from karst aquifers have yields greater than 5 l/s (DWAF, 2006).

4.2 Surface water

4.2.1 Distribution of surface water

Various surface water features (rivers, streams, and dams) intersect regions surrounding the KOSH-area. The regionally prominent southward-flowing Mooirivier River cuts through the dolomitic area for almost half of its length in the direct vicinity of Potchefstroom. The Wonderfonteinspruit is located towards the north of Potchefstroom, and the Kromdraai- and Koekemoerspruit near Stilfontein, which also flow over the dolomite. Two regionally prominent dams are situated on dolomite, including the Boskop Dam north of Potchefstroom, and the Klerkskraal Dam east of Ventersdorp (Figure 4-2). These features are often of importance in dolomitic area, due to its association with structural geological controls.

4.2.2 Precipitation, run-off and evaporation

The precipitation – which are deemed one of the primary means of groundwater recharge – relevant surface-water runoff and evapotranspiration of the various quaternary catchments are detailed in Table 4-1 below (ENPAT, 2006). These all give an indication of the groundwater recharge potential of a dolomitic area.

Table 4-1: Precipitation, runoff and evapotranspiration of various quaternary catchments

Quaternary Catchment	Mean Annual Precipitation (mm)	Mean Annual Run-off (mm)	Mean Annual Evaporation (mm)
C24B	562.5	31.8	1750
C24A	584.04	36.8	1750
C23L	611.65	35.8	1700
C23H	603.5	23.4	1700

4.3 Groundwater

4.3.1 Aquifer types and associated yield capacity

According to the hydrogeological map series of South Africa (2526 JOHANNESBURG; Barnard, 1999), three aquifer types can be distinguished across the study area. These three aquifer types are related to the degrees of porosity, and include intergranular primary aquifers, fractured secondary aquifers, and karstic tertiary aquifers. The main differences between these mentioned aquifer-types are detailed in Table 4-2.

The yield capacity of karstic aquifers may vary throughout the succession. This is predominantly due to the presence, frequency, and size of solution cavities and disseminated voids present in the dolomite bedrock. Such voids can generally range from small interconnected solution cavities and open joints to vast interconnected caverns that extend several kilometres. Well-connected saturated secondary openings may present high yields due to the high transmissivity and storativity it provides. As such these are considered productive aquifers. On the contrary, primary dolomite that is for the most part undissolved and un-fractured may be described as a confining unit with low porosity.

No primary intergranular-type aquifer is distinguishable across the study area. This type of aquifer frequently co-exists with fractured-type aquifers where unconsolidated weathered rock material overlies solid (but fractured) bedrock. In the absence of weathered surficial material, an aquifer is exclusively classified as a karst-type aquifer. Generally speaking, according to the available hydrogeological information of the area, a typical karst-type aquifer has a yielding

capacity greater than 5 l/s, with isolated areas where yields of between 0.5 and 5 l/s can be expected.

Table 4-2: Aquifer classification (after DWAF, 2006)

Porosity	Origin	Aquifer Type
Primary	Groundwater is located within original void spaces left between grains during and after deposition of sediments.	Intergranular Type
Secondary	After sediments lithified to form rock, primary porosity reduces, but fractures in the rock create secondary porosity. Groundwater is located within voids developed after lithification.	Fractured Type
Tertiary	In carbonate rocks, the rock is dissolved by acidic water infiltrating the profile along fractures. This dissolution process causes tertiary porosity.	Karst Type

4.3.2 Groundwater flow in karst aquifers

The rate of groundwater flow is for the most part many orders of magnitude lower than the rate of surface flow. This is ascribed to the occurrence of flow of groundwater being controlled by the effective porosity and hydraulic gradients in the rock, where groundwater flow occurs within pores inside the bedrock. At surface, water can flow unhindered and the flow rate is predominantly controlled by the topographic gradient.

Groundwater flow in karst aquifers generally contains the characteristics of both groundwater- and surface water flow, due to its high porosity. The nature of interconnected fractures and solution cavities of various sizes result in variations of the rate of groundwater movement, where movement rates are generally sporadic rather than uniform as in homogenous aquifers. Groundwater flow in karst aquifers can therefore occur as an open channel manner in an underground stream, or as pipe flow through conduits. (White, 1999)

4.3.3 Dewatering of karst aquifers

The link between large scale dewatering of dolomitic aquifers and sinkhole formation was realised when the Venterspost groundwater compartment was dewatered since 1935 and the Oberholtzer groundwater compartment since 1960. This resulted in the formation of numerous sinkholes and subsidences across the West Rand. The dewatering of the dolomite

compartment was aimed to aid gold mining of the auriferous conglomerates underlying the dolomite (Brink, 1979; Swart, 1991; Wolmarans, 1984). As the water level decreases, hydrostatic pressure is removed from already existing cavities in the dolomite, and the ingress of surface water after heavy rains, together with an increased relative weight of the now saturated overburden, can cause sudden (or gradual) collapse to form a sinkhole (or subsidence) (Brink, 1979). According to Brink (1979), dewatering is defined where the rate of groundwater abstraction exceeds the rate of groundwater recharge. Roux (1984) argues that natural seasonal groundwater fluctuations in dolomite aquifers are regarded as variations of up to 6 m.

Compartmentalization within the dolomite of the Far West Rand (and across other parts of the Transvaal Basin) is structurally bound by Pilanesberg-age dyke intrusions. Pyke and Kleywegt (1982) state that these compartment-forming dykes are generally vertical to sub-vertical and have a thickness of between 6 and 60 m. In the Carletonville area, dykes form impervious barriers between the various compartments, and groundwater discharge occurs at surface as springs.

Most of the dolomitic terrain on a regional scale in the area is characterised by agricultural activities, with groundwater abstraction taking place on various scales. Large-scale dewatering of karst aquifers related to mining occurs in the KOSH-area, as well as the Carletonville and Oberholtzer areas. The geographic extent of the different groundwater compartments is illustrated in Figure 4-2.

4.4 Groundwater-surface water interaction in karst landscapes

4.4.1 Groundwater discharge at springs

Groundwater discharges from karst aquifers where the hydraulic head elevation exceed that of the surface elevation. Water is discharged through fractures or slots in the bedrock, which occurs through springs if the openings are directly connected to surface, and through diffuse discharge in valley bottoms (or where the opening is covered with overburden). Brink (1979) observed that, in the Carletonville area, springs are situated at the intersection of the Wonderfonteinspruit with the western side of the northward trending Pilanesberg-age dykes in the area. This suggests that surface water features intersecting dolomite is fed by groundwater (i.e.: streams are gaining streams).

Springs often constitute more than one eye and are associated with areas where the largest volume of groundwater discharge occurs. Three of the strongest springs in the southern hemisphere (volume-wise) are located on the Malmani Subgroup dolomite in the North West

Province, namely: the Gerhard Minnebron Eye between Potchefstroom and Carletonville, the Oberholtzer Eye, and Bank Eye. The latter two both dried up in 1959 and 1969 respectively, when dewatering of dolomite compartments commenced due to gold mining of the West Rand goldfields.

4.4.2 Regional groundwater level distribution

Due to the strategic importance of karst aquifers as source of water and an associated high vulnerability (DWAF, 2006; Van Rooy & Witthuser, 2008), pro-active management is needed for groundwater abstraction from dolomite to ensure long-term sustainability of the aquifer, and to attempted to prevent sinkhole formation or groundwater pollution. Excessive abstraction across dolomite compartments can cause groundwater levels to decrease significantly, which will cause the formation of sinkholes and subsidences, if no management interventions are implemented.

Current legislation in South Africa enforces holistic and integrated groundwater management. The dominant authoritative bodies responsible for the implication of integrated water resource management (IWRM) include the Department of Water Affairs (responsible for national legislation, including the relevant planning and development thereof), Catchment Management Agencies (responsible for water resource management within its Water Management Area) and Water User Associations (responsible for representing water users) (Riemann *et al*, 2012). Watershed divides (also referred to as water management areas across tertiary- and quaternary catchments) are defined based on surface topography that separates overland runoff into different water catchments. On the contrary, groundwater divides are represented by high water table points and might have no relation with surface divides due to structural geological controls or localized groundwater abstraction. Aquifers with a generally shallow groundwater table tend to correlate well with surface water divides, while deeper aquifers that are isolated from the surface water regime may have little or no correlation with surface water divides.

Groundwater levels in dolomitic aquifers seldom mimic the surface topography (due to their characteristicly high transmissivity) and aquifer divides often represent sudden variations in groundwater levels. It is therefore regarded that groundwater levels often serve as an adequate compartmentalisation parameter as groundwater level discrepancies within a single compartment with a high transmissivity is unlikely.

4.4.3 Groundwater chemistry

Groundwater chemistry and distribution of chemical values often provide useful clues to the origin and interconnectedness of groundwater flow. As such, groundwater chemistry values can be evaluated on a regional scale using the DWAf (2006) guidelines for drinking water quality (Table 4-3), in combination with Piper Diagram plots.

Piper diagrams are ideal for comparing regional water chemistry data, in order to determine the potential origin of water (Figure 4-1). Anions are plotted in the lower right triangle, where plots in the lower right corner of this triangle represents sodium-enriched water, and plots towards the upper left portions represents unpolluted groundwater. Cations are plotted in the lower left triangle, where plots towards the lower right of this triangle represents chloride-enriched water, plots in the lower left corner represents unpolluted groundwater, and plots towards the upper parts of the cation triangle represents mine pollution. Extrapolation of anions and cations towards the upper Piper diagram-diamond gives a final indication of potential groundwater origins.

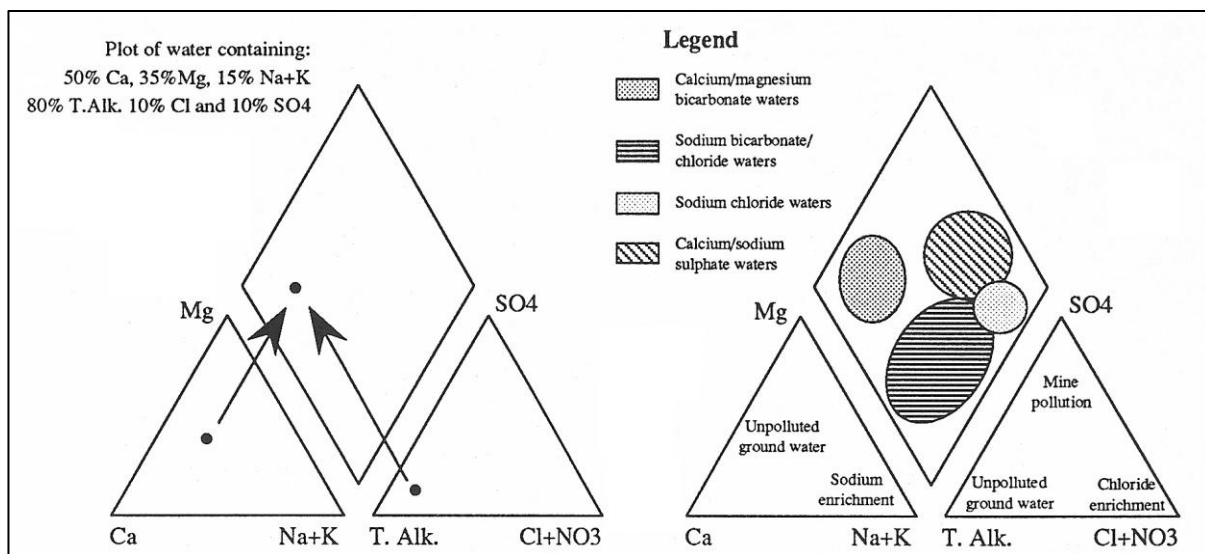


Figure 4-1: Piper diagram plotting procedure and water origins (unknown source)

As such, four potential types of groundwater are broadly recognized:

- (i) Calcium/magnesium bicarbonate (CaMg-HCO₃) water: represents recently recharged groundwater. According to Veltman (2004), high Ca²⁺ and Mg²⁺ concentrations are indicative of recently recharged water.
- (ii) Sodium bicarbonate/chloride (Na-HCO₃) water: Represents dynamic groundwater flow, where Na⁺ replaces the Ca²⁺ and Mg²⁺ in solution.

- (iii) Sodium chloride (Na-Cl) water: Represents relatively stagnant groundwater where very little recharge occurs.
- (iv) Calcium/sodium sulphate (SO_4^{2-}) water: Represents oxidation of sulphate minerals associated with mine pollution and acid mine drainage. Veltman (2004) indicates that elevated SO_4^{2-} (and Cl^- concentrations) concentrations in dolomite environments are deemed indicative of groundwater pollution.

Table 4-3: Water quality chemical classes (after DWAF, 2006)

	Class 0 (mg/l or ppm)	Class 1 (mg/l or ppm)	Class 2 (mg/l or ppm)	Class 3 (mg/l or ppm)	Class 4 (mg/l or ppm)
Physical and aesthetic determinant:					
Conductivity at 25 °C	< 70	70 -150	150 - 370	370 - 520	> 520
pH at 25 °C	5 - 9.5	4.5 - 5 or 9.5 - 10	4 - 4.5 or 10 - 10.5	3 - 4 or 10.5 - 11	< 3 or > 11
Total Dissolved Solids (TDS)	< 450	450 - 1000	1000 - 2400	2400 - 3400	> 3400
Chemical determinant (macro determinants):					
Calcium Dissolved as Ca^{2+}	< 80	60 - 150	150 -300	> 300	
Chloride as Cl^-	< 100	100 -200	200 - 600	600 - 1200	> 1200
Fluoride as F^-	< 0.7	0.7 - 1	1 - 1.5	1.5 - 3.5	< 3.5
Magnesium Dissolved as Mg^{2+}	< 70	70 - 100	100 - 200	200 -400	> 400
Nitrate as N^+	< 6	6 - 10	10 - 20	20 - 40	> 40
Sodium as Na^+	< 100	100 -200	200 - 400	400 -1000	> 1000
Sulphate as SO_4^{2-}	< 200	200 - 400	400 - 600	600 - 1000	> 1000
Potassium	< 25	25 - 50	50 - 100	100 -500	> 500
Arsenic	< .01	.01 - .05	0.05 - 0.2	0.2 - 2	>2
Iron	< .01	0.5 - 1	1 - 5	5 - 10	> 10
Cadmium	< .003	.003 - .005	.005 - .02	.02 - .05	> .05
Class 0	Ideal water quality-suitable for lifetime use.				
Class 1	Good water quality-suitable for use, rare instances of negative effects.				
Class 2	Marginal water quality-conditionally acceptable. Negative effects may occur in some sensitive groups.				
Class 3	Poor water quality-unsuitable for use without treatment. Chronic effects may occur.				
Class 4	Dangerous water quality-totally unsuitable for use. Acute effects may occur.				

4.5 Effects of re-watering on dolomite stability

The requirements to establish the effect of re-watering of dewatered dolomite compartments have been emphasized by Wagener (1982) as a topic requiring further researching.

Current understanding of re-watering of the dolomite aquifer dictates that the effect of re-watering of the dolomite compartment will have a resulting similar effect as dewatering, due to the potential for material to be mobilised. An area that has been dewatered is therefore considered to have a high susceptibility for the formation of sinkholes once dewatering ceases and natural re-watering consequently ensues. It is therefore required that stringent groundwater monitoring in combination with ground surface monitoring is employed in dewatered areas, to detect any formation of sinkholes and subsidences, or the re-activation of rehabilitated sinkholes and subsidences.

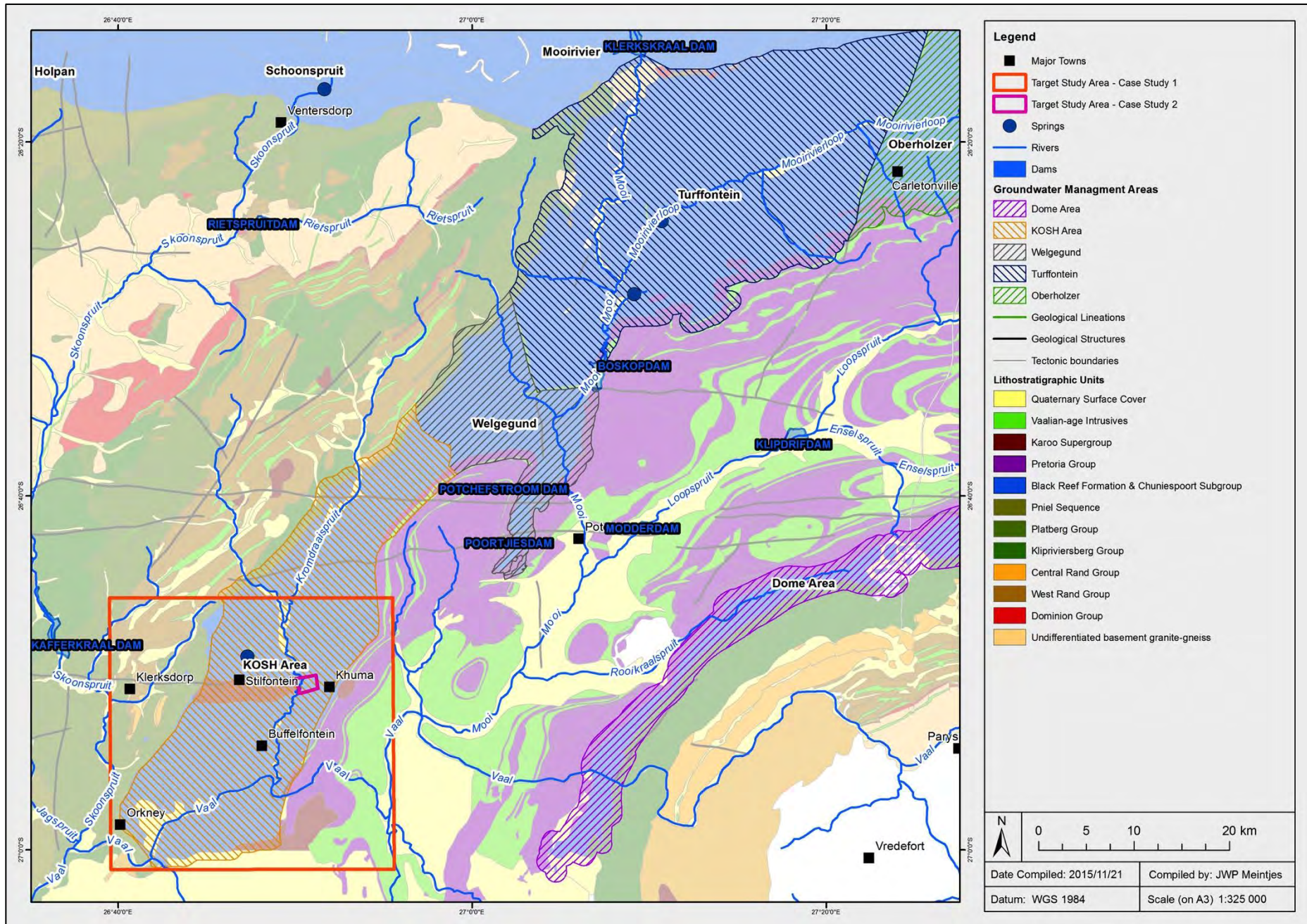


Figure 4-2: Regional distribution of groundwater and surface water features (adopted after DWAF, 2006; and Holland and Wiegman, 2009)

4.6 Development of a regional hydrogeological model

4.6.1 Methodology

The regional groundwater setting of the various dolomitic compartments as demarcated by Holland and Wiegmans (2009) is discussed in order to broadly illustrate the regional hydrogeological setting of the larger study area. The groundwater compartments in the dolomitic strata are demarcated into Groundwater Management Areas (GMAs) across the area, and groundwater management is alternatively managed in terms of quaternary catchments (Holland and Wiegmans, 2009; DWAF, 2006). The rationale behind the methodology for developing the regional groundwater model of the area is detailed in Figure 4-3, and includes the following considerations:

- (i) Groundwater level measurement data obtained from the National Groundwater Archive (NGA) for tertiary catchments C23 and C24.
- (ii) A total of 47 323 groundwater measurements were included, which were reduced to a total of 1 862 measurements after all duplicate values were removed, and only the most recent measurements intersecting the dolomite areas of the study area were considered.
- (iii) Chemical data was requested from the NGA for the relevant area, which contained 5 424 chemical analysis of which 409 were used after eliminating repetitions and data located outside the dolomite area.
- (iv) Groundwater chemistry data was evaluated in terms of the four groundwater classes (class 1 to 4) according to the current DWAF (2006) drinking water standards.
- (v) Registered groundwater use and borehole registration information (WARMS) was obtained to determine the predominant groundwater usage across the regional dolomitic area.
- (vi) Piper diagram plots were constructed in order to derive the origin of the groundwater.

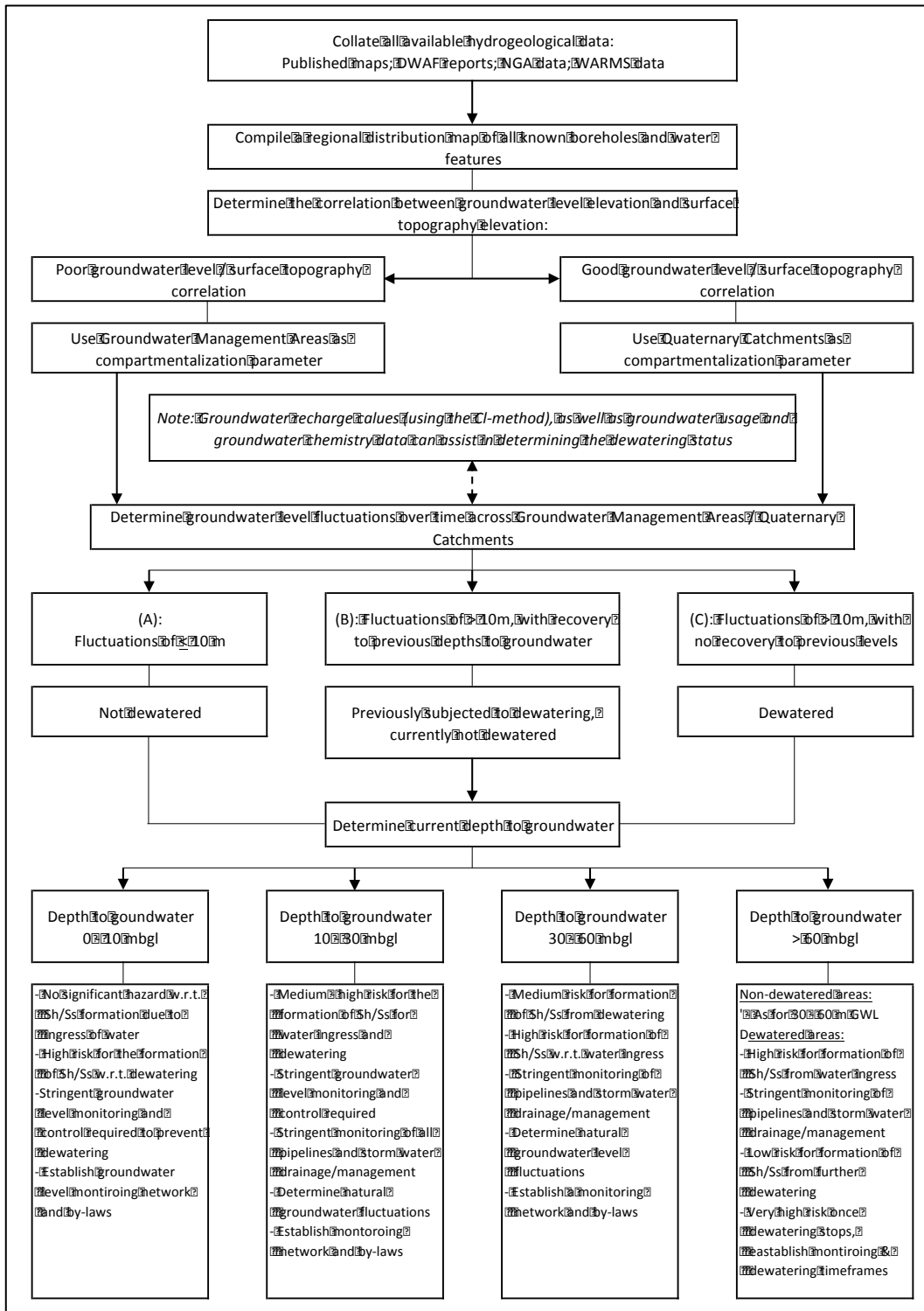


Figure 4-3: Decision support system for developing a regional conceptual hydrogeological model to determine dolomitic management considerations associated with groundwater

4.6.2 Results and discussions

4.6.2.1 Groundwater-surface water interaction

Two GMAs are situated across four quaternary catchments in the larger KOSH-area, and intersect the study area or is situated adjacent to the area (Figure 4-11 and Figure 4-15). It is required to assess adjacent GMAs to determine the effect of dewatering on a regional scale. The correlations between groundwater level elevation and topographic elevations are indicated per GMW in Figure 4-4, as well as per quaternary catchment in Figure 4-5, and are briefly discussed:

- (i) A general groundwater elevation-surface elevation correlation for the whole region might be highly probable, as a linear correlation is apparent. It is also apparent that the groundwater level and topographic elevation correlations within individual GMAs are scattered. Sub-management within these GMAs is therefore crucial for efficient groundwater management as the poor correlation and absence of a cluster or linear distribution suggest sub-compartmentalization within the GMAs. The sub-compartments are inhibiting the zones of high transmissivity to recharge any discharge zones, and balance out the decrease in water level caused by abstraction or differential recharge.
- (ii) The KOSH GMA is located in the Orkney-Stilfontein-Hartebeesfontein area and includes quaternary catchments C23L, C24B and C24A. Quaternary catchment C23L has a shallow groundwater level, while quaternary catchment C24A has a highly variable groundwater level. Scattered information is available for quaternary catchment C24B, but generally indicates shallow depths to groundwater. The quaternary management level is inadequate, as the correlations for both these areas indicate a poor groundwater level-surface elevation correlation, suggesting compartmentalisation.
- (iii) The Welgegund GMA is located in the area surrounding Potchefstroom, as well as the country towards the north and west of Potchefstroom. This GMA includes quaternary catchment C23H. Quaternary catchment C23H indicates a shallow groundwater level, with a central deeper groundwater level (30 to 40 mbgl). The deep groundwater level correlates with localised higher recharge values, supporting the caution required when evaluating recharge as compartmentalization parameter.

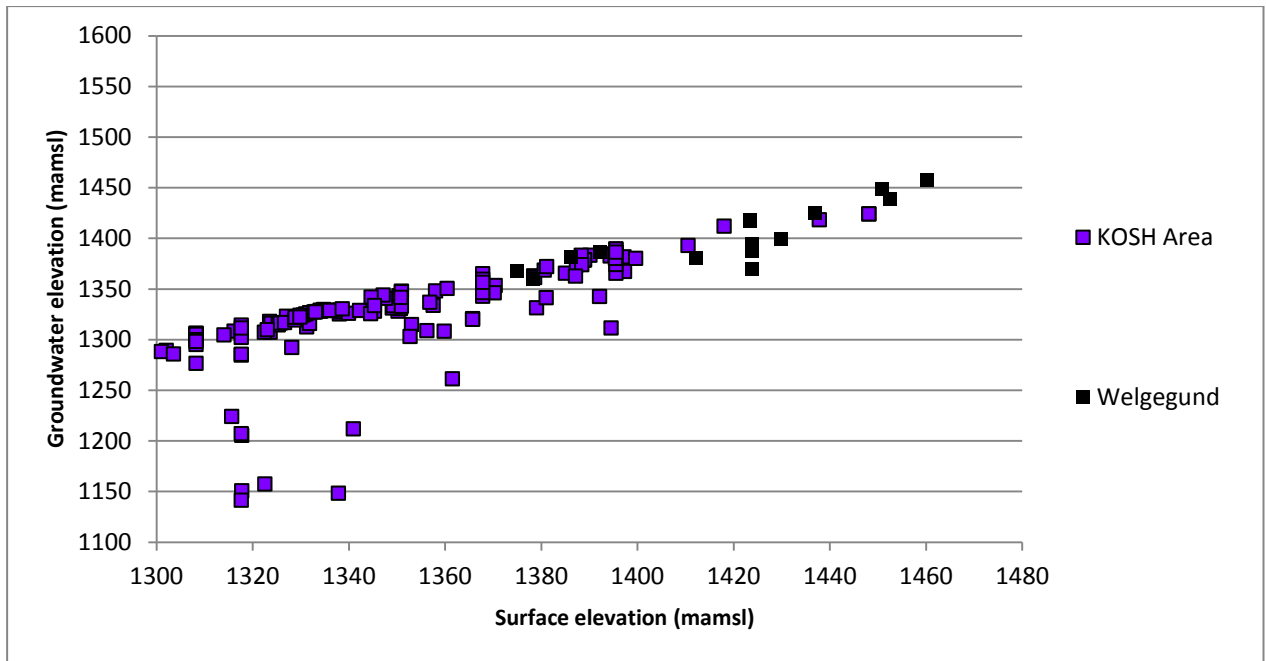


Figure 4-4: Groundwater elevation versus topographic elevation across GMAs

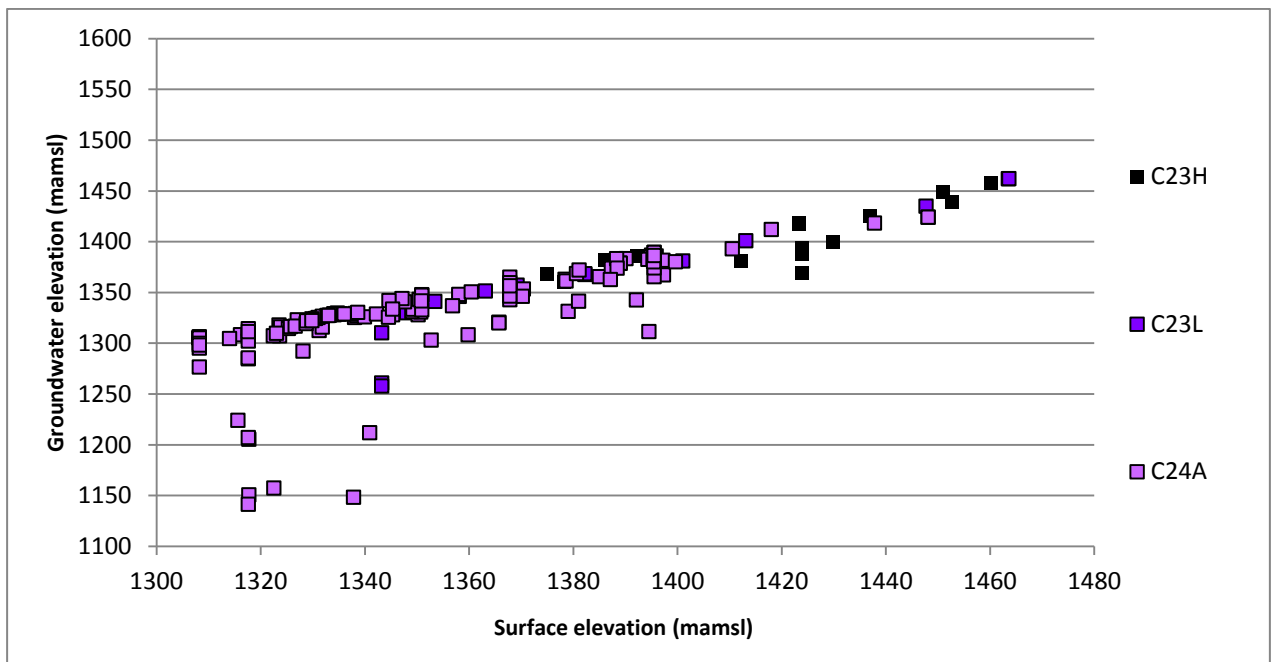


Figure 4-5: Groundwater elevation versus topographic elevation across Quaternary Catchments

4.6.2.2 Groundwater level fluctuations and dewatering

The groundwater level elevation fluctuations over time across the various dolomite compartments are illustrated in relation to each other in Figure 4-6, and local correlations between groundwater levels and precipitation are illustrated in Figure 4-7 and Figure 4-8, and the final dewatered areas for the KOSH groundwater compartment is indicated in Figure 4-10:

- (i) The KOSH GMA illustrates a good correlation between precipitation and water level during the early 1980's as water levels are deeper during times of less precipitation and shallower during times of more precipitation. From 1984 the correlation between precipitation and water levels ceases, as dewatering of the aquifer is clear since this time. While the rainfall in 1990 is similar to that of 1968, water levels are much deeper. During the timespan of between July 1967 and November 1993, the depth to groundwater increased from between 37 and 63 mbgl to between 199 and 219 mbgl in boreholes 2626DD00245, 2626DD00246, and 2626DD00251. The maximum water level fluctuations in these three boreholes were between 161.7 and 180.7 m over the time period. In the same GMA, boreholes 2626DD00240, 2626DD00241 and 2626DD00242 indicated no significant decrease in groundwater level between July 1967 and November 1993. Groundwater levels in these three boreholes fluctuated between depths of 6.3 and 20.8 mbgl, with maximum fluctuations of between 7.5 and 12.3 m. The higher groundwater level elevation of borehole 2626DD00241 is ascribed to the borehole being drilled within the Karoo Supergroup outlier south of Stilfontein, and therefore is deemed to represent a perched groundwater level. It is evident that significantly different groundwater levels occur in the same GMA, which suggest compartmentalisation and emphasises the need for local-scale groundwater management and compartment delineations.

A north-south trending Pilanesberg-age dyke intersects the geological succession in the KOSH area – approximately in the central parts of Stilfontein – which separates the KOSH dolomite compartments into A towards the west and B towards the east (as proposed by Darcy, 2002). Darcy (2002) furthermore sub-divided the KOSH compartment into compartments C and D towards the regions south of the Vaal River (also divided by the same Pilanesberg-age dyke), but no time-series groundwater information is available for these areas. Mining in the KOSH-area is dependent on pumping at Margaret Shaft (approximately 32 Ml/d) in order to prevent possible flooding of underground operations further downstream in the vicinity of the Vaal Reefs operations to the south-west, although operations at Margret Shaft ceased in 1992. The shaft was constructed through the upper

weathered aquifer and the lower karst aquifer of the chert-rich Malmani Subgroup dolomite (Veltman, 2004). Dewatering of the Karst aquifer plays a significant role in the flow dynamics of the area, due to the cone of depression created by groundwater abstraction at Margaret Shaft. Dewatering of the underground workings at Margaret Shaft influence the water levels in the karst aquifer along structural controls, to form a cone of depression, whilst the Pilanesberg-age dyke dictate the shape and extent of the drawdown cone. According to Messrs. L&W Environmental (1993) the extent of the drawdown cone is based on conceptual thinking, and they described three distinct groundwater levels in the area:

- A perched groundwater level at the interface between the overburden and solid bedrock that exhibits seasonal fluctuations of between 1 and 3 mbgl.
- The static groundwater level of the karst aquifer varies at depths of between 5 and 100 mbgl.
- The third is a deep, artificial water level in the mine, representing the level of controlled flooding within the mine workings. The resultant cone of depression has water levels that drop from 1 335 m above mean sea level (amsl), to an estimated 1 000 mamsl, towards the northern regions.

Pretorius (2004) measured water levels in the vicinity of Margaret Shaft in the upper weathered aquifer, which gave no indications to have been influenced by the cone of depression. This suggests that there is very little connection between the upper weathered aquifer and the lower karst aquifer, however, the north-south trending Pilanesberg-age diabase dyke acts as a water conduit between the mine workings and the upper karst aquifer. Rosewarne (1982) determined the areas of maximum fissure flow, with estimated flow rates within the old Stilfontein mine working. These flow rates and directions could prove to be very useful in inferring possible areas where dolomite instability could be anticipated once dewatering of the KOSH compartment B ceases (Figure 6-6). Rosewarne also determined that groundwater abstraction rates (in 1982) at the various mining areas across KOSH, as summarised in Table 4-4. Although no significant amount of water is abstracted from the dolomite aquifer itself, the karst aquifer and the underlying mine workings in the Stilfontein region was described by Rosewarne (1982) to be interconnected, and fractures and jointing in the dolomite serves as conduit to transport water into the mine workings. The abstraction rates at these mine areas can therefore be considered to represent a component of abstraction from the dolomitic aquifer. Rosewarne also stated that the mine working in the Vaal Reefs area is generally

drier, ascribed to the crystalline and generally impervious Ventersdorp Supergroup lavas that separate the dolomite from the Witwatersrand Supergroup. Spangenberg (2000) determined that the rate of groundwater abstraction in the Stilfontein mines area increased since 1982. The highest rates of abstraction was between 1988 and 1993, where approximately 60 000 kl was pumped per day. After 1993, the pumping rates gradually decreased to approximately 35 000 kl per day during 2000. Due to the escalation of re-mining activities since 2005, a significant number of sinkholes and subsidences started to form in the area (Van Deventer, 2015). This is mainly due to an increase in water-bearing infrastructure, disturbance of natural drainage courses and groundwater use.

Table 4-4: Groundwater abstraction rates at various mines across KOSH (after Rosewarne, 1982)

Mine lease area	Operating shafts	Groundwater abstraction rates	
		MI/day from Mine workings	MI/day from dolomite aquifer
Buffelsfontein	4 no. (Pioneer, Orange, Eastern & Southern)	14.4	2.8
Hartebeesfontein	6 no. (Nos. 2, & 4 to 8)	13.1	-
Stilfontein	4 no. (Toni, Charles, Scott & Margret)	49.2	-
Vaal Reefs	9 no. (Nos. 1 to 9)	19.7	-
	TOTAL	96.4	2.8

- (ii) The Welgegund GMA is characterised by groundwater levels that do not fluctuate significantly over time. This GMA was also not subjected to dewatering mainly due to the absence of mining in the GMA. Borehole TMHB03, which indicates a relatively shallower groundwater table, was drilled in Timeball Hill Formation Shale, whereas the remaining two boreholes represents groundwater level fluctuations of the dolomite aquifer. It should be considered that the available time-series information for boreholes in this GMA is concentrated towards the urbanised area in the southeast, and may not necessarily be representative of the groundwater regime of the northern parts of the compartment.

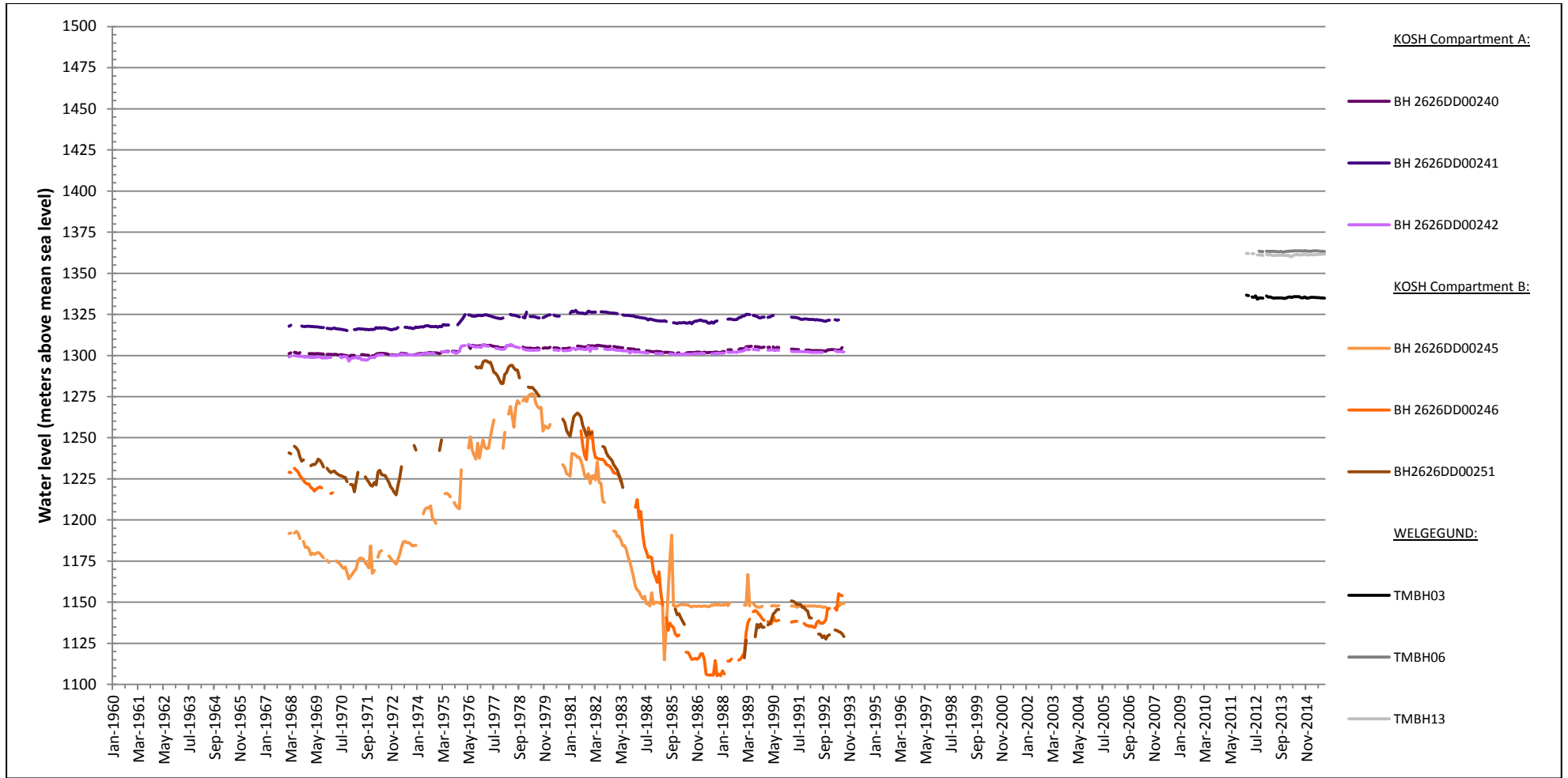


Figure 4-6: Groundwater level elevation time series across all compartments

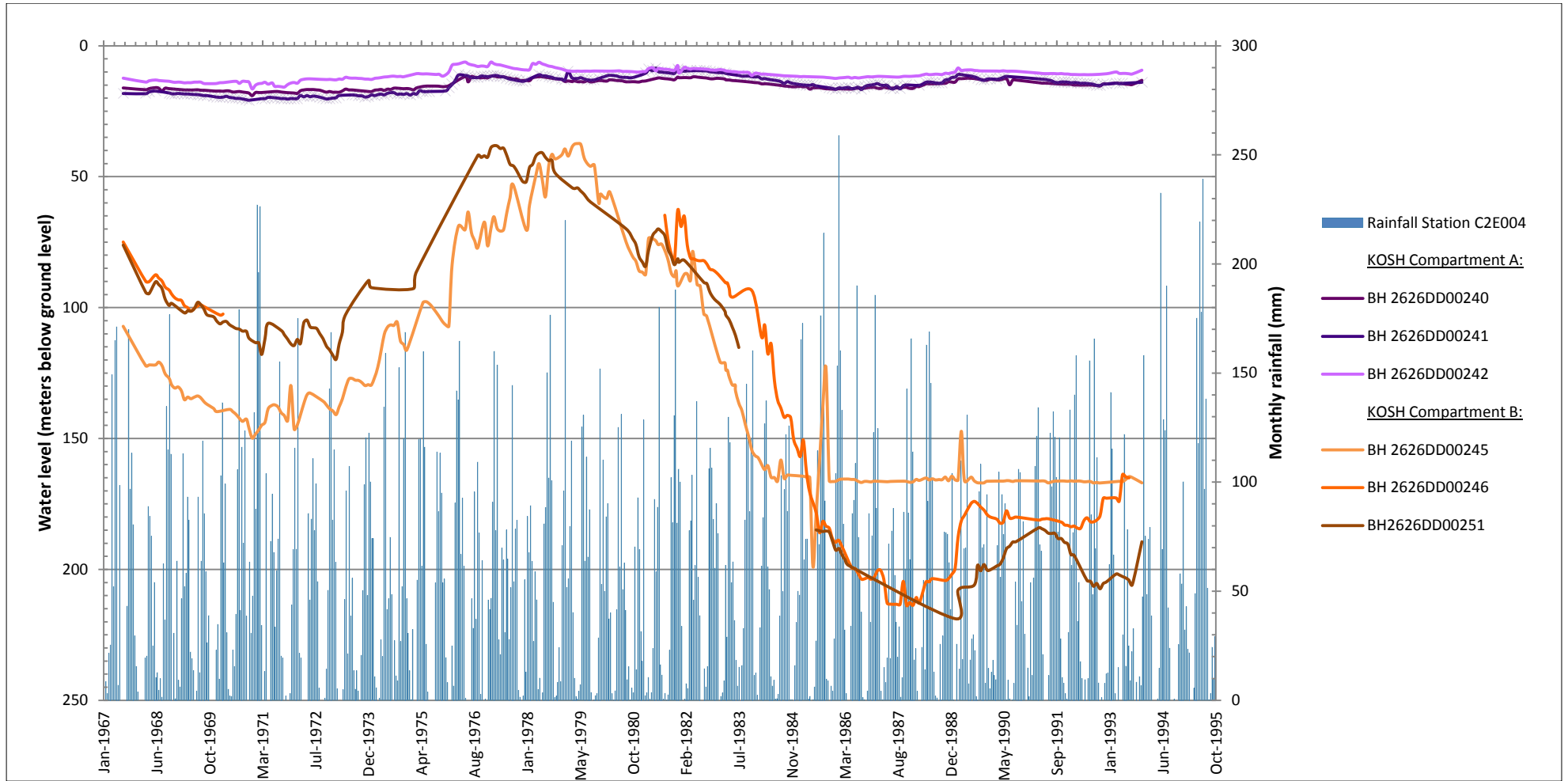


Figure 4-7: Depth to groundwater and monthly rainfall in the KOSH groundwater compartment

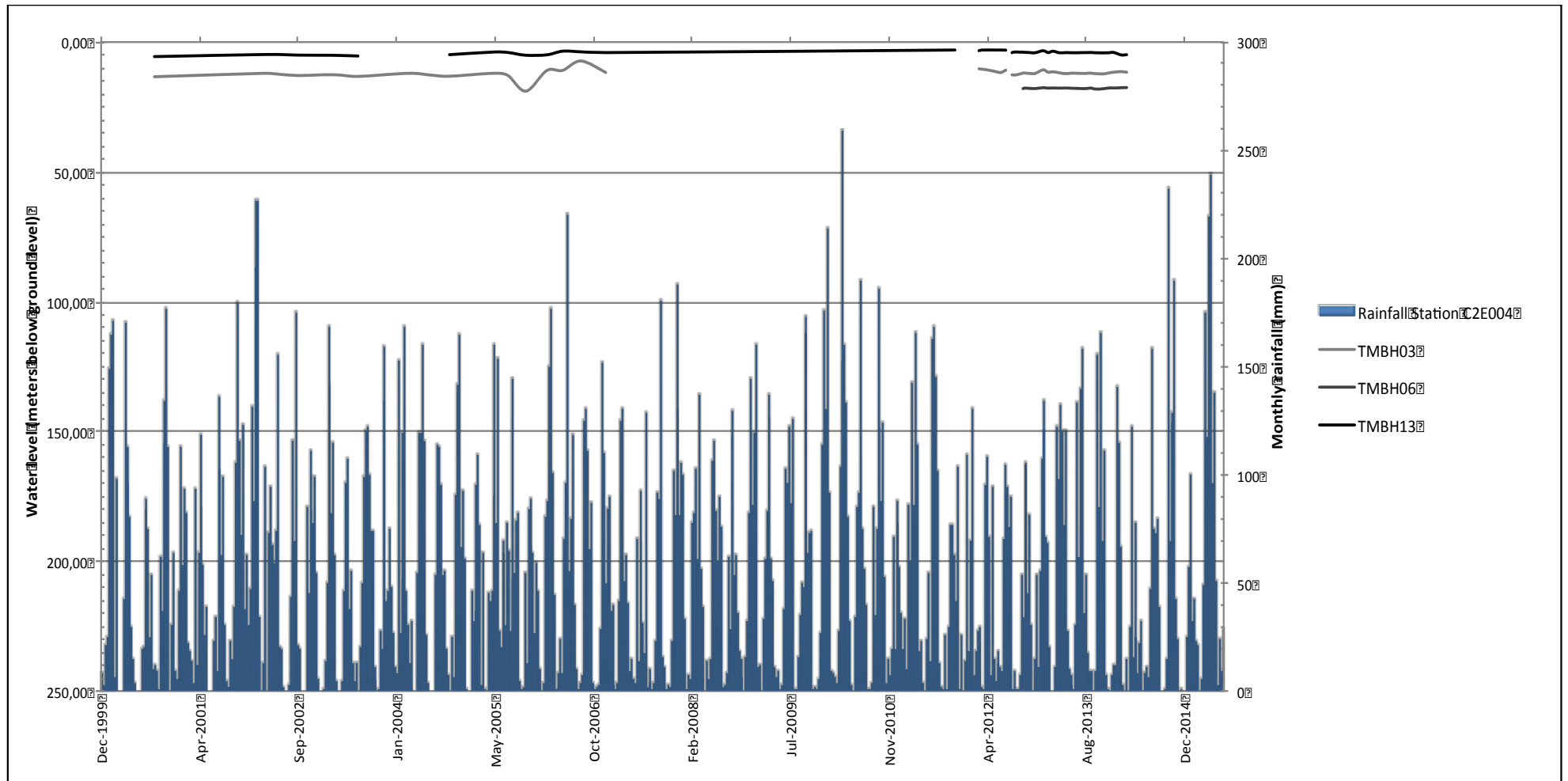


Figure 4-8: Depth to groundwater and monthly rainfall in the Welgedund groundwater compartment

4.6.2.3 Registered groundwater use and regional groundwater quality

The groundwater quality classes for the various GMAs (Figure 4-14 and Figure 4-18) can be summarised as follows:

- (i) Groundwater chemical Classes of the KOSH GMA indicated a highly variably spatial distribution, which could either suggest a highly compartmentalized aquifer, or point source pollution, of which the latter is deemed most likely to be associated with the area. Nonetheless, poor water quality Classes are mainly ascribed to elevated sulphate concentration. Class 3 and 4 groundwater quality classes are all attributed to sulphate contamination, in relationship with elevated levels of calcium, magnesium and nitrate. The isolated Class 2 water quality located in the northeastern sector of the KOSH GMA is correlated to nitrate contamination.
- (ii) The Welgegund GMA is primarily associated with groundwater Class 2.

It is clear from the WARMS data that the dominant activities within the regional dolomitic area are linked with agricultural activities (e.g.: irrigation and livestock), and mining. The distribution of registered water use for agricultural purposes (Figure 4-13 and Figure 4-17) explains the elevated nitrate levels. The mentioned Class 2 groundwater quality isolated to the northeastern sector of the KOSH GMA can be associated with elevated nitrate levels derived from agricultural activities. Groundwater quality Class 4 across the majority of the remainder of the KOSH GMA is associated with mining activity, derived from the high sulphate concentrations.

In general the anion plots of Piper diagram indicates equally concentrated Ca^{2+} and Mn^{2+} enrichments, except for some instances where elevated Mg^{2+} concentrations are encountered across the regional dolomitic area. Anion plots indicate unpolluted groundwater in some areas, and mine pollution in other areas. The overall trend across the entire dolomitic area indicates recently recharged water and acid mine drainage-associated mine pollution (Figure 4-9). The Piper diagram interpretations across the various GMAs can be summarised as follows:

- (i) KOSH GMA: Cations represents approximately equal concentrations of Ca^{2+} and Mg^{2+} , which is representative of unpolluted groundwater. Anions of this GMA are represented by a variable groundwater composition, ranging from unpolluted to mine polluted groundwater. The overall origin of groundwater in the KOSH GMA is clustered in 2 main areas, representing mine-polluted groundwater and recently recharged groundwater.

- (ii) Welgegund GMA: Chemistry data for this GMA is sparse, however available data indicated both sodium enrichment and unpolluted groundwater for this GMA. Anion plots indicate unpolluted groundwater, as well a Cl^- enrichment (deemed indicative of potential groundwater pollution derived from agricultural activities in dolomite areas). The overall groundwater origin in this GMA can be ascribed to polluted groundwater in some areas, and recently recharged groundwater in others.

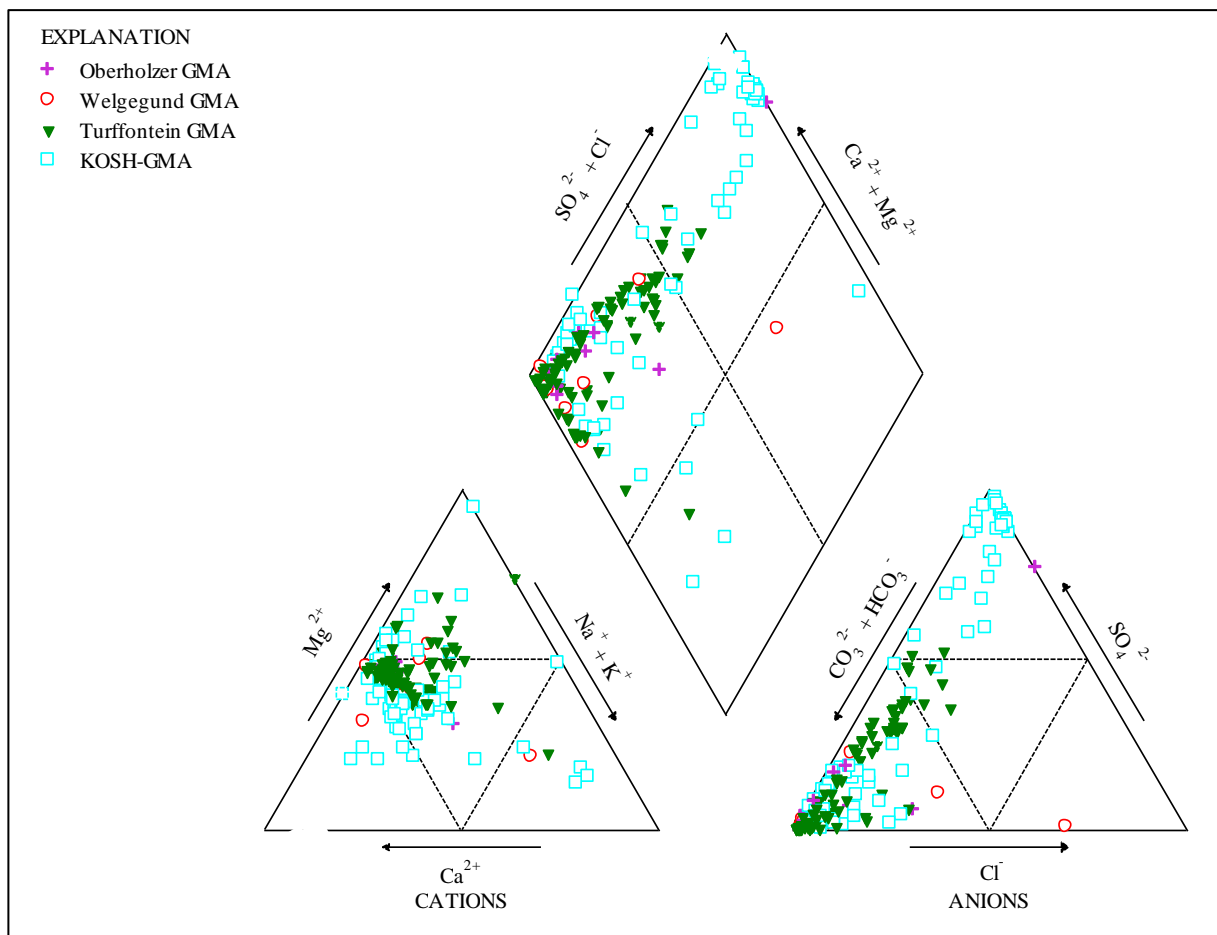


Figure 4-9: Piper diagram plot of groundwater chemistry across the regional dolomitic area

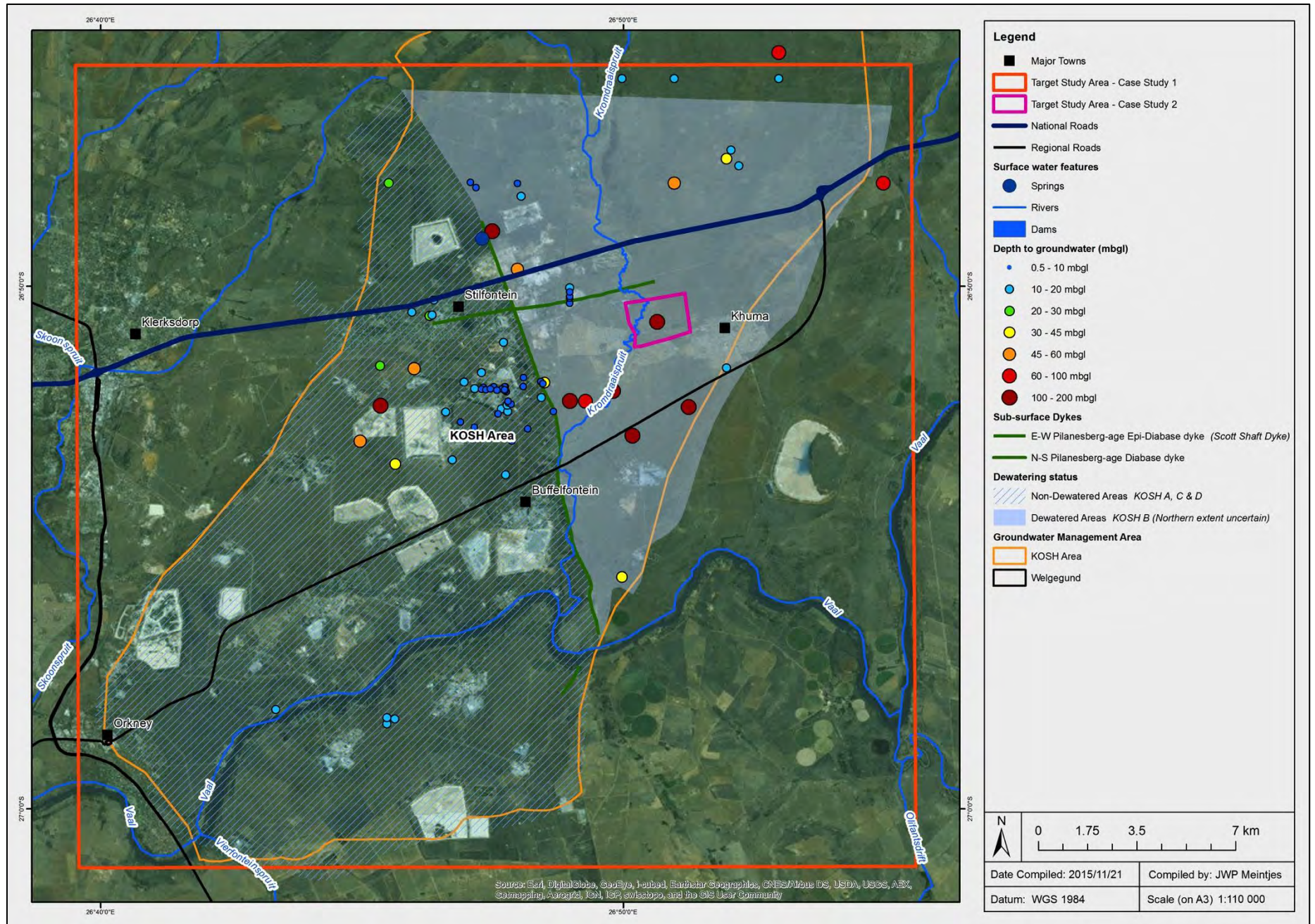


Figure 4-10: Demarcated dewatered areas in the KOSH region

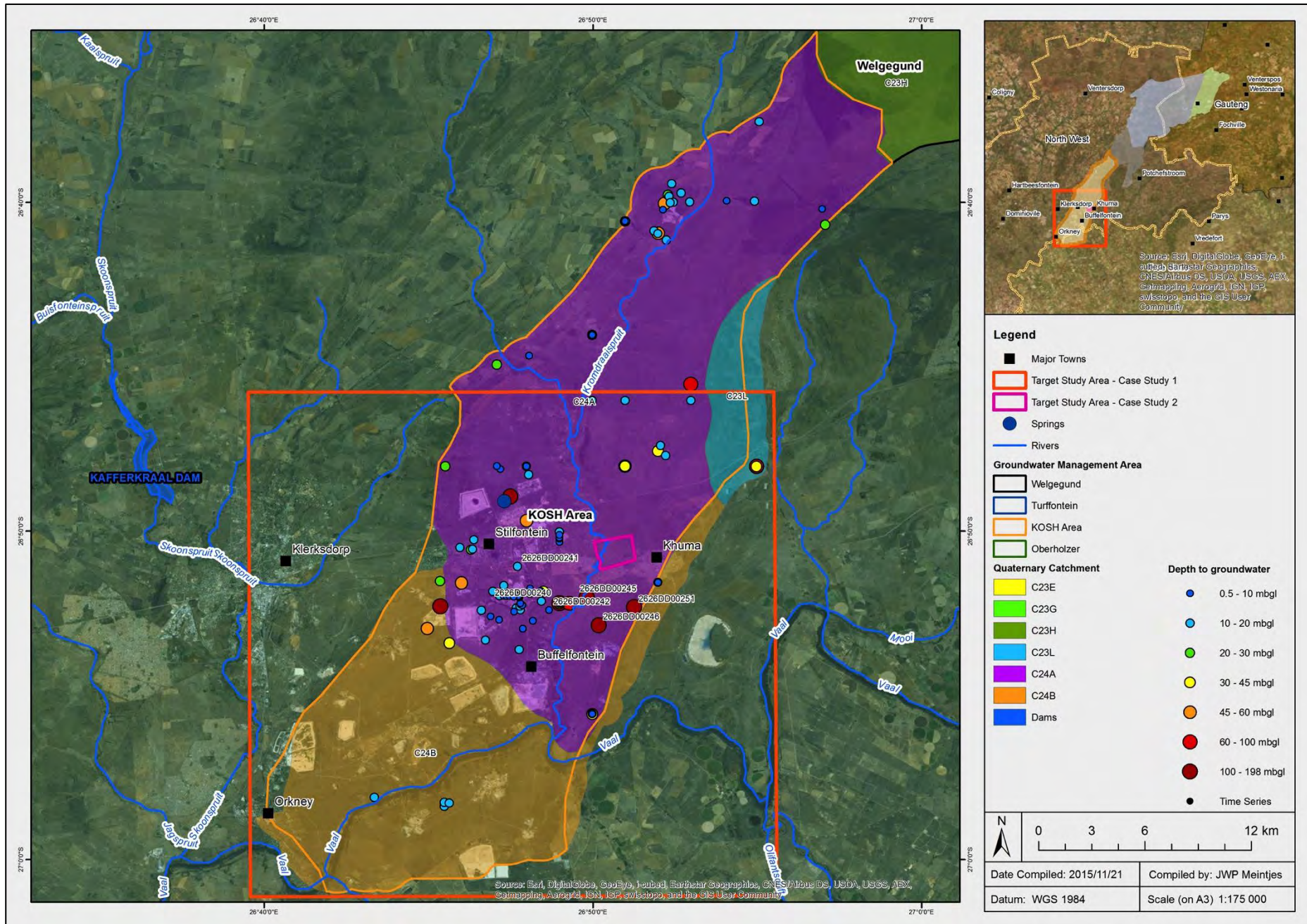


Figure 4-11: Regional groundwater assessment results – KOSH depth to groundwater

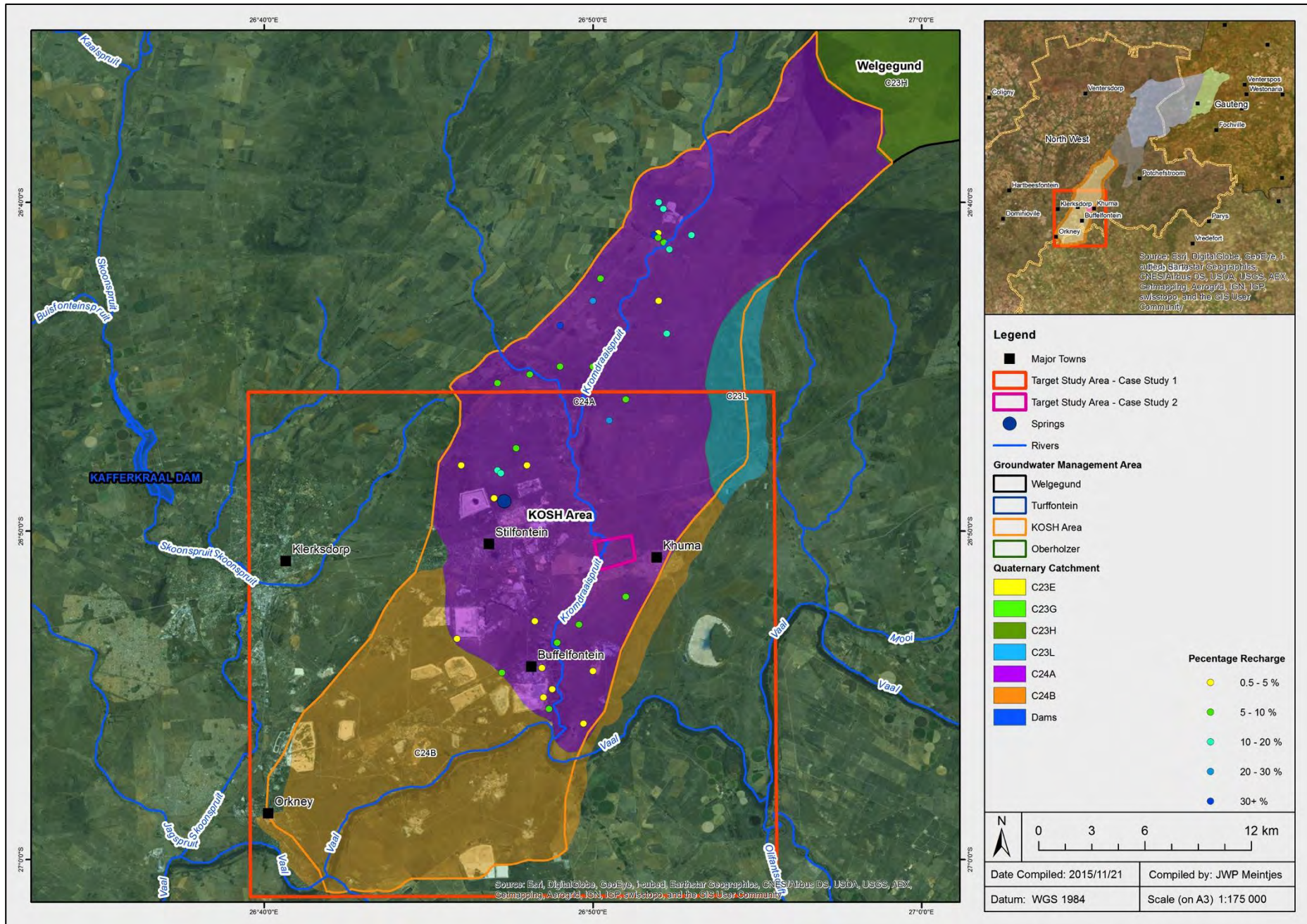


Figure 4-12: Regional groundwater assessment results – KOSH groundwater recharge values

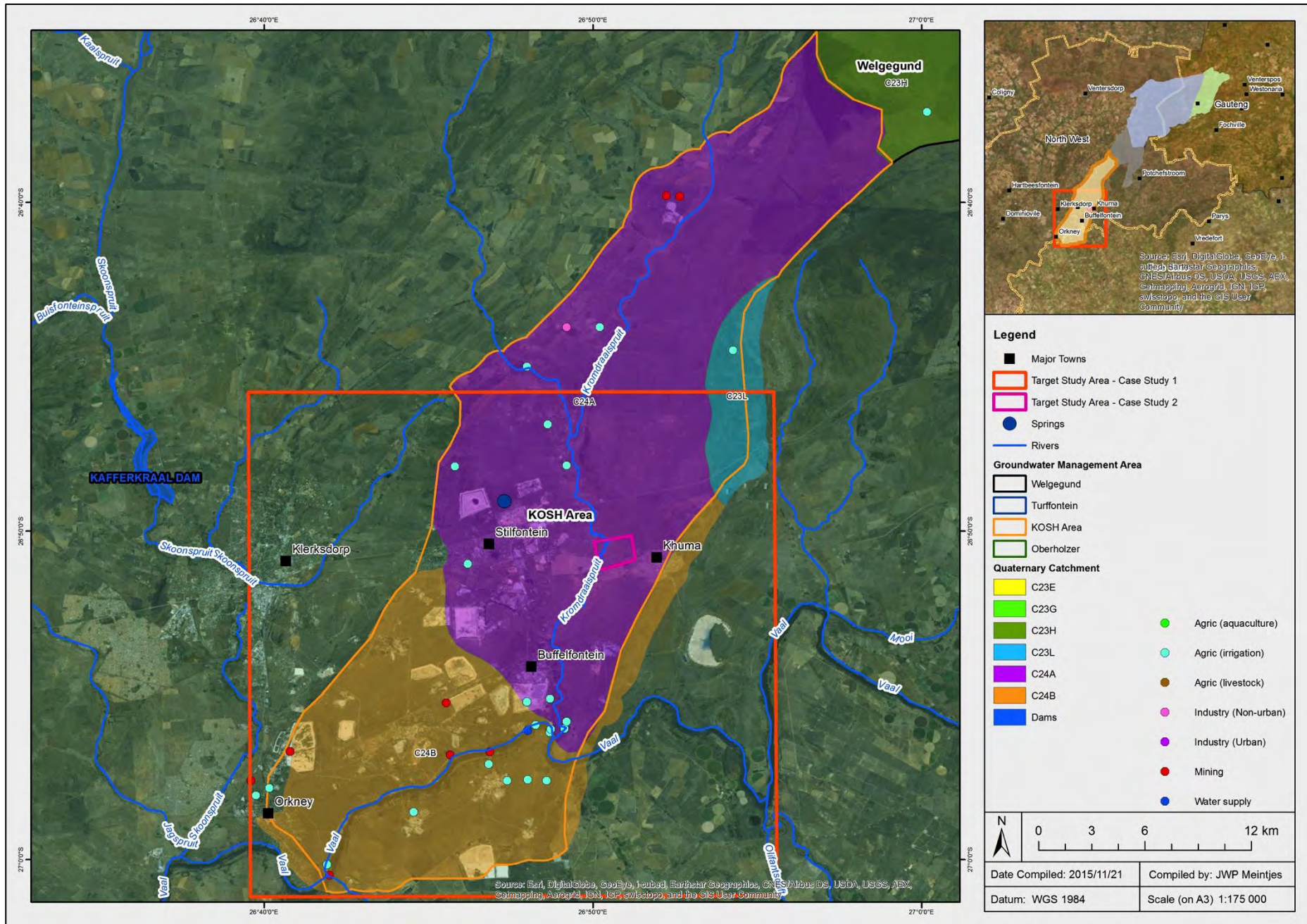


Figure 4-13: Regional groundwater assessment results – KOSH registered groundwater usage

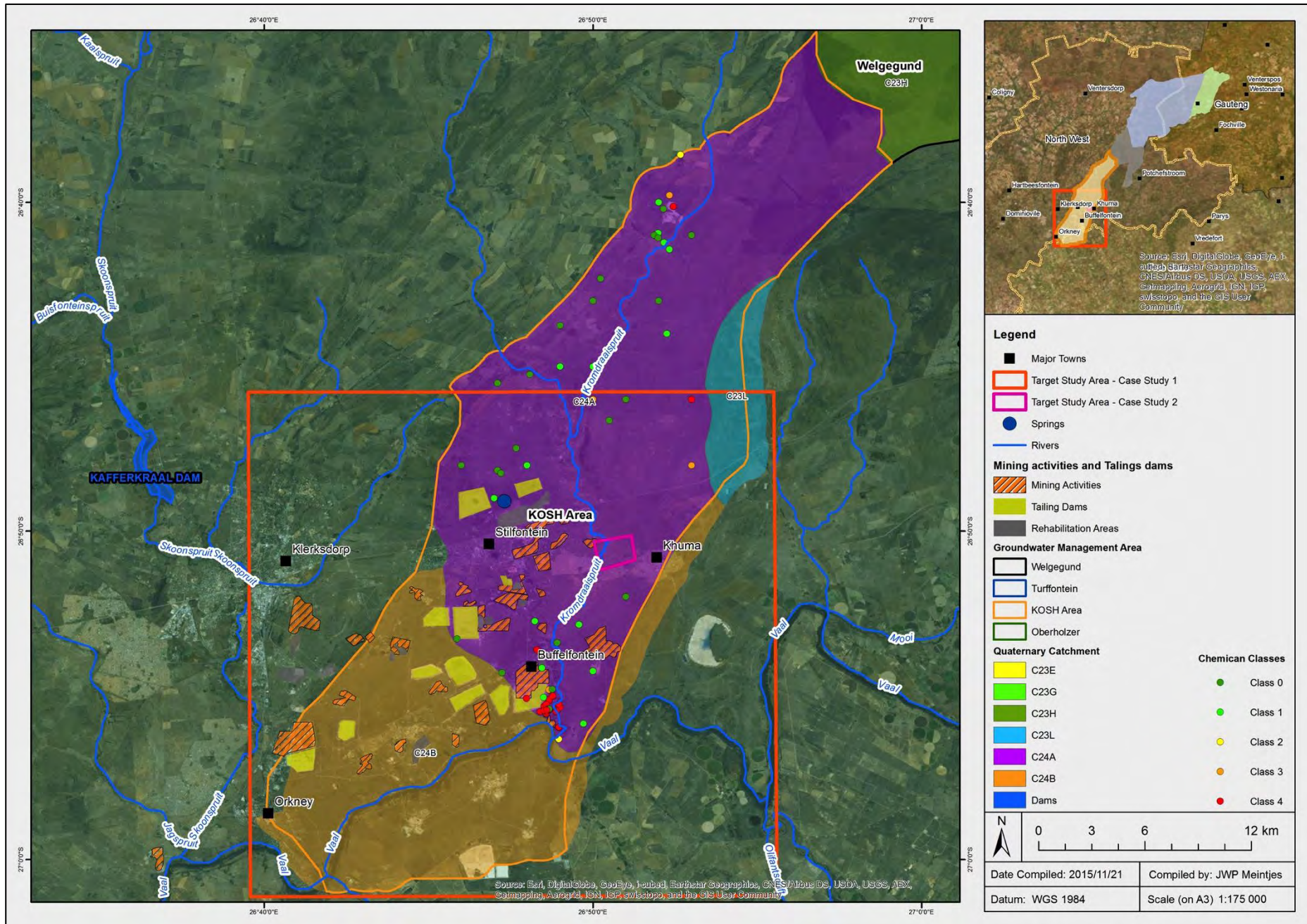


Figure 4-14: Regional groundwater assessment results – KOSH groundwater chemistry classes

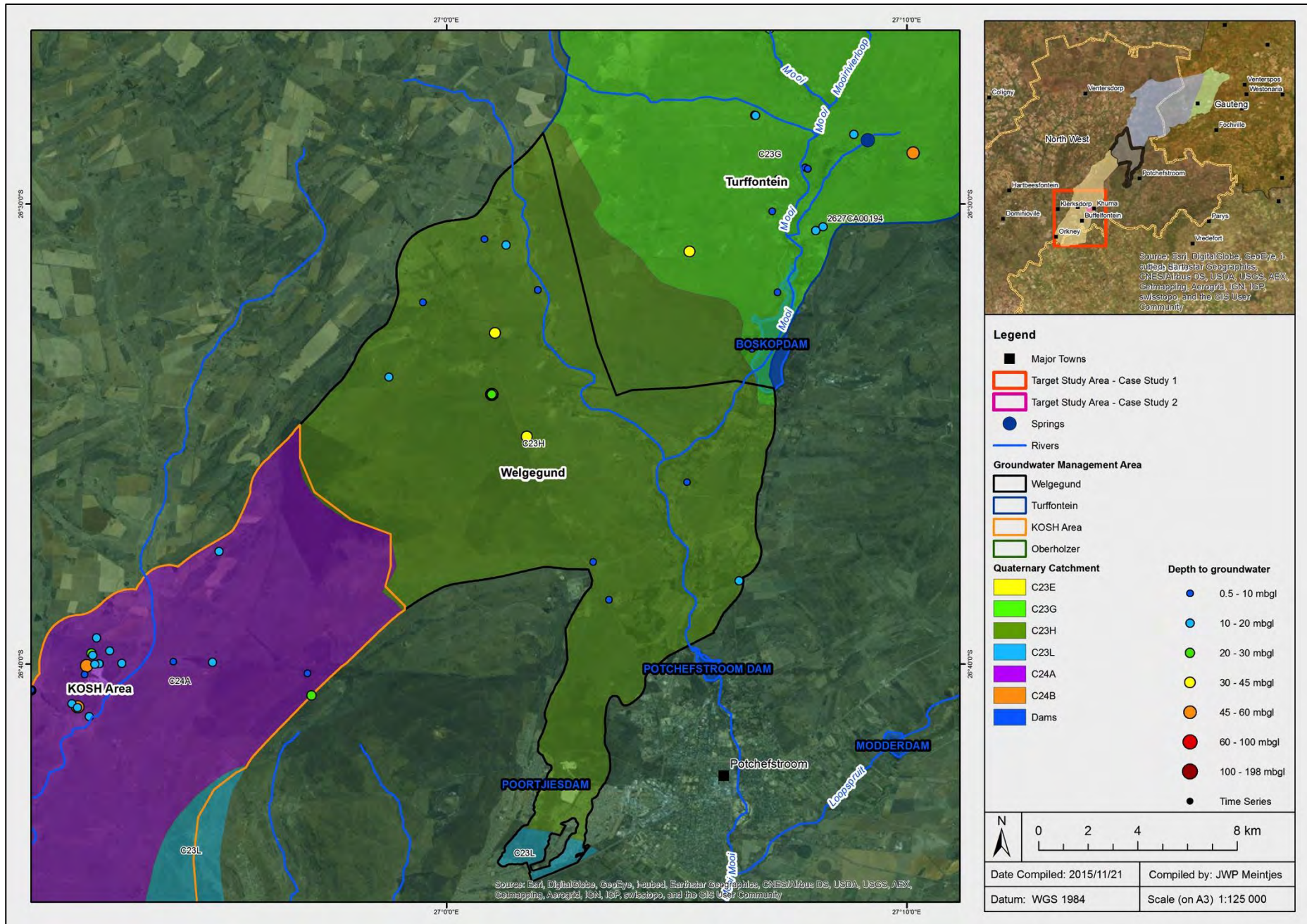


Figure 4-15: Regional groundwater assessment results – Welgegund depth to groundwater

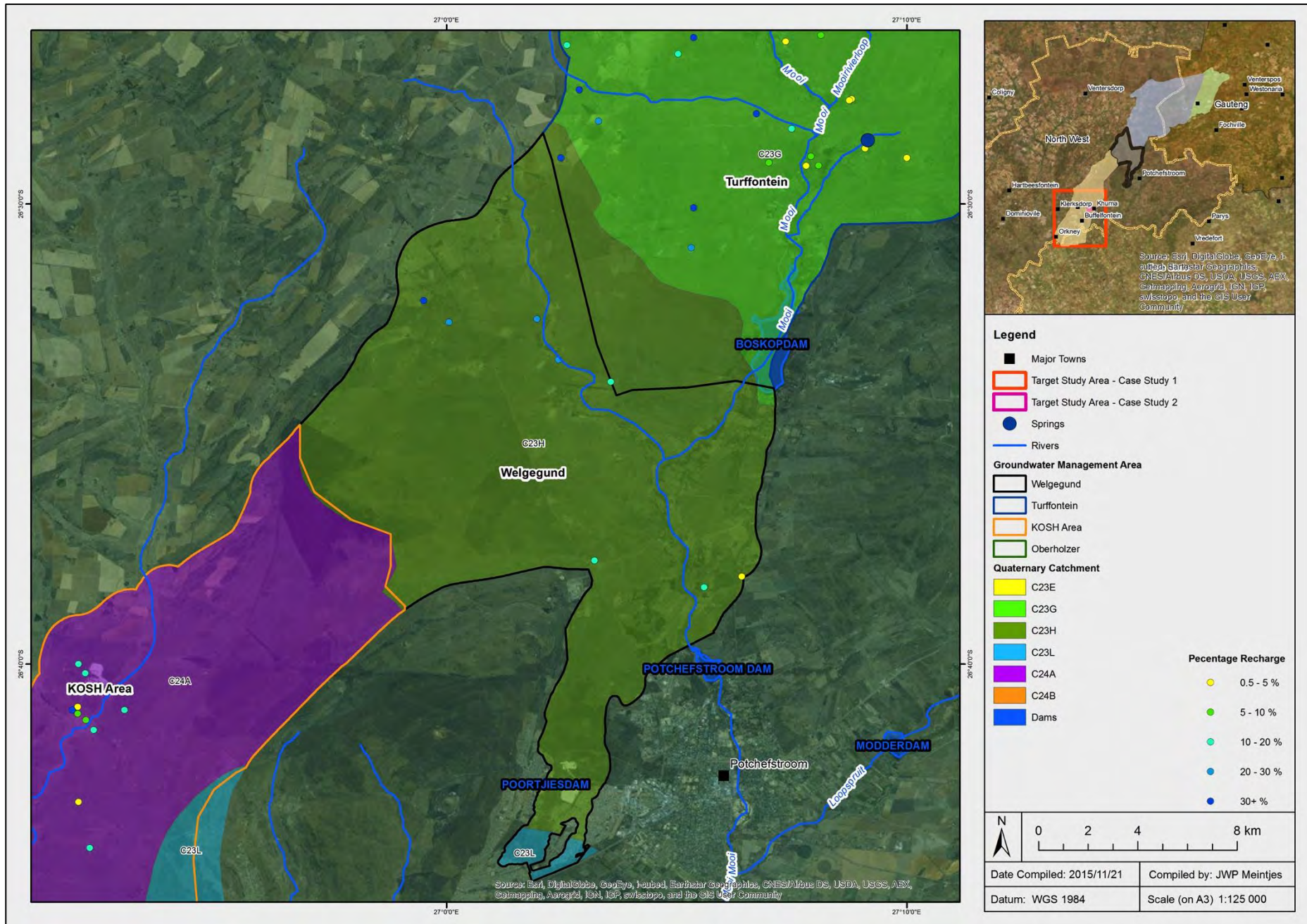


Figure 4-16: Regional groundwater assessment results – Welgegend groundwater recharge values

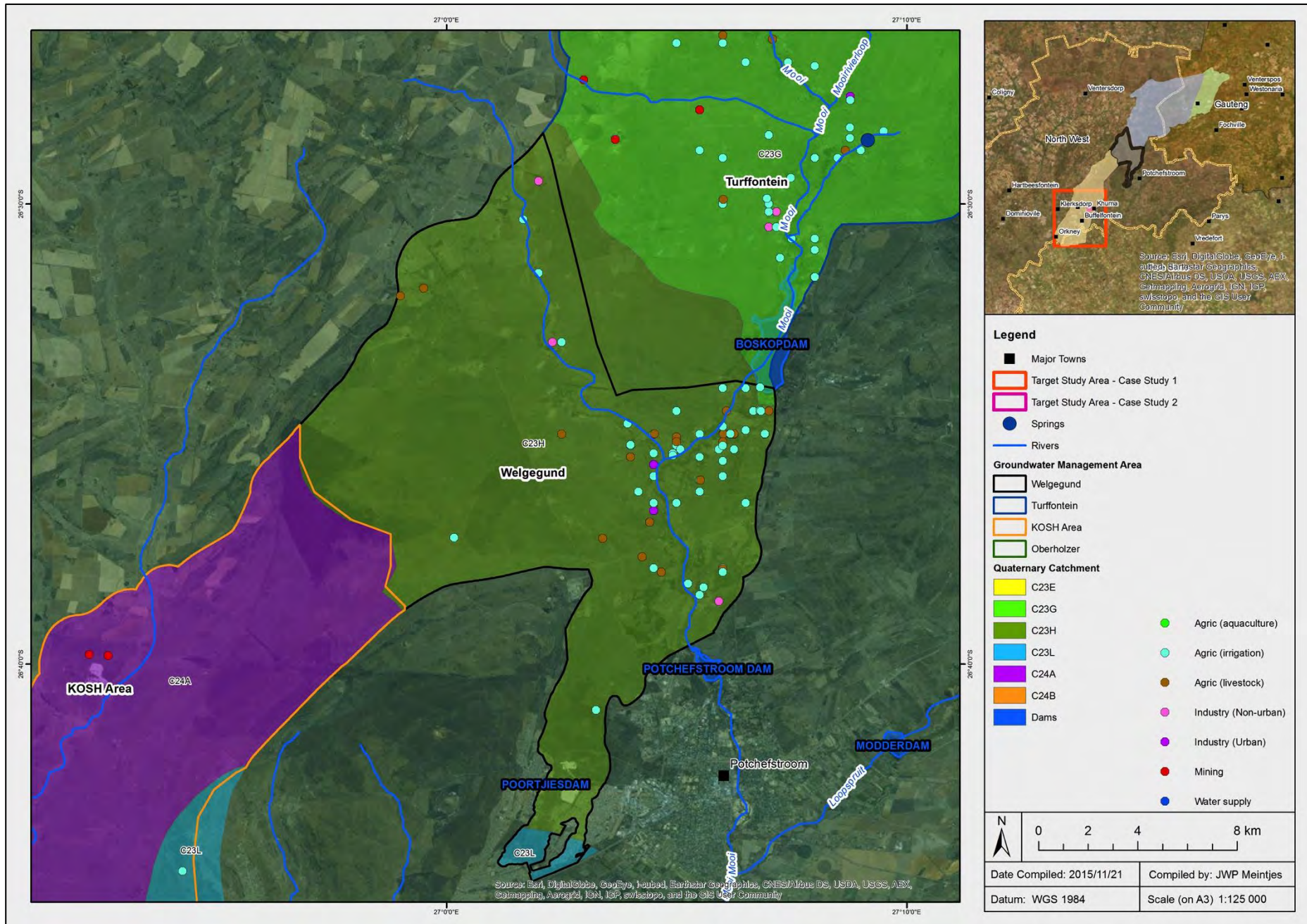


Figure 4-17: Regional groundwater assessment results – Welgegend registered groundwater usage

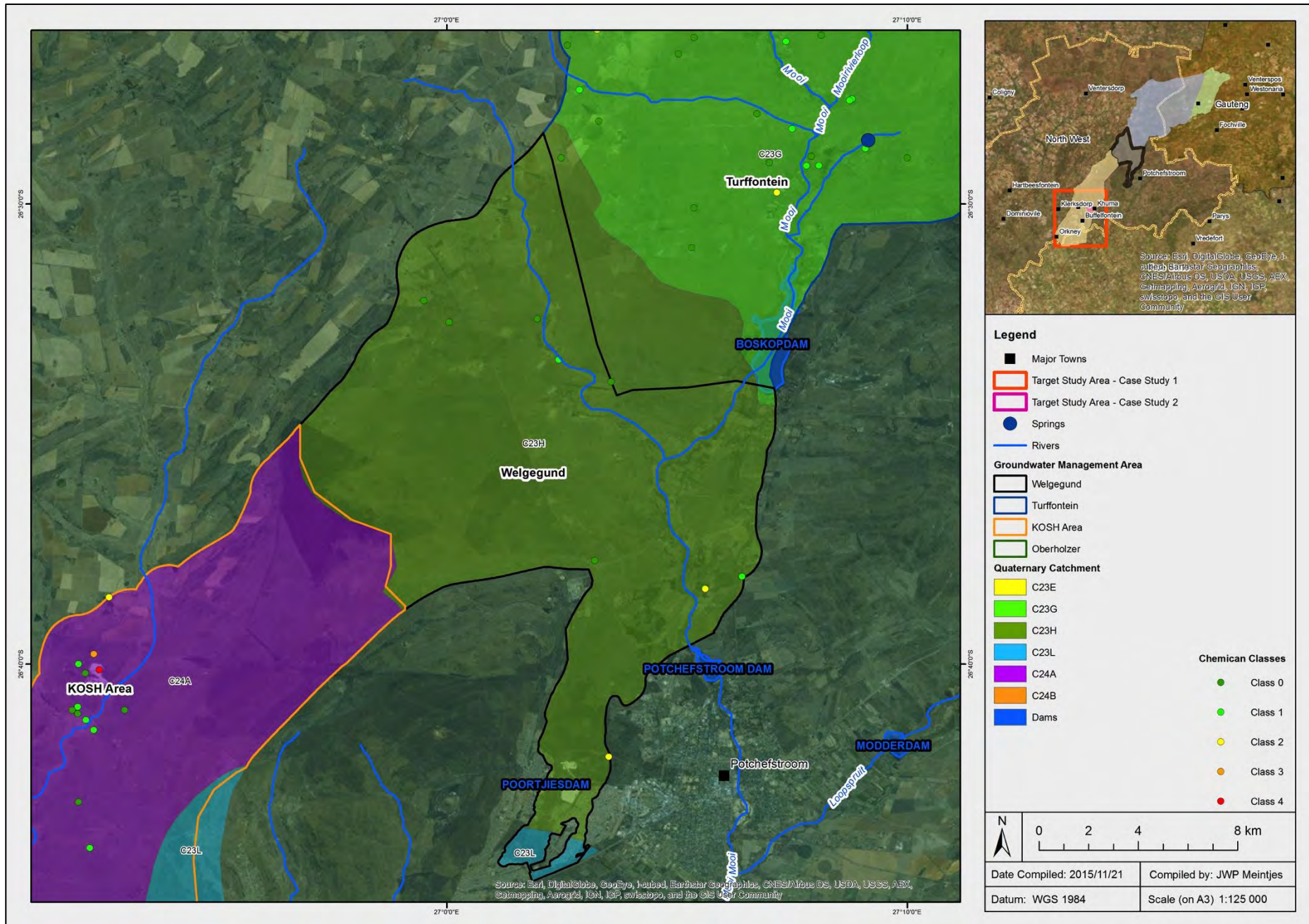


Figure 4-18: Regional groundwater assessment results – Welgegund groundwater chemistry classes

CHAPTER 5 – Case Study 1: Regional dolomite hazard assessment

5.1 Background

The development of the *indicated regional dolomitic hazard* maps, intended for regional risk management and spatial planning, is strongly based on the regional geological and structural geological setting, as well as the hydrogeological setting of the area as discussed in Chapters 3 and 4.

The geological hazard as determined during previous dolomite stability investigations were re-evaluated and incorporated into a single geotechnical hazard map, together with the newly demarcated *indicated hazard* across the area. These were collated into a final regional hazard map as “indicated risk based on inferred dolomitic hazard” and “measured risk based on proven dolomitic hazard” depending on the level and aim of the previous investigations. The boundaries of previous dolomite stability investigations are indicated in Figure 6-2. The geotechnical zoning of these area were re-considered and grouped together where low risk represents IHC 1, medium risk IHC 2 to 4 and high risk IHC 5 to 8, according to the proposed grouping for risk management by the South African Department of Public Works (2006).

5.2 Hazard assessment criteria and methodology

The geological- and hydrogeological models of the area form the basis from which the regional inherent hazard assessment is conducted. All geological, geotechnical and hydrogeological information available at the time was considered, in order to compile a representative model of each (as discussed in Chapters 3 and 4 using the developed Decision Support Systems: Figure 3-10 and Figure 4-1). The geological and structural model is regarded as the fundamental component to this model, and dictates the constraints and parameters for the overburden model as well as the hydrogeological model.

During site-specific assessments, the overburden model is developed and the regional geological- and hydrogeological models are updated using site-specific geo-scientific information obtained, such as detailed hydrocensus of the area, gravimetric surveys and a comprehensive drilling program. As discussed in Chapter 2, SANS (2012) defines the geological model required for a dolomitic terrain as a three dimensional representation of the lithostratigraphic materials that occurs in, and in close proximity, of the project area that is considered for development. This model is based on the acquisition of all geological information – both from existing sources as well as more detailed on-site investigations –

that is represented in the form of a geological map with representative cross sections to illustrate the regional structure of the area. This level of information is generally aimed at detailed geotechnical investigations in support of detailed design and construction on dolomitic terrain. The requirements for compiling the geological model of a project area that is investigated during feasibility level were detailed in section 2.7.4.1

Based on the researched- and available information detailed in Chapters 2, 3 and 4, the following regional classification was decided on, within the limitations of the available regional information. The assessment criteria is summarised in Table 5-1 and compiled into a decision support system (DSS; Table 5-2) to assist in determining the regional indicated hazard classes on a regional scale in support of regional strategic planning and regional dolomite risk management.

Table 5-1 Initial inherent hazard assessment criteria and considerations

Evaluation Criteria	Inferred hazard			
	Low	Med	High	Very High
A. GEOLOGICAL ASPECTS				
(i) Surface geology:				
<u>Areas covered by Pre-Transvaal age non-dolomitic outcrops</u>				TBD (e.g.: structural bound: overturning, folding, faulting). Higher Hazard (if applicable) due to tectonic disturbance.
<u>Areas covered by Post-Transvaal age non-dolomitic overburden:</u>				
Thickness of well consolidated material including: Pretoria Group, Karoo Supergroup & Intrusive Sills ≤ 20 m				
Thickness of well consolidated material including: Pretoria Group, Karoo Supergroup & Intrusive Sills 20 to 60 m				
Thickness of well consolidated material including: Pretoria Group, Karoo Supergroup & Intrusive Sills > 60 m				
Areas covered by > 60 m of well-consolidated, stratigraphically older non-dolomitic rocks (in non-dewatered areas)				No Hazard
Areas covered by > 100 m of well-consolidated, stratigraphically older non-dolomitic rocks (in dewatered areas)				No Hazard
Areas covered by unconsolidated material (e.g.: tertiary and quaternary transported materials of various origins) up to depths of between 60 and 100 m (in non-dewatered and dewatered areas respectively)				
<u>Areas covered by dolomitic outcrops:</u>				
Areas characterized as outcrops belonging to Black Reef Quartzite Formation				
Areas characterized as outcrops belonging to Oaktree Formation				
Areas characterized as outcrops belonging to Monte-Christo Formation				
Areas characterized as outcrops belonging to Lyttleton Formation				
Areas characterized as outcrops belonging to Eccles Formation				
(ii) Faults intersecting dolomite (and associated quartz veins & breccia):				
Areas within 500 m of faults and shear zones				
Areas within 100 m of intrusive, quartz veins and breccia zones				
B. GEOMORPHOLOGICAL ASPECTS				
Topographic low-lying areas (valley bottoms)				
Topographic intermediate areas (foot slopes & mid slopes)				
Topographic high areas (ridge crests, plateaus and escarpments)				
Areas situated within known drainage channel or flood plain, or adjacent known drainage channel or flood plain with slopes < 1% (depending on depth to groundwater)				
Occurrence of karst associated surface topographic features (i.e.: circular or oval-shaped negative topographies, lineations with negative relief etc.)				

C. CURRENT STABILITY CHARACTER OF THE AREA				
(i) Pretense of voids in overburden and/or bedrock:				
Extent of cavities and voids (from previous drilling) within 30 m of surface				
Extent of cavities and voids (from previous drilling) 30 to 60 m of surface				
Extent of cavities and voids (from previous drilling) deeper than 60 m of surface in dewatered areas				
Extent of cavities and voids (from previous drilling) deeper than 60 m of surface in non-dewatered areas				
(ii) Existing instability features and history of damages to structures:				
Areas in proximity of known/rehabilitated sinkholes and subsidences				
Damage to structures / demolishing of structures occurred historically due to instability				
D. HYDROGEOLOGICAL ASPECTS				
(i) Depth to groundwater (per groundwater compartment):				
Areas where current depth to water table is 0 to 10 mbgl, and inferred to be situated within the dolomite residuum, transported material or dolomite bedrock				
Areas where current depth to water table is 0 to 10 mbgl, and areas where the water-table is situated within stratigraphically younger non-dolomitic rocks (excluding transported material)				
Areas where current depth to water table is 10 to 30 mbgl, and inferred to be situated within the dolomite residuum or dolomite bedrock				
Areas where current water table is between 30 and 60 mbgl, and situated in dolomitic residuum or dolomite bedrock				
Areas where current water table is deeper than 60 mbgl and inferred to be situated within the dolomite residuum or dolomite bedrock				
(ii) Groundwater fluctuations over time:				
Areas where the natural water table fluctuations is ± 6 m over time, and <u>not</u> situated within 5 m of the dolomite rock head, or situated deep within the hard rock dolomite				
Areas where the natural water table fluctuations is ± 6 m over time, and situated within 5 m of the dolomite rock head				
Areas where the natural water table fluctuations is $> \pm 6$ m over time, or where the water table is situated within the dolomite residuum				
Dewatered areas - current or historically (hazard associated re-watering)				

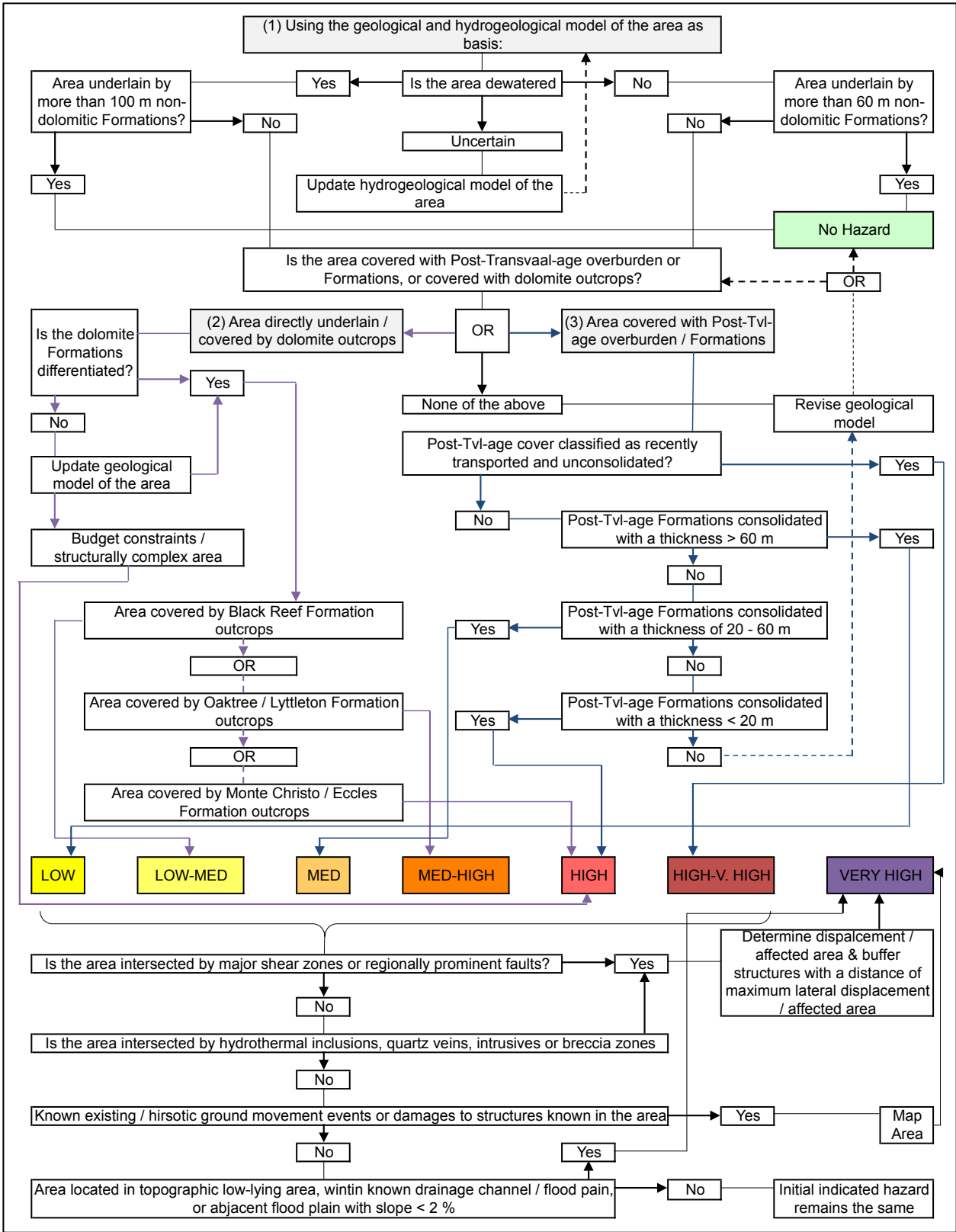


Table 5-2: Decision support system to determine indicated inherent hazard of an area for regional planning and risk management purposes

5.3 Discussion and regional hazard maps

Based on the above-mentioned criteria, *regional inherent hazard zones* were delineated across the KOSH-region, and the extent of dolomite land demarcated. These indicated hazard zones (total of 5) are indicated in Figure 5-3 and Figure 5-4.

Key areas for site-specific consideration are demarcated on the above-mentioned figures, and further geotechnical investigation requirements are detailed in Table 6-4 (Annexure 4).

5.3.1 Overview of sinkholes and subsidences across the KOSH-area

When considering the ground movement events (including sinkholes, subsidences and concentric surface cracks) that were researched and identified across the KOSH-area, the following assumptions, results and interpretations can be drawn:

- (i) The extent of ground movement events was only considered across the demarcated project area (Case Study 1 area), which covers the area from south of the Vaal River towards directly north of the N12 national route. Based on the determined extent of dolomite land (up to a depth of 100 m), a total surface area of approximately 390 km² is underlain by dolomite across the demarcated study area.
- (ii) The northern-most extent of the dewatered KOSH groundwater compartment B (discussed in Chapter 4) is uncertain. As such, this boundary was arbitrarily selected along an east-west section where the area under investigation ended. Subsequently, the dewatered extent of dolomite land across the study area covers approximately 139 km², and the non-dewatered area approximately 251 km².
- (iii) The dataset of ground movement events presented in this study is not considered to be 100 % complete. It is expected that a large number of sinkholes and subsidences previously un-reported and backfilled occurred across the area. This also include some existing features may have been missed.
- (iv) The size distributions of the various features are generally not mentioned in the researched technical correspondence, and sizes were subsequently measured from aerial photographs (except for 21 features).
- (v) Based on the research conducted, the oldest recorded ground movement event in the area occurred during 1978. As such, the timeframe used for calculating the rate of ground movement formation (e.g.: number of events / km² / annum) was taken as 37 years, ranging from 1978 to 2015.

- (vi) The ground movement events that are included as part of the statistical analysis included both inferred (from aerial photography) and field verified events.
- (vii) It was found, based on field observations and personal communications with Van Deventer (2015), that the majority of the sinkholes in the KOSH-area consist of throats that are south-east dipping (along the regional dip direction of the geology). It was found that the sinkholes identified in the field very often manifest as a number of smaller sinkholes that are inter-connected with concentric surface tension cracks. As such, it is inferred that a number of these events represent the re-activation of previously backfilled sinkholes.
- (viii) A large majority of the sinkholes and subsidences, especially along the eastern regions of the study area, were found to be closely associated with north-east/south-west trending geological structures.
- (ix) A total of 255 ground movement events were researched and identified across the study area. These features represent sinkholes, subsidences, and Paleo-sinkholes/subsidences. The following statistical analysis can be drawn from the data:
 - a. The total number of events per km² across the dewatered areas were calculated as 0.87 events / km² (e.g.: 121 events / 139 km²).
 - b. The total number of events per km² across the non-dewatered areas were calculated as 0.53 events / km² (e.g.: 134 events / 251 km²).
 - c. The combined total number of events per km² for the entire study area is 0.65 events / km² (e.g.: 255 events / 390 km²).
 - d. The rate of new sinkhole formation (NSH) across the dewatered areas is 0.02 events / km² / year (e.g.: 121 events / 139 km² / 37 years).
 - e. The rate of new sinkhole formation (NSH) across the non-dewatered areas is 0.01 events / km² / year (e.g.: 134 events / 251 km² / 37 years).
 - f. The overall rate of new sinkhole formation (NSH) for both dewatered- and non-dewatered areas was calculated as 0.02 / km² / year (e.g.: 255 events / 390 km² / 37 years). As such, according to the definitions of karst for engineering purposes proposed by Waltham & Fookes (2003), the KOSH area can be classified as “*Mature Karst*”.

g. When considering the overall rate of new sinkhole formation (NSH) across the entire study area, a total of 6.9 events can be expected per year (e.g.: $0.02 \times 390 \text{ km}^2$). It should be noted that the total number of expected events per year would be less if the dolomitic area used in the calculation was increased.

(x) The size- and feature type distributions across the various lithostratigraphic subdivisions of the Malmani Subgroup are summarised in Table 5-3 and illustrated in Figure 5-1.

Table 5-3: Distribution of sinkhole and subsidence dimensions across the various groundwater compartments and geological formations in the KOSH area

Feature type and groundwater status	Total	Vmo	Vmm	VI	Ve	Ecca	Area Size (km ²)
Number of Events - Whole Area	255	8	180	45	20	2	390
Number of Events - Dewatered Area	121	7	66	33	18	-	139
Number of Events - Non-dewatered Area	134	1	114	12	2	2	251
Number of Sinkholes - Whole Area	200	7	145	37	9	2	390
Number of Sinkholes - Dewatered Area	95	0	59	25	9	-	139
Number of Sinkholes - Non-dewatered Area	105	7	86	12	-	2	251
Number of Subsidences - Whole Area	55	1	40	8	11	0	390
Number of Subsidences - Dewatered Area	26	1	7	8	9	-	139
Number of Subsidences - Non-dewatered Area	29	0	33	0	2	-	251

*Vmo = Oaktree Formation, Vmm = Monte Christo Formation, VI = Lyttleton Formation, Ve = Eccles Formation, Ecca = Ecca Group.

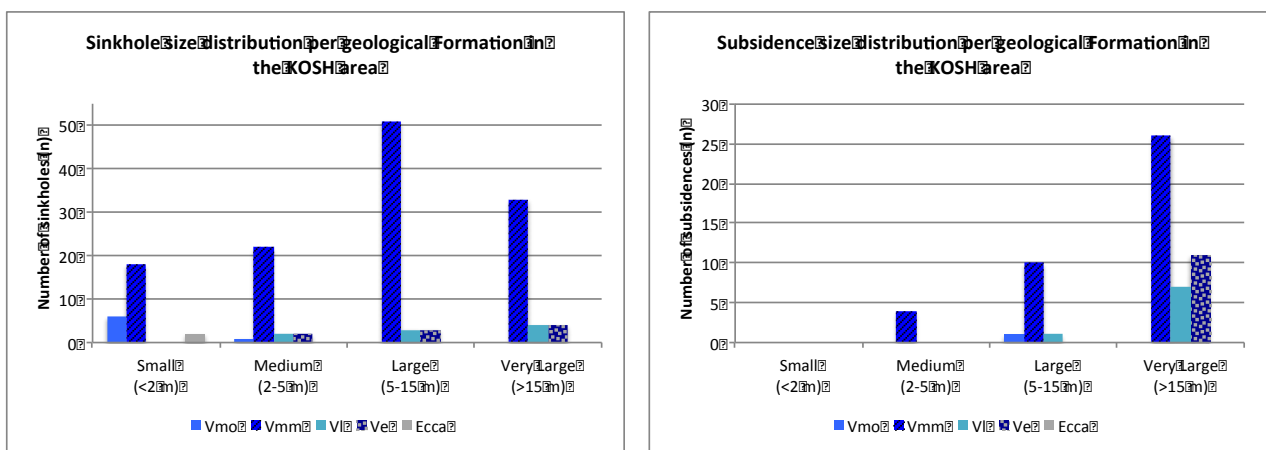


Figure 5-1: Sinkhole and subsidence size distributions across the various geological formations in the KOSH-area

Karst-related instability features identified as part of this study are spatially represented in Figure 5-1, together with the feature type and size. A detailed sinkhole and subsidence database is included in Annexure 3.

5.3.2 No hazard areas

Areas that are not defined as dolomite land according to the definition provided by SANS 1936 (2012), including areas where pre-Transvaal Supergroup rocks form outcrops, and areas where dolomite occurs in excess of 100 m below ground surface. Due to no evidence of current groundwater management and control measures being implemented in the KOSH-area – such as long-term continuous groundwater monitoring, management of groundwater abstraction rates, licensing of boreholes etc. – it is argued that a dewatering-type dolomite scenario prevails (i.e.: dolomite land defined as areas underlain by dolomite up to 100 m).

5.3.3 Low to Medium (and Low to High) hazard areas

Low to Medium hazard dolomitic areas are associated with geological and geomorphological settings characterised by the following aspects:

- Areas covered by outcrops of the Black Reef Formation at surface are regarded as reflecting a low to medium hazard for the formation of sinkholes and subsidences.
- The buffer area included towards the west and the south of the Black Reef Formation is deemed to reflect a low hazard for the formation of sinkholes and subsidences. As such, areas mapped as Ventersdorp Supergroup outcrops are included in the demarcated dolomite land due to uncertainty regarding the exact contact between the Ventersdorp Supergroup and the Black Reef Formation.
- Areas where the current groundwater table is less than 10 m from surface is regarded as reflecting a low hazard for the formation of sinkholes and subsidences from a water ingress perspective. However, these areas will require stringent groundwater monitoring and control measures to prevent the artificial lowering of the water table.
- Areas where the current groundwater table is situated in excess of 60 m from surface is regarded as reflecting a low hazard for the formation of sinkholes and subsidences from a groundwater level drawdown perspective, provided the past and current groundwater tables are situated within the dolomite bedrock, and not in the dolomite residuum.

Low to High-hazard dolomitic areas is associated with geological settings characterised by the following aspects:

- Areas that are covered by substantially thick non-dolomitic overburden (i.e.: in excess of 60 m or Karoo Supergroup sediments or intrusive material) are deemed as having a low susceptibility for the formation of sinkholes and subsidences. As such, areas that are covered by non-dolomitic strata (specifically karst-valley fill deposits) are regarded as representing a low to a high hazard for the formation of sinkholes and subsidences due to the known high variability in the thickness of such fill-deposits. It is required that the vertical extent of such Paleo-valley deposits be verified by means of rotary-air percussion drilling and accompanying geophysical methods in all instances.
- It should be noted that once the groundwater authority of the KOSH-area can prove, by means of a multi-year track record and monitoring data, that groundwater management and control measures are in place, areas that are underlain by dolomite bedrock at depths of between 60 to 100 m can be excluded from the medium to very high hazard areas. However, these areas are currently included in the dolomite hazard zones due to the absence of such proof at this time.

5.3.4 Medium to High hazard areas

Medium hazard dolomitic areas are associated with geological and geomorphological settings characterised by the following aspects:

- Areas covered by dolomitic strata belonging to the Oaktree- and the Lyttleton Formation at surface. This is ascribed to the known comparatively lower inherent hazard associated with these formations due to the absence of continuous chert bands. However, these formations are known to be associated with a dolomitic profile containing abundant highly erodible wad, leaving it potentially more susceptible to the formation of subsidences.
- Non-dewatered dolomitic compartments where the current groundwater table is situated between 10 and 60 m from surface are regarded as reflecting a medium to high hazard for the formation of sinkholes and subsidences from a groundwater level drawdown- and water ingress perspective. These areas will therefore require stringent monitoring and control measures for groundwater levels, water-bearing infrastructure, and areas associated with poor storm water management and drainage.
- It should be noted that areas that are covered by between 20 and 60 m of non-dolomitic overburden (i.e. Karoo Supergroup sediments or intrusive material) are deemed as being potentially moderately susceptible for the formation of sinkholes and subsidences.

5.3.5 High hazard areas

High-hazard dolomitic areas are associated with geological and geomorphological settings characterised by the following aspects:

- Areas covered by dolomitic strata belonging to the Monte Christo- and the Eccles Formation at surface. This is ascribed to the known inherently higher hazard associated with these formations due to an increased chert content.
- Areas underlain by dolomite that is characterised as reflecting pronounced bedrock topography on stereo-pair ortho photographs. These areas are inferred to represent shallow dolomite bedrock, and are deemed to be highly susceptible to the formation of small sinkholes, due to very little blanketing material overlying the dolomite bedrock.
- Streams and rivers crossing dolomitic areas, ascribed to the potentially concentrated ingress of water, a higher interaction between groundwater and surface water, seasonal flooding and concentrated water flow after heavy precipitation events, and the hazard for flooding.
- Non-dewatered dolomitic compartments where the current groundwater table is situated less than 10 m from surface are regarded as reflecting a high hazard for the formation of sinkholes and subsidences from a groundwater level drawdown perspective. Such areas will require stringent groundwater monitoring and control measures to prevent the artificial lowering of the groundwater table.
- Non-dewatered compartments where the groundwater table is deeper than 60 m below surface is regarded as reflecting a high hazard for the formation of sinkholes and subsidences from a water ingress perspective. Stringent monitoring of water-bearing surfaces to detect leakages, as well as areas associated with poor storm water drainage and management, must be enforced.
- Areas representing a very gentle surface topography (i.e. flat-lying and nearly flat-lying areas) are considered as reflecting a high hazard for the formation of sinkholes and subsidences ascribed to an expected concentrated ingress of water. Storm water management and control measures must be implemented in such areas.
- It should be noted that areas that are covered by less than 20 m of non-dolomitic overburden (i.e. Karoo Supergroup sediments or intrusive material) are deemed as being potentially highly susceptible for the formation of sinkholes and subsidences.

- The buffer area towards the east of the Eccles Formation is included in the high hazard area, ascribed to the known associated higher hazard of sinkhole formation between the Eccles Formation and overlying geological successions in the Carletonville area (Pretoria Group: Rooihoogte Formations and Timeball Hill).

5.3.6 Very High hazard areas

Very high-hazard areas are associated with geological settings characterised by the following aspects:

- Areas where existing (known and inferred) ground movement events occurred, and are as such known as areas being highly susceptible to sinkhole and subsidence formation. It should be noted that sinkholes in the KOSH-area are known to dip in the same direction as the regional dip of the geology. As such, the throats of most sinkholes in the area tend to dip towards the south-east.
- Areas underlain by dolomite up to a depth of 100 m that are intersected by known and inferred faults, and areas that were subject to tectonic deformation (i.e.: folding, shear zones, fault zones and thrusts, intrusives, overturned strata etc.) are all considered as very high hazard areas. Hazard zones associated with faults and tectonic deformation has been buffered by 500 m on either side. This is primarily ascribed to known sub-surface displacement of some faults in the area being as much as 200 to 500 m.
- Areas associated with hydrothermal quartz veins, intrusions and breccia zones, are regarded as being associated with tectonic deformation, and therefore represent a very high hazard. Hazard zones in these areas were buffered by 100 m on either side.
- Underpinning the geological hazard associated with the various demarcated areas, are the groundwater aspects. Areas that have been subjected to dewatering are considered as having a resultant higher hazard associated with water ingress, as well as an anticipated very high hazard for the formation of sinkholes and subsidences once the continuous dewatering of the aquifer ceases, and the dolomite compartment is re-watered. Areas that are currently dewatered are therefore considered as inherently having a very high hazard for the formation of sinkholes and subsidences from a water ingress- and a later re-watering perspective.

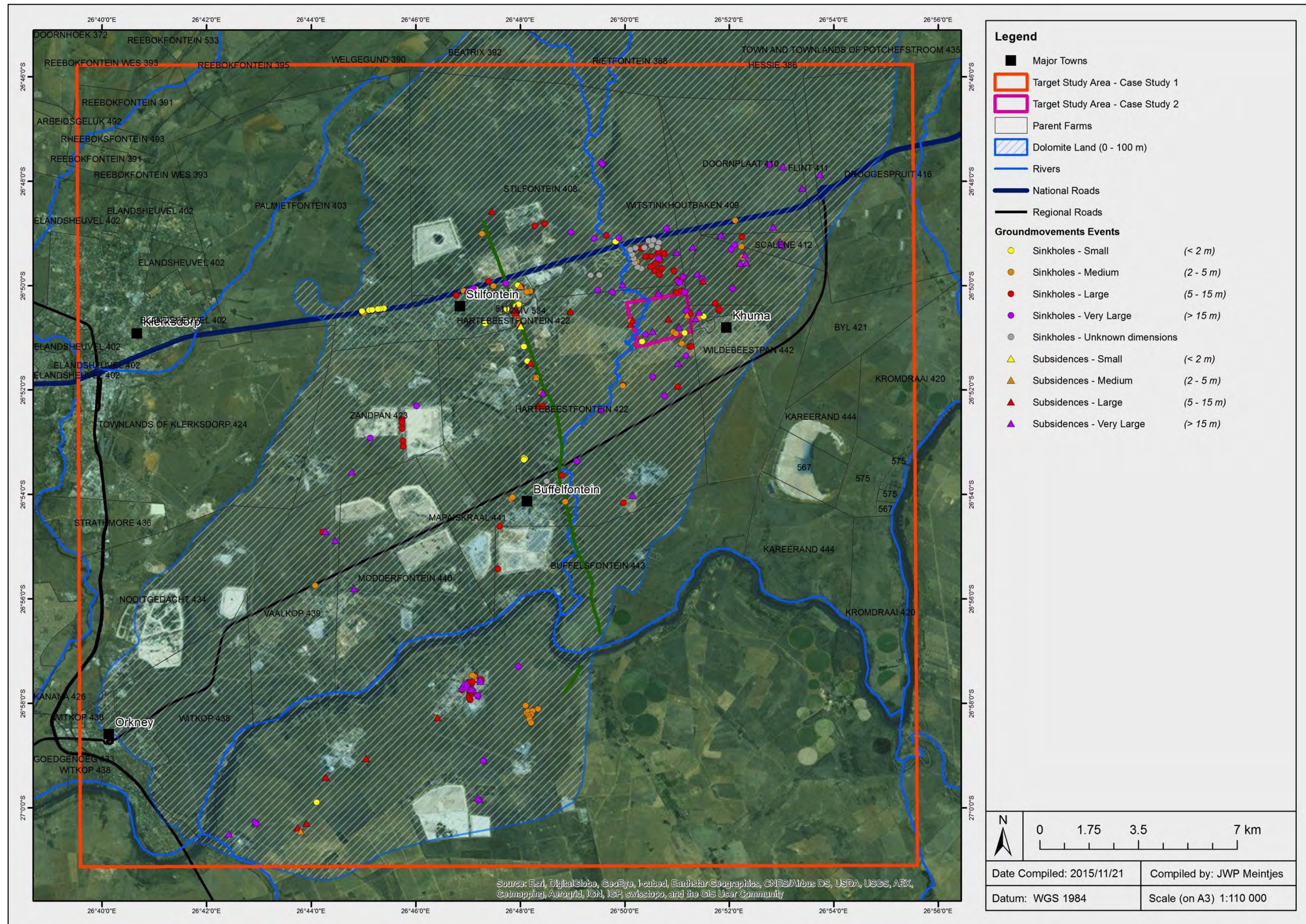


Figure 5-2: Distribution of sinkholes and subsidences across demarcated dolomite land in the KOSH-area

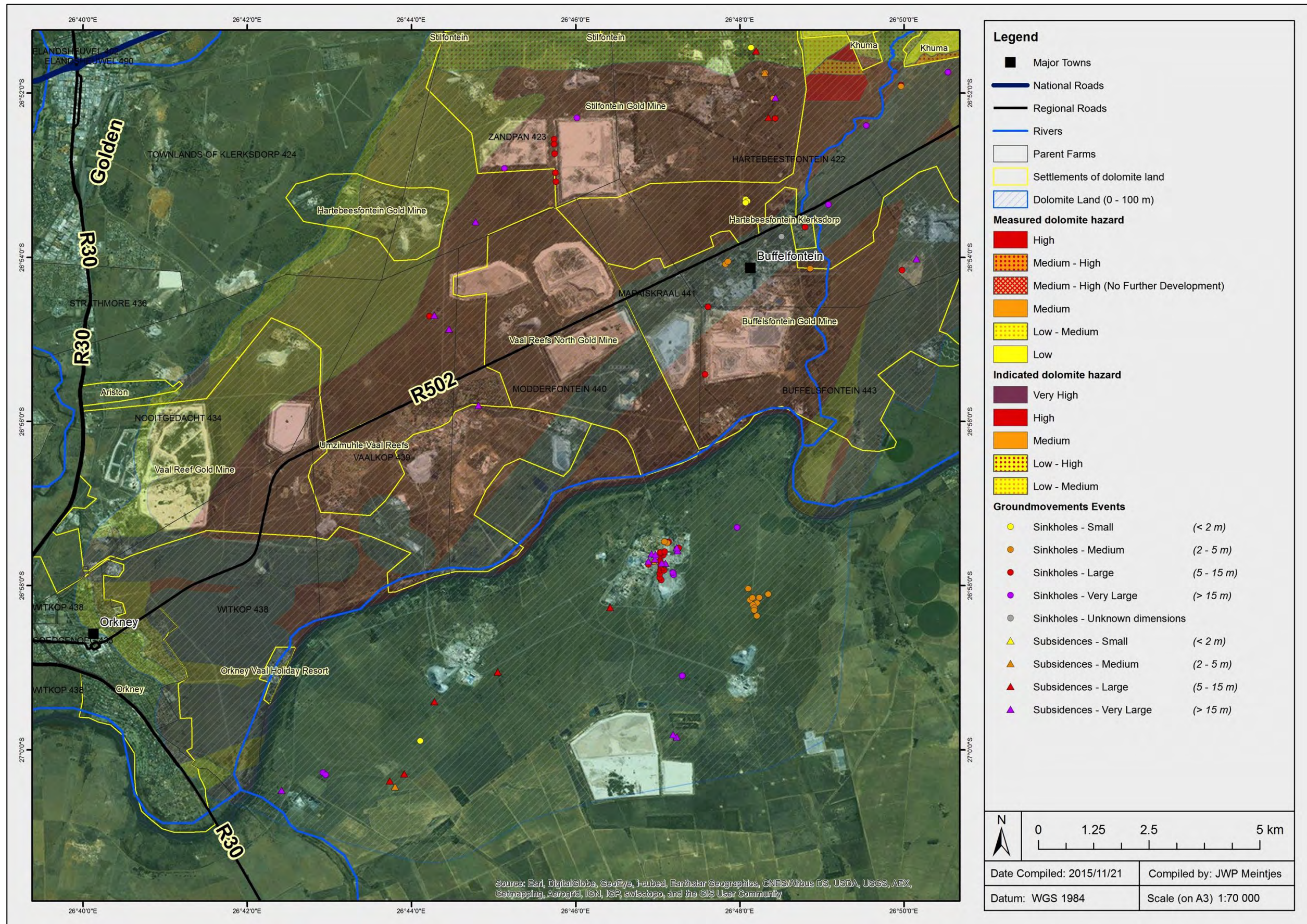


Figure 5-3: Inherent Dolomite Hazard – Orkney Area

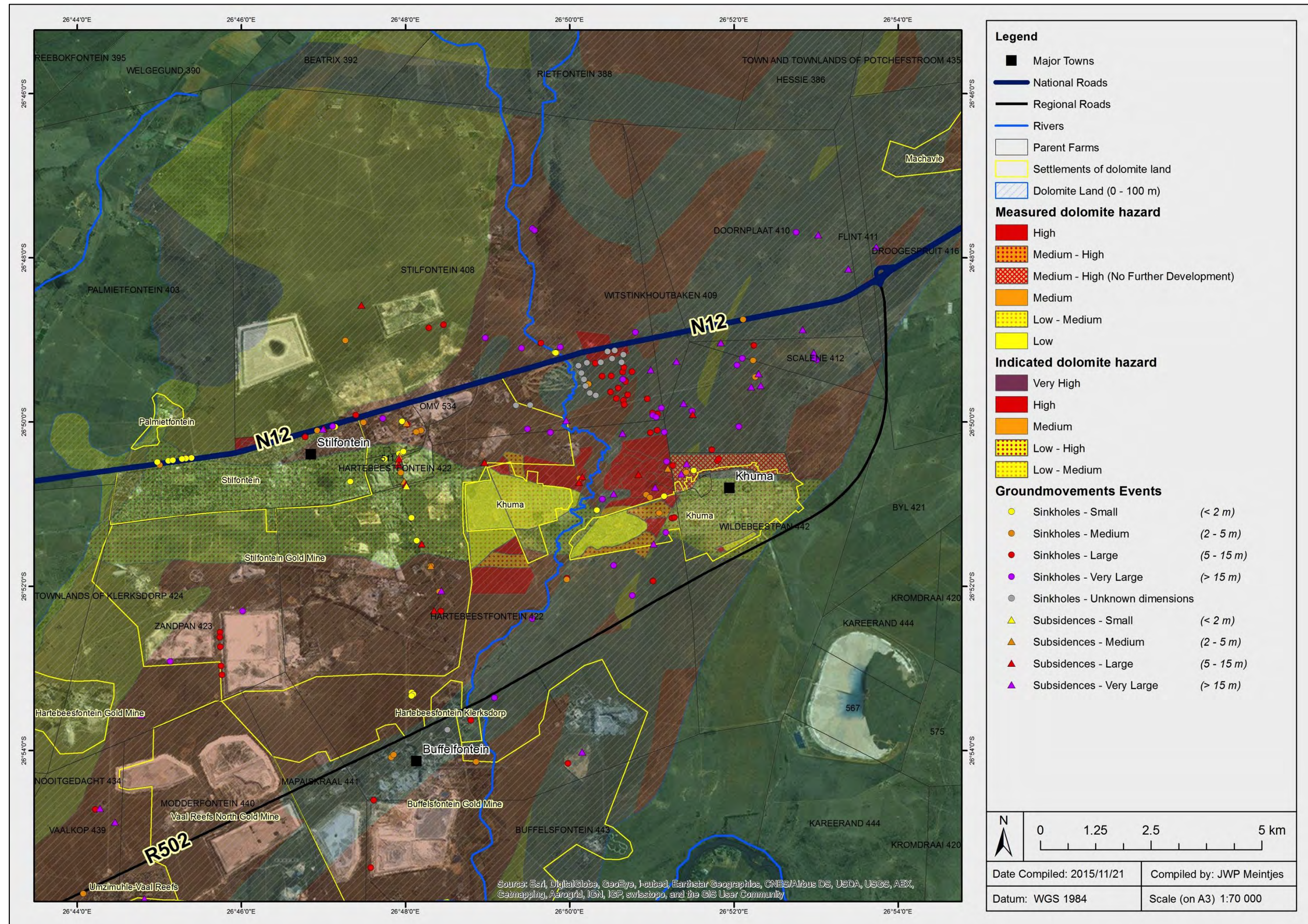


Figure 5-4: Inherent Dolomite Hazard - Stilfontein - Khuma – Hartebeesfontein Area

CHAPTER 6 – Case study 2: Detailed dolomite stability investigation on Portions 14 and 21 of the Farm Hartebeesfontein 422 IP

6.1 Background of the investigation

Where development on dolomite land is considered, a detailed dolomite stability investigation is a mandatory requirement as set out by the current industry standards in South Africa (SANS 1936:2012, as elaborated in Chapter 2). Such areas where development is considered frequently includes a pre-determined demarcated portion of land that is selected purely based on economic or town planning principles, and often lacks strategic considerations with respect to dolomite stability such as a broader understanding of the regional geological setting, the impact of structural geological features in the area, and the extent of known ground movement events.

This case study describes a typical feasibility level dolomite stability investigation in support of township establishment, with the following aims:

- Determine and evaluate the geological and hydrogeological character of the study area.
- Assess the hazard of the formation of karst-related instability features at the ground surface within the extent of the project area, using the current best-practise industry standards.
- Assess the possible size of these features, using the method of scenario supposition.
- Characterize the hazard potential of the study area through the demarcation of Inherent Hazard Class (IHC) zones that relates to various permissible land uses.

6.2 Site description

6.2.1 Location of the study area

The project area is located approximately seven kilometres due east of the Stilfontein CBD area, and directly north of Khuma Extension 6 in the North West Province of South Africa. The project area is defined as Portion 21- and the Remaining extent of Portion 14 of the Farm Hartebeesfontein 422 IP, and covers a total surface area of approximately 270 Ha. The site is located within the Matlosana Local Municipal area of jurisdiction that forms part of the Dr. KKDM (Figure 6-1).

The Stilfontein-Khuma road forms the southern boundary of the project area, with the Kromdraaispruit near the western border. The farm portion boundaries define the northern and

eastern limits of the project area. The centre point of the project area is roughly defined by the following coordinate (decimal degrees, WGS84 datum): latitude: -26.844858° S, longitude: 26.843721° E.

6.2.2 Existing infrastructure

Scattered informal settlements are located in the southern half of the project area with an average stand size of approximately 2 000 m². An oil pipeline- and power line servitude bisects the northern and southern half of the project area. Bulk services are situated along the southern-most border of the project area (bulk sewer mainline), and the south-western corner (bulk water mainline). A small portion in the extreme north-west of the project area is occupied by mine waste rock dumps, and the remainder of the project area is currently primarily used as communal cattle grazing land.

6.2.3 Regional physiographic settings

The project area is located on a gentle roughly south-west dipping slope, with steeper gradients towards the east of the project area and a flatter topography in the vicinity of the Kromdraaispruit in the west. The topographic elevation of the region is approximately 1 330 meters above mean sea level (mamsl).

Drainage across the project area is predominantly in a south-westward direction by means of sheet wash with storm water generally collecting in the regionally prominent southward flowing Koekemoerspruit. Localised ponding of surface water and inundation is observed in the eastern and south-eastern parts of the project area.

Rainfall in the area occurs mainly as thunderstorms and showers, with a mean annual precipitation of between 600 and 625 mm, mainly in the period between October and March. Climatic conditions of the project area is typical to that of the South African Highveld, with warm to hot summers and cool to cold and dry winters. Average temperatures are in the order of 30°C in the summer and 18°C in winter.

6.3 Investigative methodology

6.3.1 Desk study

During the initial stages of the investigation, all available regional geological- and geotechnical information in close proximity to the project area was collated and evaluated (Figure 6-2). The primary purpose of this is to obtain a preliminary indication of the regional geological setting and dolomite stability character, indications of structural geological features intersecting the project area and to determine any initial fatal flaws. Stereo-pair aerial photographs were assessed as

part of the desk study (Figure 6-3) to attempt to delineate any structural geological features such as geological contacts, lineaments, dykes and faults (or fault zones), according to the methodology set out by Lattman and Ray (1965).

6.3.2 Surface mapping

A walkover surface-mapping investigation was carried out in order to verify the surface geology and identify possible karst-related instability features that have already manifested within the project area (Figure 6-3).

6.3.3 Magnetic geophysical surveys

A magnetic geophysical survey was undertaken comprising of a total of seven traverse lines covering approximately 3 100 m (Figure 6-3). Traverses were laid out across lineaments derived from the interpretation of remote sensing images in an attempt to determine if these could represent intrusives. Data was collected every 10 m using a Geotron G5 magnetometer, with readings repeated a minimum three times at each point station, until an adequate standard deviation between readings was obtained. Magnetic geophysical traverse results are included as Annexure 6.

6.3.4 Gravimetric geophysical survey

A detailed gravimetric geophysical survey was conducted across the entire project area in March 2013, utilizing a grid spacing of 30 m in order to characterise the bedrock morphology (Figure 6-3). A total of 3 115 stations were laid out and measured by means of a Leica differential GPS system, and changes in gravity measured with a Scintrex Autograv gravimeter.

All field observations were reduced to Relative Bouguer values using an elevation correction of 0,189 and a theoretical gravity gradient of 0,00065 mgal per meter. The final data set was adjusted in order to generate a residual gravity map, indicating contoured gravimetric values at a 0.1 mgal interval. Residual fields were initially approximated by means of a linear plane so as to generate a provisional residual gravity map. This was then used to correlate depth to hard rock dolomite bedrock across the project area during the drilling phase. The regional gravity field was recalculated using a 200m x 200 m moving average once the drill results were available. The provisional residual gravity map was subsequently updated, and a final residual gravity map compiled. Geophysicists argue that 0.1 mgal represents 3.0 to 4.5 m depth to bedrock (Wagener, 1982).

6.3.5 Rotary air percussion borehole drilling







A rotary air percussion borehole programme was planned on the basis of the gravimetric survey and available geological information. A total of 41 boreholes were sited and drilled during April 2013 (Figure 6-3), as determined using the national standards (e.g.: 270 ha x 0.15 = 40.5 boreholes = 41 boreholes; SANS, 2012). The results of the geotechnical drilling were used to interpret the subsurface conditions of the underlying soil and rock, including; lithology, competency and effective weathering of soil and rock drilled into, the presence of possible receptacles within bedrock, water strikes and groundwater levels, and the inherent character of the prominent gravity anomalies and anomalous trends across the area.

The drill rig was equipped with a 165 mm-diameter button drill bit, and a compressor with 19-bar air pressure and a capacity of 27.6 m³/s. The following data was recorded per meter drilled: penetration rates using an electronic stopwatch, depth of groundwater strikes, hammer rates, sample loss, and air loss. Returned chip samples were collected per meter drilled and described according to the current industry standards (Brink & Bruin, 2002). Final borehole logs were compiled using the commercial *LogPlot* software package (Annexure 5).

6.4 Regional geological setting

The regional geological setting of the larger KOSH-area is discussed as part of Chapter 3. According to the available geological information as published on 1:250 000 scale geological map (2626 West Rand), the project area is underlain by the Transvaal Supergroup succession of rocks, specifically dolomite of the Malmani Subgroup, Chuniespoort Group (Figure 6-4). The geological contacts between various lithostratigraphic subdivisions of the Malmani Subgroup are not indicated on the published 1:250 000 scale surface geological map. Localised portions in direct proximity towards the west of the project area and on a more regional scale towards the east of the project area are underlain by clastic sedimentary rocks of the Karoo Succession, and the Pretoria Group volcano-sedimentary succession underlie the area towards the far-east.

Table 6-1: Regional stratigraphy of the Karoo-, Transvaal- and Ventersdorp Supergroups

STRATIGRAPHIC UNITS						
SEDIMENTARY AND VOLCANIC ROCKS					INTRUSIVE ROCKS	
	SUPERGROUP	GROUP	SUBGROUP	FORMATION		
QUATERNARY				(Alluvium)		
PALAEOZOIC	KAROO	ECCA		Undifferentiated		
VAALIAN	TRANSVAAL	CHUNIESPOORT	MALMANI	Undifferentiated		Diabase (Vdi) 
				Black Reef		
RANDIAN	VENTERSDORP	PLATBERG		Rietgat		

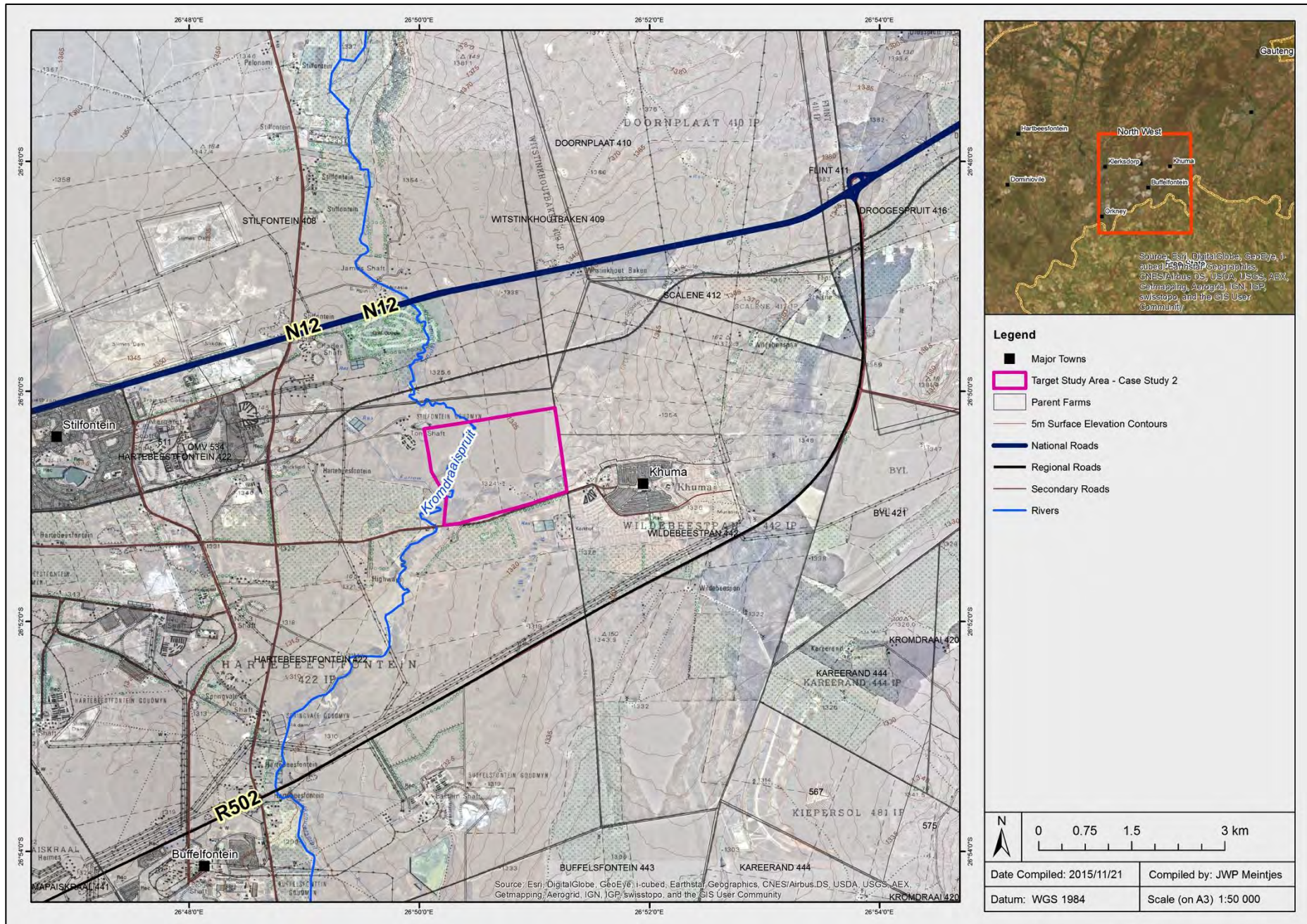


Figure 6-1: Case Study 2 project area boundaries and locality

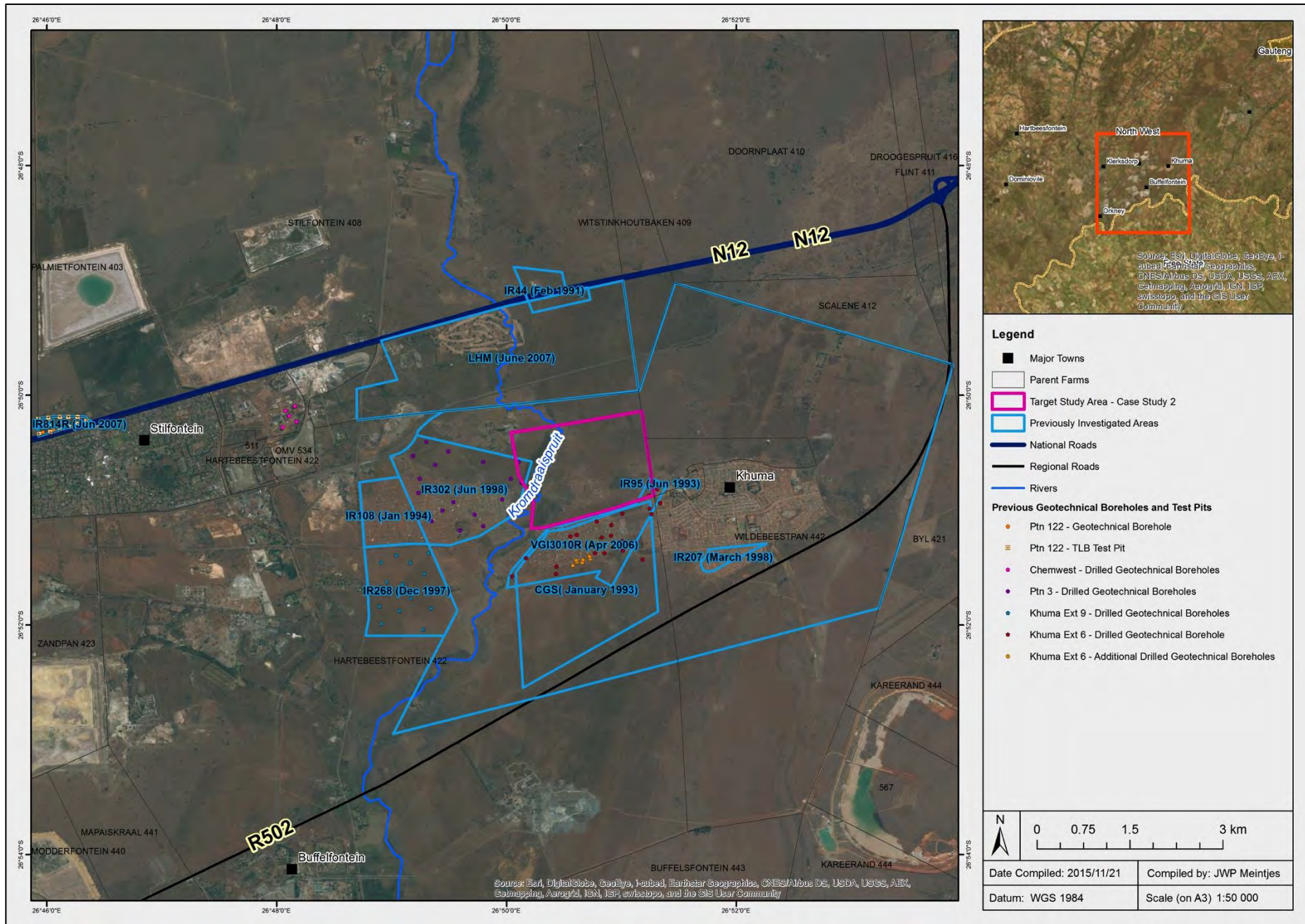


Figure 6-2: Previously investigated areas surrounding the Case Study 2 site

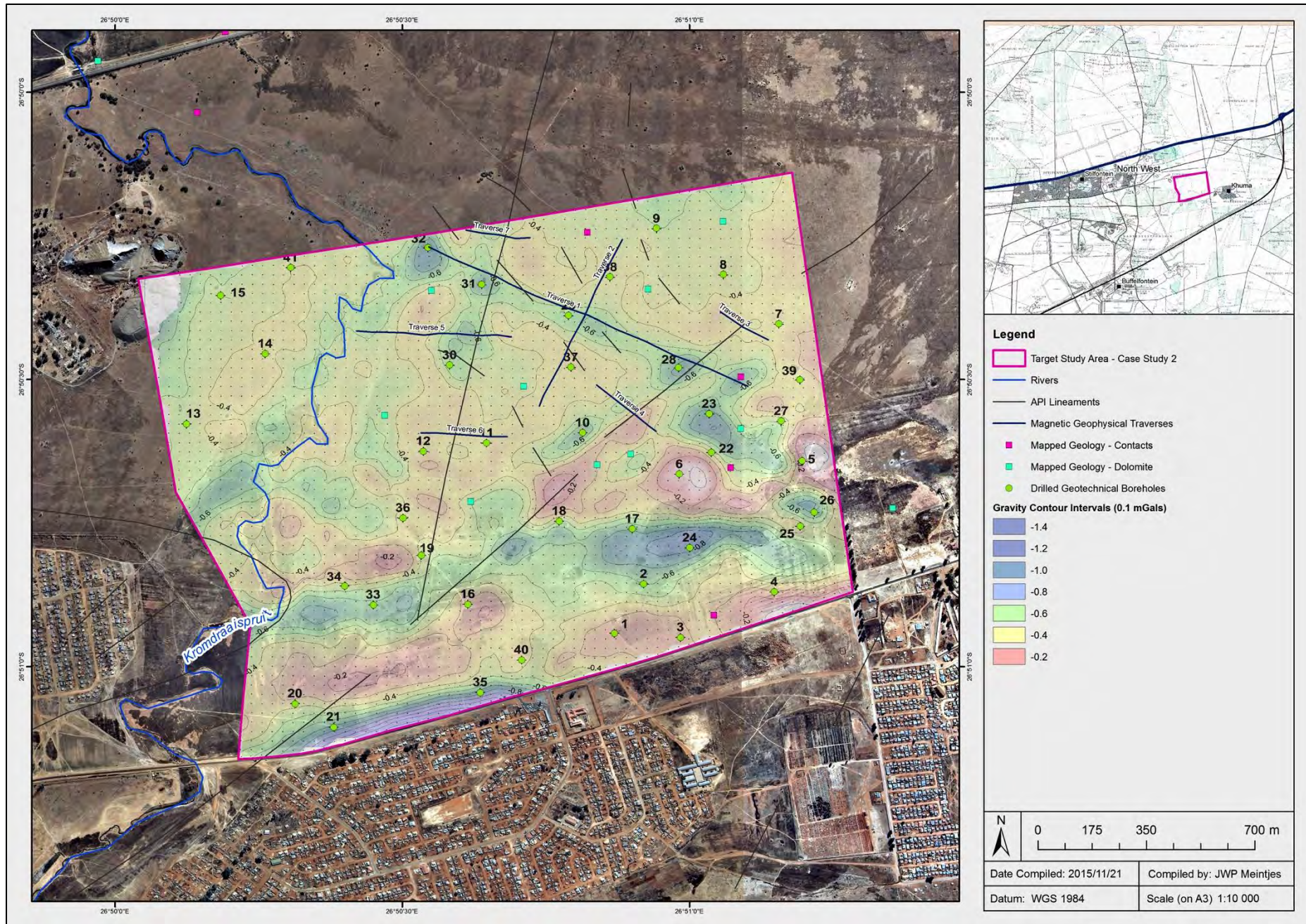


Figure 6-3: Geotechnical Investigation

6.5 Regional geological structure

On a regional scale, it is considered that the study area has been affected by the impact of the Vredefort Meteorite, where strata belonging to the Witwatersrand (c. 2 970 - 2 914 Ma), Ventersdorp (c. 2 714 Ma), and Transvaal Supergroup has been severely altered and deformed (Brink *et al.*, 2000). This represents deformation of rocks, reflecting the greatest single energy release event that occurred on the surface of the earth due to a meteorite impact, with age c. 2 023 Ma (Brink *et al.*, 2005).

Various faults and fracture zones were identified across the dolomite in-and around the project area. These faults and fault zones are not indicated on the published geological map (2626 West Rand; Figure 6-4) and are associated with quartz veins and deformation breccia at surface. Structurally, deformation appears to have a significant impact on the sub-surface dolomitic conditions, with some portions fairly heavily faulted. As discussed in Chapter 3, most faults trend north-east/south-west, are normal, and have downthrows either to the north-west or south-east. The reactivation of these fault zones during the Vredefort Meteorite Impact event gave rise to intense faulting, folding and fracturing within the dolomite.

Various Pilanesberg-age dykes intersect the geological succession in the proximity of the project area. Such dykes generally forms groundwater compartments within the dolomite bedrock, but does not form outcrops in all instances in the KOSH-area (Darcy, 2002, Veltman, 2004, Van Deventer, 2013). Dykes in the area generally trend north-south and form structural controls that compartmentalise the karst aquifer. One such a north-south trending Pilanesberg-age dyke separates the KOSH dolomite compartments A (towards the west of the project area) and B (underlying the project area).

6.6 Local geological setting

From the regional geological setting, geological mapping and percussion drilling data (both existing and new), it was determined that the project area is predominantly underlain by three lithostratigraphic successions, namely: rocks from the Eccca Group (undifferentiated) in the south-westernmost corner of the site, which is referred to as the Karoo Supergroup outlier, rocks from the Monte Christo Formation of the Malmani Subgroup across the majority of the area, and rocks from the Lyttleton Formation of the Malmani Subgroup towards the far eastern regions of the study area (Figure 6-5).

The Karoo Inlier is interpreted to be a valley fill deposit that is preserved in an east-west striking Paleo-karst valley during a post-Karoo period of erosion. However, the possibility of this outlier to be associated with glacial activity cannot be ruled out. The various lithostratigraphic sub-

divisions of the Eccca Group has not been substantiated, and some previously drilled percussion boreholes towards the south of the project area indicated the occurrence of poorly developed pockets of tillite at the base of the Karoo Inlier. The Eccca Group in the KOSH area is very highly variable in thickness and reaches a maximum vertical thickness of up to 190 m in some instances, as determined during previous geotechnical- and exploration drilling in the region. Gravimetric geophysical surveys conducted by various consultants in the vicinity of Stilfontein and Khuma indicate that the sidewalls of the in-filled Paleo-karst valley are very steep. The extent of the Karoo Inlier has been amended based on the percussion borehole drilling in the area, and was subsequently updated in the vicinity of the project area.

6.6.1 Local geological structures

The geological succession predominantly strikes south-west/north-east, and dips at a shallow angle in the western parts of the KOSH-area (roughly 3° to 12° to the east) and steeper towards the east (roughly 50° to the east). This was substantiated during the surface-mapping phase, which verified that the entire project area is underlain by chert and dolomite with more prominent outcrops and sub-outcrops towards the northern regions of the project area. No prominent outcrops were noted in the southern, and south-western most portions of the project area, as these areas are predominantly covered by transported material (colluvium and/or alluvium).

Various regionally prominent faults intersect the regions in the vicinity of the project area, and generally trend along a north-south axis (Figure 6-5). However, none of these major structural features are indicated on the 1:250 000 scale published geological map (2626 West Rand, Wilkinson, 1986).

The regionally prominent north-east/south-west striking Kromdraai Fault intersects the central portions of the project area. This fault is known in the region and was mapped in mine areas (Antrobus *et al*, 1986). The Kromdraai Fault is known to be a south dipping normal fault, and displaced the geological succession with between 700 and 3 000 m at surface, with downthrows towards the south-west of up to 200 m. This fault is associated with breccia outcrops and hydrothermal quartz vein intrusions at surface, and sympathetic faulting parallel to the main fault zone in the Khuma area is expected.

The Fakawi Fault (first described by Brink, 1996) is located towards the east of the project area. This fault is deemed to have associated sympathetically faulting parallel to the primary approximately north-east/south-west striking fault. The Fakawi fault is a east-southsouth dipping normal fault, and is known to have displaced strata with up to 3 000 m at surface, with downthrows of up to 500 m towards the south-west. As with the Kromdraai Fault, the Fakawi

Fault is associated with breccia and hydrothermal quartz vein intrusions at surface where it forms outcrops.

The Katdoornbosch Thrust Fault is located approximately 1.5 km towards the east of the project area. This thrust fault strikes approximately north-east/south-west in the vicinity of the project area, and its outcrops can be traced along breccia zones and prominent topographical depressions (in the Oaktree- and Lyttleton Formations) and ridges (in the Monte Christo- and Eccles Formations) from the Vaal River in the south towards Welverdiend in the north. According to Brink *et al.*, (2001), the Katdoornbosch Thrust Fault is also associated with chocolate tablet boudanage, pseudotachylite and chert breccia.

The aerial photograph investigation revealed an approximately east-west striking fault system that could be associated with the Karoo outlier valley-fill deposit. This fault system was found to be cut off in the vicinity of the Koekemoerspruit in the south-western corner of the project area by an approximately north-east/south-west striking fault (possibly a conjugate of the Kromdraai Fault), where the continuation of the Karoo outlier suddenly pinches out to a very narrow surface outcrop.

Numerous, approximately north-east/south-west and north-west/south-east trending, hydrothermal quartz veins intrusions and breccia zones intersect the vicinity of the project area. All these features are considered to be associated with structural deformation and fault zones that exhibit pronounced surface outcrops, traceable across long distances. Higher concentrations of these features are observable in the vicinity of the approximate positions of the regionally prominent Kromdraai-, Fakawi- and Katdoornbosch faults.

A number of sub-surface intrusives are indicated to the north-west and west of the project area. These intrusives were mapped in the underground workings at the old Stilfontein Gold Mine in the vicinity of the Toni Shaft. None of these features were found to form surface outcrops. Approximately north-south striking kimberlite dykes are indicated towards the west of the area, and varies in thickness of between 0.3 to 3 m. A prominent east-west striking sub-surface diabase dyke (inferred to be of Pilanesberg-age) is located directly north of the project area. This dyke was measured to be up to 10 m thick in the Scott Shaft area, and is referred to as the Scott Shaft Dyke.

The magnetic geophysical survey did not yield any significant anomalies, and no correlation could be drawn to the structural orientation of faults or intrusives intersecting the project area.

6.6.2 Summarised key geological factors

The geological aspects considered as part of the dolomite stability investigation plays an integral role in determining the sub-surface conditions and associated hazard for sinkhole and subsidence formation. These include delineating areas of shallow dolomite bedrock outcrops and sub-outcrops, the character of the material overlying the dolomite, and to determine – in conjunction with aerial photograph investigations and geophysical surveys – areas where drilling should commence. The following can be derived from the geological assessment:

- Aerial photograph interpretation and surface mapping assisted in the delineation of structural geological related lineaments. In this light, it was determined that the northern and north-western sectors of the project area exhibit a pronounced bedrock structure, deemed to be associated with shallow bedrock outcrop.
- The study area is underlain by chert-rich dolomite of the Monte Christo Formation across the majority of the central and western parts, and chert-poor dolomite of the Lyttleton Formation in the eastern-most parts, which both have undergone crustal deformation.
- The dolomite is covered by colluvium and chert residuum throughout the project area, with the exception of a very localised portion in the south-westernmost part, which is underlain by shale of the Ecca Group.
- A major fault runs through the study area with an east-west trending strike. This inferred fault could be a shallow association of the east-west striking karst-valley fill deposit (filled with Karoo Supergroup sediments) that is prominent in the region.
- The regionally prominent north-east/south-west striking Kromdraai Fault intersects the site in the central parts. This fault is known to be south-dipping with downthrows of up to 200 m.
- The regionally prominent north-east/south-west striking Fakawi Fault is situated directly east of the project area. This fault is known to be a normal south-dipping fault with down throws of up to 500 m.
- The regionally prominent north-east/south-west striking Katdoornbosch Thrust Fault is located approximately 1.5 km directly east of the project area. This major thrust fault, and its associated imbricates, are known to have displaced the geological succession with up to 1 000 m in some areas.
- All of the above-mentioned faults and fault zones are closely associated with the mapped quartz vein- and breccia outcrops at surface.

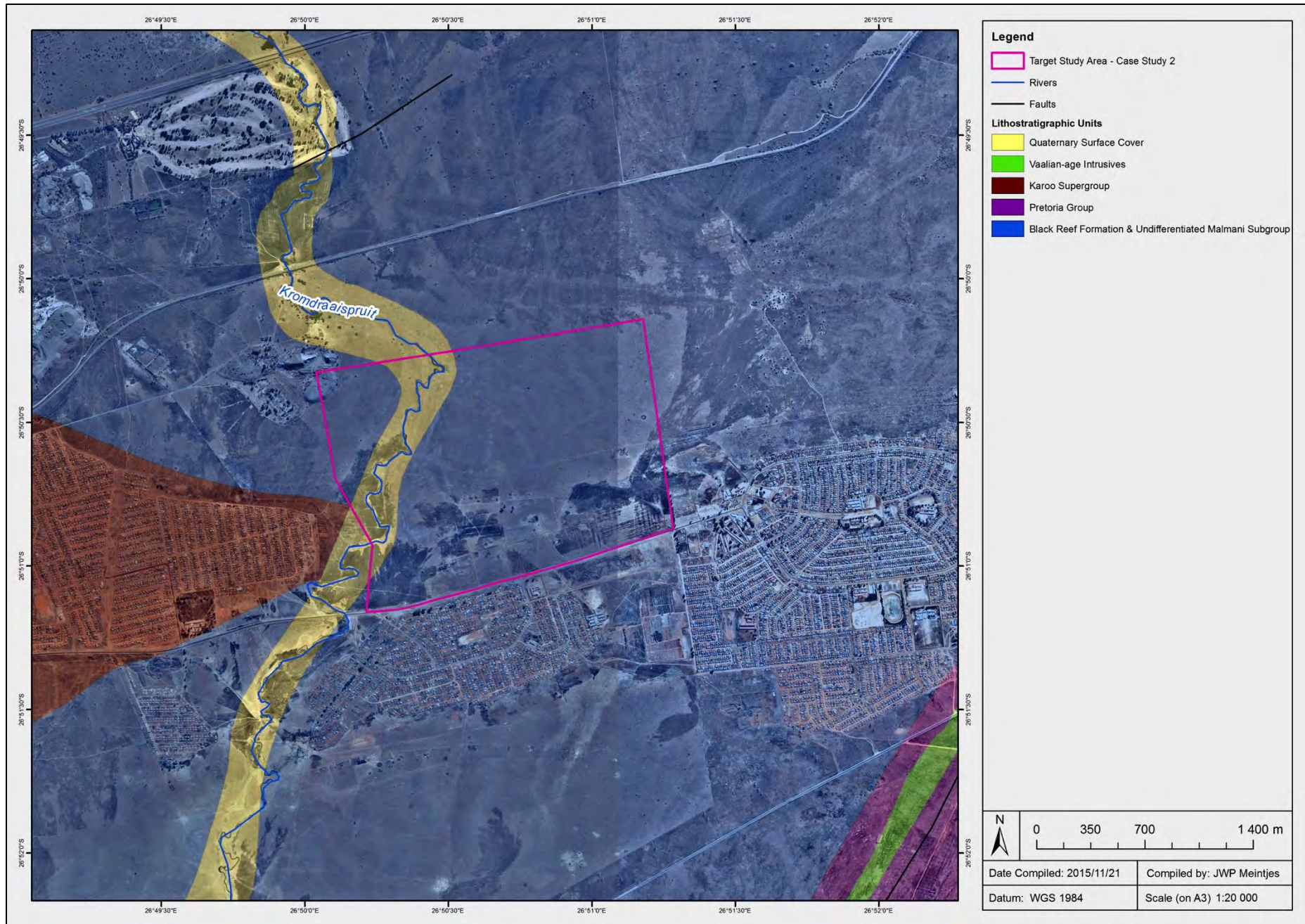


Figure 6-4: Project area in relation to the regional 1:250 000 scale geological map (after Wilkinson, 1986)

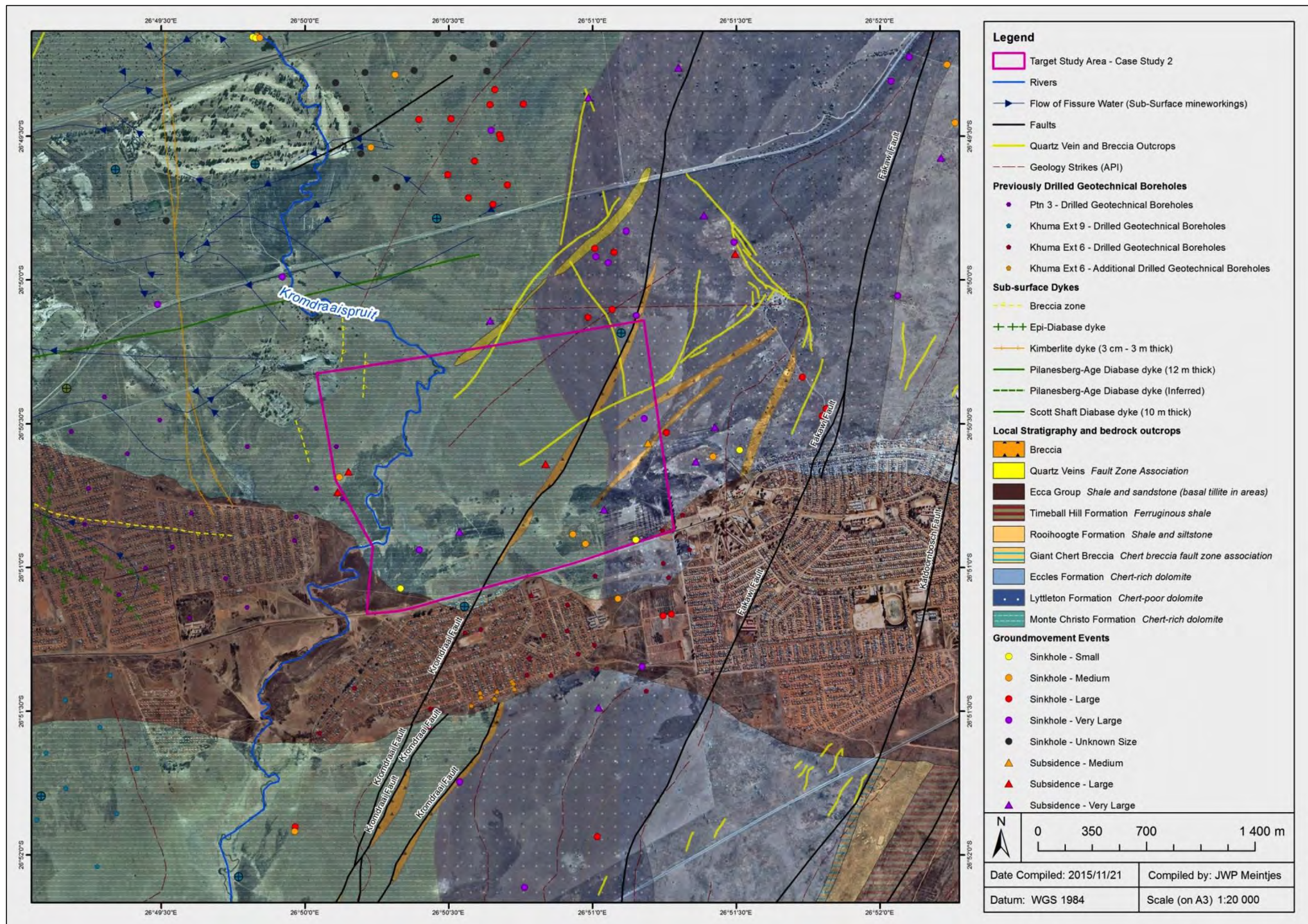


Figure 6-5: Compiled local geological setting based on previous mapping, geological information and new field investigations

6.7 Existing karst-related instability features

A number of existing karst-related instability features have been observed and documented within the boundaries of the project area during the fieldwork phase, as well as in the regions towards the east of Khuma Extension 6, as detailed in Chapter 3 and indicated in Figure 6-5. The formation of these features are inferred to be associated with the following criteria and triggering mechanisms:

- Dewatering of the KOSH groundwater compartment B.
- Seasonal inundation causing concentrated ingress of water, especially in close proximity of the Kromdraaispruit.
- As part of the inherent character of the dolomitic Formations covering the project area (especially the Monte Christo Formation) in combination with the highly tectonically disrupted structural geological setting of the area.
- Possible leakages of liquid-bearing bulk service along the Khuma-Stilfontein road.

6.8 Hydrogeological setting

Groundwater movement within the dolomitic strata in this area is associated with north-south trending structural controls (e.g.: joints, dykes and faults) that compartmentalize the karst aquifer in the KOSH area. A north-south trending Pilanesberg-age epi-diabase dyke separates dolomite compartments A and B (Figure 6-6). The project area falls within the KOSH dolomite compartment B (with the Welgegund dolomite compartment located upstream towards the north). The project area is situated within the C24A quaternary catchment that forms part of the Middle Vaal Water Management Area (WMA) (DWAF, 2004).

6.8.1 Aquifer classification

The geological strata underlying the project area dictates to primary distinguishable aquifers, which vary significantly in terms of hydraulic properties. This is primarily ascribed to the nature of the rock medium. Zones of increased permeability are associated with joints, bedding planes and cavernous zones within the Karst-type aquifers, rather than mass permeability. The primary aquifers encountered across the project area includes:

- A perched aquifer above the impervious shale of the Karoo Inlier, which serves as an aquitard.

- An intergranular- and fractured aquifer associated with the Karoo Supergroup rock types (e.g.: clastic sedimentary rocks) as well as with intrusives (i.e.: epi-diabase dykes and ilmenite dykes in the area).
- A Karst aquifer associated with the Malmani Subgroup dolomitic rocks.

Water flow and storage inside the clastic sedimentary rocks typically occur in between the individual grains (intergranular), depending on the porosity of the matrix, but is mainly transported along preferred pathways created by structures such as faults and joints. The contacts with intrusive bodies such as dykes and sills are associated with fractures in the surrounding host rock that create preferred pathways.

6.8.2 Groundwater levels

As described in Chapter 4, mining operations in the vicinity of the project area resulted in the dewatering of the KOSH-B groundwater compartment. Information obtained during March 2013 indicates that dewatering pumping is still taking place at Margaret Shaft due to current mining operations occurring further downstream towards the south-west at the Vaal Reefs mining operations. This was confirmed during a hydrocensus conducted in April 2013, where the water level in a borehole located within the project area was measured to be in excess of 100 mbgl deep.

Groundwater seepage and perched groundwater conditions were encountered at depths of between 12 and 49 mbgl in four of the 41 newly drilled geotechnical boreholes (e.g.: boreholes 20, 21, 35 and 36). These boreholes were all drilled in relative close proximity to the Kromdraaispruit. It is inferred that the seepage is due to the presence of a perched water table either representing a perched aquifer, or the seasonal accumulation of rainwater within unconsolidated material after heavy precipitation events (which occurred in the period preceding the drilling phase of this project). Groundwater seepage was not encountered in any of the other 37 boreholes drilled during this study. The latter boreholes were some drawn down to a depth of 60 mbgl.

Uncertainty still prevails regarding the effect of re-watering on the underlying dolomitic strata. It is inferred that the mobilisation of material, and subsequent increase in susceptibility for the formation of sinkholes and subsidences can be expected to take place in the event of re-watering. Rosewarne (1982) determined the groundwater flow and areas of maximum fissure flow from the underground mine workings at the old Stilfontein Gold Mine (Figure 6-6). These areas must be closely monitored once dewatering at Margret Shaft ceases, as these areas are inferred to indicate the first signs of mobilisation of material.

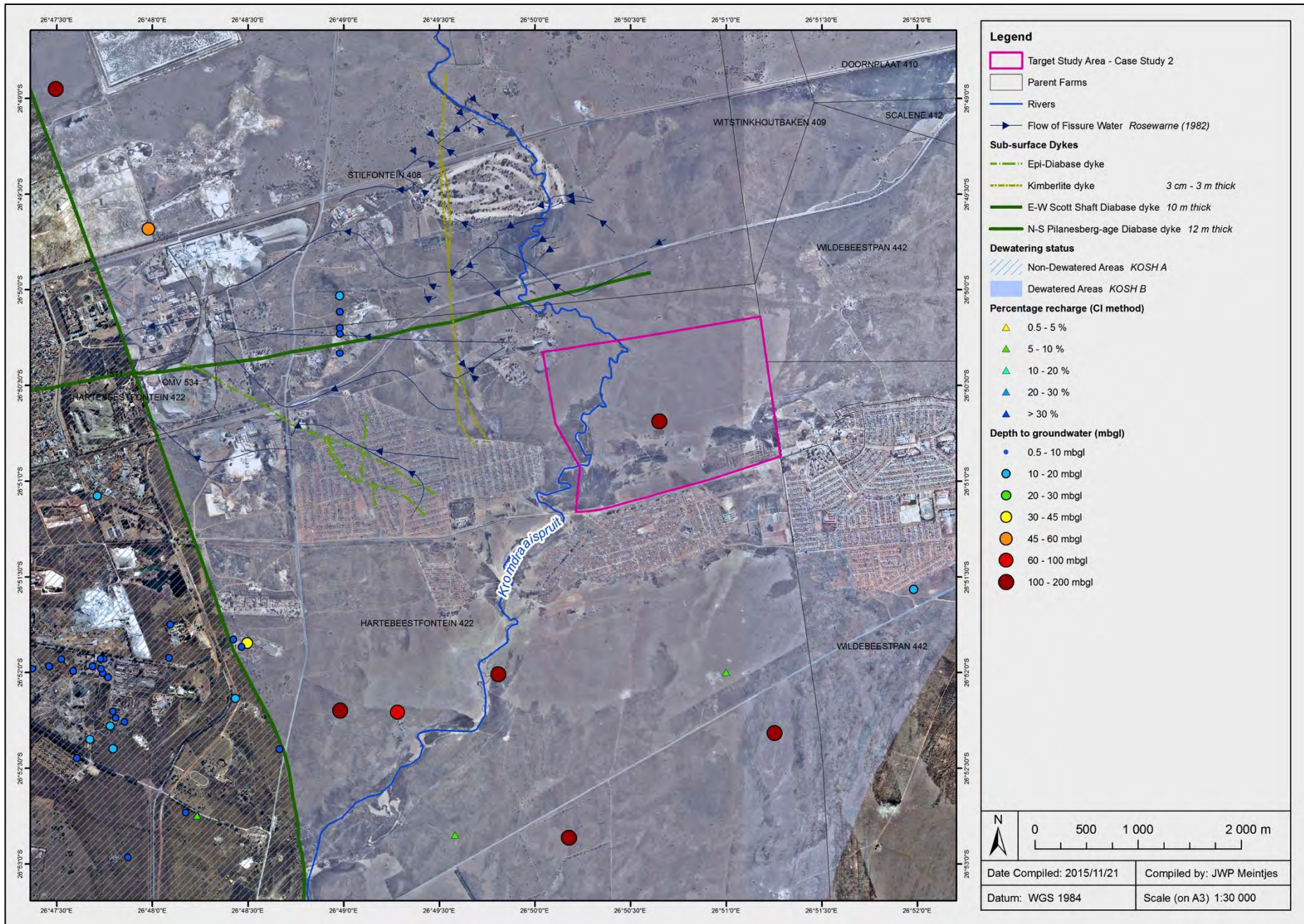


Figure 6-6: Local hydrogeological setting of the project area

6.9 Hazard characterisation and evaluation procedures

The hazard evaluation and characterisation process is done in accordance with the methodology as set out in SANS 1936 (SANS, 2012) and the detailed methodology as set out in Chapter 2. This process forms the basis for the compilation of the geotechnical model for the project area. The final geotechnical model of the project area was compiled, taking cognisance of the geotechnical investigation and drilled boreholes, geophysical investigations, hydrogeological regime of the area, and the surface geological and structural features.

6.9.1 Nature and mobilisation potential of the blanketing layer

The different materials encountered across the project area during the drilling process were considered and evaluated to determine the inherent susceptibility for mobilisation and subsequent angles of draw. A detailed table supporting the considerations to determine the various angles of draw are included in Annexure 7. Some of these considerations include: lithostratigraphic descriptions of the material, geotechnical criteria determined during drilling, material drilled into, penetration tempo, air- and sample loss, and a description of the fines and coarse content of the material. The overburden across the project area is inferred to exhibit the following characteristics:

- The *transported colluvium and alluvium* is deemed to be highly to moderately permeable and moderately to slightly cohesive, with a resultant high mobilization potential;
- The *shale* becomes more competent with depth, and grades from *completely weathered (residual) shale* composed of mainly a silty matrix, into *moderately weathered shale* composed of harder more competent bedrock. The mobilization potential is accordingly high to low.
- The *chert* encountered grades from a silty matrix containing weathered chert fragments (*chert residuum*) into *highly weathered chert* composed of abundant fragments in a silty matrix. The *chert* is considered to be composed of rubble and breccia – in some instances larger boulders/bands – with no cohesion and a relatively high permeability, with a corresponding high mobilisation potential, where chert bands are brittle and not laterally continuous.
- Both the *chert-rich- and chert-poor dolomite residuum* are composed of coarse particles moderately densely- to densely packed in a predominantly granular matrix, but the recording of irregular hammer rates in some places within these materials during drilling is indicative of

the occasional occurrence of less densely packed pockets, resulting in an inferred moderate to high mobilisation potential.

- The *dolomite bedrock* generally grades from highly to slightly weathered rock with depth, although localised widespread pockets of weak material occur within the otherwise relatively competent bedrock. The chert contents of dolomite bedrock vary between chert-free, chert-poor, and chert-rich. The corresponding mobilization potential thus varies from high to low depending on the chert content and effective weathering grade.

The angles of draw (calculated from the horizontal to the assumed sinkhole sidewalls) are inferred for the different materials underlying the project area as determined during the geotechnical-drilling phase, and are summarised in Table 6-2.

Table 6-2: Angles of draw for various lithologies (after Buttrick, 1992)

Lithology	Effective weathering		
	Highly weathered	Moderately weathered	Slightly weathered
Alluvium	75°	-	-
Colluvium	75°	-	-
Chert residuum	70°	-	-
Chert	75°	-	-
Shale	80°	85°	-
Chert-free dolomite	70°	80°	90°
Chert-poor dolomite	70°	80°	90°
Chert-rich dolomite	75°	80°	90°
WAD (clayey silt)	55°	-	-
Chert-poor dolomite residuum	60°	-	-
Chert-rich dolomite residuum	60°	-	-

6.9.2 Bedrock morphology

Variances in the bedrock morphology are considered as an integral part of the evaluation process and are built into the overall hazard evaluation of the area. Faults and fault systems are considered to cause deep leaching in the dolomite bedrock, which may act as a preferred pathway for mobilisation agents, with sudden variations in the nature of the material. Sinkholes are known to occur along fault systems in the KOSH-areas (as well as other areas in South Africa), and are therefore incorporated in all zone designations. This is ascribed to the occurrence of major fault zones across the project area, and inferred smaller sympathetic faulting along these fault zones.

The depth to dolomite was found to be reasonably well correlated with the generated gravity anomalies across the project area, and is characterised as a much-dissected plateau. Dolomite bedrock mainly forms outcrops, and sub-outcrops, in the northern portion of the site. Two prominent Paleo-karst valleys occur within the project area. The first – an east-west trending feature – occurs in the southern sector and exhibits a depth to bedrock of up to 60 meters. The second – a north-eastward trending feature – occurs in the eastern sector of the site. The dolomite bedrock is predominantly overlain by colluvium and chert residuum throughout the project area, with the exception of a very small portion in the south-west that is overlain by 18 m shale of the Ecca Group.

6.10 Dolomite hazard characterisation of the site

A total of five hazard class zones have been demarcated within the project area in accordance with above mentioned geo-scientific data and considerations, and are sequentially discussed. The hazard class zones were determined by i) using the developed geotechnical model for the project area, and ii) the detailed hazard characterisation as per borehole as included in Annexure 8. The demarcated final hazard class zones are illustrated in Figure 6-7.

6.10.1 Dolomite Hazard Zone A

6.10.1.1 Gravity signature

This Zone is defined as a prominent gravity low with a steep gradient located in the extreme south-west of the project area. This gravity anomaly is bordered by an east-west striking gravity high anomaly towards the north.

6.10.1.2 Nature of the overburden material

The blanketing layer in this Zone is characterised by the following:

- The dolomitic strata are covered by highly weathered shale with a thickness of approximately 18 m in the west.
- The blanketing layer in the south and east is composed of interlayered shale and chert with an average thickness of 18 m.
- Moderately weathered dolomite underlies the shale and chert in this area, with no residuum (wad) recorded between shale and dolomite bedrock.
- Air- and/or sample loss was not recorded in any of the boreholes drilled in this Zone.
- Irregular hammer rates were occasionally recorded in this Zone, and are associated with intercalations of chert and weathered shale.

6.10.1.3 Bedrock configuration

All boreholes were drilled at least 6 m into competent dolomite bedrock. The dolomite bedrock is overlain by shale in the western parts of this Zone.

6.10.1.4 Hydrogeology

Groundwater levels of 13,3, 13,9 and 49,0 mbgl were measured in boreholes 20, 21 and 35 respectively. These water levels are considered to represent a perched groundwater table associated with influx from the adjacent Kromdraaispruit. The original water level (OWL) in the KOSH Compartment B was measured in 1993 and found to be in excess of 100 mbgl, as confirmed during the fieldwork phase in March 2013. This zone is therefore dewatered.

6.10.1.5 Final characterisation

The blanketing layer consists of interlayered sedimentary rocks (shale and chert) with an average thickness of 18 m. This material is generally highly weathered, with a resultant high mobilisation potential. The dolomite bedrock is situated at a depth of between 15 and 22 mbgl, becoming more competent with depth. Less weathered solid dolomite bedrock occurs from a depth of between 17 and 49 mbgl.

This zone is characterised by a gravity low anomaly with a steep gradient towards the south, possibly associated with the boundary of a more regional east-west striking fault system, which

increases the inherent susceptibility from a low to a medium. The nature of the blanketing layer and the subsurface conditions result in a low to a medium inherent susceptibility for the formation of large size sinkholes and subsidence, with sub-areas resulting in a low to a medium inherent susceptibility for the formation of medium size sinkholes and subsidence, with respect to water ingress. A resulting classification is therefore given as Inherent Hazard Class 4 (with sub-areas of 3) with respect to ingress of water.

This area is characterised as reflecting a low susceptibility for the formation of all size sinkholes and subsidences with respect to further groundwater level drawdown. The composite hazard designation for this Zone is Inherent Hazard Class 4(3)//1.

6.10.2 Dolomite Hazard Zone B

6.10.2.1 Gravity signature

The area is characterised by gravity plateau anomalies and associated gravity plateau high anomalies.

6.10.2.2 Nature of the overburden material

This area does not have any substantial blanketing layer. However, the thin overburden in this Zone is characterised by the following:

- None of the boreholes drilled in this Zone reflected any air loss or sample loss.
- Some irregular hammer rates were recorded during drilling, but very irregular hammer rates indicative of possible cavernous conditions were not documented.
- The dolomite bedrock is overlain by an average of 5 m of transported colluvium, highly weathered chert, and highly weathered chert-rich and/or chert-poor dolomite, grading into moderately weathered chert-rich and/or chert-poor dolomite.

6.10.2.3 Bedrock configuration

All boreholes were drilled at least 6 m into competent dolomite bedrock. Slightly weathered dolomite bedrock was encountered at shallow depths in this Zone (between 3 and 11 mbgl), and is generally interlayered with more weathered layers with a thickness of between 1 and 3 m.

6.10.2.4 Hydrogeology

No water levels were measured in this Zone. Historic groundwater data up to 1993 indicates that this zone is dewatered.

6.10.2.5 Final characterisation

This Zone is generally covered by transported and residual material with a thickness of between 1 and 3 m, with a corresponding high mobilisation potential. A highly weathered section with a thickness of between 1 and 7m overlies the dolomite bedrock. The material within this highly weathered section predominantly includes chert-rich dolomite residuum, chert and chert-rich-and/or chert-poor dolomite, with a resultant high mobilisation potential. The nature of the overburden material and the subsurface conditions, result in a high inherent susceptibility for the formation of small size sinkholes and subsidences with respect to water ingress. The resulting classification is given as Inherent Hazard Class 5 with respect to ingress of water.

The inherent susceptibility for mobilisation is low from a groundwater level drawdown perspective. The resulting classification is an Inherent Hazard Class 1 with respect to further groundwater level drawdown.

This area is characterised as reflecting a high inherent susceptibility for the formation of small size sinkholes and subsidences with respect to ingress of water and a low susceptibility for the formation of all size sinkholes and subsidences with respect to further groundwater level drawdown. The composite hazard designation for this Zone is Inherent Hazard Class 5//1.

6.10.3 Dolomite Hazard Zone C

6.10.3.1 Gravity signature

The area is characterised by an east-west striking gravity high anomaly and a gravity low plateau anomaly in the central portions of the project area, bordered by a transition into approximately north-east/south-west and north-west/south-east striking gravity troughs.

6.10.3.2 Nature of the overburden material

No substantial blanketing layer overlies the dolomite bedrock in this Zone. The overburden material is characterised by the following:

- The dolomite bedrock is generally overlain by highly weathered material (overburden) composed of colluvium, chert residuum and chert, dolomite residuum (wad, and in some

cases chert-rich/chert-poor dolomite residuum), grading into less weathered dolomite with depth.

- The overburden is between 5 and 14 m thick in the central regions, and between 6 and 22 m in the southern parts of this Zone.
- Some of the boreholes in this Zone reflected slight air loss, and very occasionally some sample loss.
- Irregular hammer rates were recorded in this Zone.

6.10.3.3 Bedrock configuration

All boreholes were drilled at least 6 m into competent dolomite bedrock. Slightly weathered dolomite bedrock was encountered from a relatively shallow depth (between 5 and 14 mbgl) in the central regions of this Zone, and between 7 and 23 mbgl in the southern-most portions of this Zone. The bedrock morphology in this Zone is expected to be rugged between data points.

6.10.3.4 Hydrogeology

A single water level was measured (KBH 36), which is regarded as representing a perched water table due to influx from the adjacent Kromdraaispruit. The dolomite compartment is dewatered below this zone.

6.10.3.5 Final characterisation

A highly weathered section with a thickness of approximately 5 to 9 m overlies the dolomite bedrock in this Zone, with localised portions exhibiting a deeper weathered profile with depths of up to 14 to 22 m. The bedrock morphology in this Zone is expected to be relatively rugged, with the weathered material comprising colluvium, chert residuum and highly weathered chert, and dolomite residuum with wad (in some instances chert-poor and/or chert-rich residuum), grading into highly weathered dolomite. This material is characterised as having a high mobilisation potential. Subsequently, the nature of the blanketing layer and the subsurface conditions, result in a high inherent susceptibility for the formation of small size sinkholes and subsidences, and sub-areas reflecting a high inherent susceptibility for the formation of medium size sinkholes and subsidences with respect to water ingress. The resulting classification is given as Inherent Hazard Class 6 (with sub-areas of 5) with respect to ingress of water.

The compartment below this zone (KOSH Compartment B) is dewatered, with a resulting low inherent susceptibility for the formation of all size sinkholes and subsidences with respect to

further groundwater level drawdown. The Inherent Hazard Class for this Zone is 1 with respect to groundwater level drawdown.

The composite hazard designation for this Zone is Inherent Hazard Class 6(5)/1.

6.10.4 Dolomite Hazard Zone D

This area is divided into three sub-areas, namely D1 to D3.

6.10.4.1 Gravity signature

The combined area is characterised as gravity gradient areas of a highly dissected gravity plateau grading into adjacent gravity low anomalies in the east.

6.10.4.2 Nature of the overburden material

The blanketing layer in this Zone is characterised by the following:

- The area is underlain by a combination of highly to moderately weathered dolomite with different chert contents.
- Boreholes drilled in this Zone reflected some sample loss, irregular hammer rates and up to moderate air loss.
- The dolomite bedrock is overlain by between 5 to 40 m of weathered overburden, ranging from localised horizons containing wad with traces of chert to moderately weathered dolomite.

6.10.4.3 Bedrock configuration

All boreholes were drilled at least 6 m into competent bedrock, and the bedrock in this area ranges from moderately weathered to slightly weathered dolomite with varying chert contents.

The structure of the dolomite bedrock, as seen in the surrounding bedrock, has been altered in Zone D3, associated with a north-west/south-east trending lineament, possibly a fault.

6.10.4.4 Hydrogeology

No water levels were measured in this Zone. Historic groundwater data up to 1993 indicates that the KOSH compartment B is dewatered.

6.10.4.5 Final characterisation

The overburden material in this Zone is highly weathered with a resulting high mobilisation potential. The material within the highly weathered zone ranges from transported soil cover to chert and dolomite residuum (with wad) and interlayered moderately weathered dolomite bands. The resulting nature of the blanketing layer and the subsurface conditions is sub-divided into three Zones, largely reflecting the same primary character with varying sub-areas.

Zone D1 is characterised as reflecting a high inherent susceptibility for the formation of medium size (with sub areas of high susceptibility for small size) sinkholes and subsidences with respect to ingress of water the resulting classification is given as Inherent Hazard Class 6 (with sub-areas of 5) with respect to ingress of water.

Zone D2 is characterised as reflecting a high inherent susceptibility for the formation of medium size sinkholes and subsidences with respect to ingress of water. The resulting classification is given as Inherent Hazard Class 6 with respect to ingress of water.

Zone D3 is characterised as reflecting a high inherent susceptibility for the formation of medium size (with sub areas of high susceptibility for very large size) sinkholes and subsidences with respect to ingress of water. The resulting classification is given as Inherent Hazard Class 6 (with sub-areas of 8) with respect to ingress of water.

No water levels have been measured in the boreholes of this Zone (up to a depth of 60 meters) and the compartment below this zone is dewatered. The inherent susceptibility for mobilisation is low from a further groundwater level drawdown perspective. The resulting classification is an Inherent Hazard Class 1 with respect to further groundwater level drawdown.

- The composite characterisation of Zone D1 is therefore Inherent Hazard Class 6(5)//1.
- The composite characterisation of Zone D2 is therefore Inherent Hazard Class 6//1.
- The composite characterisation of Zone D3 is therefore Inherent Hazard Class 46(8)//1.

6.10.5 Dolomite Hazard Zone E

6.10.5.1 Gravity signature

This zone is characterised by a prominent east-west striking gravity low anomaly in the southern half of the project area with associated northeast-southwest striking gravity low anomalies in the south-eastern quadrant of the project area. These anomalies have a steep gradient into adjacent gravity high and plateau anomalies.

6.10.5.2 Nature of the overburden material

The dolomite bedrock in this Zone does not have any significant blanketing layer. The highly weathered material overlying the dolomite bedrock is characterised by the following:

- Dolomite bedrock is generally overlain by colluvium/alluvium, and by residual material (i.e.: chert residuum, highly weathered chert, and dolomite residuum (containing wad, in some instances), and chert-rich or chert-poor dolomite residuum). The strata generally become more competent with depth, and contain cavernous conditions with interlayered harder chert and dolomite bands/boulders, especially directly above the solid dolomite bedrock.
- All of the boreholes drilled in this Zone reflected varying degrees of air- and sample loss, with the majority of the boreholes reflecting total air- and sample loss, with very irregular hammer rates from a depth of between 15 to 40 m, possibly indicating incipient sinkholes in some instances.
- The dolomite bedrock is overlain by approximately 15 to 40 m of overburden ranging from chert and dolomite residuum with wad, to highly weathered dolomite.

6.10.5.3 Bedrock configuration

The bedrock in this Zone varies from highly weathered dolomite containing different concentrations of chert, that grades into slightly weathered dolomite bedrock (containing chert in most instances). The bedrock generally becomes more competent with depth, and is characterised by cavernous conditions within the highly weathered bedrock. The majority of the boreholes were drilled at least 6 m into competent bedrock, with one borehole (KBH 28) terminated at a depth of 60 m due to difficult drilling and cavernous conditions.

The bedrock morphology correlates with the gravity anomaly of the Zone, and is associated with deep leaching and weathering, as well as a prominent east-west striking deeply weathered section with associated smaller north-east/south-west striking weathered portions.

6.10.5.4 Hydrogeology

No water levels have been measured in the boreholes of this Zone (up to a depth of 60 m). The dolomite compartment below the Zone is dewatered.

6.10.5.5 Final characterisation

The blanketing layer of this Zone is characterised a deeply weathered profile grading into highly weathered and cavernous dolomite bedrock. The material is predominantly highly weathered down to approximately 45 m, where after the bedrock becomes less weathered.

The material within this area of the site ranges from transported soil cover, to highly weathered dolomite and wad. The succession contains different amounts of chert, and is generally cavernous. Overburden and highly weathered dolomite across this Zone is characterised as having a high mobilisation potential. The resulting nature of the blanketing layer, and the subsurface conditions, result in a high inherent susceptibility for the formation of very large size (with sub areas of high susceptibility for large size) sinkholes and subsidences with respect to water ingress. The resulting classification is given as Inherent Hazard Class 8(7) with respect to ingress of water.

The inherent susceptibility for mobilisation is low from a groundwater level drawdown perspective. The resulting classification is an Inherent Hazard Class 1 with respect to further groundwater level drawdown.

The composite hazard designation for this Zone is Inherent Hazard Class 8(7)/1.

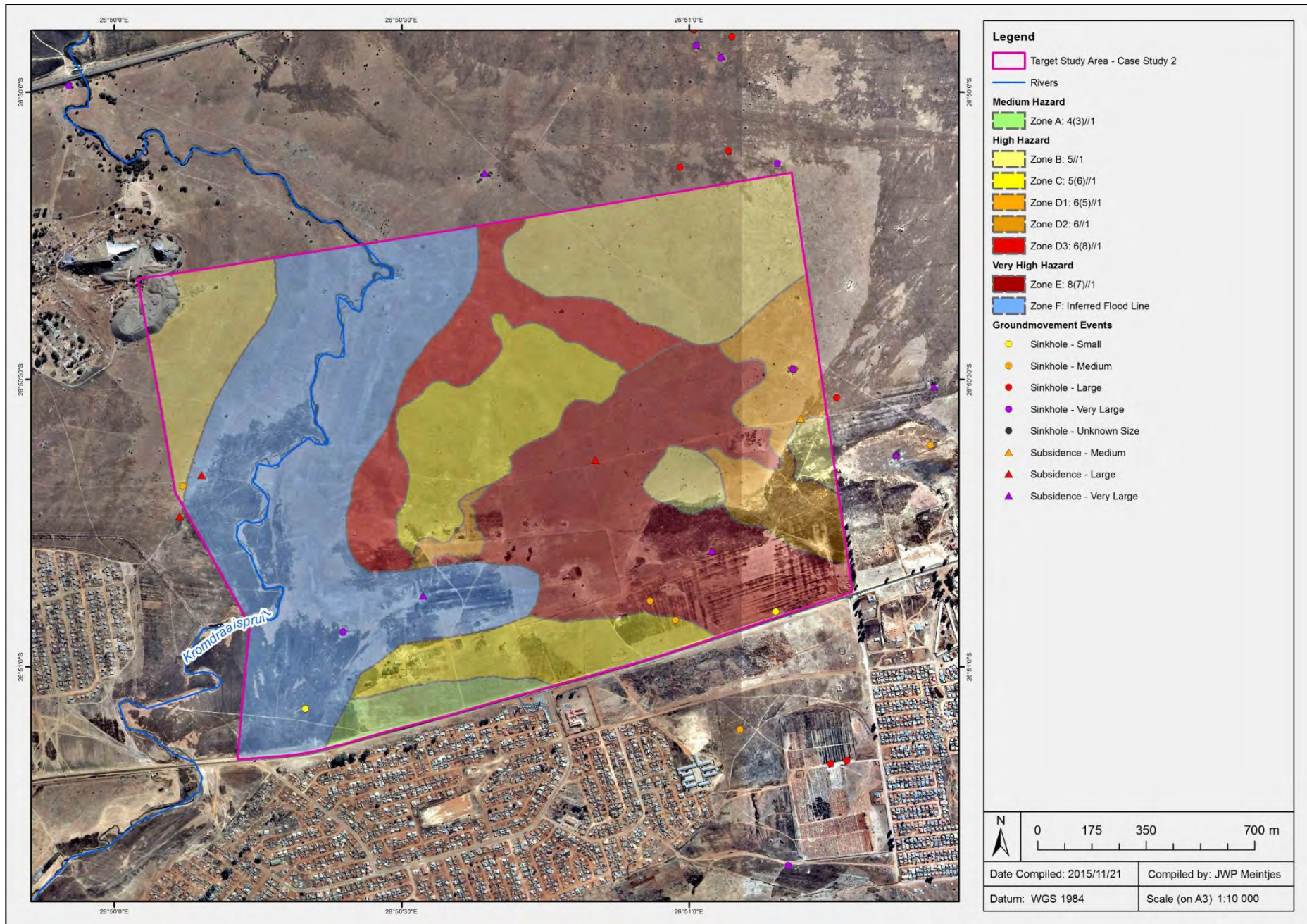


Figure 6-7: Inherent Hazard Class zones determined across the project area

CHAPTER 7 – Conclusions

Upon consideration of the available geo-scientific information across the larger KOSH-area, it is evident that without a regional context of the structural geological setting, local-scale geotechnical investigations and strategic development planning on dolomite are often skewed and wrongfully interpreted with respect to the true character of the area. Geological information contained in the widely used published maps often proves to be insufficient in determining the true regional character on the required scale to establish the expected prevailing dolomitic conditions in an area. This is largely ascribed to the regional focus of the published 1:250 000 scale geological maps that do not indicate local-scale features of significance. Local geological maps across large parts of South Africa (i.e.: 1:50 000 scale mapping) have also not been compiled.

As part of this study, three decision support models were compiled in order to assist in the development of a high-level regional indication of the inherent hazard across dolomite land. The three models include a geological decision tree, hydrogeological considerations to determine the groundwater status and management thereof, and a decision matrix to determine the various regional extents of *indicated dolomite hazard zones* across the demarcated dolomite land. It should be regarded that the demarcated *indicated dolomite hazard zones* are not intended to replace site-specific dolomite stability investigations, but rather assist in strategic- and regional planning and to provide an initial conceptual geological and hydrogeological model of the region, prior to local scale investigations. Additionally, this study will form the basis for a regional dolomite risk management strategy for the KOSH-area. An initial sinkhole and subsidence database was also compiled for the KOSH-area.

After assessing the structural geological setting across the KOSH-area from a dolomite risk management perspective, the following can be concluded:

- (a) The various lithostratigraphic sub-divisions have not previously been differentiated across the entire area. Some local mapping across mining properties indicated the extent of possible contacts between these successions and the stratigraphy of dolomite in the area. Areas where no geological information could be obtained were subsequently mapped to determine geological contacts and to verify existing geological information in close proximity of these areas. This will provide – at least on a sub-regional scale – some idea towards where future development should take place, based on the inherent higher hazard associated with the chert-rich dolomitic formations and the extent of major structural geological features intersecting the area.

- (b) In addition to the broad mapping of the different dolomitic Formations across the region, it was determined that the east-west striking Karoo Supergroup outcrops in the area can be interpreted as an in-filled paleo-karst valley. The extent of this Paleo-karst valley was amended based on the available borehole information in the region, seeing as this feature does not form outcrops in the area. The possibility that this east-west striking feature could be the result of deep scouring of the dolomite bedrock by glacial activity, rather than deep leaching of the dolomite along structural controls, could not be determined or ruled out. The stability of this Karoo Supergroup Inlier must be considered with care, where conventionally it is deemed “safe land” to develop upon. It is known that this feature was deposited on a Paleo-karst bedrock topography, and as such varies greatly in depth across the area (e.g.: between 5 and 190 m in thickness). Very deep (but small-diameter) sinkholes are also associated with this feature, where sinkholes of up to 300 m deep were reported in the past. The geological contacts of the outlier with the surrounding dolomitic formations are also considered to be more prone to sinkhole formation. This could be due to differential settlement along contacts, large-scale seasonal shrink and heave action along the contacts, as well as a high relative difference in the degree of permeability along the contacts of the Karoo outlier with the surrounding dolomitic strata.
- (c) The published 1:250 000 scale geological map was found to be incomplete in terms of the extent of linear features, dykes, quartz vein intrusions, and faults intersecting the dolomite in the KOSH-area. A large number of these features were identified on previously compiled geological maps of the region as well as stereography and field mapping. It was found that a large number of ground movement events occur along such north-east/south-west trending features, and proves to be a critical consideration when assessing dolomitic sites in this area. The concentration of instability features along geological structures are inferred to be due to deep leaching and a higher degree of weathering that occurs along these vertical to sub-vertical lineations. Exactly this was confirmed by the drilling of percussion boreholes towards the eastern parts of the area, where a larger concentration of these features coalesce. Fault- and shear-zone associated indications – such as deformation breccia and quartz vein intrusions – must be regarded as very high-risk areas from a dolomite stability perspective and assessed with great caution.
- (d) The dolomitic strata across the entire KOSH-area have been extensively altered by tectonic deformation (faulting, folding and tilting). This was caused by three prominent historic stages of deformation: the (i) re-activation of Ventersdorp-age tectonism where residual stress was relieved along existing Ventersdorp-age fault planes after the deposition of the Transvaal Supergroup, (ii) Transvaal-age deformation, and (iii) the

Vredefort Meteor Impact event. The Vredefort event was found to have resulted in the most significant structural deformation of the dolomitic strata in the area. It was observed that the western parts of the Malmani Subgroup (and the Black Reef Formation) were not as significantly affected by the Vredefort Meteor Impact as the eastern parts. The western parts are more associated with large-scale folding, whereas the eastern parts are associated with folding, faulting, and thrusting.

- (e) Various periods of erosion occurred in the area. This can be observed in the stratigraphy of the region. The first stage of erosion was prior the deposition of the Black Reef Formation, where the Black Reef Formation was subsequently deposited on a paleo-topography of the Ventersdorp Supergroup. The second era of erosion was during the various depositional stages of the Malmani Subgroup, and prior to the deposition of the Pretoria Group, leaving a rugged topography on which each subsequent stratigraphically younger formation was deposited. The last significant period of erosion was after the deposition of the Karoo Supergroup in the area, where the entire regional stratigraphic succession was eroded to the current-day surface. A number of unconformities in the area are associated with faulting and tectonic deformation, especially due to the Vredefort Meteorite Impact.
- (f) Outcomes of the hydrogeological assessment conducted across the region confirmed that the eastern parts of the KOSH-area is currently dewatered, and the larger extent of the western parts have not been subjected to large-scale dewatered. However, evidence exist that the western parts are subjected to occasional and sporadic local-scale dewatering. It was determined that the Welgegund groundwater compartment situated towards the north of the KOSH-area is not currently dewatered. The overall regional area was considered from a dewatering dolomite scenario, largely ascribed to the currently dewatered regions in combination with the absence of groundwater monitoring and control measures currently in place across the larger KOSH-region. The need for stringent groundwater monitoring and management measures as well as vigilance will be required across the entire urbanised eastern region once dewatering ceases, seeing as it is expected that a significant number of ground movement events will occur during this time.
- (g) Based on the new understanding of the structural geological setting and hydrogeological regime of the KOSH-area, the extent of dolomite land was demarcated for a dewatering-type scenario (e.g.: dolomite land is classified as areas underlain by dolomite up to a depth of 100 m) across the area.

- (h) As part of the compiled sinkholes and subsidence database, an initial total of 255 ground movement events (un-rehabilitated sinkholes and subsidences, paleo sinkholes and subsidences, rehabilitated features, and inferred other karst-related features) were accounted for across the larger KOSH-area. Statistics conducted using this compiled dataset indicates an overall total of 0.65 events / km² across the combined dewatered and non-dewatered dolomitic area of approximately 390 km². Available information suggests that ground movement events occurring across the KOSH-area formed over a period of 37 years, seeing as no information could be obtained prior to 1978. This could be due to no records being kept prior to 1978, and is not necessarily ascribed to any features forming prior to 1978. A larger number of sinkholes were found to have occurred since 2005, primarily due to the initiation of re-mining of existing mine tailings in the area. The rate of new sinkhole formation (NSH) across the KOSH-area was calculated to be 0.02 events / km² / year, which translates to an expected total of 6.9 events per year. This is substantially lower than the initially expected 25.5 events per year that was inferred from the study across the Carletonville area conducted by Richardson (2013). The total number of events per year more closely correlates with the Pretoria-area.
- (i) The most sinkholes and subsidences occurred across the chert-rich dolomite of the Monte Christo Formation. This is due to the relatively larger surface area covered by this formation across the KOSH-area, much of the mining developments in the area being constructed across this Formation, as well as an inherently higher hazard associated with this Formation due to continuous chert bands. Sinkholes are generally large in diameter (e.g.: 5 to 15 m) in the KOSH-region, although some very large features are present in the area (up to 70 x 200 m in diameter). The majority of the sinkholes across the KOSH-area are relatively shallow (less than 5 m deep) and represents typical buried or suffosion sinkholes. Some deep textbook concentric sinkholes also exist in the region. Subsidences also tend to be more associated with the chert-rich Formations (Monte Christ Formation followed by the Eccles Formation), with some subsidences also prevalent in the Lyttleton Formation. The majority of subsidences in the KOSH-area are very large in diameter (e.g.: in excess of 15 m). Very little ground movement events were observed/recorded across the Oaktree Formation.
- (j) An association is evident in the KOSH-area between the dip direction of the regional geological succession and the direction of sinkhole throats. These tend to be in the same directions across the KOSH-area.

- (k) Sinkhole statistics imply that the regional area (taking into consideration the various identified ground movement events) is characterised as *Mature Karst* according to the engineering classification proposed by Waltham & Fookes (2003). This suggests that the area is underlain by caves that are mostly less than 5 m across, an extensively fissured rock head that varies less than 5 m prevails across the region, a large number of secondary openings and fissures are present in the bedrock, and mostly suffosion and dropout sinkholes with small collapsed and buried sinkholes can be expected. However, *Extreme Karst* conditions are inferred to occur across areas that have been subjected to more intense structural deformation.
- (l) The local-scale dolomite stability investigation conducted in the area presented compelling evidence that *Extreme Karst* conditions prevail. This could be ascribed to the connotation to a large concentration of structural features in the vicinity of the eastern parts that were induced by the Vredefort Meteor Impact.
- (m) The compiled regional *indicated dolomite hazard zones* (Case Study 1) were found to correlate well with the anticipated hazard in the demarcated zones, as verified during a local-scale dolomite stability investigation (Case Study 2). This investigation confirmed the demarcated “very high hazard” *indicated dolomite hazard zones* across the majority of the eastern parts of the area, seeing as the Vredefort Meteor Impact more significantly affected this area, in comparison with the western parts. The detailed dolomite stability investigation concluded that the majority of the area east of the old Khuma that is not underlain by the Karoo Inlier is undevelopable, and large parts were determined to be high-risk dolomite (i.e.: IHC 5 to 8). Sinkholes and subsidences occur in the project area.

CHAPTER 8 – Recommendations for further studies

Based on the outcomes of this research, the following additional studies area proposed:

- (a) A detailed sedimentological study across the broadly demarcated lithostratigraphic sub-divisions of the Malmani Subgroup dolomite is proposed, in line with the initial work done by Obbes (2000) in the Pretoria-area. This study can include the areas from south of the Vaal River to Carletonville. Core drilled in the area by mine houses could be re-interpreted to assist in the demarcation of different geological contacts.
- (b) A regional thermal line-scanning infrared survey is proposed across the demarcated dolomite land to determine the Paleo drainage regime of the area, and classify the region according to the criteria proposed by Van Rooy (1984).
- (c) Regional air borne gravimetric and magnetic survey information should be assessed across the area to verify the regional extent of dykes and extent of smaller local faults. The gravimetric survey could also be incorporated into the existing regionally derived indicated dolomite hazard zones and refined, based on the criteria proposed by Brink (1979) and Kleywegt and Enslin (1973).
- (d) Incorporating land-uses, infrastructure conditions, socio-economic, and social vulnerability aspects into the demarcated inherent dolomite hazard zones is proposed to work towards a risk determination model of the area.
- (e) The risk model should be accompanied by detailed geotechnical and dolomite stability investigations across developed areas to demarcate measured inherent hazard areas across the region. A list of proposed township areas and further investigations are included in Table 7-2, Annexure 4.
- (f) The application of the developed Decision Support Systems for the compilation of a geological, hydrogeological and indicated hazard of a region is proposed to be applied elsewhere to determine the performance of the systems in other geological settings. It could be that the systems might require some tweaking to accommodate region-specific geological aspects elsewhere.
- (g) Geochemical analysis of the different dolomitic formations in the KOSH-area could provide valuable information regarding the depositional model, as well as more accurate contents of insoluble residues (e.g.: wad) in the geological profile. These findings could be correlated with the work done by Buttrick (1986), Roux (1984), Wagener (1982) and

Wolmarans (1996) elsewhere, and will assist in understanding the nature of the overburden across the various lithostratigraphic sub-divisions.

- (h) A highly focussed site-specific assessment of the joint structure and orientations at different sinkhole site in the West Rand and Far West Rand could provide valuable information regarding the regional trends of sinkhole occurrences in relation to the regional geological structure. The sinkhole databases compiled by Oosthuizen (2013) and Richardson (2013) could be updated with geological and anthropogenic components to the sinkhole formation and distribution.
- (i) It is recommended that the aquifer vulnerability mapping using the modified COP method (referred to as the VUKA index) as set out by Leyland *et al.*, (2008) be applied to the Welgegund- and KOSH groundwater compartments. This method takes into consideration the concentration of flow (C-factor), the overlying layers – including soil and lithology – (O-factor), and the precipitation of the area (P-factor). Leyland *et al.*, (2008) is of the opinion that it is required to compile an aquifer vulnerability map of an area prior to any development as part of the Dolomite Stability Investigation process.
- (j) It could be of value to determine the relative ages of various stalactites and stalagmites that formed in the various caves throughout the West Rand to correlate the relative ages of the caves. This can be achieved by collecting samples from various stalactites and stalagmites (generally retrieved by means of horizontal core boring to the centre of the stalagmite or stalactite), and conducting age determinations of the samples. It is hypothesized that the central parts of the stalagmite or stalactite will be the oldest, and the cave will be just older than the oldest determined age.
- (k) A comparative study to determine the current status and advancements of South African guidelines to characterise the inherent hazard posed by dolomite with other parts of the world could provide a holistic understanding of where South Africa stands with respect to the rest of the world on dolomite assessments.

Bibliography

- ALCANTARA, A. 2002. Geomorphology, natural hazards, vulnerability and prevention of natural disasters in developing countries. *Geomorphology* Volume 47. Elsevier SO169-555X(02)00088-1.
- ALTERMANN, W. & WITHERSPOON, J. Mc D. 1995. The carbonates of the Transvaal and Griqualand West Sequences of the Kaapvaal Craton, with reference to the Lime Acres limestone deposit. *Mineralium Deposita*, 30, 124-134 pp.
- ANTROBUS, E.S.A., BRINK, W.C.J., BRINK, M.C., CAULKIN, J. HUTCHINSON, R.I., THOMAS, D.E., VAN GRAAN, J.A., VILJOEN, J.J. 1986. The Klerksdorp goldfield. *Mineral Deposits of Southern Africa (1986)*, pp. 549- 598.
- AVUTIA, D. & KALUMBA. D. 2014. Geomechanical response towards sinkhole propagation in Centurion, South Africa. *Proceedings of the Dolomite Seminar 2014, 25 & 26 June 2014, UP*
- BARNARD, H.C. 1999. 1:500 000 general hydrogeological Map, Johannesburg 2526. DWAF, Geohydrology. Pretoria.
- BARNARD, H.C. 2000. An explanation of the 1:500 000 general hydrogeological Map, Johannesburg 2526. DWAF, Geohydrology. Pretoria.
- BECK, B.F. & SINCLAIR, W.C. 1986. Sinkholes in Florida: an introduction. Florida sinkhole research institute / the United States Geological Survey. Orlando, Florida, 1986.
- BEUKES, N.J. 1987. Facies relationships, depositional environments and diagenesis in a major early Proterozoic stromatolitic carbonate platform to basinal sequence, Campbellrand Subgroup, Transvaal Supergroup, South Africa. *Sedimentary Geology*. Volume 54, pp. 1-56.
- BISSCHOFF, A.A. 1992. Potchefstroom Dorp en Dorpsgronde Geologiese Kaart. 1 : 50 000.
- BOSCH, P.J.A. 2007. A holistic approach in geological information interpretation and representation to optimize and aim engineering geological zonation on dolomite hazardous land. Council for Geoscience.
- BRADLEY, W.F., BURST, J.F. & GRAF, D.L. 1953. Crystal chemistry and differential thermal effects of dolomite. *Amer. Min.* Volume 28, 207 pp.

- BRINK M.C., WAANDERS, F.B. & BISSCHOFF, A.A. 2005. The potential effect of prospecting or mining on the Vredefort Dome World Heritage Site. Proceedings 2nd International Conference of Chemistry and the Environment, 2005, 274-278. School of Chemical and Minerals Engineering, North-West University, Potchefstroom, 2520, South Africa.
- BRINK, A.B.A. & BRUIN, R.M.H. 2001. Guidelines for Soil and Rock Logging in South Africa, 2nd Impression. Proceedings, Geoterminology Workshop organised by AEG, SAICE and SAIEG, 1990.
- BRINK, A.B.A. & PARTRIDGE, T.C. 1965. Transvaal karst – some considerations of development and morphology with special reference to sinkhole and subsidence's on the Far West Rand. The S. A. Journal, Volume XLVII, December 1965.
- BRINK, A.B.A. 1979. Engineering Geology of Southern Africa. Volume 1. Building Publications, Silverton, 1979.
- BRINK, A.B.A. 1981. Geology and Geomorphology. Seminar on the Engineering geology of dolomite areas, University of Pretoria, Pretoria, 26-27 November 1981.
- BRINK, A.B.A. 1996. Mechanisms of sinkhole and doline formation. Seminar on the Engineering geology of dolomite areas, University of Pretoria, Pretoria, 18 January 1996.
- BRINK, A.B.A., PARTRIDGE, T.C. & WILLIAMS, A.A.B. 1982. Soil survey for engineering. Monographs on soil survey. Clarendon Press, Oxford, 1982.
- BRINK, M.C., WAANDERS, F.B. & BISSCHOFF, A.A. 1999. The Katdoornbosch-Witpoortjie Fault: A ring thrust of Vredefort age. University of the Witwatersrand, Economic Geology Research Unit, Information Circular No 333. Published by University of the Witwatersrand, Johannesburg. ISBN 1-86838-294-4.
- BRINK, M.C., WAANDERS, F.B., BISSCHOFF, A.A. & GAY, N.C. 2000. The Foch Thrust-Potchefstroom Fault structural system, Vredefort, South Africa: a model for impact-related tectonic movement over a pre-existing barrier. Journal of African Earth Sciences, 30(1):99-117.
- BUTTON, A. 1972. The stratigraphic history of the Malmani Dolomite in the eastern and north eastern Transvaal. University of the Witwatersrand, Economic Geology Research Unit, Johannesburg: No. 73.

BUTTRICK, D.B. & ROUX, P. 1993. The safety of high density informal settlements on the dolomites of South Africa. Applied karst geology, Beck (ed) Proceedings. Balkema, Rotterdam (1993). pp 291-294.

BUTTRICK, D.B. & VAN SCHALKWYK, A. 1995. The method of scenario supposition for stability evaluation of sites on dolomitic land in South Africa. Journal of South Africa Institution of Civil Engineers, 37(4), 4-14, 1995.

BUTTRICK, D.B. 1986. The role of wad in stability evaluation. Seminar on the engineering geological evaluation of sites on dolomite. South African Geological Survey and University of Pretoria, Pretoria.

BUTTRICK, D.B. 2014. Annual dolomite seminar. Pretoria, South Africa.

BUTTRICK, D.B., 1992. Characterization and appropriate development on sites on dolomite. Unpublished Ph. D. thesis, University of Pretoria, Pretoria, 1992.

BUTTRICK, D.B., AND VAN SCHALKWYK, A. 1996. Stability Evaluation and appropriate development. Seminar on the engineering geology of dolomite areas, university of Pretoria, Pretoria, 18 January 1996.

BUTTRICK, D.B., TROLLIP, N.Y.G., WATERMEYER, R.B., PIETERSE, N.D. & GERBER, A.G. 2011. A performance based approach to dolomite risk management. Environmental Earth Sciences, January 201. pp 1127-1138.

BUTTRICK, D.B., VAN SCHALKWYK, A., KLEYWEGT, R.J. & WATERMEYER, R.B. 2001. Proposed method for dolomite land hazard and risk assessment in South Africa. Journal of the South African Institution of civil engineering. Volume 43. Number 2, 2001. pp 27-36.

CALITZ, F. 2015. Personal communications. Potchefstroom.

CLENDENIN, C. W. 1989. Tectonic influence on the evolution of the early Proterozoic Transvaal Sea, Southern Africa. Ph.D. thesis (unpublished, University of the Witwatersrand, Johannesburg, South Africa).

COETZEE, H.P.A. 1996. The stratigraphy and sedimentology of the Black Reef Quartzite Formation, Transvaal Sequence, in the area of Carletonville and West Rand goldfields. Unpublished M. Sc. thesis, North West University, Potchefstroom, 1996.

COLLINS DICTIONARY OF GEOLOGY. 1990. Glasgow: HarperCollins Publishers.

COUNCIL FOR GEOSCIENCE AND SOUTH AFRICAN INSTITUTE FOR ENGINEERING AND ENVIRONMENTAL GEOLOGISTS. 2003. Guideline for engineering-geological characterisation and development of dolomitic land. Council for Geoscience Publication, 66 pp.

COUNCIL OF GEOSCIENCE. 2007. Consultants guide: Approach to sites on dolomite land.

DARCY GROUNDWATER SCIENTISTS AND CONSULTANTS (DARCY). 2002. A catchment management plan for the Schoonspruit and Koekemoerspruit catchments: A groundwater situation analysis. The department of Water Affairs and Forestry, Bloemfontein, South Africa.

DAY, P.W. 1981. Properties of wad: evaluation of investigation results – Dumprock and chert gravel mattresses. Seminar of Engineering geology of dolomite areas. Department of Geology. University of Pretoria, November 1981.

DE BEER, J.H. 1981. Evaluation of dolomite areas. Seminar on engineering geology for dolomite areas. University of Pretoria, Pretoria, November, 1981.

DE KOCK, W.P. 1964. The dolomite water and its attendant problems. Geology of some ore deposits in South Africa. South African Geological Society, Volume 1, pp. 375-381.

ENSLIN, J.F. & SMIT, P.J. 1955. Geophysical surveys for foundations in South Africa with special reference to the sinkholes in the dolomite south of Pretoria. Transactions of the South African Institute of Civil Engineering. Volume 5, September, 1955.

ERIKSSON, K.A. & TRUSWELL, J.F. 1974. Tidal flat associations from the lower proterozoic carbonate sequence in South Africa. Journal of Sedimentology, Volume 21, pp 293-309.

ERIKSSON, K.A. & WARREN, J.K. 1983. A Paleohydrologic model for early Proterozoic dolomitization and silicification. Precambrian research, Volume 21, pp. 299-321.

ERIKSSON, K.A., McCARTHY, T.S. & TRUSWELL, J.F. 1975. Limestone formation and dolomitisation in a lower Proterozoic succession from South Africa. J. Sediment. Petrol, pp. 604-614.

ERIKSSON, P.G. & ALTERMANN, W. 1998. An overview of the geology of the Transvaal Supergroup dolomites (South Africa). Environmental Geology. Volume 36, pp. 179-188.

ERIKSSON, P.G. & RECZKO, B.F.F. 1995. The sedimentary and tectonic setting of the Transvaal Supergroup floor rocks to the Bushveld Complex. Journal of Afr. Earth. Sci., Volume 21, pp. 487- 504.

ERIKSSON, P.G. 1972. Cyclic sedimentation in the Malmani Dolomite, Potchefstroom Synclonorium. Transactions of the Geological Society of South Africa. Volume 75, pp. 86-97.

ERIKSSON, P.G., ALTERMANN, W. & HARTZER, F.J. 2006. The Transvaal Supergroup and its precursors. The Geology of South Africa. Published jointly by the Geological Society of South Africa, Johannesburg, and the Council of Geoscience, Pretoria.

ERIKSSON, P.G., ALTERMANN, W., CATUNEANU, O., VAN DER MERWE, R. & BUMBY, A.J. 2001. Major influences on the evolution of the 2.67-2.1 GA Transvaal basin, Kaapvaal craton. Sedimentary Geology. Volume 141-142. pp. 205-231.

FORD, D.C. & WILLIAMS, P. 2007. Karst Hydrogeology and Geomorphology. Second Edition, Wiley March 2007.

HARTOPP, P.G. 1978. Use of thermal linescanning imagery for engineering geological investigations in dolomite terrain. AEG newsletter (SA Section) Volume 2, No. 3, 1978.

HOLLAND, M. & WIEGMANS, F. 2009. Desktop development of a dolomite hydrogeological compartment map and explanation booklet. Submitted to the Department of Water Affairs, South Africa under the project: Geohydrology guideline development: Implementation of Dolomite Guideline – Phase 1. Project No. 14/14/5/2.

IRWIN, M.L. 1965. General theory of epeiric clear water sedimentation. Bulletin of American Association of Petroleum Geology. Volume 49, No. 4, April 1965.

JANSEN, H. 1967. Explanatory notes to 2626 WES-RAND 1:250000 Geological Series Map. Pretoria: Government Printer.

JENNINGS, J.E. 1966. Building on dolomites in the Transvaal. The Civil Engineer in South Africa, February 1966.

JENNINGS, J.E., BRINK, A.B.A. & WILLIAMS, A.A.B. 1973. Revised guide to soil profiling for Civil Engineering Purposes in South Africa. The Civil Engineer in South Africa, January, 1973.

JENNINGS, J.E., BRINK, A.B.A., LOUW, A. & GOWAN, G.D. 1965. Sinkholes and subsidences in the Transvaal dolomite of South Arica. In; Proceedings 6th International conference of soil Mechanics and foundation engineering, Montreal, pp 51-54.

JOHNSON, M.R., VAN VUUREN, C.J., VISSER, J.N.J., COLE, D.I., WICKENS, H. DE V., CHISTIE, A.D.M., ROBERTS, D.L. & BRANDL, G. 2006. The Geology of South Africa. Edited

by Johnson, M.R., Anhaeuser, C.R. and Thomas, R.J. Published jointly by the Geological Society of South Africa, Johannesburg, and the Council of Geoscience, Pretoria.

JONES, D.H. 1984. Unstable ground conditions associated with Karoo outliers in the dolomitic environment of the Far West Rand. Unpublished M. Sc. thesis. University of Pretoria, Pretoria, September 1987.

KIRSTEN, H.A.D., HEATH, G.J., VENTER, I.S., TROLLIP, N.Y.G. & OOSTHUIZEN, A.C. 2009. The issue of personal safety on dolomite: a probability based evaluation with respect to single-storey residential houses. *Journal of the South African Institution of Civil Engineering*, 51(1):26-36.

KLEINHANS, I. & VAN ROOY, J. L. 2014. The formation of Sinkholes of Subsidences and related Geotechnical Models. Proceedings of the Dolomite Seminar 2014, 25 & 26 June 2014, UP.

KLEYWEGT, R. 1987. Keynote address. Seminar on the engineering geological evaluation of site on dolomite. South African Geological Survey and University of Pretoria, Pretoria, November 1987.

KLEYWEGT, R.J. & ENSLIN, J.F. 1973. The application of the gravity method to the problem of ground settlement and sinkhole formation in dolomite in the far west rand, South Africa. Proceedings: IAEG Symposium on sinkholes and subsidence Engineering-Geological Problems related to soluble rocks, Hannover, pp 1-15, 1973.

KLEYWEGT, R.J. & PIKE, D.R. 1982. Surface subsidence and sinkholes caused by lowering of the dolomitic water table on the Far West Rand Gold Field of South Africa. *Anal of Geological Survey of South Africa*. Volume 16, pp. 77– 105.

KLEYWEGT, R.J. 1980. Engineering geological problems associated with soluble rocks in the Republic of South Africa. *Ground profile Newsletter in Geological Division of the South African Institute of Civil Engineering*. No. 23, July 1980.

L&W ENVIRONMENTAL (L&W). 1993. KOSH Regional Groundwater Study. A report to the KOSH Mine Managers Association, Klerksdorp, South Africa.

LATTMAN, L.H. & RAY, R.G. 1965. *Aerial photographs in field geology*: Holt, Reinhart and Winston, New York.

MARTINELLI, E. & HUBERT, G.L. 1980. The application of geo-electrical measurements to the definition of a shale/dolomite contact in the Witwatersrand area. *The Civil Engineer in South Africa*. November 1980.

MARTINI, J.E.J. 2006. Karst and Caves. In: Johnson, M.R., Anhausser, C.R., THOMAS, R.J. Eds. 2006. *The Geology of South Africa*. Geological Society of South Africa, Johannesburg / Council for Geoscience, Pretoria, 661-668 pp.

MELLOR, E.T. 1934. KF589 Map of Potchefstroom – Showing fifteen-mile radius. Council of Geoscience.

MINETT, R.C.A. 1979. Krugersdorp remote sensing research project: Spectral Africa, Report 15.

NEL, L.T. 1934. Geological Map of Klerksdorp-Ventersdorp; 1:60 000 (Sheet 1). *Geol. Surv. S. Afr.*, Government Printer, Pretoria.

NEL, L.T. 1935. The geology of the Klerksdorp-Ventersdorp area. *Spec. Publ. Geol. Surv. S. Afr.*, 9, 130 pp.

OBBER, A.M. 2000. The structure, stratigraphy and sedimentology of the Black Reef-Malmani-Rooihoghte succession of the Transvaal Supergroup southwest of Pretoria. *Bulletin 27 Council for Geoscience*.

OOSTHUIZEN, A.C. 2013. The hazard of sinkhole formation in Centurion CBD and surrounding areas: Pretoria, Gauteng. Unpublished M. Sc. thesis, University of Pretoria, Pretoria, 2013.

PARROCK, A. L. 2014. Calculation of Sinkhole Size for the Design of Structures using available Geotechnical Parameters. *Proceedings of the Dolomite Seminar 2014, 25 & 26 June 2014, UP*.

PRETORIUS, D.A. 1979. The depositional environment of the Witwatersrand goldfields: A chronological review of speculations and observations. In: *Some sedimentary basins and associated ore deposits of South Africa*. Geological Society of South Africa. Special Publication No. 6, 1979, pp. 33 – 55.

PRETORIUS, J. 2004. Water Use License Application Report for pumping Underground water at Stilfontein Gold Mine. Institute for Groundwater Studies, Bloemfontein, South Africa.

RICHARDSON, S. 2013. Sinkhole and subsidence record in the Chuniespoort Group dolomite, Gauteng, South Africa. Unpublished M. Sc. thesis, University of Pretoria, Pretoria, 2013

RIEMANN, K., CHIMBOZA, N. & FUBESI, M. 2012. A proposal for groundwater management framework for municipalities in South Africa. International Conference on Groundwater Special Edition 38(3).

ROSEWARNE, P.N. 1982. Extension of the Far West Rand Project – Potchefstroom to the Vaal River. Technical report no. GH 3216. Pretoria, Department of Environmental Affairs, Directorate of Water Affairs.

ROUX, P. 1981. Investigation techniques on dolomite. Seminar on the Engineering geology of dolomite areas, Department of Geology, university of Pretoria, Pretoria, November 1981.

ROUX, P. 1984. Geotegniese ondersoek vir dorpsontwikkeling in dolomietgebiede. Unpublished D. Sc. dissertation, university of Pretoria, 1984.

SCH NIN , W.L. 1990. Verspreiding van singate en versakkings in die dolomietgebiede suid van Pretoria. Unpublished M.Sc. thesis, University of Pretoria, Pretoria, 1990.

SCH NIN , W.L. 1996. Distribution of sinkholes and dolines in the area south of Pretoria. Seminar on the engineering geological evaluation of sites on dolomite areas, University of Pretoria, Pretoria, 18 January 1996.

SOUTH AFRICA: DEPARTMENT OF PUBLIC WORKS (DPW). 2006. Appropriate development of infrastructure on dolomite: Manual for consultants. Pretoria: Government Printer. 1 – 375 p.

SOUTH AFRICA: DEPARTMENT OF WATER AFFAIRS AND FORESTRY (DWAF). 2006. A guideline for the assessment, planning and management of groundwater resources within dolomitic areas in South Africa Volume 2.

SOUTH AFRICA: DEPARTMENT OF WATER AFFAIRS AND FORESTRY (DWAF). 2004. Lower Vaal Water Management Area: Internal Strategic Perspective. Prepared by PDNA, WRP Consulting Engineers (Pty) Ltd, WMB and Kwezi-V3 on behalf of the Directorate: National Water Resource Planning. DWAF Report No P WMA 10/000/00/0304).

SOUTH AFRICA. 2002. NATIONAL DEPARTMENT OF HOUSING Generic specification for green fields subsidy-linked housing developments (GFSH 2).

SOUTH AFRICAN NATIONAL STANDARDS (SANS) 1936. 2012. Development of dolomite land - Part 1: General principles and requirements.

SOUTH AFRICAN NATIONAL STANDARDS (SANS) 1936. 2012. Development of dolomite land - Part 2: Geotechnical investigation and determinations.

SOUTH AFRICAN NATIONAL STANDARDS (SANS) 1936. 2012. Development of dolomite land - Part 3: Design and construction of buildings, structures and infrastructure.

SOUTH AFRICAN NATIONAL STANDARDS (SANS) 1936. 2012. Development of dolomite land - Part 4: Risk management.

SPANGENBERG, A. 2000. The management of recharge and quality of underground water in the Klerksdorp area with specific reference to post-closure at the Stilfontein Gold Mine (1952-2000). Unpublished M. Sc. thesis, Rand Afrikaanse Universiteit, Johannesburg, October 2000.

STEPHAN, L.A. 1975. Stability prediction from borehole logs of dolomite areas. Unpublished report, South African Geological Survey.

STRATIGRAPHY OF SOUTH AFRICA (SACS). 1980. By the South African Committee for Stratigraphy.

SWART, C.J.U. 1991. Grouting practices for the evaluation and improvement of dolomitic sites in the Far west Rand, South Africa. Pretoria: UoP. (Dissertation – D.Phil.).

TROLLIP, N.Y.G. 2006. The Geology of an area south of Pretoria, with reference to Dolomite Stability. Unpublished M. Sc. thesis, University of Pretoria, Pretoria, 2006.

TROLLIP, N.Y.G., VAN ROOY, J.L. & ERIKSSON, P.G. 2008. Analysis of the occurrence and importance of slot development (grykes) within shallow dolomite zones in a selected type area of the Eccles Formation. South African Journal of Geology, September 2008. Volume 111, no.2-3. pp 333-344.

VAN DEVENTER, P.W. 2013. Personal communications. Potchefstroom.

VAN DEVENTER, P.W. 2015. Personal communications. Potchefstroom.

VAN ROOY, J.L. & WITTHUSER, K.T. 2008. Vulnerability and risk in karst terrain. SAICE conference: Problems Soils in South Africa. Midrand, 3-4 November 2008.

VAN ROOY, J.L. 1984. Sonering van 'n dolomietgebied suid van Pretoria met behulp van 'n meervoudige-faktor klassifikasiesstelsel. Unpublished M. Sc. thesis, University of Pretoria, Pretoria, 1984.

VAN ROOY, J.L. 1996. Classification systems applied to dolomite terrain, a review. Seminar on the engineering geology of dolomite areas, university of Pretoria, Pretoria, 18 January 1996.

VAN ROOY, J.L. 2014. Annual dolomite seminar. Pretoria, South Africa.

VAN SCHALKWYK, A. 1981. Ontwikkelingspatroon en risiko-evaluasie in dolomietgebiede. The engineering geology of dolomite areas. Department of Geology, University of Pretoria, November 1981.

VELTMAN, S. 2004. A method for groundwater management in dolomitic terrains with the Schoonspruit compartment as pilot area. Bloemfontein: UFS. (Dissertation – M.Sc.)

VENTER, I. S. 2014. SANS 1936-1:2012 Development of Dolomite Land; Part 2: Geotechnical Investigations and Determinations. Proceedings of the Dolomite Seminar 2014, 25 & 26 June 2014, UP.

VENTER, I.S. 1981. Evaluasie van dolomietgebiede - 'n klassifikasie benadering. Seminar on the engineering geology of dolomite sites, University of Pretoria, 26-27 November 1981.

VENTER, L. 2015. Personal communications. Potchefstroom.

VICK, S.G. 1994. Geotechnical risk and reliability – from theory to practice in dam safety. Proceedings: Earth engineers and Education – a symposium in honour of Robert Whitman, Cambridge, Massachusetts.

VILJOEN, R.P. 1980. Thermal scanning techniques as applied to dolomites. Dip. of Mun. Eng. SAICE, Kelvin House, June 1980.

WAGENER, F VON M. 1982. Engineering Construction on dolomite. Ph. D. thesis, University of Natal, November 1982.

WAGENER, F VON M. 1985. Dolomites. Problems of soils in South Africa - state of the Art. The Civil Engineer in South Africa, July 1985. pp 395- 407.

WALRAVEN, F. & MARTINI, J.E.J. 1995. Zircon Pb-evaporation age determinations of the Oaktree Formation, Chuniespoort Group, Transvaal Sequence: Implications for the Transvaal-Griqualand West Basin correlations.

- WALTHAM, A.C. & FOOKES, P.G. 2003. Engineering classification of karst ground conditions. Quarterly Journal of Engineering Geology and Hydrogeology. Volume 36 2003 pp. 101-118.
- WALTHAM, A.C., BELL, F.G. & CULSHAW, M.G. 2005. Sinkholes and Subsidence: Karst and cavernous rocks in engineering and construction. Praxis Publishing Ltd, Chichester, UK, 2005.
- WEAVER, J.M. 1979. Geological investigation conducted at T.E.K. Base Single Quarters, Verwoerdburg. Report number J90/1 for Department Community Development, May 1979.
- WHITE, L.P. 1977. Aerial photography and remote sensing for soil surveys. Monographs on soil survey, Clarendon Press, Oxford.
- WHITE, L.P. 1977. Aerial photography and remote sensing for soil survey. Monographs on soil survey, Clarendon Press, Oxford, 1977.
- WHITE, W.B. 1999. Groundwater flow and transport in karst. *In*: The handbook of groundwater engineering. Delleur J.W. (Editor-in-Chief). CRC Press LCC, Boca Raton.
- WIELAND, F. 2006. Structural analysis of impact-related deformation in the collar rocks of the Vredefort Dome, South Africa. University of the Witwatersrand.
- WILKINSON, K.J. 1986. 2626 WES-RAND 1:250000 Geological Series Map. Pretoria: Government Printer.
- WOLMARANS, J.F. 1984. Ontwatering van die dolomietgebied aan die verre Wes Rand: Gebeure in perpektief. Unpublished D.Sc. thesis, university of Pretoria, 1984.
- WOLMARANS, J.F. 1996. Sinkholes and subsidences on the Far West rand. Seminar on the engineering geology of dolomite areas, university of Pretoria, Pretoria, 18 January 1996.

Annexures

Annexure 1: List of technical reports used in geological assessments of the KOSH area

Table 6-3: Detailed list of Technical Reports conducted by other consultants used in the assessment

REPORT NAME	PORTION / STAND	FARM NAME	REPORT/ CORRESPONDENCE	CONSULTANT	REPORT DATE	LOCAL	DISTRICT
Stilfontein Extensions	-	Hartebeesfontein 422 IP,Zandpan 423 IP	Report	Steffen Robertson & Kirsten	May 1981	Matlosana	Dr Kenneth Kuanda
Stilfontein 408 IP	Portion 122	Stilfontein 408 IP	Report	Intraconsult CC	June 2007	Matlosana	Dr Kenneth Kuanda
Stilfontein Chemwes Gold & Uranium CBE (Chemwes 2)	-	-	Report	Moore Spence Jones (Pty) Ltd	21 January 2008	Matlosana	Dr Kenneth Kuanda
Khuma Ext 6	-	-	Report	VGI Consult	April 2006	Matlosana	Dr Kenneth Kuanda
Stilfontein 408 IP	Portion 61	Stilfontein 408 IP	Report	Intraconsult CC	February 1991	Matlosana	Dr Kenneth Kuanda
Khuma South West Extension	-	-	Report	CGS	January 1993	Matlosana	Dr Kenneth Kuanda
Stilfontein Ext 9	-	-	Report	Intraconsult CC	December 1997	Matlosana	Dr Kenneth Kuanda
Stilfontein Ext 8	Portion 2	Hartebeesfontein 422 IP	Report	Intraconsult CC	January 1994	Matlosana	Dr Kenneth Kuanda
Khuma Greater Area	-	Hartebeesfontein 422 IP	Report	Intraconsult CC	June 1993	Matlosana	Dr Kenneth Kuanda

Annexure 2: Existing geological maps

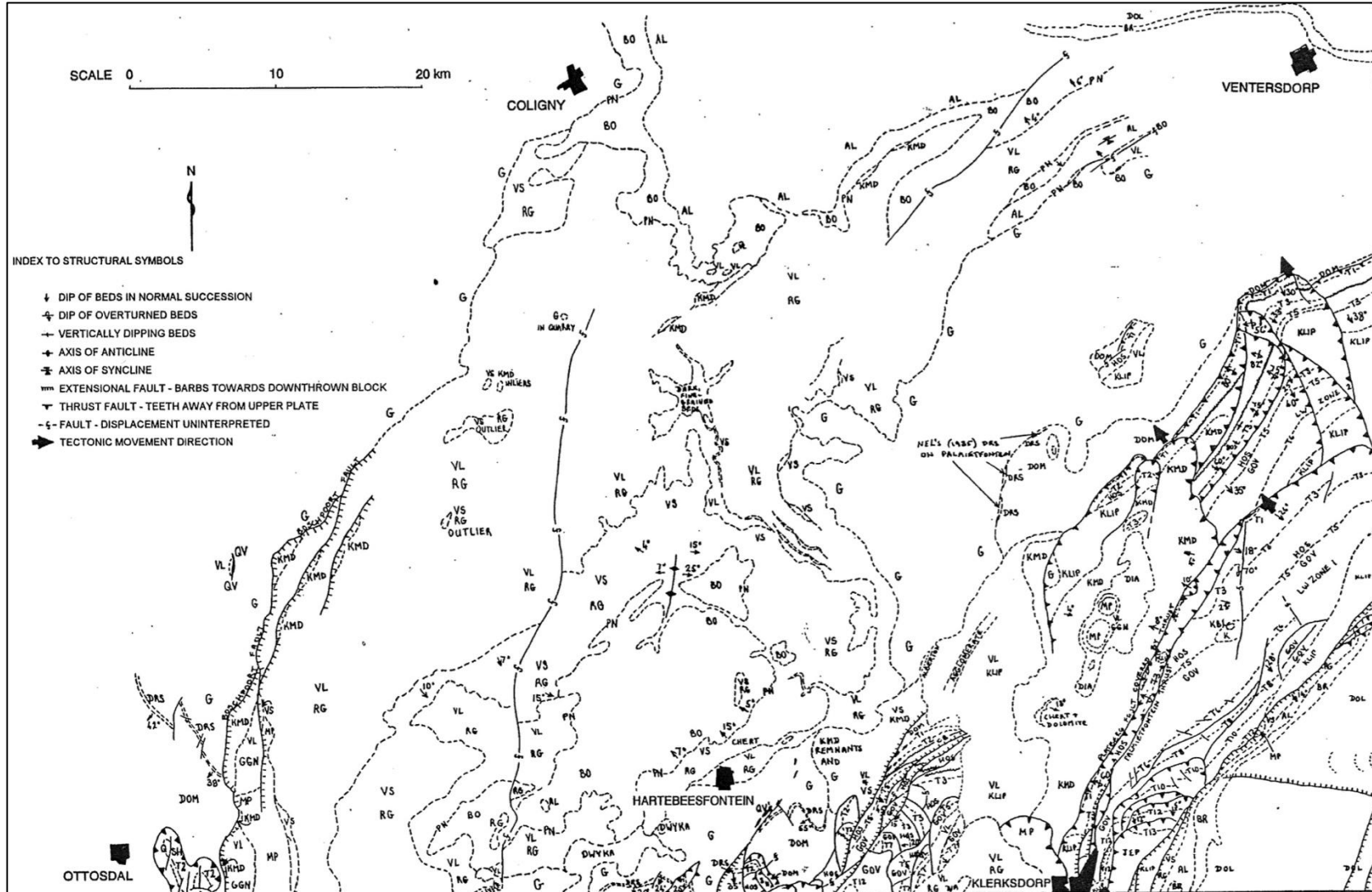


Figure 6-9: Structural mapping of the Klerksdorp-Ventersdorp-Carletonville-Fochville-Parys-Potchefstroom area – Map 1 (Brink, 1996)

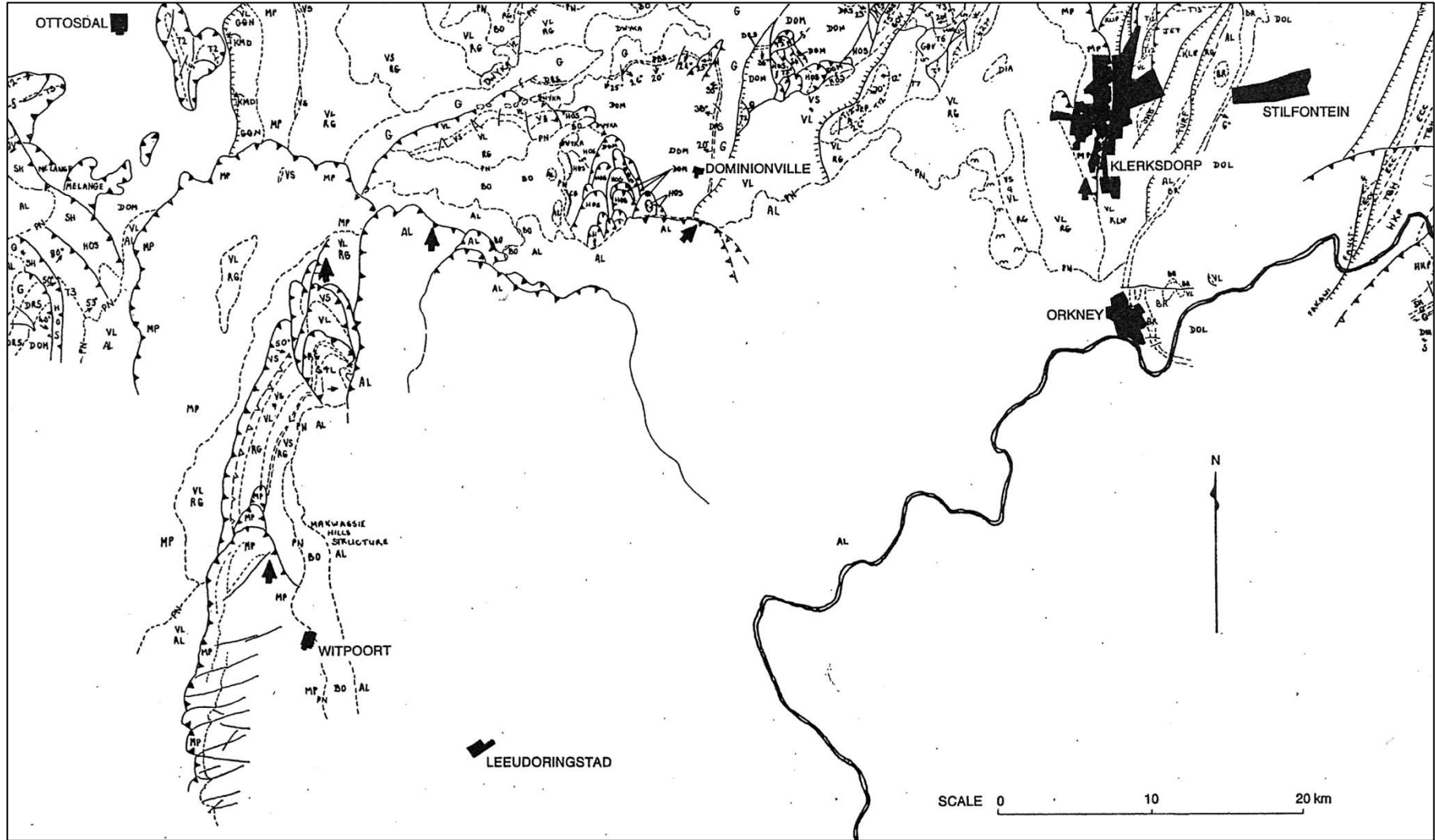


Figure 6-10: Structural mapping of the Klerksdorp-Ventersdorp-Carletonville-Fochville-Parys-Potchefstroom area – Map 2 (Brink, 1996)

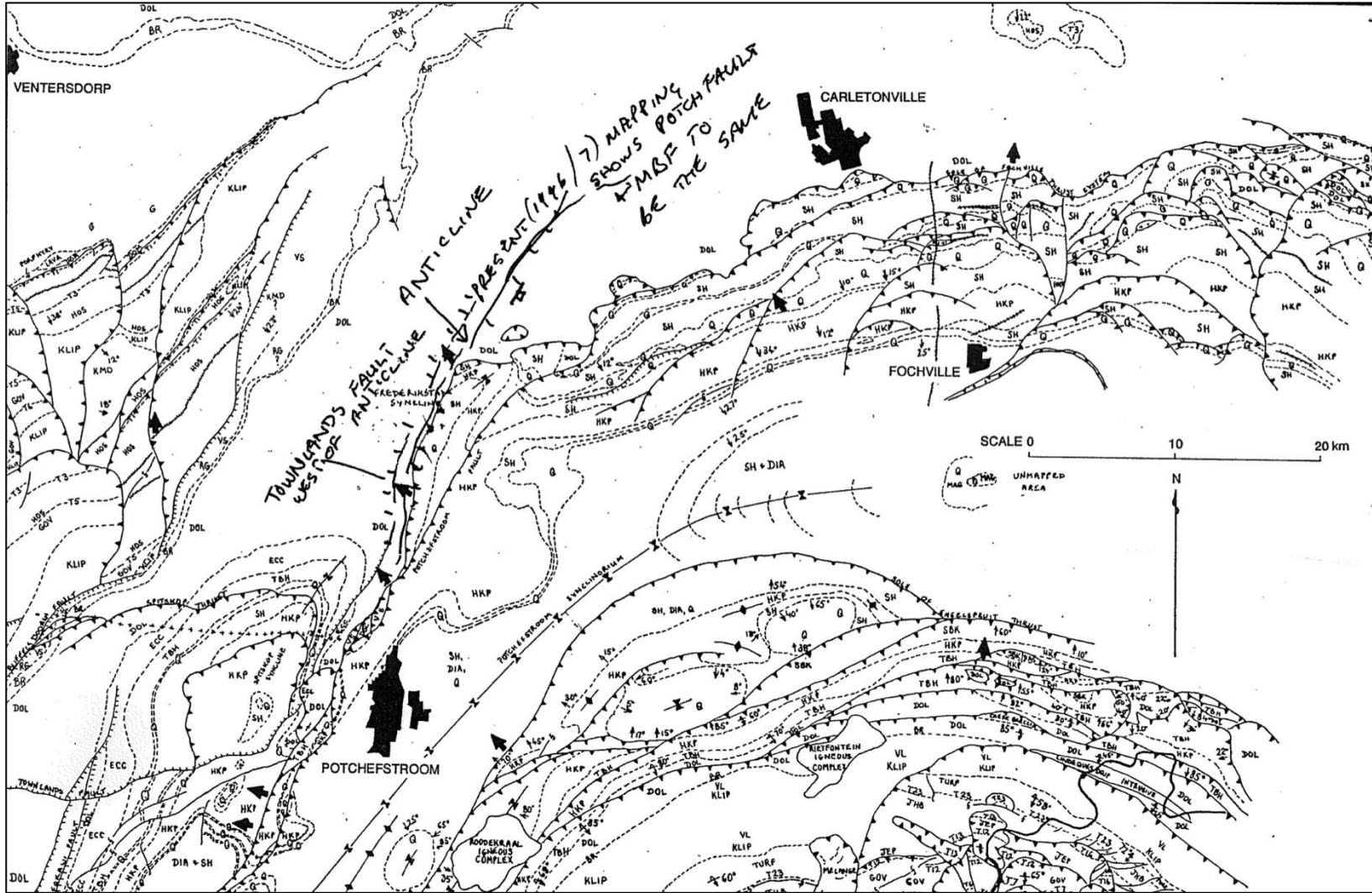


Figure 6-11: Structural mapping of the Klerksdorp-Ventersdorp-Carletonville-Fochville-Parys-Potchefstroom area – Map 3 (Brink, 1996)

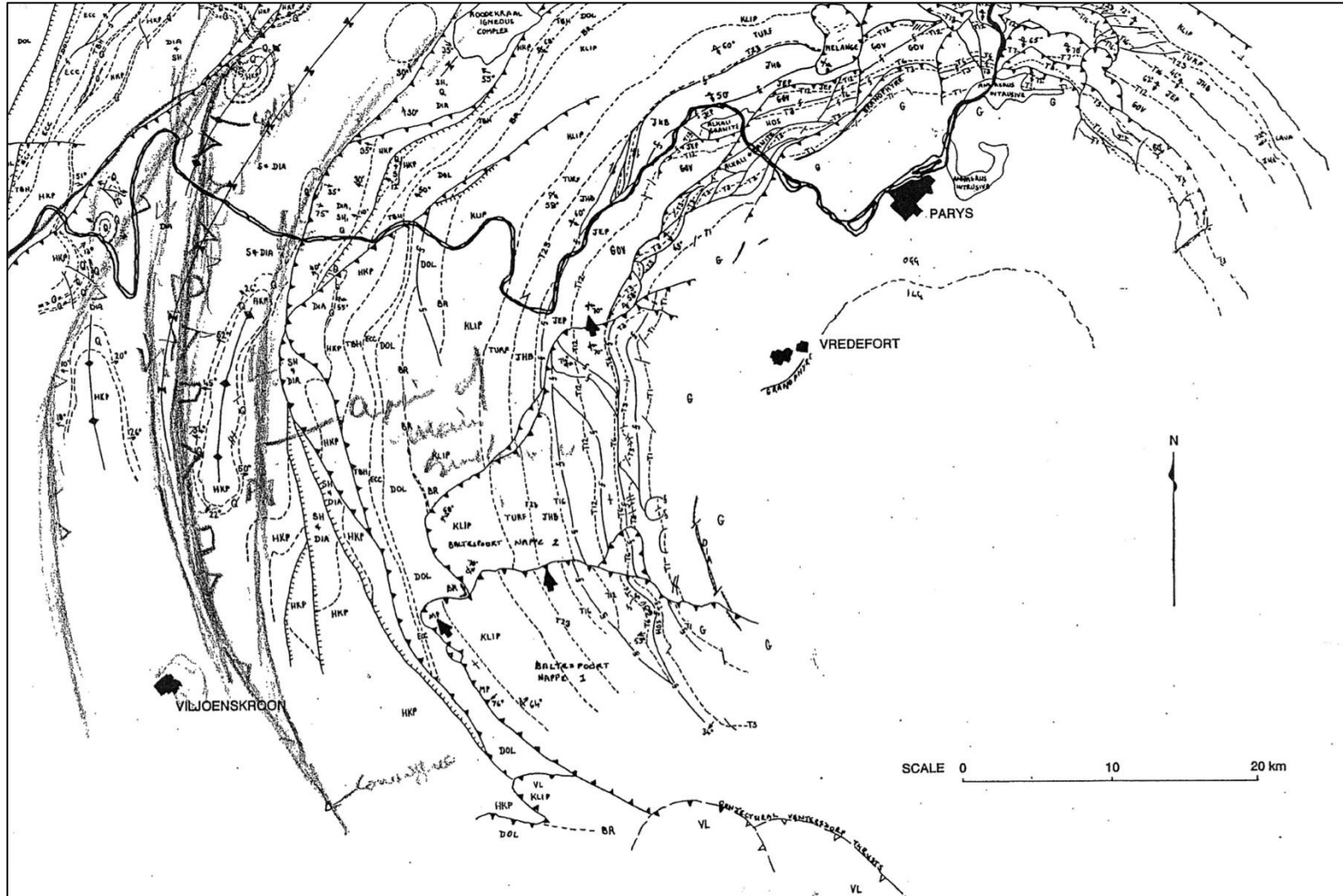


Figure 6-12: Structural mapping of the Klerksdorp-Ventersdorp-Carletonville-Fochville-Parys-Potchefstroom area – Map 4 (Brink, 1996)

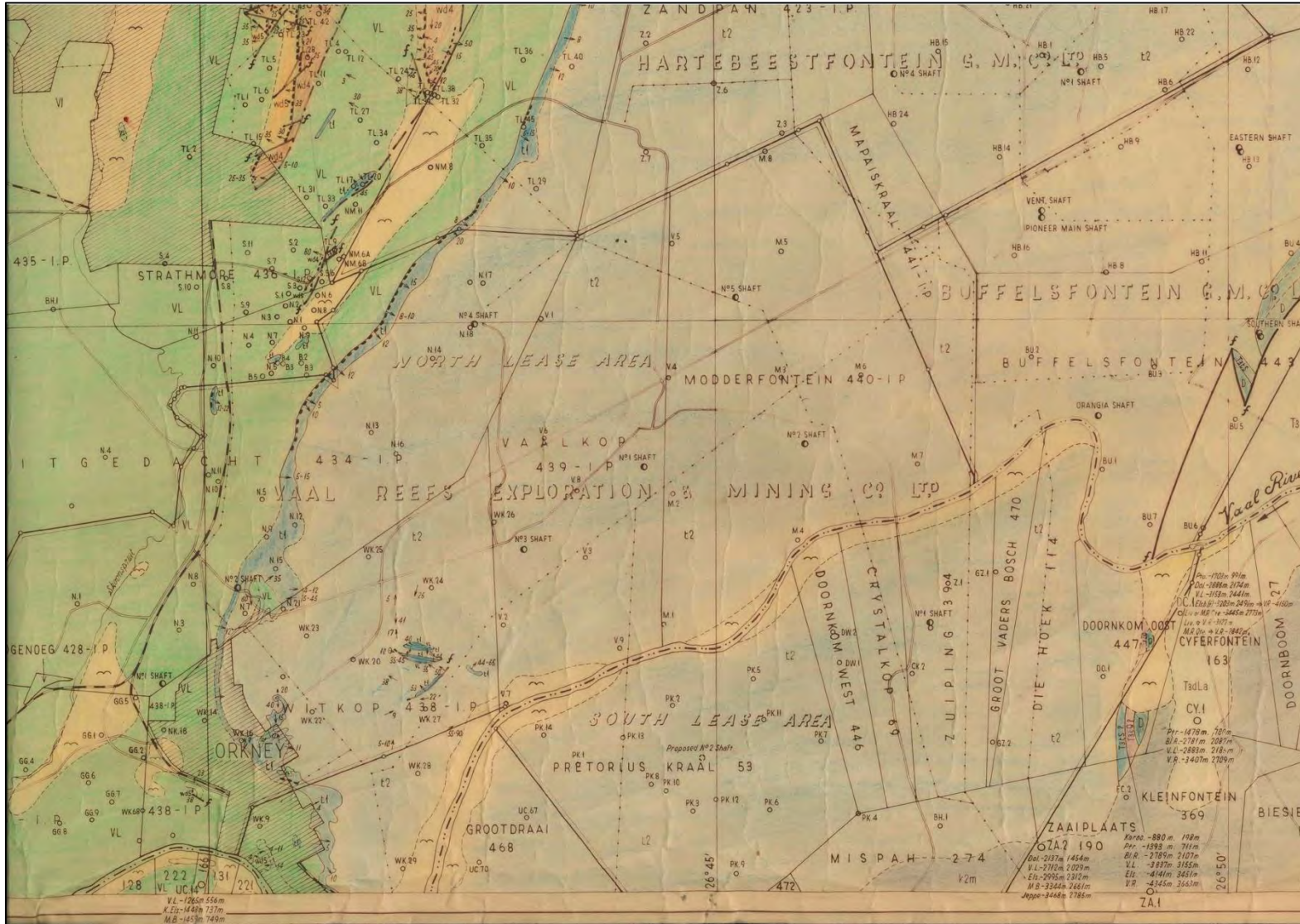


Figure 6-13: 1:50 000 scale Potchefstroom gap geological map – selection of map 1 of 3

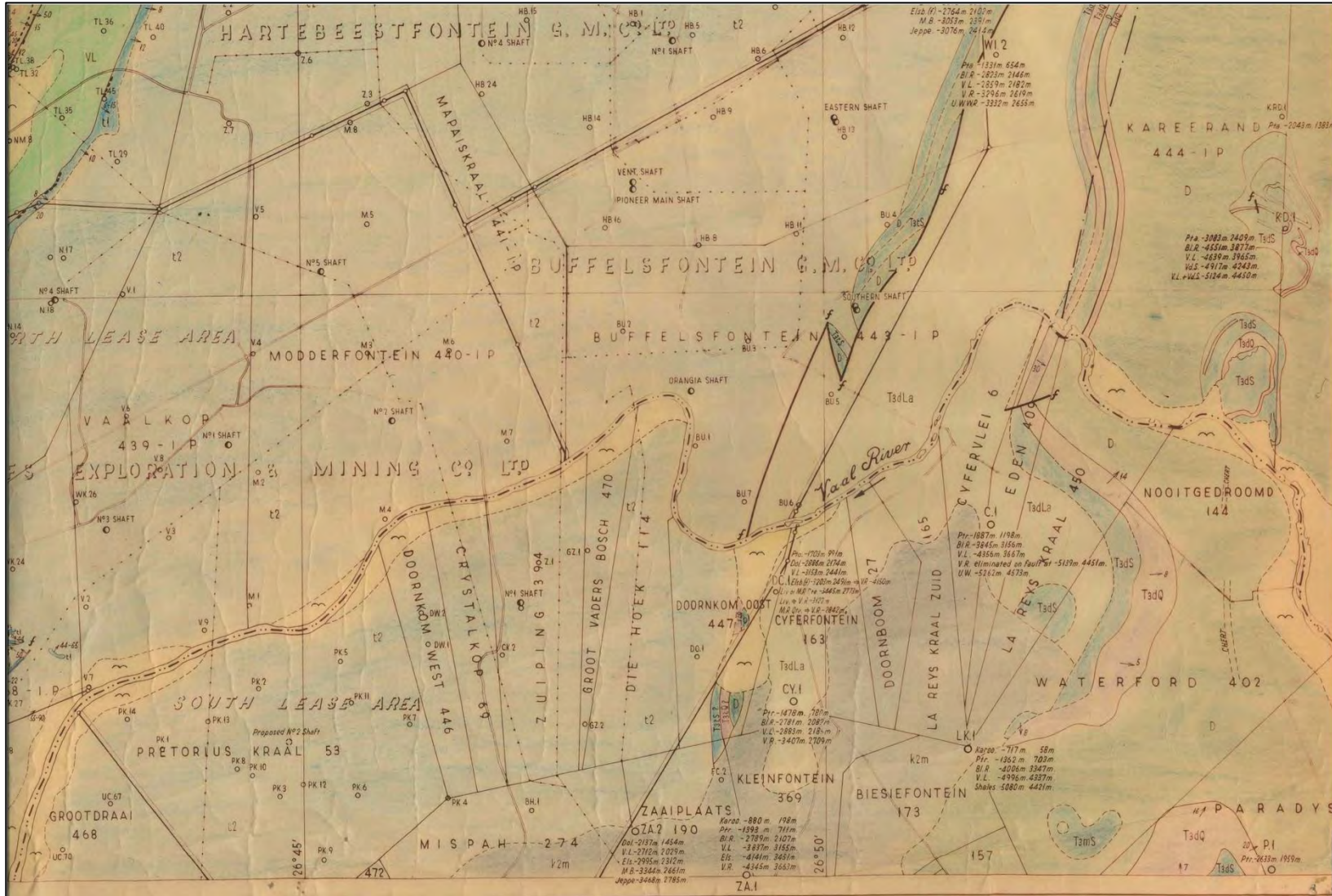


Figure 6-14: 1:50 000 scale Potchefstroom gap geological map – selection of map 2 of 3



Figure 6-15: 1:50 000 scale Potchefstroom gap geological map – selection of map 3 of 3

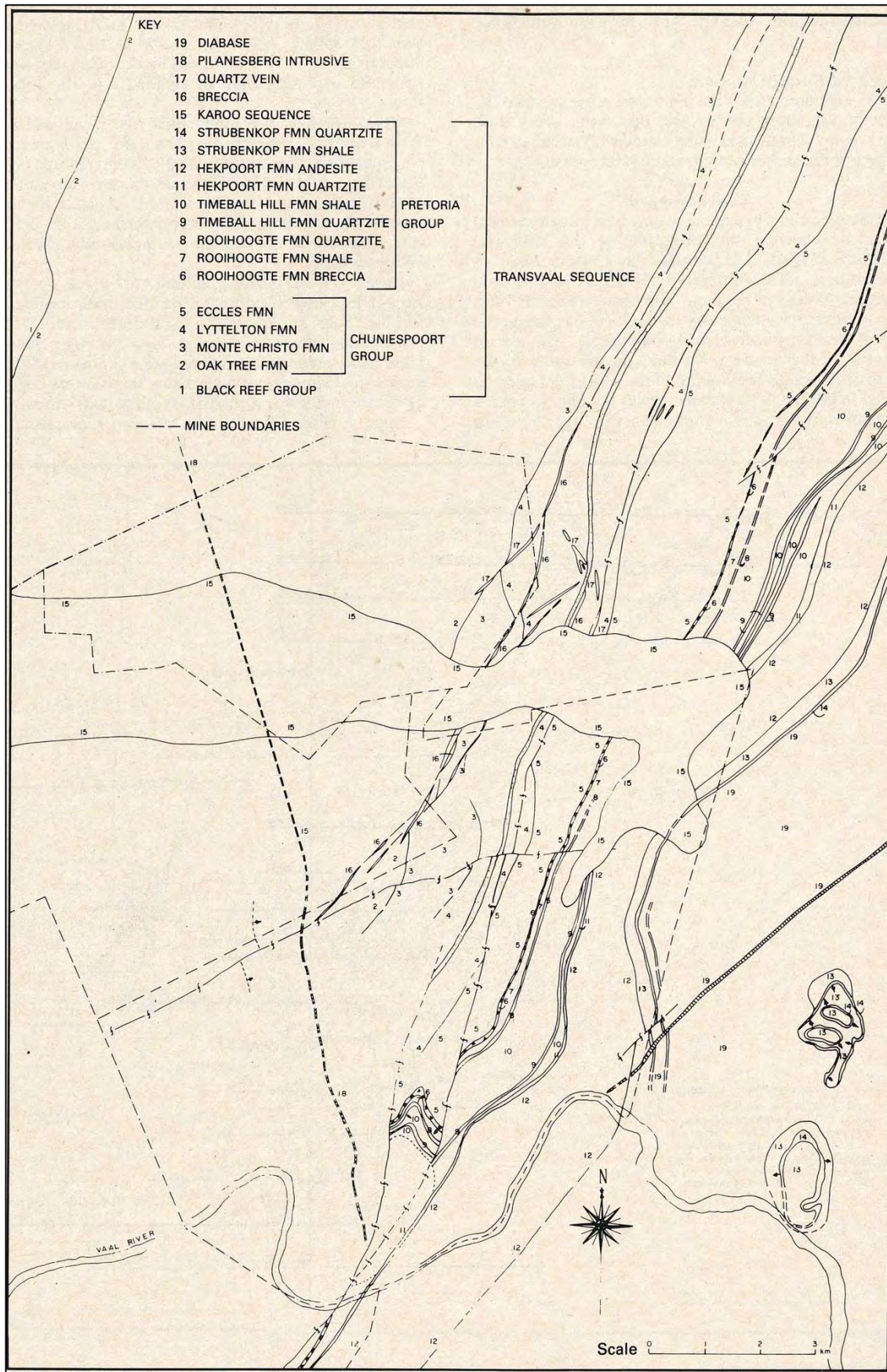


Figure 6-17: Surface geological map of the Buffelsdoorn mine lease area (Brink, 1986)

Annexure 3: Sinkhole and subsidence database for the KOSH area

Regional Location	Geological Formation	Notes	Feature Type	Feature Size	Confidence
North of old Khuma	Eccles Formation	Shallow, partially backfilled sinkhole with diameter of approximately 9 m	Sinkhole	Large	Certain
North of old Khuma	Eccles Formation	Shallow, partially backfilled sinkhole with diameter of approximately 12 m	Sinkhole	Large	Certain
South of railway line, North of old Khuma	Eccles Formation	Backfilled sinkhole that re-activated. Surface diameter of approximately 12 m	Sinkhole	Large	Certain
North of old Khuma	Eccles Formation	Combination of 2 backfilled sinkhole in Eskom servitude	Sinkhole	Medium	Certain
South of N12 near railway line	Eccles Formation	-	Sinkhole	Very Large	Paleo Feature
South of N12 near railway line	Eccles Formation	-	Sinkhole	Very Large	Paleo Feature
North of N12	Eccles Formation	-	Subsidence	Very Large	Paleo Feature
North of N12	Eccles Formation	-	Subsidence	Very Large	Paleo Feature
North of N12	Eccles Formation	-	Subsidence	Very Large	Paleo Feature
South of N12 near railway line	Eccles Formation	-	Subsidence	Very Large	Paleo Feature
South of N12 near railway line	Eccles Formation	-	Subsidence	Very Large	Paleo Feature
South of N12 near railway line	Eccles Formation	-	Subsidence	Very Large	Inferred from API
South of Vaal River	Eccles Formation	Diameter of approximately 56 m	Subsidence	Very Large	Certain
South of Vaal River	Eccles Formation	Diameter of approximately 30 m	Subsidence	Very Large	Certain
North of old Khuma	Eccles Formation	Paleo-subsidence associated with Camel Thorn trees. Verified in field	Subsidence	Very Large	Certain
North of old Khuma	Eccles Formation	Paleo-subsidence associated with Camel Thorn trees. Verified in field	Subsidence	Very Large	Certain
Mineworkers Village	Eccles Formation	Sagging chert bands exposed in railway cutting	Subsidence	Very Large	Certain

Strath Vaal Primary School, Stilfontein	Karoo Supergroup (300 m deep)	2 m at surface, 300 m deep (through entire Karoo Inlier). Early 1980's - location approximate	Sinkhole	Small	Certain
Stilfontein town	Karoo Supergroup / Monte-Christo Formation (contact)	Small sinkhole on contact with Monte Christo & Karoo	Sinkhole	Small	Certain
South of railway line, North of old Khuma	Lyttleton / Eccles Formation (across contact)	-	Sinkhole	Medium	Certain
North of old Khuma	Lyttleton / Eccles Formation (across contact)	Approximately 220 x 70 m diameter. Surface cracks visible from airplane. Northwest-southeast strike	Sinkhole	Very Large	Certain
Khuma Extension 6 Cemetery	Lyttleton Formation	-	Sinkhole	Large	Certain
Khuma Extension 6 Cemetery	Lyttleton Formation	-	Sinkhole	Large	Certain
South of Khuma Extension 6	Lyttleton Formation	Backfilled sinkhole. Diameter \pm 14 m	Sinkhole	Large	Inferred from API
North of old Khuma, south of railway line	Lyttleton Formation	-	Sinkhole	Large	Paleo Feature
North of old Khuma, south of railway line	Lyttleton Formation	-	Sinkhole	Large	Paleo Feature
South-east of Eagles Creek Gold Course	Lyttleton Formation	-	Sinkhole	Large	Paleo Feature
South-east of Eagles Creek Gold Course	Lyttleton Formation	-	Sinkhole	Large	Paleo Feature
North of Khuma Extension 6	Lyttleton Formation	Partially developed sinkhole verified in field	Sinkhole	Large	Certain
North of old Khuma	Lyttleton Formation	Shallow partially developed sinkhole with diameter of approximately 13 m. Dolomite pinnacles visible between eroded overburden	Sinkhole	Large	Certain

Khuma Extension 6	Lyttleton Formation	Approximately 4 m diameter and 3 m deep. Developed 1993/01/02	Sinkhole	Medium	Inferred from API
N12 east of Stilfontein	Lyttleton Formation	Rehabilitated sinkhole, formed between midway of the N12	Sinkhole	Medium	Certain
North-west of old Khuma	Lyttleton Formation	-	Sinkhole	Medium	Inferred from API
South of Vaal River	Lyttleton Formation	-	Sinkhole	Medium	Inferred from API
South of Vaal River	Lyttleton Formation	-	Sinkhole	Medium	Inferred from API
South of Vaal River	Lyttleton Formation	-	Sinkhole	Medium	Inferred from API
South of Vaal River	Lyttleton Formation	-	Sinkhole	Medium	Inferred from API
South of Vaal River	Lyttleton Formation	-	Sinkhole	Medium	Inferred from API
South of Vaal River	Lyttleton Formation	-	Sinkhole	Medium	Inferred from API
South of Vaal River	Lyttleton Formation	-	Sinkhole	Medium	Inferred from API
South of Vaal River	Lyttleton Formation	-	Sinkhole	Medium	Inferred from API
South of Vaal River	Lyttleton Formation	-	Sinkhole	Medium	Inferred from API
South of Vaal River	Lyttleton Formation	-	Sinkhole	Medium	Inferred from API
South of Vaal River	Lyttleton Formation	-	Sinkhole	Medium	Inferred from API
Northeast of Khuma Extension 6	Lyttleton Formation	Diameter of less than 1 m.	Sinkhole	Small	Certain
North-west of old Khuma	Lyttleton Formation	Partially developed sinkhole verified in field	Sinkhole	Small	Certain
North-east of Khuma Extension 6	Lyttleton Formation	Approximately 28 m diameter	Sinkhole	Very Large	Certain
Khuma Extension 6 Cemetery	Lyttleton Formation	Approximately 25 m diameter & 20 m deep. Developed 1993/01/01	Sinkhole	Very Large	Certain
North of N12	Lyttleton Formation	-	Sinkhole	Very Large	Paleo Feature
South of Khuma Extension 6	Lyttleton Formation	-	Sinkhole	Very Large	Inferred from API
North of old Khuma, south of railway line	Lyttleton Formation	-	Sinkhole	Very Large	Paleo Feature

North of old Khuma, south of railway line	Lyttleton Formation	-	Sinkhole	Very Large	Paleo Feature
South-east of Eagles Creek Gold Course	Lyttleton Formation	-	Sinkhole	Very Large	Paleo Feature
South-east of Eagles Creek Gold Course	Lyttleton Formation	-	Sinkhole	Very Large	Paleo Feature
South-east of Eagles Creek Gold Course	Lyttleton Formation	-	Sinkhole	Very Large	Paleo Feature
South of Vaal River	Lyttleton Formation	-	Sinkhole	Very Large	Paleo Feature
South of Vaal River	Lyttleton Formation	-	Sinkhole	Very Large	Paleo Feature
South of railway line, North of old Khuma	Lyttleton Formation	Paleo-sinkhole defined by Camel Thorn trees with a circular configuration in the field	Sinkhole	Very Large	Certain
South of railway line, North of old Khuma	Lyttleton Formation	Paleo-sinkhole defined by Camel Thorn trees with a circular configuration in the field	Sinkhole	Very Large	Certain
North of old Khuma, south of railway line	Lyttleton Formation	-	Subsidence	Large	Inferred from API
South of Eastern Shaft	Lyttleton Formation	Approximately 500 x 300 m. North-west/south-east strike	Subsidence	Very Large	Inferred from API
South of Khuma Extension 6	Lyttleton Formation	Approximately 170 x 60 m diameter. North-west/south-east strike.	Subsidence	Very Large	Inferred from API
East of Eagles Creek Golf Course	Lyttleton Formation	-	Subsidence	Very Large	Inferred from API
South of N12 near railway line	Lyttleton Formation	-	Subsidence	Very Large	Paleo Feature
North-west of old Khuma	Lyttleton Formation	Seasonal inundation due to topographic depression caused by subsidence	Subsidence	Very Large	Certain
North-west of old Khuma	Lyttleton Formation	Seasonal inundation due to topographic depression caused by subsidence	Subsidence	Very Large	Certain
North of old Khuma, south of railway line	Lyttleton Formation	-	Subsidence	Very Large	Inferred from API

North of Khuma Extension 6	Monte Christo / Lyttleton Formation (across contact)	Approximately 600 x 300 m diameter. East-West strike.	Subsidence	Very Large	Certain
East of Eagles Creek Golf Course	Monte Christo / Lyttleton Formation (across contact)	-	Subsidence	Very Large	Paleo Feature
Buffelsfontein mine offices	Monte Christo Formation	Two sinkholes. Last known sinkhole was 2002.	Sinkhole	Large	Certain
East of Stilfontein golf course	Monte Christo Formation	Backfilled sinkhole (August 2007)	Sinkhole	Large	Certain
East of Stilfontein golf course	Monte Christo Formation	Backfilled sinkhole (August 2007)	Sinkhole	Large	Certain
East of Stilfontein golf course	Monte Christo Formation	Backfilled sinkhole (August 2007)	Sinkhole	Large	Certain
East of Stilfontein golf course	Monte Christo Formation	Backfilled sinkhole (August 2007)	Sinkhole	Large	Certain
East of Stilfontein golf course	Monte Christo Formation	Backfilled sinkhole (August 2007)	Sinkhole	Large	Certain
East of Stilfontein golf course	Monte Christo Formation	Backfilled sinkhole (August 2007)	Sinkhole	Large	Certain
East of Stilfontein golf course	Monte Christo Formation	Backfilled sinkhole (August 2007)	Sinkhole	Large	Certain
East of Stilfontein golf course	Monte Christo Formation	Backfilled sinkhole (August 2007)	Sinkhole	Large	Certain
East of Stilfontein golf course	Monte Christo Formation	Backfilled sinkhole (August 2007)	Sinkhole	Large	Certain
East of Stilfontein golf course	Monte Christo Formation	Backfilled sinkhole (August 2007)	Sinkhole	Large	Certain
East of Stilfontein golf course	Monte Christo Formation	Backfilled sinkhole (August 2007)	Sinkhole	Large	Certain
South of Khuma Extension 6	Monte Christo Formation	Backfilled sinkhole. Diameter \pm 7 m	Sinkhole	Large	Inferred from API

Vaal Reefs 8 Shaft (Free State)	Monte Christo Formation	From Wagener (1982). Formed due to poor storm water management (1978-1981)	Sinkhole	Large	Certain
Vaal Reefs 8 Shaft (Free State)	Monte Christo Formation	From Wagener (1982). Formed due to poor storm water management (1978-1981)	Sinkhole	Large	Certain
Vaal Reefs 8 Shaft (Free State)	Monte Christo Formation	From Wagener (1982). Formed due to poor storm water management (1978-1981)	Sinkhole	Large	Certain
Vaal Reefs 8 Shaft (Free State)	Monte Christo Formation	From Wagener (1982). Formed due to poor storm water management (1978-1981)	Sinkhole	Large	Certain
Vaal Reefs 8 Shaft (Free State)	Monte Christo Formation	From Wagener (1982). Formed due to poor storm water management (1978-1981)	Sinkhole	Large	Certain
Vaal Reefs 8 Shaft (Free State)	Monte Christo Formation	From Wagener (1982). Formed due to poor storm water management (1978-1981)	Sinkhole	Large	Certain
Vaal Reefs 8 Shaft (Free State)	Monte Christo Formation	From Wagener (1982). Formed due to poor storm water management (1978-1981)	Sinkhole	Large	Certain
Vaal Reefs 8 Shaft (Free State)	Monte Christo Formation	From Wagener (1982). Formed due to poor storm water management (1978-1981)	Sinkhole	Large	Certain
Vaal Reefs 8 Shaft (Free State)	Monte Christo Formation	From Wagener (1982). Formed due to poor storm water management (1978-1981)	Sinkhole	Large	Certain
Vaal Reefs 8 Shaft (Free State)	Monte Christo Formation	From Wagener (1982). Formed due to poor storm water management (1978-1981)	Sinkhole	Large	Certain
Vaal Reefs 8 Shaft (Free State)	Monte Christo Formation	From Wagener (1982). Formed due to poor storm water management (1978-1981)	Sinkhole	Large	Certain
Vaal Reefs 8 Shaft (Free State)	Monte Christo Formation	From Wagener (1982). Formed due to poor storm water management (1978-1981)	Sinkhole	Large	Certain
Vaal Reefs 8 Shaft (Free State)	Monte Christo Formation	From Wagener (1982). Formed due to poor storm water management (1978-1981)	Sinkhole	Large	Certain
Vaal Reefs 8 Shaft (Free State)	Monte Christo Formation	From Wagener (1982). Formed due to poor storm water management (1978-1981)	Sinkhole	Large	Certain

Vaal Reefs 8 Shaft (Free State)	Monte Christo Formation	From Wagener (1982). Formed due to poor storm water management (1978-1981)	Sinkhole	Large	Certain
Vaal Reefs 8 Shaft (Free State)	Monte Christo Formation	From Wagener (1982). Formed due to poor storm water management (1978-1981)	Sinkhole	Large	Certain
Vaal Reefs 8 Shaft (Free State)	Monte Christo Formation	From Wagener (1982). Formed due to poor storm water management (1978-1981)	Sinkhole	Large	Certain
Vaal Reefs 8 Shaft (Free State)	Monte Christo Formation	From Wagener (1982). Formed due to poor storm water management (1978-1981)	Sinkhole	Large	Certain
Vaal Reefs 8 Shaft (Free State)	Monte Christo Formation	From Wagener (1982). Formed due to poor storm water management (1978-1981)	Sinkhole	Large	Certain
Vaal Reefs 8 Shaft (Free State)	Monte Christo Formation	From Wagener (1982). Formed due to poor storm water management (1978-1981)	Sinkhole	Large	Certain
Vaal Reefs 8 Shaft (Free State)	Monte Christo Formation	From Wagener (1982). Formed due to poor storm water management (1978-1981)	Sinkhole	Large	Certain
Vaal Reefs 8 Shaft (Free State)	Monte Christo Formation	From Wagener (1982). Formed due to poor storm water management (1978-1981)	Sinkhole	Large	Certain
Vaal Reefs 8 Shaft (Free State)	Monte Christo Formation	From Wagener (1982). Formed due to poor storm water management (1978-1981)	Sinkhole	Large	Certain
Vaal Reefs 8 Shaft (Free State)	Monte Christo Formation	From Wagener (1982). Formed due to poor storm water management (1978-1981)	Sinkhole	Large	Certain
North of N12	Monte Christo Formation	-	Sinkhole	Large	Inferred from API
67 Jan Van Riebeeck Avenue, Stilfontein	Monte Christo Formation	Developed during 1981.	Sinkhole	Large	Certain
East of Eagles Creek Golf Course	Monte Christo Formation	Re-activation of previously backfilled sinkhole. Diameter of ± 8 m	Sinkhole	Large	Certain

North of Mineworkers Village	Monte Christo Formation	Backfilled sinkhole with trees established. Diameter of approximately 12 m	Sinkhole	Large	Certain
Hartebeesfontein Nos. 5 & 6 TDF	Monte Christo Formation	Large sinkholes with diameter 20 m, south of penstock decant, and water accumulation on access ramp. Backfilled sinkholes re-activated 3 times. Last re-activations during January 2009	Sinkhole	Very Large	Certain
Along pipeline parallel with N12, 100 m west of Stilfontein GM Transport office	Monte Christo Formation	Sinkhole with dimensions 4 x 5 m and 3 m deep developed during 2007. Sinkhole was backfilled.	Sinkhole	Large	Certain
Buffelsfontein No 3 TDF	Monte Christo Formation	Combination of 3 sinkholes developed on south-western corner of TDF in January 2009. Sinkholes have diameters of 10 m and are spaced across 50 m, connected with concentric surface tension cracks	Sinkhole	Large	Certain
Anglo Midway Pump Station north of Buffelsfontein	Monte Christo Formation	Sinkhole developed during April 2011. Diameter approximately 2m. Developed after water spillage.	Sinkhole	Small	Certain
Anglo Midway Pump Station north of Buffelsfontein	Monte Christo Formation	Sinkhole developed during April 2011. Diameter approximately 2m. Developed after water spillage.	Sinkhole	Small	Certain
Anglo Midway Pump Station north of Buffelsfontein	Monte Christo Formation	Sinkhole developed during April 2011. Diameter approximately 2m. Developed after water spillage.	Sinkhole	Small	Certain
Northeast of Khuma Extension 6	Monte Christo Formation	Cover collapse sinkhole of approximately 6 m diameter, 2 m deep. Filled with trees	Sinkhole	Medium	Certain
Northeast of Khuma Extension 6	Monte Christo Formation	Cover collapse sinkhole of approximately 10 m diameter, 2 m deep. Filled with trees	Sinkhole	Medium	Certain
South of Khuma Extension 6	Monte Christo Formation	Backfilled sinkhole. Diameter ±5 m	Sinkhole	Medium	Inferred from API
Vaal Reefs 8 Shaft (Free State)	Monte Christo Formation	From Wagener (1982). Formed due to poor storm water management (1978-1981)	Sinkhole	Medium	Certain

Vaal Reefs 8 Shaft (Free State)	Monte Christo Formation	From Wagener (1982). Formed due to poor storm water management (1978-1981)	Sinkhole	Medium	Certain
Vaal Reefs 8 Shaft (Free State)	Monte Christo Formation	From Wagener (1982). Formed due to poor storm water management (1978-1981)	Sinkhole	Medium	Certain
Vaal Reefs 8 Shaft (Free State)	Monte Christo Formation	From Wagener (1982). Formed due to poor storm water management (1978-1981)	Sinkhole	Medium	Certain
N12 at Stilfontein	Monte Christo Formation	Partially developed sinkhole. Diameter of approximately 3 m	Sinkhole	Medium	Certain
Mineworkers Village	Monte Christo Formation	-	Sinkhole	Medium	Inferred from API
North of N12	Monte Christo Formation	-	Sinkhole	Medium	Inferred from API
North of N12	Monte Christo Formation	Within drainage of Kromdraaispruit	Sinkhole	Medium	Certain
East of Eagles Creek Golf Course	Monte Christo Formation	Re-activation of previously backfilled sinkhole	Sinkhole	Medium	Certain
North of Khuma Extension 6	Monte Christo Formation	Sinkhole verified in field. Associated with Kromdraaispruit drainage	Sinkhole	Medium	Certain
Hartebeesfontein Nos. 1 to 4 TDF	Monte Christo Formation	Several sinkholes due to damage pipeline and accumulation of run-off water next to TDF	Sinkhole	Very Large	Certain
Hartebeesfontein Nos. 1 to 4 TDF	Monte Christo Formation	Several sinkholes due to damage pipeline and accumulation of run-off water next to TDF	Sinkhole	Large	Certain
Hartebeesfontein Nos. 1 to 4 TDF	Monte Christo Formation	Several sinkholes due to damage pipeline and accumulation of run-off water next to TDF	Sinkhole	Large	Certain
Hartebeesfontein Nos. 1 to 4 TDF	Monte Christo Formation	Several sinkholes due to damage pipeline and accumulation of run-off water next to TDF	Sinkhole	Large	Certain
Hartebeesfontein Nos. 1 to 4 TDF	Monte Christo Formation	Several sinkholes due to damage pipeline and accumulation of run-off water next to TDF	Sinkhole	Large	Certain
Hartebeesfontein Nos. 1 to 4 TDF	Monte Christo Formation	Several sinkholes due to damage pipeline and accumulation of run-off water next to TDF	Sinkhole	Large	Certain

North of Khuma Extension 6	Monte Christo Formation	Cluster of 3 small sinkholes with diameters of less than 0.8 m, 0,6 m deep	Sinkhole	Small	Certain
Stilfontein water towers and reservoir	Monte Christo Formation	Small sinkholes, part of larger structure that is re-activating. First sinkhole developed in 2002. Reactivated in 2004, 2011, and ±2014	Sinkhole	Small	Certain
Stilfontein water towers and reservoir	Monte Christo Formation	Small sinkholes, part of larger structure that is re-activating. First sinkhole developed in 2002. Reactivated in 2004, 2011, and ±2014	Sinkhole	Small	Certain
Stilfontein water towers and reservoir	Monte Christo Formation	Small sinkholes, part of larger structure that is re-activating. First sinkhole developed in 2002. Reactivated in 2004, 2011, and ±2014	Sinkhole	Small	Certain
North of N12	Monte Christo Formation	Within drainage of Kromdraaispruit	Sinkhole	Small	Certain
North of N12	Monte Christo Formation	Within drainage of Kromdraaispruit	Sinkhole	Small	Certain
South of Vaal River	Monte Christo Formation	-	Sinkhole	Small	Inferred from API
Along pipeline parallel with N12, 100 m west of Stilfontein GM Transport office	Monte Christo Formation	Several small sinkholes developed along pipeline prior to 2002. All sinkholes were backfilled	Sinkhole	Small	Certain
South of Chemwes Plant near Stilfontein	Monte Christo Formation	South of Chemwes Plant, North of Pinnacle school underneath Chemwes-Buffelsfontein pipeline Several small sinkholes developed associated with pipeline during 2007. Sinkholes were backfilled, subsidences are still present. Large number of sinkholes associated with dolomite-Karoo contact across this area due to consolidation of the Karoo Inlier over a time period of more than 10 years along the formed cone of depression	Sinkhole	Small	Certain

Chemwest Thickener tanks near Stilfontein	Monte Christo Formation	Sinkholes developed next to new U-plant thickener tanks - 26 January 2009. outh-east dipping feature.	Sinkhole	Medium	Certain
Chemwest Thickener tanks near Stilfontein	Monte Christo Formation	Sinkhole at Chemwes plan. South-east dipping feature.	Sinkhole	Medium	Certain
South of Stilfontein golf course	Monte Christo Formation	Backfilled sinkhole (August 2007)	Sinkhole	Unknown dimensions	Certain
South of Stilfontein golf course	Monte Christo Formation	Backfilled sinkhole (August 2007)	Sinkhole	Unknown dimensions	Certain
East of Stilfontein golf course	Monte Christo Formation	Backfilled sinkhole (August 2007)	Sinkhole	Unknown dimensions	Certain
East of Stilfontein golf course	Monte Christo Formation	Backfilled sinkhole (August 2007)	Sinkhole	Unknown dimensions	Certain
East of Stilfontein golf course	Monte Christo Formation	Backfilled sinkhole (August 2007)	Sinkhole	Unknown dimensions	Certain
East of Stilfontein golf course	Monte Christo Formation	Backfilled sinkhole (August 2007)	Sinkhole	Unknown dimensions	Certain
East of Stilfontein golf course	Monte Christo Formation	Backfilled sinkhole (August 2007)	Sinkhole	Unknown dimensions	Certain
East of Stilfontein golf course	Monte Christo Formation	Backfilled sinkhole (August 2007)	Sinkhole	Unknown dimensions	Certain
East of Stilfontein golf course	Monte Christo Formation	Backfilled sinkhole (August 2007)	Sinkhole	Unknown dimensions	Certain
East of Stilfontein golf course	Monte Christo Formation	Backfilled sinkhole (August 2007)	Sinkhole	Unknown dimensions	Certain
East of Stilfontein golf course	Monte Christo Formation	Backfilled sinkhole (August 2007)	Sinkhole	Unknown dimensions	Certain
East of Stilfontein golf course	Monte Christo Formation	Backfilled sinkhole (August 2007)	Sinkhole	Unknown dimensions	Certain
East of Stilfontein golf course	Monte Christo Formation	Backfilled sinkhole (August 2007)	Sinkhole	Unknown dimensions	Certain
East of Stilfontein golf course	Monte Christo Formation	Backfilled sinkhole (August 2007)	Sinkhole	Unknown dimensions	Certain
East of Stilfontein golf course	Monte Christo Formation	Backfilled sinkhole (August 2007)	Sinkhole	Unknown dimensions	Certain
D. Scott Hospital south of Stilfontein	Monte Christo Formation	Sinkhole developed along Buffelsfontein-Chemwes pipeline close to D. Scott Hospital during 2007	Sinkhole	Medium	Certain

South of Vaal River near Dolomite Mine	Monte Christo Formation	Very large sinkhole, approximately 22 m across	Sinkhole	Very Large	Certain
South of Vaal River near Dolomite Mine	Monte Christo Formation	Partially developed sinkhole, approximately 23 m across	Sinkhole	Very Large	Certain
Spoornet Railway line crossing at Koekemoerspruit (east of Stilfontein)	Monte Christo Formation	Cluster of 7 sinkholes. Formed before 2007. Re-activated 2007	Sinkhole	Very Large	Certain
Spoornet Railway line crossing at Koekemoerspruit (east of Stilfontein)	Monte Christo Formation	Combination of 2 subsidences directly adjacent the railway intersection with the Koekemoerspruit	Subsidence	Very Large	Certain
Spoornet Railway line crossing east of Koekemoerspruit	Monte Christo Formation	Sinkhole developed directly on the southern side of the railway line during 2012	Sinkhole	Large	Certain
Spoornet Railway line crossing east of Koekemoerspruit	Monte Christo Formation	Sinkhole developed directly on the southern side of the railway line during 2013	Sinkhole	Large	Certain
North of Khuma Extension 6	Monte Christo Formation	Approximately 50 m across 15 m deep	Sinkhole	Very Large	Certain
South of Khuma Extension 6	Monte Christo Formation	Approximately 24m diameter. Deemed old back-filled sinkhole	Sinkhole	Very Large	Inferred from API
South of Stilfontein golf course	Monte Christo Formation	Backfilled sinkhole (August 2007)	Sinkhole	Very Large	Certain
East of Stilfontein golf course	Monte Christo Formation	Backfilled sinkhole (August 2007)	Sinkhole	Very Large	Certain
South of Khuma Extension 6	Monte Christo Formation	Combination of 2 sinkholes. Diameters of approximately 48 and 30 m respectively	Sinkhole	Very Large	Inferred from API
Vaal Reefs 8 Shaft (Free State)	Monte Christo Formation	From Wagener (1982). Formed due to poor storm water management (1978-1981)	Sinkhole	Very Large	Certain
Vaal Reefs 8 Shaft (Free State)	Monte Christo Formation	From Wagener (1982). Formed due to poor storm water management (1978-1981)	Sinkhole	Very Large	Certain
N12 at Stilfontein	Monte Christo Formation	Combination of 8 sinkholes connected with concentric surface cracks. Total combined surface cracks / partially developed sinkhole diameter of 25 m. Developed November 2015	Sinkhole	Very Large	Certain

R502 near Buffelsfontein mine	Monte Christo Formation	Diameter of approximately 78 m	Sinkhole	Very Large	Paleo Feature
North of N12	Monte Christo Formation	-	Sinkhole	Very Large	Paleo Feature
North of N12	Monte Christo Formation	-	Sinkhole	Very Large	Inferred from API
North of N12	Monte Christo Formation	-	Sinkhole	Very Large	Paleo Feature
North of N12	Monte Christo Formation	-	Sinkhole	Very Large	Paleo Feature
North of N12	Monte Christo Formation	-	Sinkhole	Very Large	Paleo Feature
North of N12	Monte Christo Formation	-	Sinkhole	Very Large	Paleo Feature
North of N12 between old Stilfontein tailings.	Oaktree Formation	Partially developed sinkhole activated after intersecting cavity between 1 to 2 mbgl during drilling of groundwater abstraction borehole. Sinkholes ± 1 m deep.	Sinkhole	Medium	Certain
North of N12 at Stilfontein	Monte Christo Formation	Deep excavation revealed sagging chert bands filled with red Kalahari sand. Diameter approximately 5 m across.	Sinkhole	Large	Paleo Feature
Reservoirs north-west of Chemwes	Monte Christo Formation	Sinkhole developed in 2003 directly south-west of the reservoirs. Associated with leakages from reservoirs.	Sinkhole	Medium	Certain
South of N12 at Stilfontein	Monte Christo Formation	Paleo sinkhole exposed in quarry. 6 m deep red aeolian transported soil to base of quarry. Location approximate. Quarry currently filled with rubble	Sinkhole	Very Large	Certain
Mineworkers Village	Monte Christo Formation	Formed during 1979. From Wagener (1982)	Sinkhole	Unknown dimensions	Certain
Mineworkers Village	Monte Christo Formation	Formed during 1979. From Wagener (1982)	Sinkhole	Unknown dimensions	Certain
Mineworkers Village	Monte Christo Formation	Formed during 1979. From Wagener (1982)	Sinkhole	Unknown dimensions	Certain
Mineworkers Village	Monte Christo Formation	Formed during 1979. From Wagener (1982)	Sinkhole	Unknown dimensions	Certain
Mineworkers Village	Monte Christo Formation	Formed during 1979. From Wagener (1982)	Sinkhole	Unknown dimensions	Certain

Buffelsfontein eastern Shaft	Monte Christo / Lyttleton Formation (across contact)	Covered sinkholes with diameter of approx 10m where decant water from mine shaft accumulated next to dam wall.	Sinkhole	Large	Certain
N12 at Stilfontein	Monte Christo Formation	Shallow subsidence with a diameter of 8 x 14 m	Subsidence	Large	Certain
South of Vaal River	Monte Christo Formation	-	Subsidence	Large	Inferred from API
South of Vaal River	Monte Christo Formation	-	Subsidence	Large	Inferred from API
South of Vaal River	Monte Christo Formation	-	Subsidence	Large	Inferred from API
South of Vaal River	Monte Christo Formation	Associated with north-south trending lineation of trees	Subsidence	Large	Certain
South of Vaal River	Monte Christo Formation	-	Subsidence	Large	Inferred from API
East of Stilfontein along railway line	Monte Christo Formation	Sagging chert bands visible in railway cutting	Subsidence	Large	Certain
North of Khuma Extension 6	Monte Christo Formation	Subsidence verified in field. Associated with Kromdraaispruit drainage	Subsidence	Large	Certain
North of Khuma Extension 6	Monte Christo Formation	Subsidence verified in field. Associated with Kromdraaispruit drainage	Subsidence	Large	Certain
North of Khuma Extension 6	Monte Christo Formation	Subsidence verified in field	Subsidence	Large	Certain
South of Vaal River	Monte Christo Formation	-	Subsidence	Medium	Inferred from API
North of Khuma Extension 6	Monte Christo Formation	Subsidence verified in field	Subsidence	Medium	Certain
D. Scott Hospital south of Stilfontein	Monte Christo Formation	Subsidence formed 10 m from previous sinkhole 27 January 2009. Surface cracks are associated with settlement	Subsidence	Medium	Certain
Along pipeline parallel with N12, 100 m west of Stilfontein GM Transport office	Monte Christo Formation	Depression at construction camp 100 m from Stilfontein GM Transport office on 30 January 2009	Subsidence	Medium	Certain

South of Vaal River near Dolomite Mine	Monte Christo Formation	Large depression, approximate diameter of 90 m across around buried pipeline	Subsidence	Very Large	Inferred from API
East of old Stilfontein mine	Monte Christo Formation	Cluster of 3 subsidences with a combined diameter of 200 x 70 m. Possibly ascribed to undermining of the Black Reef in the area.	Subsidence	Very Large	Inferred from API
North of Khuma Extension 6	Monte Christo Formation	Approximately 19 m diameter. East-west strike.	Subsidence	Very Large	Certain
South of old Stilfontein Tailings Dams	Monte Christo Formation	Sinking stream where wetland disappears into dolomite.	Sinkhole	Large	Certain
South of old Stilfontein Tailings Dams	Monte Christo Formation	Sinking stream where wetland disappears into dolomite.	Sinkhole	Large	Certain
Vaal Reefs 8 Shaft (Free State)	Monte Christo Formation	From Wagener (1982). Formed due to poor storm water management (1978-1981)	Subsidence	Very Large	Certain
Vaal Reefs 8 Shaft (Free State)	Monte Christo Formation	From Wagener (1982). Formed due to poor storm water management (1978-1981)	Subsidence	Very Large	Certain
Vaal Reefs 8 Shaft (Free State)	Monte Christo Formation	From Wagener (1982). Formed due to poor storm water management (1978-1981)	Subsidence	Very Large	Certain
Vaal Reefs 8 Shaft (Free State)	Monte Christo Formation	From Wagener (1982). Formed due to poor storm water management (1978-1981)	Subsidence	Very Large	Certain
Vaal Reefs 8 Shaft (Free State)	Monte Christo Formation	From Wagener (1982). Formed due to poor storm water management (1978-1981)	Subsidence	Very Large	Certain
Vaal Reefs 8 Shaft (Free State)	Monte Christo Formation	From Wagener (1982). Formed due to poor storm water management (1978-1981)	Subsidence	Very Large	Certain
Vaal Reefs 8 Shaft (Free State)	Monte Christo Formation	From Wagener (1982). Formed due to poor storm water management (1978-1981)	Subsidence	Very Large	Certain
Vaal Reefs 8 Shaft (Free State)	Monte Christo Formation	From Wagener (1982). Formed due to poor storm water management (1978-1981)	Subsidence	Very Large	Certain

N12 at Stilfontein	Monte Christo Formation	Partially developed sinkhole. Diameter approximately 18 x 15 m	Subsidence	Very Large	Certain
South-east of Eagles Creek Gold Course	Monte Christo Formation	-	Subsidence	Very Large	Paleo Feature
North of Mineworkers Village	Monte Christo Formation	North-north-west/south-south-east trending surface drainage depression.	Subsidence	Very Large	Certain
North of Mineworkers Village	Monte Christo Formation	Combination of 3 subsidences.	Subsidence	Very Large	Certain
South of N12 at Stilfontein	Oaktree Formation	Sinkhole developed in servitude next to N12. Backfilled 1993	Sinkhole	Medium	Certain
North of N12 at Stilfontein	Oaktree Formation	Sinkhole developed in servitude next to N12. Backfilled 1993	Sinkhole	Small	Certain
North of N12 at Stilfontein	Oaktree Formation	Sinkhole developed in servitude next to N12. Backfilled 1993	Sinkhole	Small	Certain
North of N12 at Stilfontein	Oaktree Formation	Sinkhole developed in servitude next to N12. Backfilled 1993	Sinkhole	Small	Certain
North of N12 at Stilfontein	Oaktree Formation	Sinkhole developed in servitude next to N12. Backfilled 1993	Sinkhole	Small	Certain
North of N12 at Stilfontein	Oaktree Formation	Sinkhole developed in servitude next to N12. Backfilled 1993	Sinkhole	Small	Certain
North of N12 at Stilfontein	Oaktree Formation	Sinkhole developed in servitude next to N12. Backfilled 1993	Sinkhole	Small	Certain
North of Stilfontein and N12	Oaktree Formation	North-westwardly trending feature.	Subsidence	Large	Inferred from API
Chemwes-Buffelsfontein Mega Tailings Dam Pipeline	Monte Christo / Karoo Inlier (along contact)	Gryke filled with Karoo Supergroup sediments. Concentric surface cracks visible and small sinkhole formed (1.5m diameter)	Sinkhole	Small	Certain
Chemwes-Buffelsfontein Mega Tailings Dam Pipeline	Karoo Supergroup	From M.J. Meyer (2011): Concentric surface cracks at surface	Subsidence	Medium	Certain
Chemwes-Buffelsfontein Mega Tailings Dam Pipeline	Karoo Supergroup	From M.J. Meyer (2011): Concentric surface cracks at surface	Subsidence	Small	Certain

Chemwes-Buffelsfontein Mega Tailings Dam Pipeline	Karoo Supergroup	From M.J. Meyer (2011): Concentric surface cracks at surface	Subsidence	Medium	Certain
Chemwes-Buffelsfontein Mega Tailings Dam Pipeline	Karoo Supergroup	From M.J. Meyer (2011): Combination of 3 small partially developed sinkholes indicating inter-linked concentric surface-cracks	Sinkhole	Medium	Certain
Chemwes-Buffelsfontein Mega Tailings Dam Pipeline	Karoo Supergroup	From M.J. Meyer (2011): Concentric surface cracks at surface	Subsidence	Medium	Certain
Chemwes-Buffelsfontein Mega Tailings Dam Pipeline	Karoo Supergroup	From M.J. Meyer (2011): Large surface cracks 10 m long, 5 cm wide along pipeline.	Subsidence	Large	Certain
Chemwes-Buffelsfontein Mega Tailings Dam Pipeline	Karoo Supergroup	From M.J. Meyer (2011): Small (2m diamated) sinkhole adjacent pipeline	Sinkhole	Small	Certain
Chemwes-Buffelsfontein Mega Tailings Dam Pipeline	Monte Christo Formation	From M.J. Meyer (2011): Small sinkhole close to pipeline	Sinkhole	Small	Certain
Chemwes-Buffelsfontein Mega Tailings Dam Pipeline	Monte Christo Formation	From M.J. Meyer (2011): Vegetation anomaly (Camel Thorn Trees) in red soil in combination with concentric surface cracks	Sinkhole	Medium	Certain
Chemwes-Buffelsfontein Mega Tailings Dam Pipeline	Monte Christo Formation	From M.J. Meyer (2011): Surface depression	Subsidence	Large	Certain
Chemwes-Buffelsfontein Mega Tailings Dam Pipeline	Monte Christo Formation	From M.J. Meyer (2011): Vegetation anomaly (Camel Thorn Trees) in red soil in combination with concentric surface cracks	Sinkhole	Large	Certain
Chemwes-Buffelsfontein Mega Tailings Dam Pipeline	Monte Christo Formation	From M.J. Meyer (2011): Numerous Camel Thorn Trees in combination with red soil cover and occasional concentric surface cracks	Subsidence	Very Large	Certain

Chemwes-Buffelsfontein Mega Tailings Dam Pipeline	Monte Christo Formation	From M.J. Meyer (2011): Deep red soil cover	Subsidence	Large	Certain
Chemwes-Buffelsfontein Mega Tailings Dam Pipeline	Karoo Supergroup	From M.J. Meyer (2011): Concentric surface cracks next to pipeline route	Subsidence	Small	Certain
Chemwes-Buffelsfontein Mega Tailings Dam Pipeline	Karoo Supergroup	From M.J. Meyer (2011): Large surface crack along pipeline together with saturated soil	Subsidence	Large	Certain
Chemwes-Buffelsfontein Mega Tailings Dam Pipeline	Monte Christo / Karoo Inlier (along contact)	From M.J. Meyer (2011): Surface tension cracks along geological contact	Subsidence	Large	Certain
Chemwes-Buffelsfontein Mega Tailings Dam Pipeline	Monte Christo Formation	From M.J. Meyer (2011): Backfilled sinkhole showing signs of re-activation (concentric surface cracks)	Sinkhole	Medium	Certain
Chemwes-Buffelsfontein Mega Tailings Dam Pipeline	Monte Christo Formation	From M.J. Meyer (2011): Large concentric surface cracks with diameter of 7 x 6 m next to pipeline	Sinkhole	Large	Certain
Chemwes-Buffelsfontein Mega Tailings Dam Pipeline	Monte Christo Formation	From M.J. Meyer (2011): Medium (2 x 3 m diameter) sinkhole next to pipeline	Sinkhole	Medium	Certain
Chemwes-Buffelsfontein Mega Tailings Dam Pipeline	Monte Christo Formation	From M.J. Meyer (2011): Medium-sized sinkholes 20 m away from pipeline	Sinkhole	Medium	Certain
Chemwes-Buffelsfontein Mega Tailings Dam Pipeline	Monte Christo Formation	From M.J. Meyer (2011): Backfilled sinkhole, size unknown	Sinkhole	Unknown dimensions	Certain
Chemwes-Buffelsfontein Mega Tailings Dam Pipeline	Monte Christo Formation	From M.J. Meyer (2011): Small sinkholes with diameter of 1 x 3 m	Sinkhole	Medium	Certain

North of old Khuma	Lyttleton / Eccles Formation (across contact)	Approximately 220 x 70 m diameter. Surface cracks visible from airplane. Northwest-southeast strike	Sinkhole	Very Large	Certain
Khuma Extension 6 Cemetery	Lyttleton Formation	-	Sinkhole	Large	Certain
Khuma Extension 6 Cemetery	Lyttleton Formation	-	Sinkhole	Large	Certain
South of Khuma Extension 6	Lyttleton Formation	Backfilled sinkhole. Diameter \pm 14 m	Sinkhole	Large	Inferred from API
North of old Khuma, south of railway line	Lyttleton Formation	-	Sinkhole	Large	Paleo Feature
North of old Khuma, south of railway line	Lyttleton Formation	-	Sinkhole	Large	Paleo Feature
South-east of Eagles Creek Gold Course	Lyttleton Formation	-	Sinkhole	Large	Paleo Feature
South-east of Eagles Creek Gold Course	Lyttleton Formation	-	Sinkhole	Large	Paleo Feature
North of Khuma Extension 6	Lyttleton Formation	Partially developed sinkhole verified in field	Sinkhole	Large	Certain
North of old Khuma	Lyttleton Formation	Shallow partially developed sinkhole with diameter of approximately 13 m. Dolomite pinnacles visible between eroded overburden	Sinkhole	Large	Certain
Khuma Extension 6	Lyttleton Formation	Approximately 4 m diameter and 3 m deep. Developed 1993/01/02	Sinkhole	Medium	Inferred from API
N12 east of Stilfontein	Lyttleton Formation	Rehabilitated sinkhole, formed between midway of the N12	Sinkhole	Medium	Certain
North-west of old Khuma	Lyttleton Formation	-	Sinkhole	Medium	Inferred from API
South of Vaal River	Lyttleton Formation	-	Sinkhole	Medium	Inferred from API
South of Vaal River	Lyttleton Formation	-	Sinkhole	Medium	Inferred from API
South of Vaal River	Lyttleton Formation	-	Sinkhole	Medium	Inferred from API
South of Vaal River	Lyttleton Formation	-	Sinkhole	Medium	Inferred from API
South of Vaal River	Lyttleton Formation	-	Sinkhole	Medium	Inferred from API
South of Vaal River	Lyttleton Formation	-	Sinkhole	Medium	Inferred from API
South of Vaal River	Lyttleton Formation	-	Sinkhole	Medium	Inferred from API
South of Vaal River	Lyttleton Formation	-	Sinkhole	Medium	Inferred from API
South of Vaal River	Lyttleton Formation	-	Sinkhole	Medium	Inferred from API

South of Vaal River	Lyttleton Formation	-	Sinkhole	Medium	Inferred from API
Northeast of Khuma Extension 6	Lyttleton Formation	Diameter of less than 1 m.	Sinkhole	Small	Certain
North-west of old Khuma	Lyttleton Formation	Partially developed sinkhole verified in field	Sinkhole	Small	Certain
North-east of Khuma Extension 6	Lyttleton Formation	Approximately 28 m diameter	Sinkhole	Very Large	Certain
Khuma Extension 6 Cemetery	Lyttleton Formation	Approximately 25 m diameter & 20 m deep. Developed 1993/01/01	Sinkhole	Very Large	Certain
North of N12	Lyttleton Formation	-	Sinkhole	Very Large	Paleo Feature
South of Khuma Extension 6	Lyttleton Formation	-	Sinkhole	Very Large	Inferred from API
North of old Khuma, south of railway line	Lyttleton Formation	-	Sinkhole	Very Large	Paleo Feature
North of old Khuma, south of railway line	Lyttleton Formation	-	Sinkhole	Very Large	Paleo Feature
South-east of Eagles Creek Gold Course	Lyttleton Formation	-	Sinkhole	Very Large	Paleo Feature
South-east of Eagles Creek Gold Course	Lyttleton Formation	-	Sinkhole	Very Large	Paleo Feature
South-east of Eagles Creek Gold Course	Lyttleton Formation	-	Sinkhole	Very Large	Paleo Feature
South of Vaal River	Lyttleton Formation	-	Sinkhole	Very Large	Paleo Feature
South of Vaal River	Lyttleton Formation	-	Sinkhole	Very Large	Paleo Feature
South of railway line, North of old Khuma	Lyttleton Formation	Paleo-sinkhole defined by Camel Thorn trees with a circular configuration in the field	Sinkhole	Very Large	Certain
South of railway line, North of old Khuma	Lyttleton Formation	Paleo-sinkhole defined by Camel Thorn trees with a circular configuration in the field	Sinkhole	Very Large	Certain
North of old Khuma, south of railway line	Lyttleton Formation	-	Subsidence	Large	Inferred from API
South of Eastern Shaft	Lyttleton Formation	Approximately 500 x 300 m. North-west/south-east strike	Subsidence	Very Large	Inferred from API
South of Khuma Extension 6	Lyttleton Formation	Approximately 170 x 60 m diameter. North-west/south-east strike.	Subsidence	Very Large	Inferred from API
East of Eagles Creek Golf Course	Lyttleton Formation	-	Subsidence	Very Large	Inferred from API
South of N12 near railway line	Lyttleton Formation	-	Subsidence	Very Large	Paleo Feature
North-west of old Khuma	Lyttleton Formation	Seasonal inundation due to topographic depression caused by subsidence	Subsidence	Very Large	Certain

North-west of old Khuma	Lyttleton Formation	Seasonal inundation due to topographic depression caused by subsidence	Subsidence	Very Large	Certain
North of old Khuma, south of railway line	Lyttleton Formation	-	Subsidence	Very Large	Inferred from API
North of Khuma Extension 6	Monte Christo / Lyttleton Formation (across contact)	Approximately 600 x 300 m diameter. East-West strike.	Subsidence	Very Large	Certain
East of Eagles Creek Golf Course	Monte Christo / Lyttleton Formation (across contact)	-	Subsidence	Very Large	Paleo Feature
Buffelsfontein mine offices	Monte Christo Formation	Several sinkholes. Last known sinkhole was 2002.	Sinkhole	Large	Certain
East of Stilfontein golf course	Monte Christo Formation	Backfilled sinkhole (August 2007)	Sinkhole	Large	Certain
East of Stilfontein golf course	Monte Christo Formation	Backfilled sinkhole (August 2007)	Sinkhole	Large	Certain
East of Stilfontein golf course	Monte Christo Formation	Backfilled sinkhole (August 2007)	Sinkhole	Large	Certain
East of Stilfontein golf course	Monte Christo Formation	Backfilled sinkhole (August 2007)	Sinkhole	Large	Certain
East of Stilfontein golf course	Monte Christo Formation	Backfilled sinkhole (August 2007)	Sinkhole	Large	Certain
East of Stilfontein golf course	Monte Christo Formation	Backfilled sinkhole (August 2007)	Sinkhole	Large	Certain
East of Stilfontein golf course	Monte Christo Formation	Backfilled sinkhole (August 2007)	Sinkhole	Large	Certain
East of Stilfontein golf course	Monte Christo Formation	Backfilled sinkhole (August 2007)	Sinkhole	Large	Certain
East of Stilfontein golf course	Monte Christo Formation	Backfilled sinkhole (August 2007)	Sinkhole	Large	Certain
East of Stilfontein golf course	Monte Christo Formation	Backfilled sinkhole (August 2007)	Sinkhole	Large	Certain
East of Stilfontein golf course	Monte Christo Formation	Backfilled sinkhole (August 2007)	Sinkhole	Large	Certain
South of Khuma Extension 6	Monte Christo Formation	Backfilled sinkhole. Diameter \pm 7 m	Sinkhole	Large	Inferred from API
Vaal Reefs 8 Shaft (Free State)	Monte Christo Formation	From Wagener (1982). Formed due to poor storm water management (1978-1981)	Sinkhole	Large	Certain

Vaal Reefs 8 Shaft (Free State)	Monte Christo Formation	From Wagener (1982). Formed due to poor storm water management (1978-1981)	Sinkhole	Large	Certain
Vaal Reefs 8 Shaft (Free State)	Monte Christo Formation	From Wagener (1982). Formed due to poor storm water management (1978-1981)	Sinkhole	Large	Certain
North of N12	Monte Christo Formation	-	Sinkhole	Large	Inferred from API
67 Jan Van Riebeeck Avenue, Stilfontein	Monte Christo Formation	Developed during 1981.	Sinkhole	Large	Certain
East of Eagles Creek Golf Course	Monte Christo Formation	Re-activation of previously backfilled sinkhole. Diameter of ± 8 m	Sinkhole	Large	Certain
North of Mineworkers Village	Monte Christo Formation	Backfilled sinkhole with trees established. Diameter of approximately 12 m	Sinkhole	Large	Certain
Hartebeesfontein Nos. 5 & 6 TDF	Monte Christo Formation	Several sinkholes south of penstock decant, and water accumulation on access ramp. Backfilled sinkholes re-activated during January 2009	Sinkhole	Large	Certain
Along pipeline parallel with N12, 100 m west of Stilfontein GM Transport office	Monte Christo Formation	Sinkhole with dimensions 4 x 5 m and 3 m deep developed during 2007. Sinkhole was backfilled.	Sinkhole	Large	Certain
Buffelsfontein No 3 TDF	Monte Christo Formation	Combination of 3 sinkholes developed on south-western corner of TDF in January 2009. Sinkholes are connected with concentric surface tension cracks	Sinkhole	Large	Certain
Anglo Midway Pump Station north of Buffelsfontein	Monte Christo Formation	Sinkhole developed during April 2011	Sinkhole	Medium	Certain
Northeast of Khuma Extension 6	Monte Christo Formation	Cover collapse sinkhole of approximately 6 m diameter, 2 m deep. Filled with trees	Sinkhole	Medium	Certain
Northeast of Khuma Extension 6	Monte Christo Formation	Cover collapse sinkhole of approximately 10 m diameter, 2 m deep. Filled with trees	Sinkhole	Medium	Certain
South of Khuma Extension 6	Monte Christo Formation	Backfilled sinkhole. Diameter ± 5 m	Sinkhole	Medium	Inferred from API
Vaal Reefs 8 Shaft (Free State)	Monte Christo Formation	From Wagener (1982). Formed due to poor storm water management (1978-1981)	Sinkhole	Medium	Certain
Vaal Reefs 8 Shaft (Free State)	Monte Christo Formation	From Wagener (1982). Formed due to poor storm water management (1978-1981)	Sinkhole	Medium	Certain
Vaal Reefs 8 Shaft (Free State)	Monte Christo Formation	From Wagener (1982). Formed due to poor storm water management (1978-1981)	Sinkhole	Medium	Certain
Vaal Reefs 8 Shaft (Free State)	Monte Christo Formation	From Wagener (1982). Formed due to poor storm water management (1978-1981)	Sinkhole	Medium	Certain
N12 at Stilfontein	Monte Christo Formation	Partially developed sinkhole. Diameter of approximately 3 m	Sinkhole	Medium	Certain

Mineworkers Village	Monte Christo Formation	-	Sinkhole	Medium	Inferred from API
North of N12	Monte Christo Formation	-	Sinkhole	Medium	Inferred from API
North of N12	Monte Christo Formation	Within drainage of Kromdraaispruit	Sinkhole	Medium	Certain
East of Eagles Creek Golf Course	Monte Christo Formation	Re-activation of previously backfilled sinkhole	Sinkhole	Medium	Certain
North of Khuma Extension 6	Monte Christo Formation	Sinkhole verified in field. Associated with Kromdraaispruit drainage	Sinkhole	Medium	Certain
Hartebeesfontein Nos. 1 to 4 TDF	Monte Christo Formation	Several sinkholes due to damage pipeline and accumulation of run-off water next to TDF	Sinkhole	Medium	Certain
North of Khuma Extension 6	Monte Christo Formation	Cluster of 3 small sinkholes with diameters of less than 0.8 m, 0,6 m deep	Sinkhole	Small	Certain
Stilfontein water towers and reservoir	Monte Christo Formation	Small sinkholes, part of larger structure that is re-activating. First sinkhole developed in 2002. Reactivated in 2004, 2011, and ±2014	Sinkhole	Small	Certain
Stilfontein water towers and reservoir	Monte Christo Formation	Small sinkholes, part of larger structure that is re-activating. First sinkhole developed in 2002. Reactivated in 2004, 2011, and ±2014	Sinkhole	Small	Certain
Stilfontein water towers and reservoir	Monte Christo Formation	Small sinkholes, part of larger structure that is re-activating. First sinkhole developed in 2002. Reactivated in 2004, 2011, and ±2014	Sinkhole	Small	Certain
North of N12	Monte Christo Formation	Within drainage of Kromdraaispruit	Sinkhole	Small	Certain
North of N12	Monte Christo Formation	Within drainage of Kromdraaispruit	Sinkhole	Small	Certain
South of Vaal River	Monte Christo Formation	-	Sinkhole	Small	Inferred from API
Along pipeline parallel with N12, 100 m west of Stilfontein GM Transport office	Monte Christo Formation	Several small sinkholes developed along pipeline prior to 2002. All sinkholes were backfilled	Sinkhole	Small	Certain
South of Chemwes Plant near Stilfontein	Monte Christo Formation	South of Chemwes Plant, North of Pinnacle school underneath Chemwes-Buffelsfontein pipeline Several small sinkholes developed associated with pipeline during 2007. Sinkholes were backfilled, subsidences are still present	Sinkhole	Small	Certain
Chemwest Thickener tanks near Stilfontein	Monte Christo Formation	Sinkholes developed next to new U-plant thickener tanks - 26 January 2009	Sinkhole	Small	Certain
South of Stilfontein golf course	Monte Christo Formation	Backfilled sinkhole (August 2007)	Sinkhole	Unknown dimensions	Certain

South of Stilfontein golf course	Monte Christo Formation	Backfilled sinkhole (August 2007)	Sinkhole	Unknown dimensions	Certain
East of Stilfontein golf course	Monte Christo Formation	Backfilled sinkhole (August 2007)	Sinkhole	Unknown dimensions	Certain
East of Stilfontein golf course	Monte Christo Formation	Backfilled sinkhole (August 2007)	Sinkhole	Unknown dimensions	Certain
East of Stilfontein golf course	Monte Christo Formation	Backfilled sinkhole (August 2007)	Sinkhole	Unknown dimensions	Certain
East of Stilfontein golf course	Monte Christo Formation	Backfilled sinkhole (August 2007)	Sinkhole	Unknown dimensions	Certain
East of Stilfontein golf course	Monte Christo Formation	Backfilled sinkhole (August 2007)	Sinkhole	Unknown dimensions	Certain
East of Stilfontein golf course	Monte Christo Formation	Backfilled sinkhole (August 2007)	Sinkhole	Unknown dimensions	Certain
East of Stilfontein golf course	Monte Christo Formation	Backfilled sinkhole (August 2007)	Sinkhole	Unknown dimensions	Certain
East of Stilfontein golf course	Monte Christo Formation	Backfilled sinkhole (August 2007)	Sinkhole	Unknown dimensions	Certain
East of Stilfontein golf course	Monte Christo Formation	Backfilled sinkhole (August 2007)	Sinkhole	Unknown dimensions	Certain
East of Stilfontein golf course	Monte Christo Formation	Backfilled sinkhole (August 2007)	Sinkhole	Unknown dimensions	Certain
East of Stilfontein golf course	Monte Christo Formation	Backfilled sinkhole (August 2007)	Sinkhole	Unknown dimensions	Certain
East of Stilfontein golf course	Monte Christo Formation	Backfilled sinkhole (August 2007)	Sinkhole	Unknown dimensions	Certain
East of Stilfontein golf course	Monte Christo Formation	Backfilled sinkhole (August 2007)	Sinkhole	Unknown dimensions	Certain
East of Stilfontein golf course	Monte Christo Formation	Backfilled sinkhole (August 2007)	Sinkhole	Unknown dimensions	Certain
D. Scott Hospital south of Stilfontein	Monte Christo Formation	Sinkhole developed along Buffelsfontein-Chemwes pipeline close to D. Scott Hospital during 2007	Sinkhole	Unknown dimensions	Certain
South of Vaal River near Dolomite Mine	Monte Christo Formation	Very large sinkhole, approximately 22 m across	Sinkhole	Very Large	Certain
South of Vaal River near Dolomite Mine	Monte Christo Formation	Partially developed sinkhole, approximately 23 m across	Sinkhole	Very Large	Certain
Spoornet Railway line crossing at Koekemoerspruit (east of Stilfontein)	Monte Christo Formation	Cluster of 7 sinkholes. Formed before 2007. Re-activated 2007	Sinkhole	Very Large	Certain
North of Khuma Extension 6	Monte Christo Formation	Approximately 50 m across 15 m deep	Sinkhole	Very Large	Certain

South of Khuma Extension 6	Monte Christo Formation	Approximately 24m diameter. Deemed old back-filled sinkhole	Sinkhole	Very Large	Inferred from API
South of Stilfontein golf course	Monte Christo Formation	Backfilled sinkhole (August 2007)	Sinkhole	Very Large	Certain
East of Stilfontein golf course	Monte Christo Formation	Backfilled sinkhole (August 2007)	Sinkhole	Very Large	Certain
South of Khuma Extension 6	Monte Christo Formation	Combination of 2 sinkholes. Diameters of approximately 48 and 30 m respectively	Sinkhole	Very Large	Inferred from API
Vaal Reefs 8 Shaft (Free State)	Monte Christo Formation	From Wagener (1982). Formed due to poor storm water management (1978-1981)	Sinkhole	Very Large	Certain
Vaal Reefs 8 Shaft (Free State)	Monte Christo Formation	From Wagener (1982). Formed due to poor storm water management (1978-1981)	Sinkhole	Very Large	Certain
N12 at Stilfontein	Monte Christo Formation	Combination of 8 sinkholes connected with concentric surface cracks. Total combined surface cracks / partially developed sinkhole diameter of 25 m. Developed November 2015	Sinkhole	Very Large	Certain
R502 near Buffelsfontein mine	Monte Christo Formation	Diameter of approximately 78 m	Sinkhole	Very Large	Paleo Feature
North of N12	Monte Christo Formation	-	Sinkhole	Very Large	Paleo Feature
North of N12	Monte Christo Formation	-	Sinkhole	Very Large	Inferred from API
North of N12	Monte Christo Formation	-	Sinkhole	Very Large	Paleo Feature
North of N12	Monte Christo Formation	-	Sinkhole	Very Large	Paleo Feature
North of N12	Monte Christo Formation	-	Sinkhole	Very Large	Paleo Feature
North of N12	Monte Christo Formation	-	Sinkhole	Very Large	Paleo Feature
South of N12 at Stilfontein	Monte Christo Formation	Paleo sinkhole exposed in quarry. 6 m deep red aeolian transported soil to base of quarry. Location approximate. Quarry currently filled with rubble	Sinkhole	Very Large	Certain
Mineworkers Village	Monte Christo Formation	Formed during 1979. From Wagener (1982)	Sinkhole	Unknown dimensions	Certain
Mineworkers Village	Monte Christo Formation	Formed during 1979. From Wagener (1982)	Sinkhole	Unknown dimensions	Certain
Mineworkers Village	Monte Christo Formation	Formed during 1979. From Wagener (1982)	Sinkhole	Unknown dimensions	Certain

Mineworkers Village	Monte Christo Formation	Formed during 1979. From Wagener (1982)	Sinkhole	Unknown dimensions	Certain
Mineworkers Village	Monte Christo Formation	Formed during 1979. From Wagener (1982)	Sinkhole	Unknown dimensions	Certain
N12 at Stilfontein	Monte Christo Formation	Shallow subsidence with a diameter of 8 x 14 m	Subsidence	Large	Certain
South of Vaal River	Monte Christo Formation	-	Subsidence	Large	Inferred from API
South of Vaal River	Monte Christo Formation	-	Subsidence	Large	Inferred from API
South of Vaal River	Monte Christo Formation	-	Subsidence	Large	Inferred from API
South of Vaal River	Monte Christo Formation	Associated with north-south trending lineation of trees	Subsidence	Large	Certain
South of Vaal River	Monte Christo Formation	-	Subsidence	Large	Inferred from API
East of Stilfontein along railway line	Monte Christo Formation	Sagging chert bands visible in railway cutting	Subsidence	Large	Certain
North of Khuma Extension 6	Monte Christo Formation	Subsidence verified in field. Associated with Kromdraaispruit drainage	Subsidence	Large	Certain
North of Khuma Extension 6	Monte Christo Formation	Subsidence verified in field. Associated with Kromdraaispruit drainage	Subsidence	Large	Certain
North of Khuma Extension 6	Monte Christo Formation	Subsidence verified in field	Subsidence	Large	Certain
South of Vaal River	Monte Christo Formation	-	Subsidence	Medium	Inferred from API
North of Khuma Extension 6	Monte Christo Formation	Subsidence verified in field	Subsidence	Medium	Certain
D. Scott Hospital south of Stilfontein	Monte Christo Formation	Subsidence formed 10 m from previous sinkhole 27 January 2009. Surface cracks are associated with settlement	Subsidence	Medium	Certain
Along pipeline parallel with N12, 100 m west of Stilfontein GM Transport office	Monte Christo Formation	Depression at construction camp 100 m from Stilfontein GM Transport office on 30 January 2009	Subsidence	Medium	Certain
South of Vaal River near Dolomite Mine	Monte Christo Formation	Large depression, approximate diameter of 90 m across around buried pipeline	Subsidence	Very Large	Inferred from API
East of old Stilfontein mine	Monte Christo Formation	Cluster of 3 subsidences with a combined diameter of 200 x 70 m. Possibly ascribed to underming of the Black Reef in the area.	Subsidence	Very Large	Inferred from API

North of Khuma Extension 6	Monte Christo Formation	Approximately 19 m diameter. East-west strike.	Subsidence	Very Large	Certain
Vaal Reefs 8 Shaft (Free State)	Monte Christo Formation	From Wagener (1982). Formed due to poor storm water management (1978-1981)	Subsidence	Very Large	Certain
Vaal Reefs 8 Shaft (Free State)	Monte Christo Formation	From Wagener (1982). Formed due to poor storm water management (1978-1981)	Subsidence	Very Large	Certain
Vaal Reefs 8 Shaft (Free State)	Monte Christo Formation	From Wagener (1982). Formed due to poor storm water management (1978-1981)	Subsidence	Very Large	Certain
Vaal Reefs 8 Shaft (Free State)	Monte Christo Formation	From Wagener (1982). Formed due to poor storm water management (1978-1981)	Subsidence	Very Large	Certain
Vaal Reefs 8 Shaft (Free State)	Monte Christo Formation	From Wagener (1982). Formed due to poor storm water management (1978-1981)	Subsidence	Very Large	Certain
Vaal Reefs 8 Shaft (Free State)	Monte Christo Formation	From Wagener (1982). Formed due to poor storm water management (1978-1981)	Subsidence	Very Large	Certain
Vaal Reefs 8 Shaft (Free State)	Monte Christo Formation	From Wagener (1982). Formed due to poor storm water management (1978-1981)	Subsidence	Very Large	Certain
Vaal Reefs 8 Shaft (Free State)	Monte Christo Formation	From Wagener (1982). Formed due to poor storm water management (1978-1981)	Subsidence	Very Large	Certain
N12 at Stilfontein	Monte Christo Formation	Partially developed sinkhole. Diameter approximately 18 x 15 m	Subsidence	Very Large	Certain
South-east of Eagles Creek Gold Course	Monte Christo Formation	-	Subsidence	Very Large	Paleo Feature
North of Mineworkers Village	Monte Christo Formation	North-north-west/south-south-east trending surface drainage depression.	Subsidence	Very Large	Certain
North of Mineworkers Village	Monte Christo Formation	Combination of 3 subsidences.	Subsidence	Very Large	Certain
South of N12 at Stilfontein	Oaktree Formation	Sinkhole developed in servitude next to N12. Backfilled 1993	Sinkhole	Medium	Certain
North of N12 at Stilfontein	Oaktree Formation	Sinkhole developed in servitude next to N12. Backfilled 1993	Sinkhole	Small	Certain
North of N12 at Stilfontein	Oaktree Formation	Sinkhole developed in servitude next to N12. Backfilled 1993	Sinkhole	Small	Certain
North of N12 at Stilfontein	Oaktree Formation	Sinkhole developed in servitude next to N12. Backfilled 1993	Sinkhole	Small	Certain
North of N12 at Stilfontein	Oaktree Formation	Sinkhole developed in servitude next to N12. Backfilled 1993	Sinkhole	Small	Certain
North of N12 at Stilfontein	Oaktree Formation	Sinkhole developed in servitude next to N12. Backfilled 1993	Sinkhole	Small	Certain
North of N12 at Stilfontein	Oaktree Formation	Sinkhole developed in servitude next to N12. Backfilled 1993	Sinkhole	Small	Certain
North of Stilfontein and N12	Oaktree Formation	North-westwardly trending feature.	Subsidence	Large	Inferred from API

Annexure 4: Detailed inherent hazard assessments of key developments and infrastructure across the KOSH area

Table 6-4: Detailed hazard assessment per area across the larger KOSH area dolomite land

Focus Area Designation	Area Name	Local Municipality	Approximate size of dolomitic area (ha)	Regional geological setting	Groundwater status	Known instability features	Previous Investigations	Regional Hazard Zone	Other considerations	Further requirements
TOWNS AND SETTLEMENTS										
A	Orkney - Eastern suburbs	Matlosana	363	Ventersdorp Supergroup towards the far west Black Reef Formation and Oaktree Formation towards the east. Faults indicated towards the north and south.	Part of KOSH western groundwater compartments (i.e. KOSH A). Historic groundwater level between 6 and 21 mbgl up to Nov 1993. Fluctuations of between 7.5 and 12.3 m total. Not deemed subjected to dewatering.	No known instability features were observed or researched in the area	Orkney Ext 2 (1981) No boreholes drilled.	<u>INDICATED RISK:</u> Zone 1 (Low to Med Risk) along the western perimeter of dolomite area Zone 2 (Med Risk) towards the east of town. Zone 5 (Very High Risk) towards the north and south-east	Tailings dams situated towards north of town. Possible environmental hazard.	Reconnaissance drilling to define extent of Black Reef Formation Detailed geotechnical investigations (gravity and drilling) across the remainder of the delineated dolomite area Dolomite Risk Management Plan and - Strategy
B	Orkney Vaal Holiday Resort	Matlosana	40	Oaktree and Monte Christo Formation Large north-east trending fault intersects the southern parts of the area	Part of KOSH western groundwater compartments (i.e. KOSH A). Historic groundwater level between 6 and 21 mbgl up to Nov 1993. Fluctuations of between 7.5 and 12.3 m total. Not deemed subjected to dewatering.	No known instability features were observed or researched in the area	No known geotechnical investigation exists for this area	<u>INDICATED RISK:</u> Zone 3 (Medium to High Risk) towards the central parts Zone 4 (High Risk) towards the north Zone 5 (Very High Risk) towards the south	-	Detailed geotechnical investigation required (including gravimetric survey, drilling of boreholes, geotechnical report) Dolomite Risk Management Plan and - Strategy
C	Umzimuhle-Vaal Reefs	Matlosana	488	Entire area underlain by Monte Christo Formation Faults inferred towards the southwest and southeast.	Part of KOSH western groundwater compartments (i.e. KOSH A). Historic groundwater level between 6 and 21 mbgl up to Nov 1993. Fluctuations of between 7.5 and 12.3 m total. Not deemed subjected to dewatering.	5 known sinkholes developed in the formalized area during and after construction (early 1980's)	Some boreholes and gravity survey (1978)	<u>INDICATED RISK:</u> Zone 3 (Medium to High Risk) Indications of shallow bedrock outcrops towards the south and the north of area	-	Updated geotechnical investigations and zoning required to comply with current industry standards (SANS 1936, 2012) Dolomite Risk Management Plan and - Strategy

C	Ariston	Matlosana	6.7	Primarily situated on the Black Reef Formation	Part of KOSH western groundwater compartments (i.e. KOSH A). Historic groundwater level between 6 and 21 mbgl up to Nov 1993. Fluctuations of between 7.5 and 12.3 m total. Not deemed subjected to dewatering. Dewatering currently occurring at Margret shaft to ensure dry working conditions at Vaal Reefs mining areas (southern parts)	No known instability features were observed or researched in the area	No available geotechnical reports from the Council for Geoscience databank.	<u>INDICATED RISK:</u> Zone 1 (Low to Medium Risk) across entire central and southern area. Zone 5 (Very High Risk) in the northeastern-most corner of area.	-	Dolomite Risk Management Plan and - Strategy required
D	Hartebeesfontein - Klerksdorp	Matlosana	76	Entirely underlain by Monte Christo Formation. Numerous north-trending faults and thrusts indicated along the eastern parts of area.	KOSH compartment B (Dewatered) towards the east. KOSH compartment A in the eastern parts of the area (non-dewatered)	No known instability features were observed or researched in the area	No available geotechnical reports from the Council for Geoscience databank.	<u>INDICATED RISK:</u> Zone 5 (Very High Risk) across the majority of the area. Zone 4 (High Risk) in the northwestern-most parts of the area	-	Dolomite Risk Management Plan and - Strategy required
E	Stilfontein Gold Mine	Matlosana	3433	Southern and northern parts underlain by Monte Christo Formation. Central (east-west) parts situated across Karoo Supergroup sediments Paleo-karst valley infill. Southwestern-most parts underlain by Oaktree Formation. No major faults are inferred to intersect the area. Folding of the dolomitic strata indicated towards the western parts.	KOSH compartment B (Dewatered) towards the east. KOSH compartment A in the eastern parts of the area (non-dewatered)	Known instability features are indicated towards the northern parts of the area.	No available geotechnical reports from the Council for Geoscience databank.	<u>INDICATED RISK:</u> Zone 4 (High Risk) towards the northern and southern parts. Zone 3 (Medium to High Risk) in the southwestern and northwestern parts of the area. Zone 2 (Low to High Risk) along the central east-west area.	Various mine tailings and redundant infrastructure located across dolomite area Groundwater level and quality monitoring needs to be verified	Dolomite Risk Management Plan and - Strategy required

F	Vaal Reefs Gold Mine	Matlosana	2509	Majority of area located across Monte Christo Formation. Oaktree- and Black Reef Formation towards the west. Various geological structures inferred along the southern perimeter, and in the south-east of the area	Part of KOSH western groundwater compartments (i.e. KOSH A). Historic groundwater level between 6 and 21 mbgl up to Nov 1993. Fluctuations of between 7.5 and 12.3 m total. Not deemed subjected to dewatering. Dewatering currently occurring at Margret shaft to ensure dry working conditions at Vaal Reefs mining areas (southern parts)	Instability features directly north of the area in the Umzimhule-Vaal Reefs village.	No available geotechnical reports from the Council for Geoscience databank.	<u>INDICATED RISK:</u> Zone 4 (High Risk) across the majority of the area, with Zones 3 and 1 (Medium to High and Low to Medium) towards the western-most parts. Zone 5 (Very High Risk) along the southern and southeastern perimeter.	Various mine tailings and redundant infrastructure located across dolomite area Groundwater level and quality monitoring needs to be verified	Dolomite Risk Management Plan and - Strategy required
G	Vaal Reefs North Gold Mine	Matlosana	1455	Entire area underlain by Monte Christo Formation. Regionally prominent structures indicated towards the southern parts of the area.	KOSH compartment A (non-dewatered) across the entire area	No known instability features were observed or researched in the area	No available geotechnical reports from the Council for Geoscience databank.	<u>INDICATED RISK:</u> Zone 4 (High Risk) across the majority of the area. Zone 5 (Very High Risk) in the southern section of the area.	Various mine tailings and redundant infrastructure located across dolomite area Groundwater level and quality monitoring needs to be verified	Dolomite Risk Management Plan and - Strategy required
H	Buffelsfontein Gold Mine	Matlosana	2552	Entire western portions of the area underlain by Monte Christo Formation. Eastern parts underlain by Lyttleton and Eccles Formations. Numerous north-trending faults and thrusts known in the area.	KOSH compartment B (Dewatered) towards the east. KOSH compartment A in the eastern parts of the area (non-dewatered)	No known instability features were observed or researched in the area	No available geotechnical reports from the Council for Geoscience databank.	<u>INDICATED RISK:</u> Zone 4 (High Risk) towards the entire western section, and eastern-most parts. Zone 5 (Very High Risk) along the entire eastern parts.	Old waste-rock dumps situated on area. Groundwater quality and depth needs to be verified.	Dolomite Risk Management Plan and - Strategy required

I	Hartebeesfontein Gold Mine	Matlosana	308	<p>Majority of the area underlain by Oaktree Formation. Black Reef Formation along the western boundary of the area. No major faults or structures inferred to intersect the area.</p>	<p>Part of KOSH western groundwater compartments (i.e. KOSH A). Historic groundwater level between 6 and 21 mbgl up to Nov 1993. Fluctuations of between 7.5 and 12.3 m total. Not deemed subjected to dewatering. Dewatering currently occurring at Margret shaft to ensure dry working conditions at Vaal Reefs mining areas (southern parts)</p>	No known instability features were observed or researched in the area	No available geotechnical reports from the Council for Geoscience databank.	<p><u>INDICATED RISK</u> Zone 3 (Medium to High Risk) across the majority of the area. Zone 1 (Low to Medium Risk) along the western boundary</p>	Old waste-rock dumps situated on area. Groundwater quality and depth needs to be verified.	Dolomite Risk Management Plan and - Strategy required
J	Palmietfontein	Matlosana	33	<p>Western parts located across Black Reef Formation. Eastern-most parts located across Oaktree Formation. Na major structures indicated to intersect the area</p>	KOSH compartment A (non-dewatered) across the entire area	No known instability features were observed or researched in the area	No available geotechnical reports from the Council for Geoscience databank.	<p><u>INDICATED RISK</u> Zone 1 (Low to Medium Risk) in the central and western parts. Zone 3 (Medium to High Risk) in the eastern parts.</p>	-	<p>Detailed geotechnical investigation required (including gravimetric survey, drilling of boreholes, geotechnical report) Dolomite Risk Management Plan and - Strategy</p>
K	Greater Khuma area	Matlosana	820	<p>Majority of area situated on karst-valley fill deposit of Karoo Supergroup Sediments. Horizontal thickness of inlier highly variable and extend in some areas extrapolated. The Karoo Inlier is underlain by the Monte Christo Formation in the west, and the Lyttleton and Eccles Formations in the east. Numerous major faults and associated quartz veins with a north-south strike intersect the area.</p>	<p>Primarily part of KOSH compartment B. Historic groundwater levels between 37 and 218 mbgl up to Nov 1993. Fluctuations of between 150 and 180 m total. Area dewatered.</p>	A number of sinkholes and subsidences occur within, north and south of Khuma Ext. 6, and north of Khuma East extensions	Phase 1 dolomite stability investigations conducted for: Khuma Extensions 1, 2, 3, 4, 5, 6, 11, east, south-west, Hartebeesfontein Ptn 3 Stilfontein Ext. 8 & 9	<p><u>MEASURED RISK:</u> Generally Low to Medium Risk along central (east west_ areas including western parts of Khuma Ext. 6 Remaining areas Medium to High Risk (IHC 4 to 8) <u>INDICATED RISK:</u> Zone 2 (Low to High Risk) in the central east-west areas Zones 4 and 5 (High to Very High Risk) in eastern parts (north and south of inlier)</p>	It is inferred that some illegal / informal settlement may have occurred in the western parts of Khuma Ext. 6 Area is highly vulnerable to re-watering of the dolomitic compartment	<p>Updated detailed geotechnical reports with integrated gravimetric survey, infill geotechnical drilling to determine the extent and thickness of Karoo inlier and dolomitic hazard, integrated updated geotechnical report Dolomite Risk Management Plan and - Strategy</p>

L	Stilfontein	Matlosana	744	<p>Majority of area situated on karst-valley fill deposit of Karoo Supergroup Sediments. Horizontal thickness of inlier highly variable and extend in the entire area extrapolated.</p> <p>The Karoo Inlier is underlain by the Monte Christo Formation in the east and the Oaktree Formation in the west.</p> <p>The northern and western-most parts are directly underlain by the Oaktree Formation.</p> <p>No known major faults intersect the area.</p>	<p>No known geotechnical investigations conducted in the formal Stilfontein township</p> <p>Geotechnical investigation conducted for Stilfontein Chemwes Gold & Uranium CBE (2007)</p>	<p>Known sinkholes at: Strathvall Primary - 300 m deep sinkhole (1981)</p> <p>Chemwest Uranium Plant (2012)</p> <p>67 Jan van Riebeeck Ave (2003)</p> <p>Ext. 5 (1980)</p> <p>At Midvaal water company offices (Stilfontein east)</p> <p>Railway crossing with the Koekemoer Spruit</p>	<p>Portion 61 of Stilfontein Eagles Creek Golf Estate</p> <p>Various correspondence on sinkholes</p>	<p><u>INDICATED RISK:</u></p> <p>Zone 2 (Low to High Risk) for the most of southern half of the east-west town area</p> <p>Zone 3 (Medium to High Risk) towards the far north and east</p> <p>Zone 4 (High Risk) in north-eastern parts</p>	<p>The eastern parts deemed highly vulnerable to the formation of sinkholes and subsidences once re-watering of the dolomite compartment commences</p>	<p>Integrated Dolomite Stability Investigation required for the entire Stilfontein and Khuma area, including gravimetric and geophysical surveys, drilling of boreholes, integrated geotechnical report</p> <p>Dolomite Risk Management Plan and - Strategy</p>
INFRASTRUCTURE										
INF 1	N12 national route (Potchefstroom - Klerksdorp)	National		<p>Across all dolomitic formations</p>	<p>KOSH groundwater compartment A towards the west (non-dewatered) and B towards the east (dewatered)</p>	<p>Known sinkhole between two lanes east of Stilfontein (1994)</p>	<p>No known geotechnical / dolomite stability investigations</p>	<p>Zones 1 to 5 (Low to High Risk)</p>	-	<p>Existing dolomite stability investigation to be verified.</p> <p>Dolomite Risk Management Plan and - Strategies to be verified / compiled.</p>
INF 2	Khuma Reservoirs	Matlosana		<p>Eccles Formation Regions surrounding area subjected to intense tectonic deformation</p>	<p>KOSH groundwater compartment B. Dewatered area.</p>	<p>Known very large sinkhole (270 x 70 m) occur towards the north-west of reservoir</p>	<p>No known geotechnical / dolomite stability investigations</p>	<p>Zone 5 (Very High Risk)</p>	<p>Reservoirs was found to be excessively leaking (July 2015)</p>	<p>Existing dolomite stability investigation to be verified.</p> <p>Dolomite Risk Management Plan and - Strategies to be verified / compiled.</p>

INF 3	Stilfontein - Potchefstroom railway Line, Orkney - Potchefstroom railway Line	Matlosana		Across all dolomitic formations	KOSH groundwater compartment A towards the west (non-dewatered) and B towards the east (dewatered).	Sagging chert bands - deemed indicative of Paleo sinkholes observed in railway cutting in eastern parts of Vaal Reefs Village and directly east of Stilfontein. 7 Sinkholes in 200 m radius at railway crossing with Koekemoer Spruit. Large sinkhole in far-eastern part of railway line north of Khuma (previously rehabilitated, in process of re-activation)	No known geotechnical / dolomite stability investigations	Zones 1 to 5 (Low to High Risk)	Various sinkholes and indications of Paleo sinkholes was observed along the railway routes	Existing dolomite stability investigation to be verified. Dolomite Risk Management Plan and - Strategies to be verified / compiled.
INF 4	R502 (Orkney - N12 route)	Matlosana		Across all dolomitic formations	KOSH groundwater compartment A towards the west (non-dewatered) and B towards the east (dewatered)	No known sinkholes within or adjacent road surface	No known geotechnical / dolomite stability investigations	Zones 1 to 5 (Low to High Risk)	-	Existing dolomite stability investigation to be verified. Dolomite Risk Management Plan and - Strategies to be verified / compiled.
INF 5	Vaal Reefs Village - Klerksdorp Road	Matlosana		Monte Christo Formation towards the south. Oaktree and Black Reef Formations towards the north	KOSH groundwater compartment A (non-dewatered)	No known sinkholes within or adjacent road surface	No known geotechnical / dolomite stability investigations	Zone 1 (Low to Medium Risk) towards the far north Zone 3 (Medium to High Risk) in central parts Zone 4 (High Risk) in southern parts	-	Existing dolomite stability investigation to be verified. Dolomite Risk Management Plan and - Strategies to be verified / compiled.
INF 6	Khuma - Buffelsdoorn Road	Matlosana		Primarily Monte Christo Formation for southern and central parts Oaktree and Black Reef Formations for northern parts	KOSH groundwater compartment A towards the west (non-dewatered) and B towards the east (dewatered)	No known sinkholes within or adjacent road surface	No known geotechnical / dolomite stability investigations	Zone 1 (Low to Medium Risk) towards the north Zone 3 (Medium to High Risk) in northern parts Zone 4 (High Risk) in central and southern parts	-	Existing dolomite stability investigation to be verified. Dolomite Risk Management Plan and - Strategies to be verified / compiled.

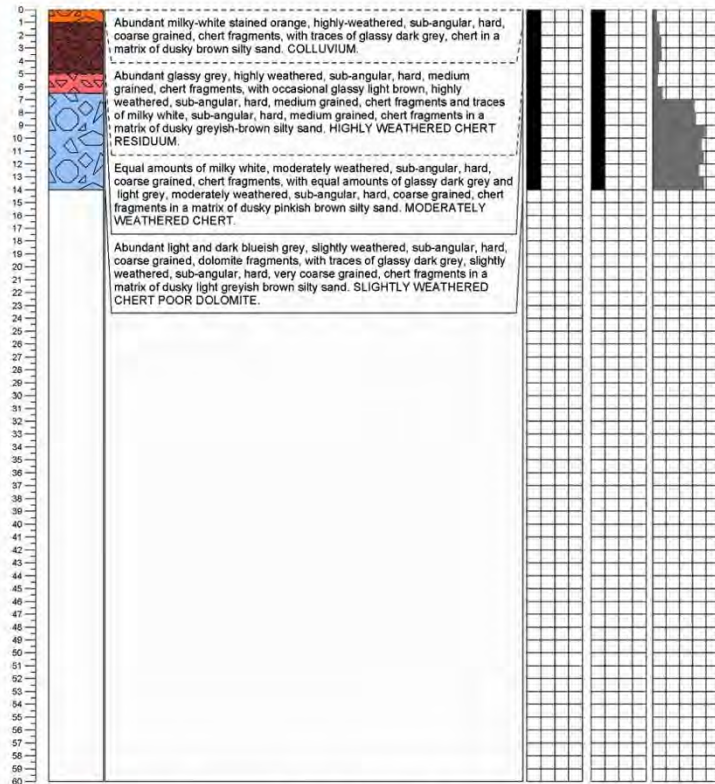
INF 7	Khuma - Stilfontein Road	Matlosana		Predominantly across inferred Karoo inlier Underlain by Monte Christo, Lyttleton, and Eccles Formations (from west to east)	KOSH groundwater compartment B. Dewatered area.	Known sinkholes adjacent Khuma Ext. 6 area	No known geotechnical / dolomite stability investigations	Zone 2 (Low to High Risk) in western and central Zone 5 (Very High Risk) in eastern parts	-	Existing dolomite stability investigation to be verified. Dolomite Risk Management Plan and - Strategies to be verified / compiled.
INF 8	Electrical lines south of Khuma	Matlosana		Across all dolomitic formations	KOSH groundwater compartment A towards the west (non-dewatered) and B towards the east (dewatered)	No known sinkholes within or adjacent servitude area	No known geotechnical / dolomite stability investigations	Zones 1 to 5 (Low to High Risk)	-	Existing dolomite stability investigation to be verified. Dolomite Risk Management Plan and - Strategies to be verified / compiled.
INF 9	Bulk fuel line north of Khuma	Matlosana		Across all dolomitic formations	KOSH groundwater compartment B. Dewatered area.	Known sinkholes adjacent Khuma Ext. 6 area	No known geotechnical / dolomite stability investigations	Zones 1 to 5 (Low to High Risk)	-	Existing dolomite stability investigation to be verified. Dolomite Risk Management Plan and - Strategies to be verified / compiled.
INF 10	Reservoirs north of Orkney	Matlosana		Western reservoirs located on Black Reef Formation Eastern reservoir underlain by Oaktree Formation	KOSH groundwater compartment A (non-dewatered)	No known sinkholes within or adjacent servitude area	No known geotechnical / dolomite stability investigations	Zone 1 (Low to Medium Risk) in the west Zone 3 (Medium to High Risk) in the east Localized Zone 5 (Very High Risk) intersecting the area	-	Existing dolomite stability investigation to be verified. Dolomite Risk Management Plan and - Strategies to be verified / compiled.

**Annexure 5: Rotary air percussion borehole logs drilled on the farm
Hartebeesfontein 422 IP**

PROJECT:

CLIENT:	LATITUDE:	BOREHOLE NO.:
CONTRACTOR: Hennie Erwe Drilling.	LONGITUDE:	DATE DRILLED: 2013/09/04
MACHINE TYPE: Super Rock 165mm / 1900kpa.	ELEVATION: 1323 mamsl	DATE LOGGED: 2013/09/04
COMPRESSOR: 19 bar	ORIENTATION: Vertical	LOGGED BY: WM & EH

Depth Lithology Description (m)

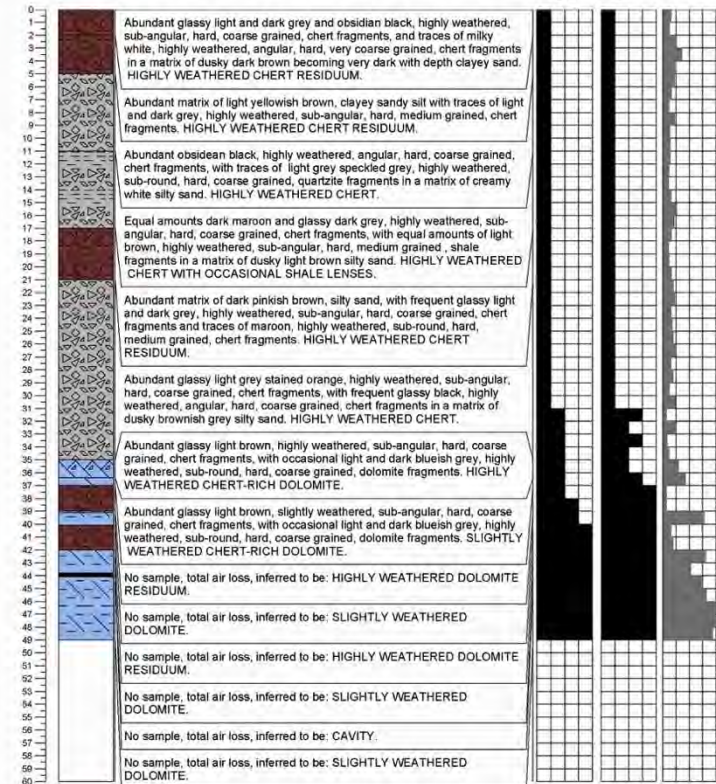


Notes:
 Drilling stopped 14 mbgl.
 No water was added during drilling.
 Irregular hammer rate at 0-1, 25-26 meters.
 Borehole dry.
 Coordinate measured with hand-held GPS (WGS84).
 Elevation inferred from 5m contours (GIS).

PROJECT:

CLIENT:	LATITUDE:	BOREHOLE NO.:
CONTRACTOR: Hennie Erwe Drilling	LONGITUDE:	DATE DRILLED: 2013/09/04
MACHINE TYPE: Super Rock 165mm / 1900kpa	ELEVATION: 1323 mamsl	DATE LOGGED: 2013/09/04
COMPRESSOR: 19 bar	ORIENTATION: Vertical	LOGGED BY: WM & EH

Depth Lithology Description (m)

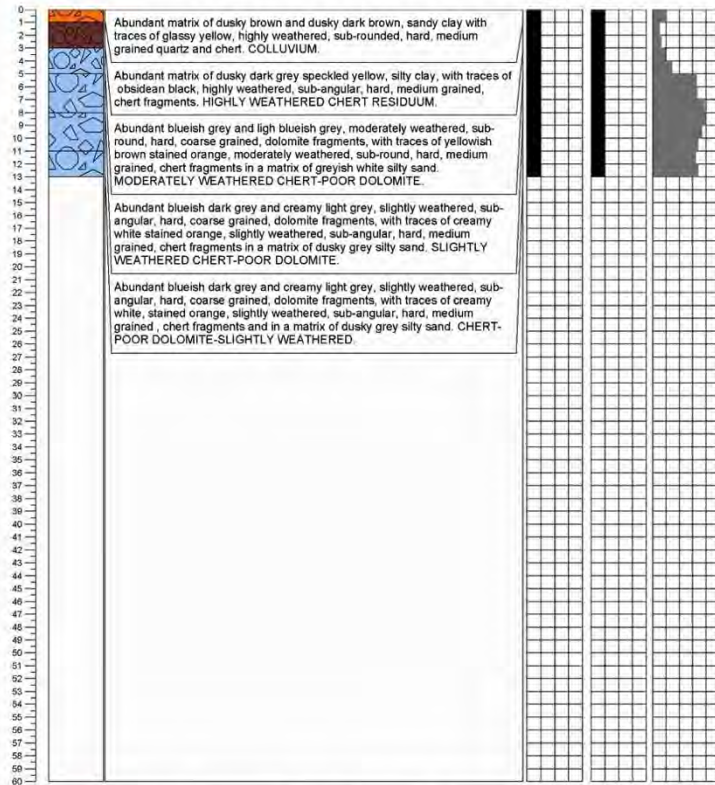


Notes:
 Drilling stopped 49 mbgl.
 No water was added during drilling.
 Irregular hammer rates at 0-1, 5-6, 32-34, 36-41, 44-46 m.
 Borehole dry.
 Coordinate measured with hand-held GPS (WGS84).
 Elevation inferred from 5m contours (GIS).

PROJECT:

CLIENT:	LATITUDE:	BOREHOLE NO.: KBH05	
CONTRACTOR: Hennie Erwee Drilling	LONGITUDE:	DATE DRILLED:	2013/10/04
MACHINE TYPE: Super Rock 165mm / 1500kpa	ELEVATION: 1324 mamsl	DATE LOGGED:	2013/10/04
COMPRESSOR: 19 bar	ORIENTATION: Vertical	LOGGED BY:	WM & EH

Depth Lithology Description
(m)

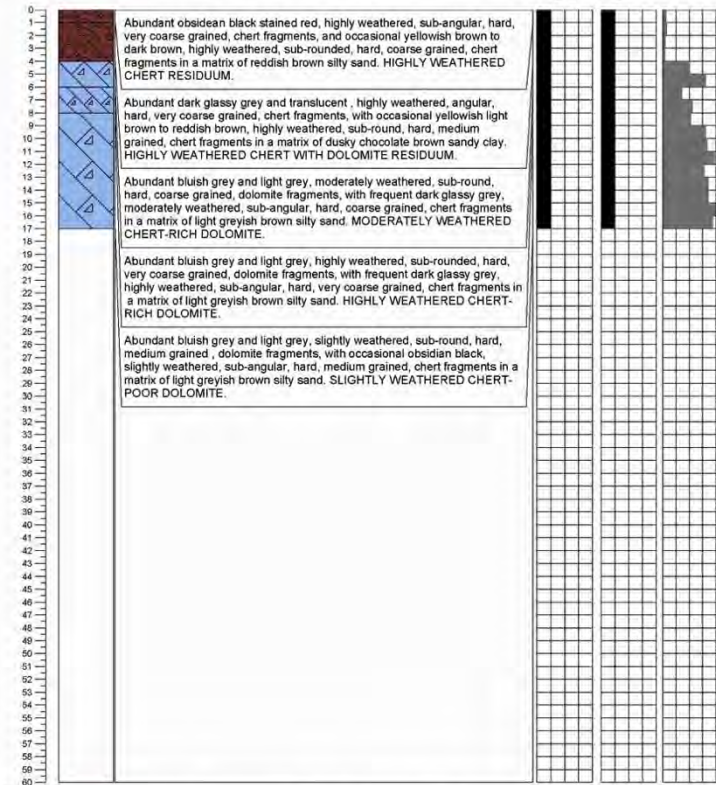


Notes: Drilling stopped 13 m bgl
No water was added during drilling.
Irregular hammer rates at: 1-2, 3-4 m.
Borehole dry.
Coordinate measured with hand-held GPS (WGS84)
Elevation inferred from 5m contours (GIS)

PROJECT:

CLIENT:	LATITUDE:	BOREHOLE NO.: KBH06	
CONTRACTOR: Hennie Erwee Drilling	LONGITUDE:	DATE DRILLED:	2013/10/04
MACHINE TYPE: Super Rock 165mm / 1500kpa	ELEVATION: 1325 mamsl	DATE LOGGED:	2013/10/04
COMPRESSOR: 19 bar	ORIENTATION: Vertical	LOGGED BY:	WM & EH

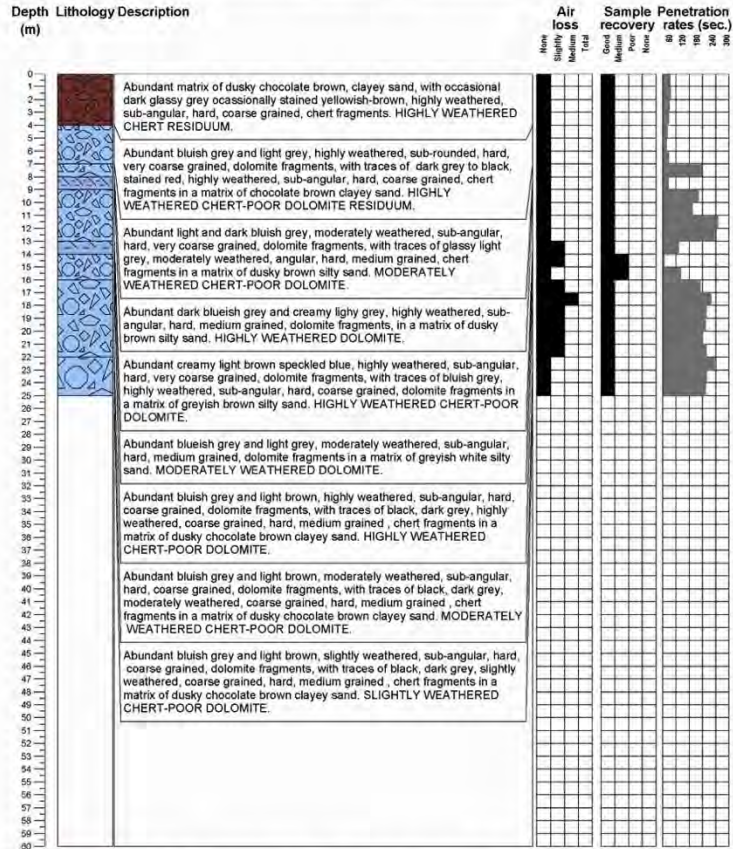
Depth Lithology Description
(m)



Notes: Drilling stopped 17 m bgl
No water was added during drilling.
Irregular hammer rates at: 0-1, 1-2, 2-3, 3-4, 4-5, 6-7, 8-9 m.
Borehole dry.
Coordinate measured with hand-held GPS (WGS84)
Elevation inferred from 5m contours (GIS)

PROJECT:

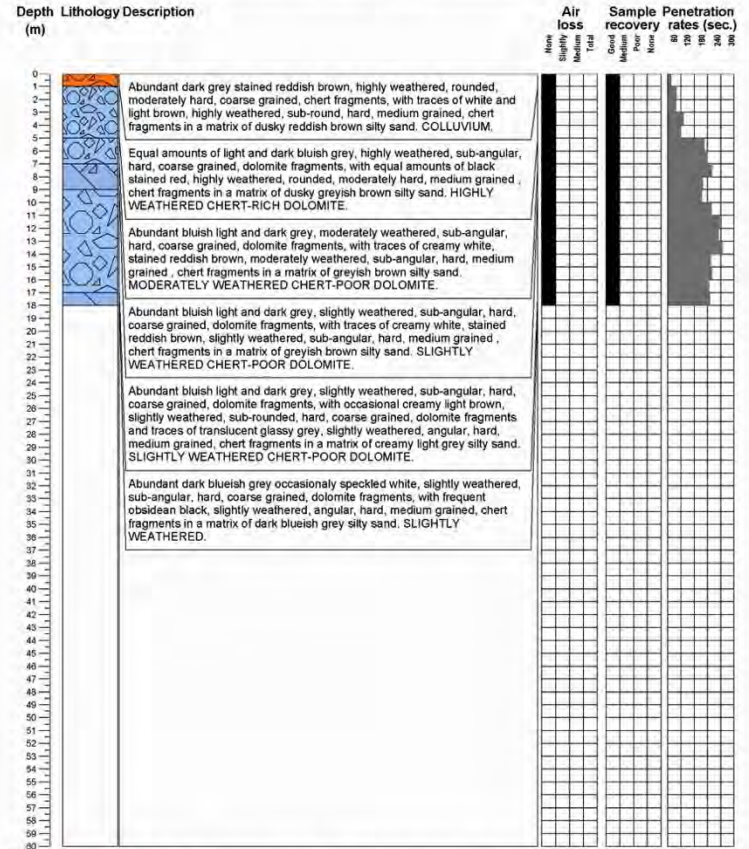
CLIENT:	LATITUDE:	BOREHOLE NO.:	KBH07		
CONTRACTOR:	Hennie Erwee Drilling	LONGITUDE:	DATE DRILLED:	2013/10/04	
MACHINE TYPE:	Super Rock 165mm / 1900kpa	ELEVATION:	1326 mamsl	DATE LOGGED:	2013/10/04
COMPRESSOR:	19 bar	ORIENTATION:	Vertical	LOGGED BY:	WM & EH



Notes: Drilling stopped at 25 mbl
 No water was added during drilling.
 Irregular hammer rates at: 5-6, 6-7, 7-8, 8-9, 9-10, 10-11, 13-14, 14-15, 16-17 m.
 Borehole dry.
 Coordinate measured with hand-held GPS (WGS84)
 Elevation inferred from 5m contours (GIS)

PROJECT:

CLIENT:	LATITUDE:	BOREHOLE NO.:	KBH08		
CONTRACTOR:	Hennie Erwee Drilling	LONGITUDE:	DATE DRILLED:	2013/10/04	
MACHINE TYPE:	Super Rock 165mm / 1900kpa	ELEVATION:	1326 mamsl	DATE LOGGED:	2013/10/04
COMPRESSOR:	19 bar	ORIENTATION:	Vertical	LOGGED BY:	WM & EH

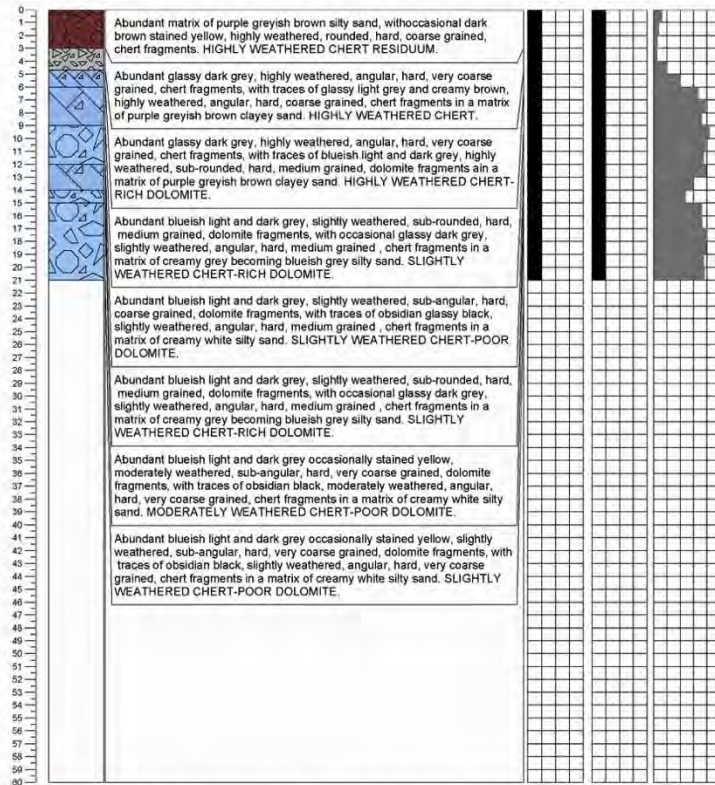


Notes: Drilling stopped at 18 mbl
 No water was added during drilling.
 Irregular hammer rates at: 0-1, 3-4, 4-5, 5-6, 6-7, 8-9, 9-10 m.
 Borehole dry.
 Coordinate measured with hand-held GPS (WGS84)
 Elevation inferred from 5m contours (GIS)

PROJECT:

CLIENT:	LATITUDE:	BOREHOLE NO.:
CONTRACTOR: Hennie Erwee Drilling	LONGITUDE:	DATE DRILLED: 2013/10/04
MACHINE TYPE: Super Rock 165mm / 1900kpa	ELEVATION: 1326 mamsl	DATE LOGGED: 2013/10/04
COMPRESSOR: 19 bar	ORIENTATION: Vertical	LOGGED BY: WM & EH

Depth Lithology Description
(m)

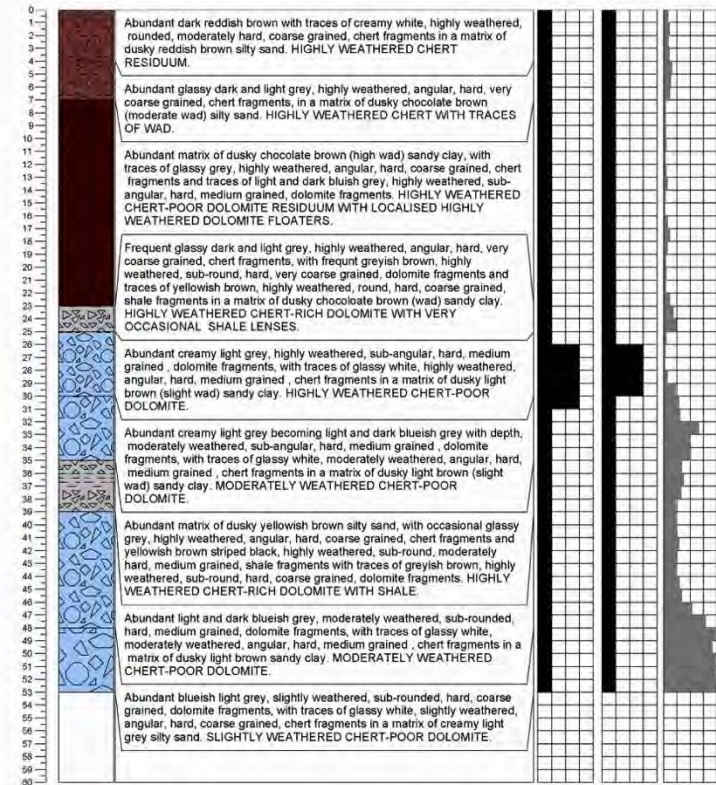


Notes: Drilling stopped at 21 magl
 No water was added during drilling.
 Irregular hammer rates at: 0-1, 2-3, 3-4, 4-5, 5-6, 13-14, 14-15 m.
 Borehole dry.
 Coordinate measured with hand-held GPS (WGS84)
 Elevation inferred from 5m contours (GIS)

PROJECT:

CLIENT:	LATITUDE:	BOREHOLE NO.:
CONTRACTOR: Hennie Erwee Drilling	LONGITUDE:	DATE DRILLED: 2013/10/04
MACHINE TYPE: Super Rock 165mm / 1900kpa	ELEVATION: 1324 mamsl	DATE LOGGED: 2013/10/04
COMPRESSOR: 19 bar	ORIENTATION: Vertical	LOGGED BY: WM & EH

Depth Lithology Description
(m)

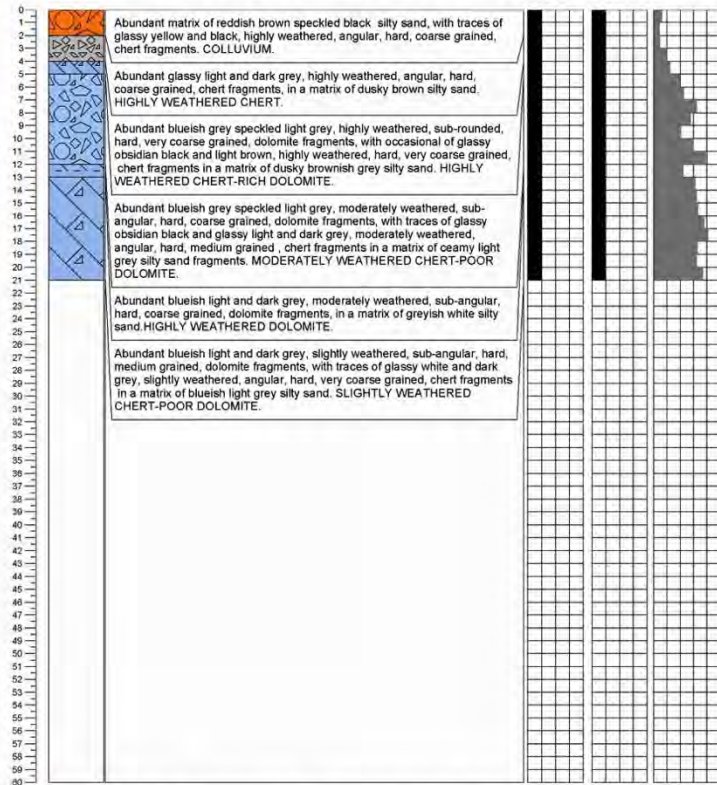


Notes: Drilling stopped at 53 magl
 Water was added at: 2-4, 4-8, 8-10, 11-14, 15-20, 23-24, 26-28, 28-33 m.
 Irregular hammer rates at: 0-2, 7-13, 14-15, 19-22, 25-30, 32-33, 38-39, 46-47m.
 Borehole dry.
 Coordinate measured with hand-held GPS (WGS84)
 Elevation inferred from 5m contours (GIS)

PROJECT:

CLIENT:	LATITUDE:	BOREHOLE NO.:	KBH11		
CONTRACTOR:	Hennie Erwee Drilling	LONGITUDE:	DATE DRILLED:	2013/10/04	
MACHINE TYPE:	Super Rock 165mm / 1900kpa	ELEVATION:	1323 mamsl	DATE LOGGED:	2013/10/04
COMPRESSOR:	19 bar	ORIENTATION:	Vertical	LOGGED BY:	WM & EH

Depth Lithology Description (m)

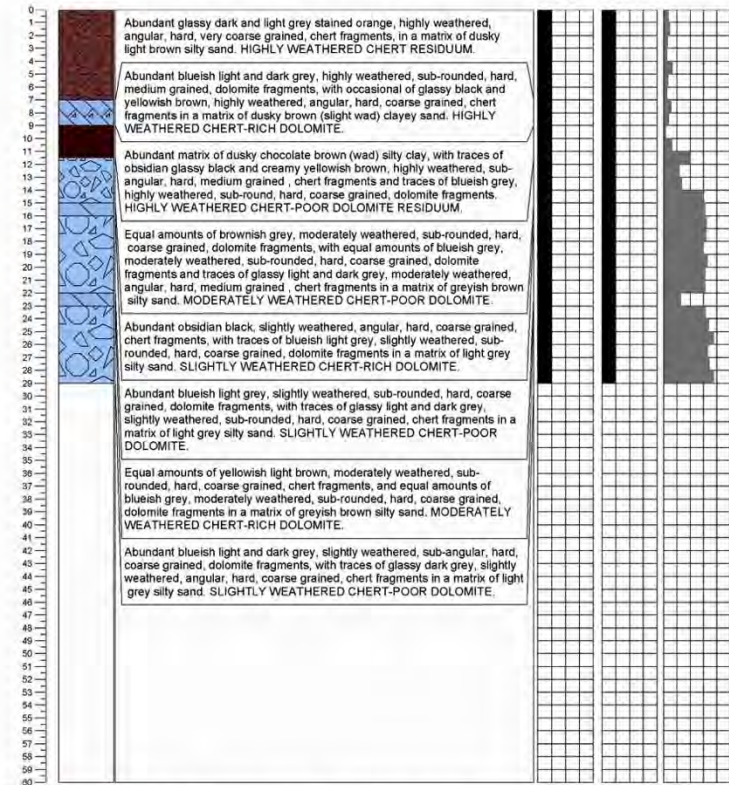


Notes: Drilling stopped at 15 mbl
 No water was added during drilling.
 Irregular hammer rates at: 0-1, 3-4, 5-6, 6-7, 8-9, 9-10, 12-13 m.
 Borehole dry.
 Coordinate measured with hand-held GPS (WGS84)
 Elevation inferred from 5m contours (GIS)

PROJECT:

CLIENT:	LATITUDE:	BOREHOLE NO.:	KBH12		
CONTRACTOR:	Hennie Erwee Drilling	LONGITUDE:	DATE DRILLED:	2013/10/04	
MACHINE TYPE:	Super Rock 165mm / 1900kpa	ELEVATION:	1322 mamsl	DATE LOGGED:	2013/10/04
COMPRESSOR:	19 bar	ORIENTATION:	Vertical	LOGGED BY:	WM & EH

Depth Lithology Description (m)



Notes: Drilling stopped at 29 mbl
 Water was added at: 6-7, 8-9, 9-10 m.
 Irregular hammer rates at: 0-1, 2-3, 8-9, 9-10, 11-12, 12-13, 14-15, 22-23 m.
 Borehole dry.
 Coordinate measured with hand-held GPS (WGS84)
 Elevation inferred from 5m contours (GIS)

PROJECT:

CLIENT:	LATITUDE:	BOREHOLE NO.:	KBH13		
CONTRACTOR:	Hennie Erwee Drilling	LONGITUDE:	DATE DRILLED:	2013/10/04	
MACHINE TYPE:	Super Rock 165mm / 1900kpa	ELEVATION:	1322 mamsl	DATE LOGGED:	2013/10/04
COMPRESSOR:	19 bar	ORIENTATION:	Vertical	LOGGED BY:	WM & EH

Depth Lithology Description (m)

Depth (m)	Lithology Description	Air loss				Sample recovery rates (sec.)			
		None	Slightly	Medium	Total	Good	Poor	None	Total
0									
1									
2	Abundant creamy orange brown and dark reddish brown, highly weathered, sub-angular, hard, very coarse grained, chert fragments, in a matrix of dusky reddish brown silty sand. HIGHLY WEATHERED CHERT RESIDUUM.								
3									
4									
5	Equal amounts of blueish light and dark grey, sub-rounded, hard, coarse grained, dolomite fragments, with equal amounts of creamy light brown and yellowish brown, highly weathered, sub-angular, hard, coarse grained, chert fragments in a matrix of dusky brown silty sand. HIGHLY WEATHERED CHERT-RICH DOLOMITE.								
6									
7									
8									
9									
10									
11	Abundant blueish light and dark grey, highly weathered, sub-angular, hard, coarse grained, dolomite fragments, with occasional purple grey, highly weathered, sub-rounded, moderately hard, medium grained, shale fragments and traces of glassy black, highly weathered, sub-angular, hard, medium grained, chert fragments in a matrix of greyish brown silty sand. HIGHLY WEATHERED CHERT-POOR DOLOMITE WITH SHALE.								
12									
13									
14									
15									
16									
17									
18									
19	Abundant blueish light and dark grey, moderately weathered, sub-angular, hard, coarse grained, dolomite fragments, with occasional purple grey, moderately weathered, sub-rounded, moderately hard, medium grained, shale fragments and traces of glassy black, moderately weathered, sub-angular, hard, medium grained, chert fragments in a matrix of greyish brown silty sand. MODERATELY WEATHERED CHERT-POOR DOLOMITE WITH SHALE.								
20									
21									
22									
23									
24									
25									
26									
27	Abundant blueish light and dark grey, moderately weathered, sub-angular, hard, medium grained, dolomite fragments, with traces of creamy white stained reddish brown and glassy light grey, moderately weathered, sub-angular, hard, medium grained, chert fragments in a matrix of creamy light grey silty sand. MODERATELY WEATHERED CHERT-POOR DOLOMITE WITH LOCALISED HARDERCHERTBANDS.								
28									
29									
30									
31									
32									
33									
34	Abundant blueish light and dark grey, slightly weathered, sub-angular, hard, medium grained, dolomite fragments, with traces of creamy white stained reddish brown and glassy light grey, slightly weathered, sub-angular, hard, medium grained, chert fragments in a matrix of creamy light grey silty sand. SLIGHTLY WEATHERED CHERT-POOR DOLOMITE WITH LOCALISED HARDERCHERTBANDS.								
35									
36									
37									
38									
39									
40									
41									
42									
43									
44									
45									
46									
47									
48									
49									
50									
51									
52									
53									
54									
55									
56									
57									
58									
59									
60									

Notes: Drilling stopped at 19 mbgl
 Water was added at: 2-3 m.
 Irregular hammer rates at: 3-4, 6-7, 10-11 m.
 Borehole dry.
 Coordinate measured with hand-held GPS (WGS84)
 Elevation inferred from 5m contours (GIS)

PROJECT:

CLIENT:	LATITUDE:	BOREHOLE NO.:	KBH14		
CONTRACTOR:	Hennie Erwee Drilling	LONGITUDE:	DATE DRILLED:	2013/10/04	
MACHINE TYPE:	Super Rock 165mm / 1900kpa	ELEVATION:	1322 mamsl	DATE LOGGED:	2013/10/04
COMPRESSOR:	19 bar	ORIENTATION:	Vertical	LOGGED BY:	WM & EH

Depth Lithology Description (m)

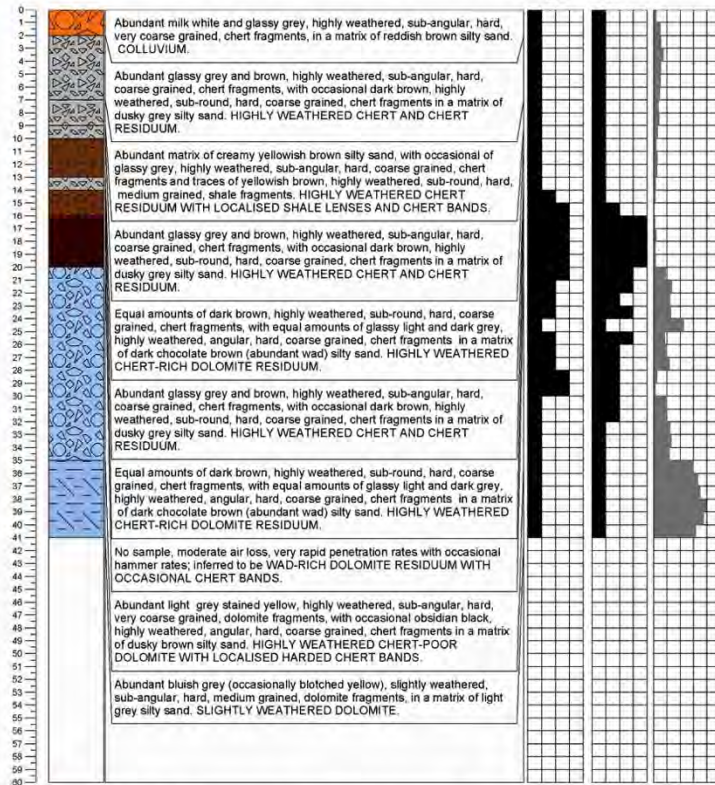
Depth (m)	Lithology Description	Air loss				Sample recovery rates (sec.)			
		None	Slightly	Medium	Total	Good	Poor	None	Total
0									
1									
2	Frequent glassy dark grey and white, highly weathered, angular, hard, very coarse grained, chert fragments, in a matrix of of dusky brown silty sand. HIGHLY WEATHERED CHERT RESIDUUM.								
3									
4	Abundant light and dark blueish grey and brownish grey, moderately weathered, sub-angular, hard, very coarse grained, dolomite fragments, with occasional glassy light grey, moderately weathered, angular, hard, very coarse grained, chert fragments in a matrix of greyish brown silty sand. MODERATELY WEATHERED CHERT-RICH DOLOMITE.								
5									
6									
7									
8									
9									
10									
11	Abundant light blueish grey, slightly weathered, sub-angular, hard, medium grained, dolomite fragments, with frequent glassy black, slightly weathered, angular, hard, coarse grained, chert fragments in a matrix of light grey silty sand. SLIGHTLY WEATHERED CHERT-RICH DOLOMITE.								
12									
13									
14									
15									
16									
17									
18	Abundant glassy dark grey and black, moderately weathered, angular, hard, coarse grained, chert fragments, with occasional light blueish grey, moderately weathered, sub-angular, hard, medium grained, dolomite fragments, and occasional creamy light brown, moderately weathered, sub-rounded, soft, medium grained, shale fragments in a matrix of grey silty sand. MODERATELY WEATHERED CHERT-RICH DOLOMITE WITH SHALE.								
19									
20									
21									
22									
23									
24									
25									
26									
27	Abundant light blueish grey, slightly weathered, sub-round, hard, medium grained, dolomite fragments, with occasional glassy light and dark grey, slightly weathered, angular, hard, coarse grained, chert fragments in a matrix of light grey silty sand. SLIGHTLY WEATHERED CHERT-RICH DOLOMITE.								
28									
29									
30									
31									
32	Abundant greyish light brown, moderately weathered, sub-rounded, hard, coarse grained, dolomite fragments, with occasional black stained grey, moderately weathered, sub-round, hard, very coarse grained, shale fragments and traces of glassy black, moderately weathered, angular, hard, medium grained, chert fragments in a matrix of creamy light brown silty sand. MODERATELY WEATHERED CHERT-POOR DOLOMITE WITH SHALE.								
33									
34									
35									
36									
37									
38									
39									
40									
41	Abundant blueish light and dark grey, slightly weathered, sub-angular, hard, coarse grained, dolomite fragments, with traces of glassy dark grey, slightly weathered, angular, hard, coarse grained, chert fragments. SLIGHTLY WEATHERED CHERT-POOR DOLOMITE.								
42									
43									
44									
45									
46									
47									
48									
49									
50									
51									
52									
53									
54									
55									
56									
57									
58									
59									
60									

Notes: Drilling stopped at 19 mbgl
 Water was added at: 17-18 m.
 Irregular hammer rates at: 3-4, 4-5, 5-6, 9-10, 15-16 m.
 Borehole dry.
 Coordinate measured with hand-held GPS (WGS84)
 Elevation inferred from 5m contours (GIS)

PROJECT:

CLIENT:	LATITUDE:	BOREHOLE NO.:
CONTRACTOR: Hennie Erwee Drilling	LONGITUDE:	DATE DRILLED: 2013/10/04
MACHINE TYPE: Super Rock 165mm / 1900kpa	ELEVATION: 1324 mamsl	DATE LOGGED: 2013/10/04
COMPRESSOR: 19 bar	ORIENTATION: Vertical	LOGGED BY: WM & EH

Depth Lithology Description
(m)

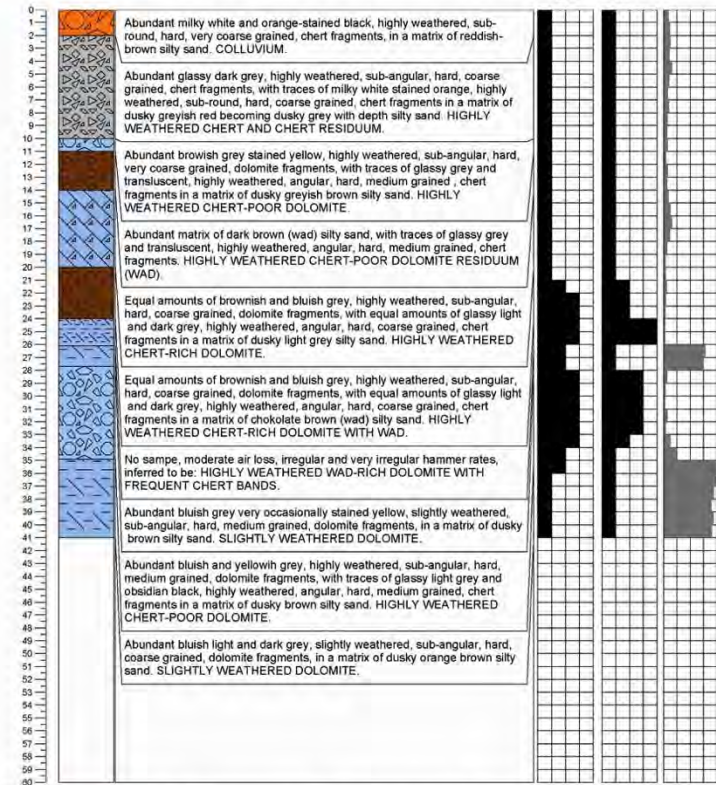


Notes: Drilling stopped at 41 mbl
Water added at: 17-26 m.
Irregular hammer rates at: 0-1, 6-7, 10-21, 25-27, 29-30 m.
Borehole dry.
Coordinate measured with hand-held GPS (WGS84)
Elevation inferred from 5m contours (GIS)

PROJECT:

CLIENT:	LATITUDE:	BOREHOLE NO.:
CONTRACTOR: Hennie Erwee Drilling	LONGITUDE:	DATE DRILLED: 2013/04/12
MACHINE TYPE: Super Rock 165mm / 1900kpa	ELEVATION: 1324 mamsl	DATE LOGGED: 2013/04/12
COMPRESSOR: 19 bar	ORIENTATION: Vertical	LOGGED BY: WM & EH

Depth Lithology Description
(m)



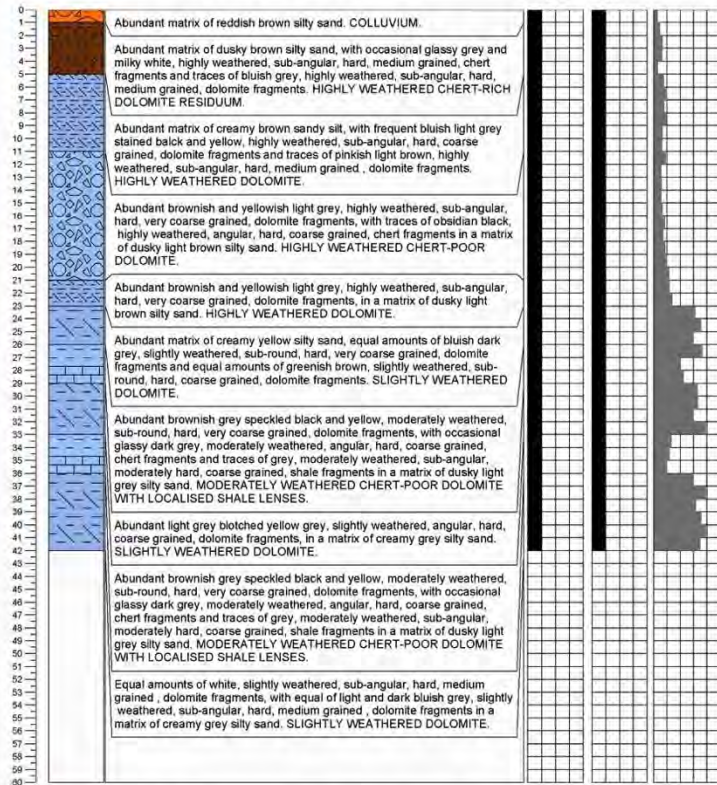
Notes: Drilling stopped at 41 mbl
Water added at: 15-16, 19-26 m.
Irregular hammer rates at: 0-1, 6-7, 9-10, 13-14, 18-33, 34-35 m.
Borehole dry.
Coordinate measured with hand-held GPS (WGS84)
Elevation inferred from 5m contours (GIS)

PROJECT:

CLIENT:	LATITUDE:	BOREHOLE NO.:	KBH19		
CONTRACTOR:	Hennie Erwee Drilling	LONGITUDE:	DATE DRILLED:	2013/04/12	
MACHINE TYPE:	Super Rock 165mm / 1900kpa	ELEVATION:	1322 mamsl	DATE LOGGED:	2013/04/12
COMPRESSOR:	19 bar	ORIENTATION:	Vertical	LOGGED BY:	WM & EH

Depth Lithology Description (m)

Air loss Sample Penetration recovery rates (sec.)



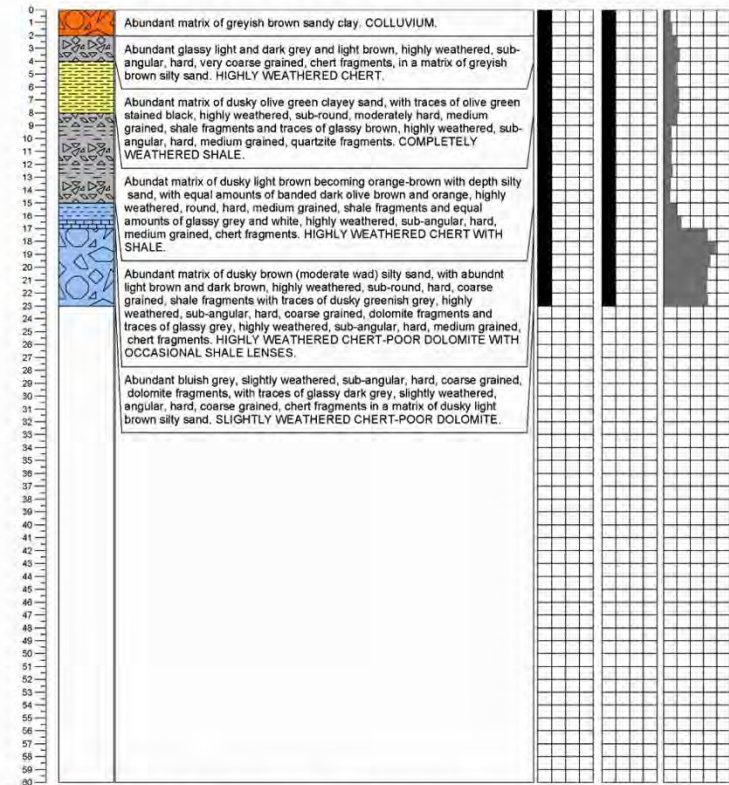
Notes: Drilling stopped at 42 magl
 Water added at: 26-27 m.
 Irregular hammer rates at: 0-1, 19-19, 33-34 m.
 Borehole dry.
 Coordinate measured with hand-held GPS (WGS84)
 Elevation inferred from 5m contours (GIS)

PROJECT:

CLIENT:	LATITUDE:	BOREHOLE NO.:	KBH20		
CONTRACTOR:	Hennie Erwee Drilling	LONGITUDE:	DATE DRILLED:	2013/04/12	
MACHINE TYPE:	Super Rock 165mm / 1900kpa	ELEVATION:	1319 mamsl	DATE LOGGED:	2013/04/12
COMPRESSOR:	19 bar	ORIENTATION:	Vertical	LOGGED BY:	WM & EH

Depth Lithology Description (m)

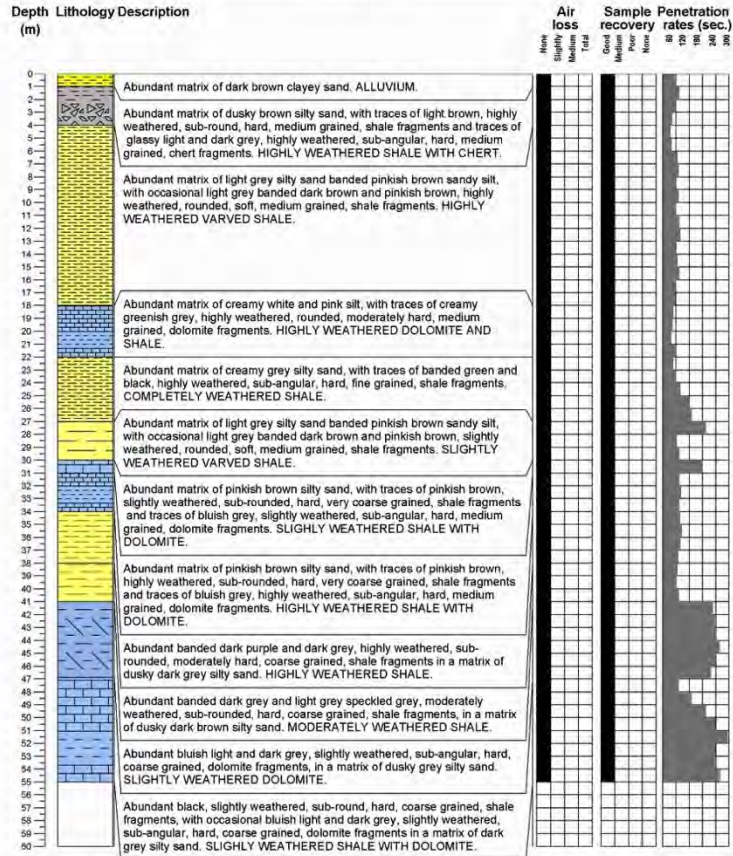
Air loss Sample Penetration recovery rates (sec.)



Notes: Drilling stopped at 23 magl
 Water added at: 26-27 m.
 Irregular hammer rates at: 0-1, 19-19, 33-34 m.
 Borehole dry.
 Coordinate measured with hand-held GPS (WGS84)
 Elevation inferred from 5m contours (GIS)

PROJECT:

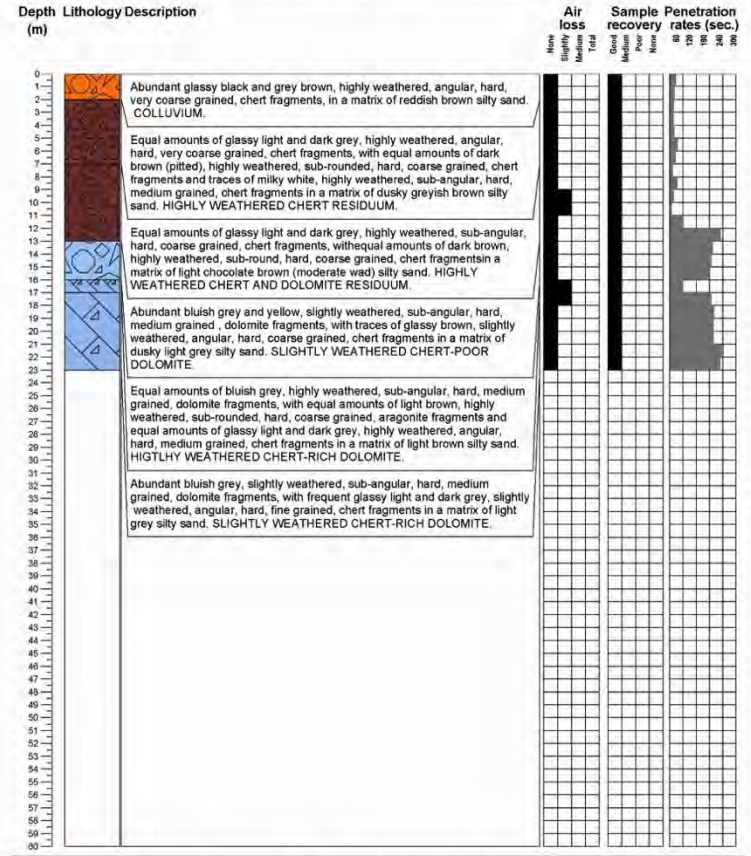
CLIENT:	LATITUDE:	BOREHOLE NO.:	KBH21		
CONTRACTOR:	Hennie Erwee Drilling	LONGITUDE:	DATE DRILLED:	2013/04/15	
MACHINE TYPE:	Super Rock 165mm / 1900kpa	ELEVATION:	1321 mamsl	DATE LOGGED:	2013/04/15
COMPRESSOR:	19 bar	ORIENTATION:	Vertical	LOGGED BY:	WM & EH



Notes: Drilling stopped at 55 mbgl
 No water was added during drilling
 Irregular hammer rates at: 5-7, 23-24, 25-26, 28-29, 30-31, 46-47, 48-49 m.
 Borehole dry.
 Coordinates measured with hand-held GPS (WGS84)
 Elevation inferred from 5m contours (GIS)

PROJECT:

CLIENT:	LATITUDE:	BOREHOLE NO.:	KBH22		
CONTRACTOR:	Hennie Erwee Drilling	LONGITUDE:	DATE DRILLED:	2013/04/15	
MACHINE TYPE:	Super Rock 165mm / 1900kpa	ELEVATION:	1326 mamsl	DATE LOGGED:	2013/04/15
COMPRESSOR:	19 bar	ORIENTATION:	Vertical	LOGGED BY:	WM & EH

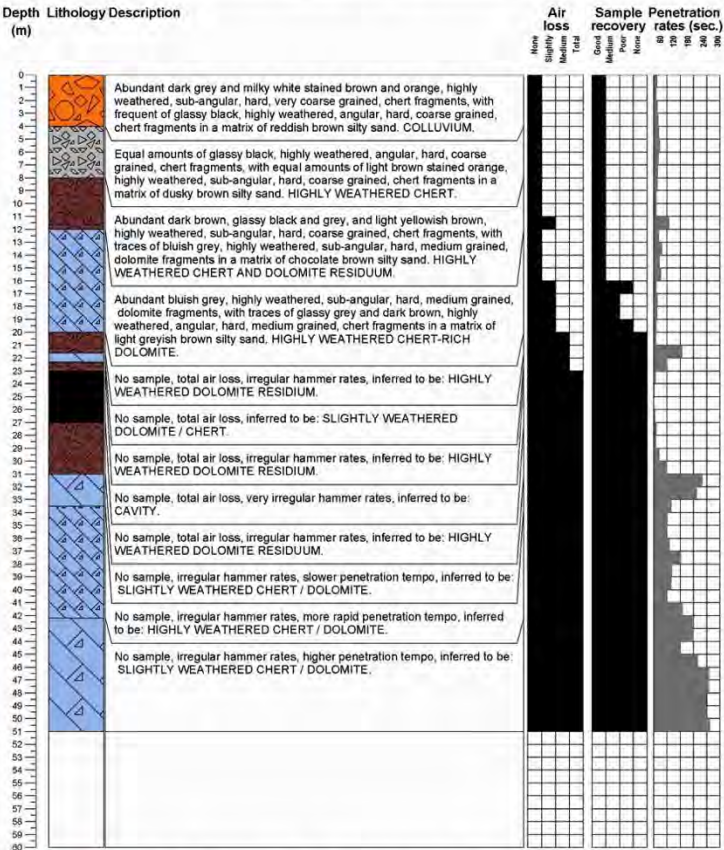


Notes: Drilling stopped at 23 mbgl
 Water added at: 5-8, 19-20, 20-21 m.
 Irregular hammer rates at: 0-3, 7-8, 9-10, 10-11, 11-12 m.
 Borehole dry.
 Coordinates measured with hand-held GPS (WGS84)
 Elevation inferred from 5m contours (GIS)

PROJECT:

CLIENT:	LATITUDE:	BOREHOLE NO.:	KBH23		
CONTRACTOR:	Hennie Erwee Drilling	LONGITUDE:	DATE DRILLED:	2013/04/15	
MACHINE TYPE:	Super Rock 165mm / 1900kpa	ELEVATION:	1326 mamsl	DATE LOGGED:	2013/04/15
COMPRESSOR:	19 bar	ORIENTATION:	Vertical	LOGGED BY:	WM & EH

Depth Lithology Description (m)

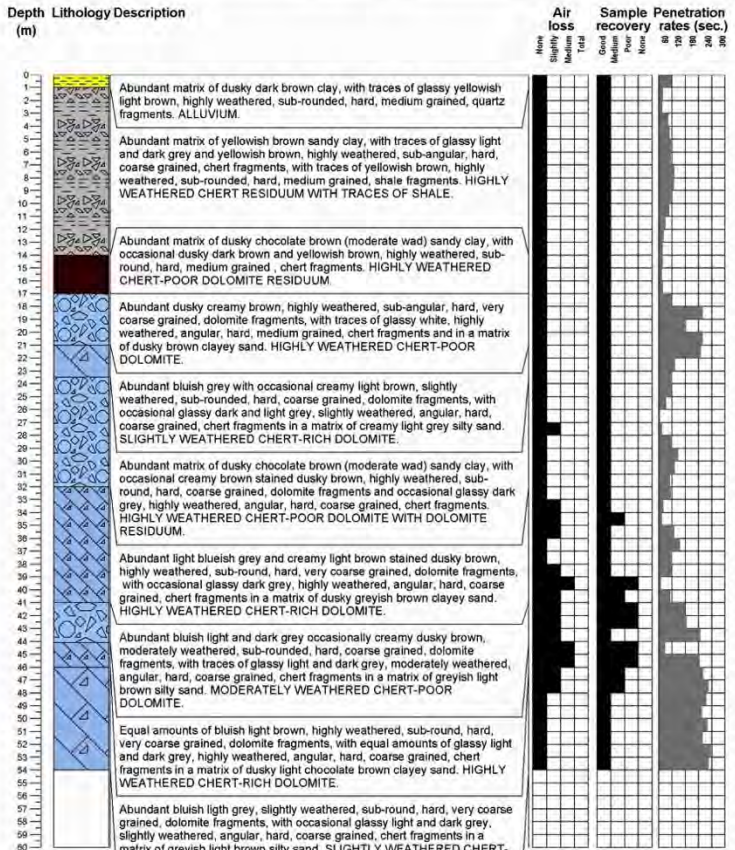


Notes: Drilling stopped at 51 mbgl
 Water was added at: 7-9, 10-12, 16-26, 27-36, 37-51 m.
 Irregular hammer rates at: 0-2, 7-8, 9-12, 17-25, 26-31, 33-34, 42-43, 44-45 m.
 Borehole dry.
 Coordinate measured with hand-held GPS (WGS84)
 Elevation inferred from 5m contours (GIS)

PROJECT:

CLIENT:	LATITUDE:	BOREHOLE NO.:	KBH24		
CONTRACTOR:	Hennie Erwee Drilling	LONGITUDE:	DATE DRILLED:	2013/04/15	
MACHINE TYPE:	Super Rock 165mm / 1900kpa	ELEVATION:	1324 mamsl	DATE LOGGED:	2013/04/15
COMPRESSOR:	19 bar	ORIENTATION:	Vertical	LOGGED BY:	WM & EH

Depth Lithology Description (m)

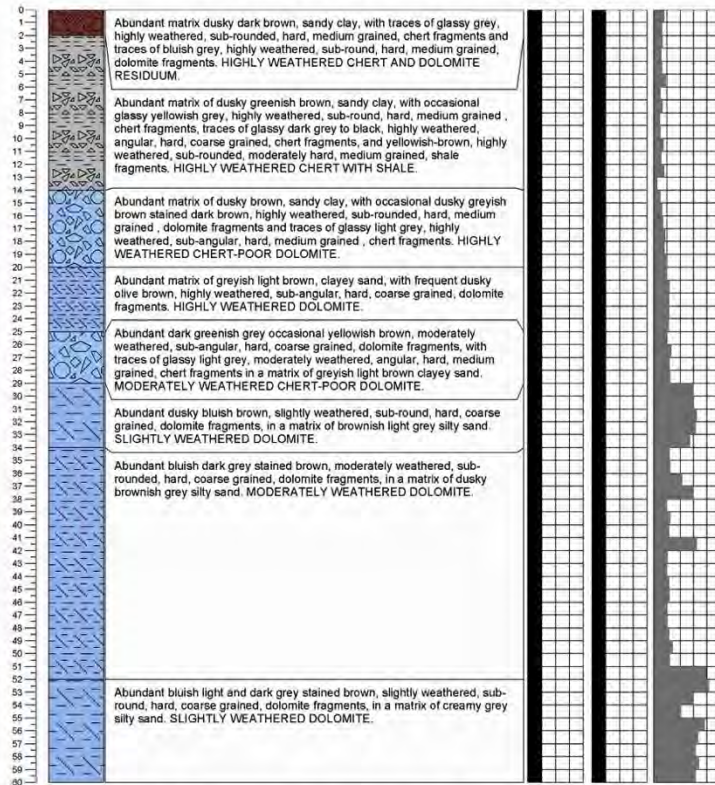


Notes: Drilling stopped at 51 mbgl
 Water was added at: 0-2, 3-4, 21-24, 26-28, 32-33, 34-37, 38-39, 40-45, 46-49 m.
 Irregular hammer rates at: 0-3, 14-18, 19-20, 22-23, 25-29, 33-36, 37-40, 41-43, 44-45 m.
 Borehole dry.
 Coordinate measured with hand-held GPS (WGS84)
 Elevation inferred from 5m contours (GIS)

PROJECT:

CLIENT:	LATITUDE:	BOREHOLE NO.:
CONTRACTOR: Hennie Erwee Drilling	LONGITUDE:	DATE DRILLED: 2013/04/17
MACHINE TYPE: Super Rock 165mm / 1900kpa	ELEVATION: 1324 mamsl	DATE LOGGED: 2013/04/17
COMPRESSOR: 19 bar	ORIENTATION: Vertical	LOGGED BY: WM & EH

Depth Lithology Description
(m)

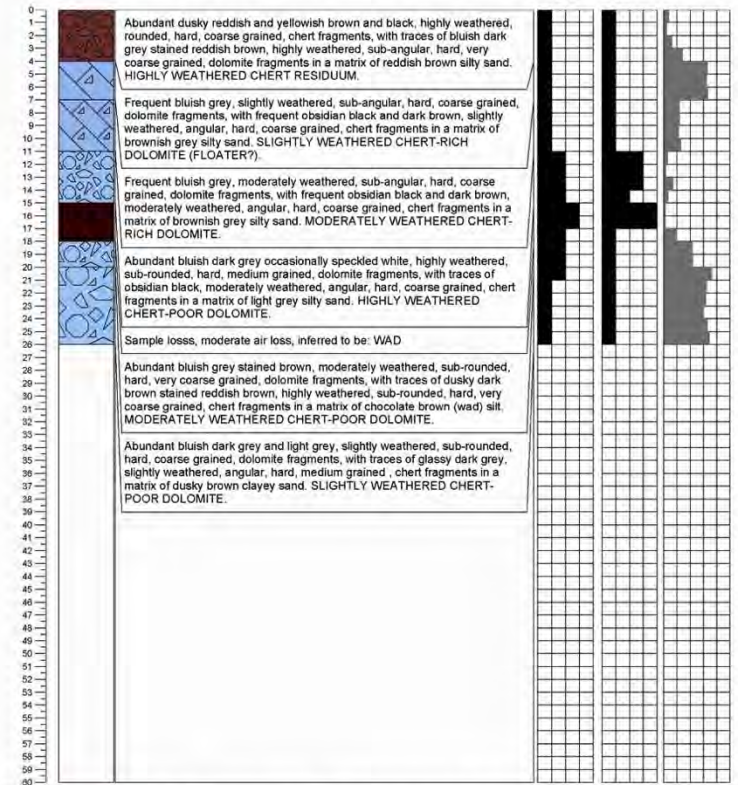


Notes: Drilling stopped at 61 mbl
 Water was added at: 33-35, 57-58 m.
 Irregular hammer rates at: 0-1, 13-14, 25-27, 29-30, 33-34, 36-37, 42-43, 55-56 m.
 Borehole dry.
 Coordinate measured with hand-held GPS (WGS84)
 Elevation inferred from 5m contours (GIS)

PROJECT:

CLIENT:	LATITUDE:	BOREHOLE NO.:
CONTRACTOR: Hennie Erwee Drilling	LONGITUDE:	DATE DRILLED: 2013/04/17
MACHINE TYPE: Super Rock 165mm / 1900kpa	ELEVATION: 1326 mamsl	DATE LOGGED: 2013/04/17
COMPRESSOR: 19 bar	ORIENTATION: Vertical	LOGGED BY: WM & EH

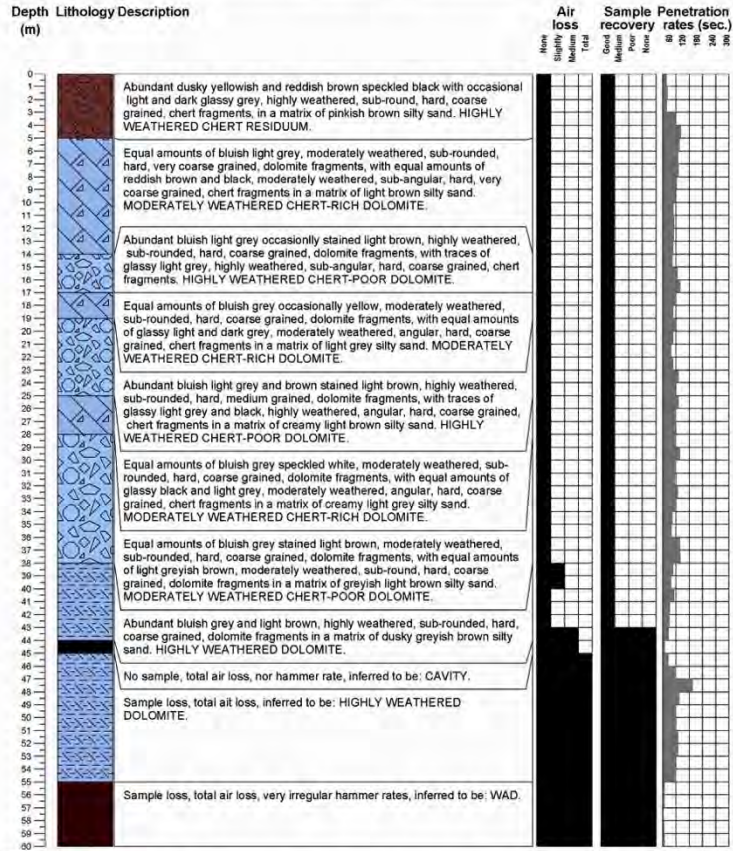
Depth Lithology Description
(m)



Notes: Drilling stopped at 26 mbl
 Water added at: 0-3, 13-20 m.
 Irregular hammer rates at: 0-2, 3-4, 7-9, 11-18 m.
 Borehole dry.
 Coordinate measured with hand-held GPS (WGS84)
 Elevation inferred from 5m contours (GIS)

PROJECT:

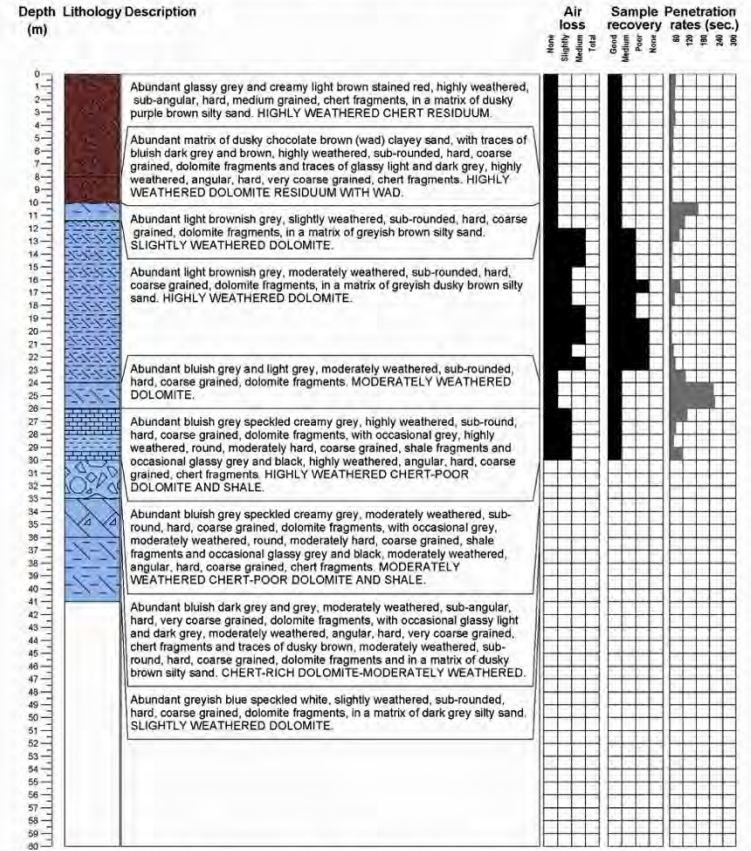
CLIENT:	LATITUDE:	BOREHOLE NO.:	KBH28		
CONTRACTOR:	Hennie Erwee Drilling	LONGITUDE:	DATE DRILLED:	2013/04/17	
MACHINE TYPE:	Super Rock 165mm / 1900kpa	ELEVATION:	1326 mamsl	DATE LOGGED:	2013/04/17
COMPRESSOR:	19 bar	ORIENTATION:	Vertical	LOGGED BY:	WM & EH



Notes: Drilling stopped at 60 mbl
 Water added at: 23-24, 33-35, 37-41, 42-51, 52-55 m.
 Irregular hammer rates at: 0-1, 3-4, 19-19, 31-32, 33-36, 38-40, 43-49, 54-60 m.
 Borehole dry.
 Coordinate measured with hand-held GPS (WGS84)
 Elevation inferred from 5m contours (GIS)

PROJECT:

CLIENT:	LATITUDE:	BOREHOLE NO.:	KBH29		
CONTRACTOR:	Hennie Erwee Drilling	LONGITUDE:	DATE DRILLED:	2013/04/18	
MACHINE TYPE:	Super Rock 165mm / 1900kpa	ELEVATION:	1324 mamsl	DATE LOGGED:	2013/04/18
COMPRESSOR:	19 bar	ORIENTATION:	Vertical	LOGGED BY:	WM & EH

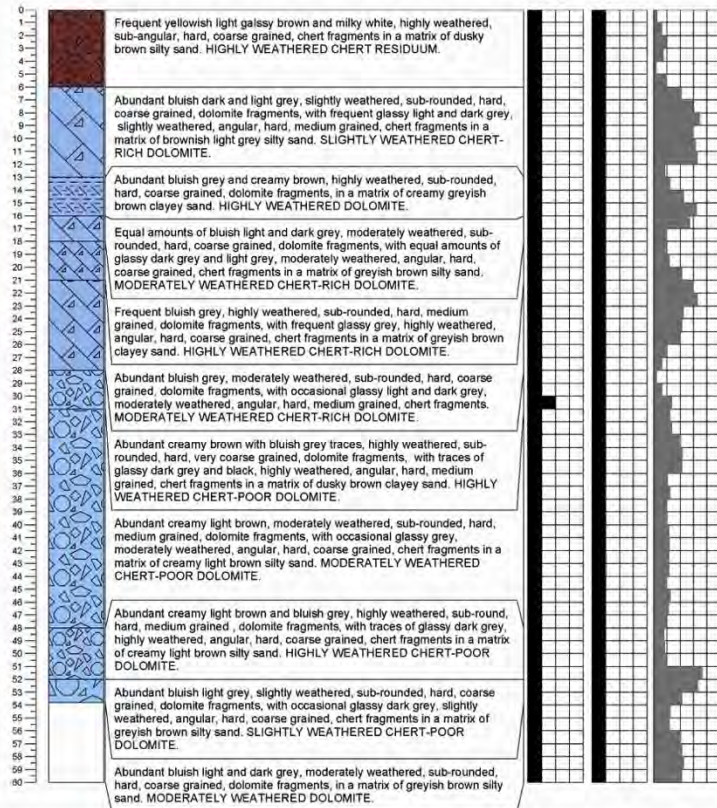


Notes: Drilling stopped at 41 mbl
 Water added at: 12-15, 16-18, 20-23 m.
 0-1, 4-6, 9-16, 17-22, 26-30 m.
 Borehole dry.
 Coordinate measured with hand-held GPS (WGS84)
 Elevation inferred from 5m contours (GIS)

PROJECT:

CLIENT:	LATITUDE:	BOREHOLE NO.:	KBH30		
CONTRACTOR:	Hennie Erwee Drilling	LONGITUDE:	DATE DRILLED:	2013/04/23	
MACHINE TYPE:	Super Rock 165mm / 1900kpa	ELEVATION:	1322 mamsl	DATE LOGGED:	2013/04/23
COMPRESSOR:	19 bar	ORIENTATION:	Vertical	LOGGED BY:	WM & EH

Depth Lithology Description
(m)

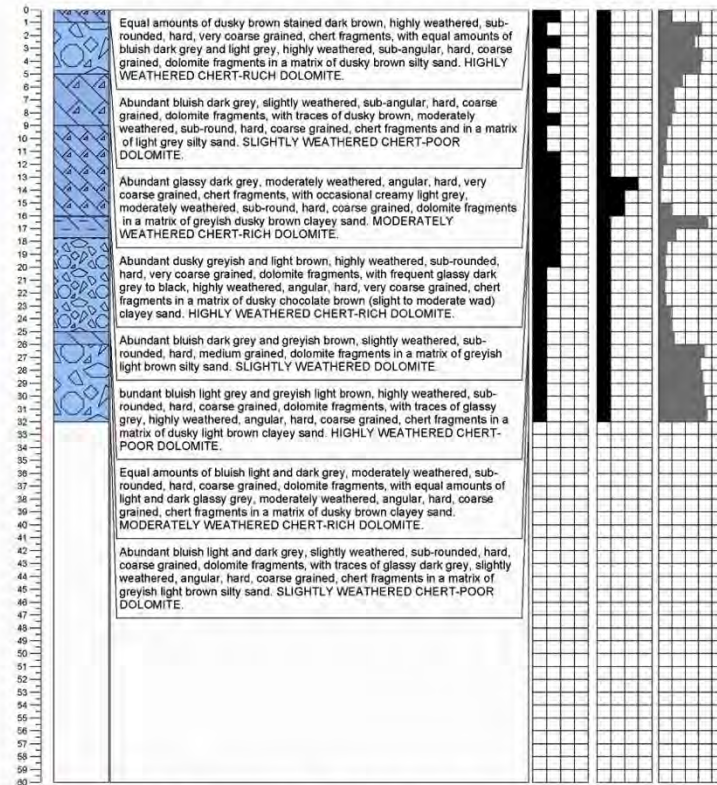


Notes: Drilling stopped at 60 mbgl
Water added at: 4-6, 8-10, 14-18, 20-21, 25-27, 28-32, 39-40, 41-44, 50-53, 55-56, 57-60 m.
Irregular hammer rates at: 0-1, 4-6, 7-8, 12-21, 23-24, 26-27, 28-29, 30-31, 33-34, 47-48, 53-54 m.
Borehole dry.
Coordinate measured with hand-held GPS (WGS84)
Elevation inferred from 5m contours (GIS)

PROJECT:

CLIENT:	LATITUDE:	BOREHOLE NO.:	KBH31		
CONTRACTOR:	Hennie Erwee Drilling	LONGITUDE:	DATE DRILLED:	2013/04/23	
MACHINE TYPE:	Super Rock 165mm / 1900kpa	ELEVATION:	1323 mamsl	DATE LOGGED:	2013/04/23
COMPRESSOR:	19 bar	ORIENTATION:	Vertical	LOGGED BY:	WM & EH

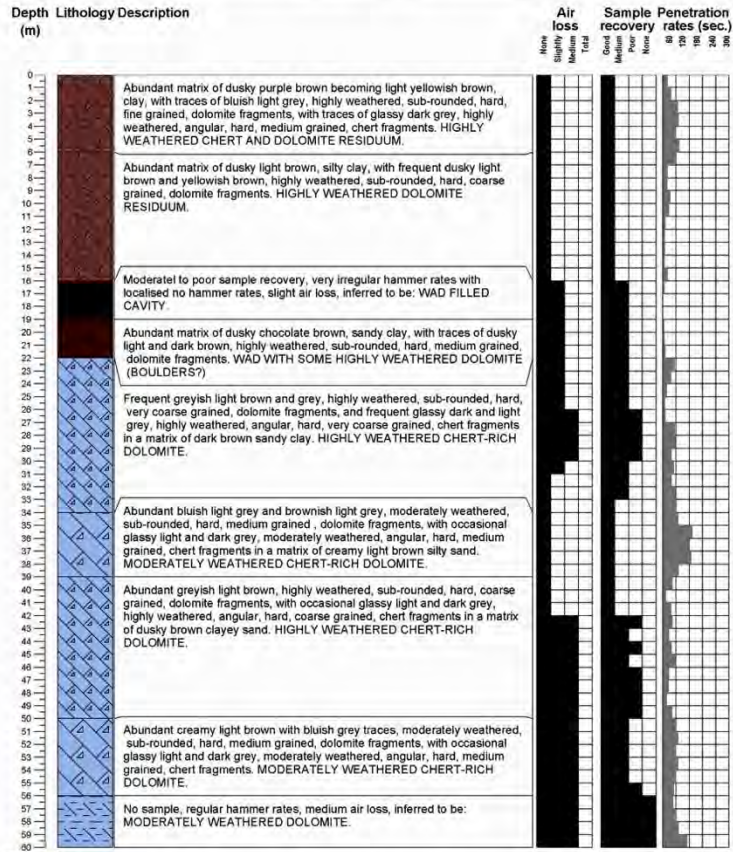
Depth Lithology Description
(m)



Notes: Drilling stopped at 32 mbgl
Water added at: 2-5, 14-16, 18-20, 21-25 m.
0-1, 2-3, 5-6, 9-8, 11-20 m.
Borehole dry.
Coordinate measured with hand-held GPS (WGS84)
Elevation inferred from 5m contours (GIS)

PROJECT:

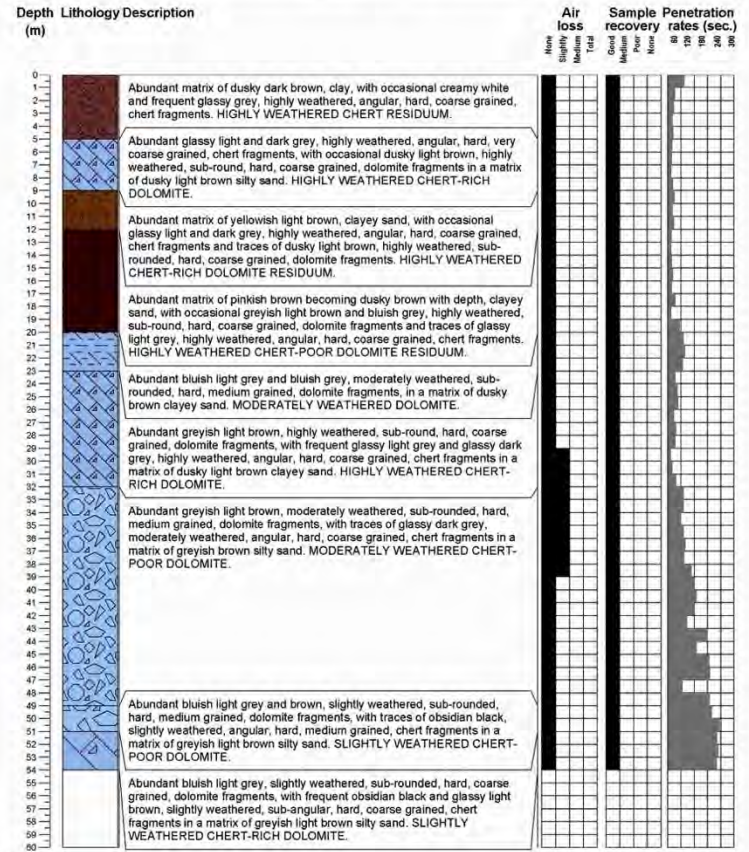
CLIENT:	LATITUDE:	BOREHOLE NO.:
CONTRACTOR: Hennie Erwe Drilling	LONGITUDE:	DATE DRILLED: 2013/04/23
MACHINE TYPE: Super Rock 165mm / 1900kpa	ELEVATION: 1323 mamsl	DATE LOGGED: 2013/04/23
COMPRESSOR: 19 bar	ORIENTATION: Vertical	LOGGED BY: WM & EH



Notes: Drilling stopped at 60 mbl
 Water added at: 10-11, 13-15, 17-18, 19-21, 22-24, 25-27, 30-31, 43-50, 51-60 m.
 Irregular hammer rates at: 0-1, 6-7, 11-15, 18-17, 19-27, 32-33, 35-36, 39-41, 43-44, 46-48, 54-56 m.
 Borehole dry.
 Coordinate measured with hand-held GPS (WGS84)
 Elevation inferred from 5m contours (GIS)

PROJECT:

CLIENT:	LATITUDE:	BOREHOLE NO.:
CONTRACTOR: Hennie Erwe Drilling	LONGITUDE:	DATE DRILLED: 2013/04/29
MACHINE TYPE: Super Rock 165mm / 1900kpa	ELEVATION: 1321 mamsl	DATE LOGGED: 2013/04/29
COMPRESSOR: 19 bar	ORIENTATION: Vertical	LOGGED BY: WM & EH

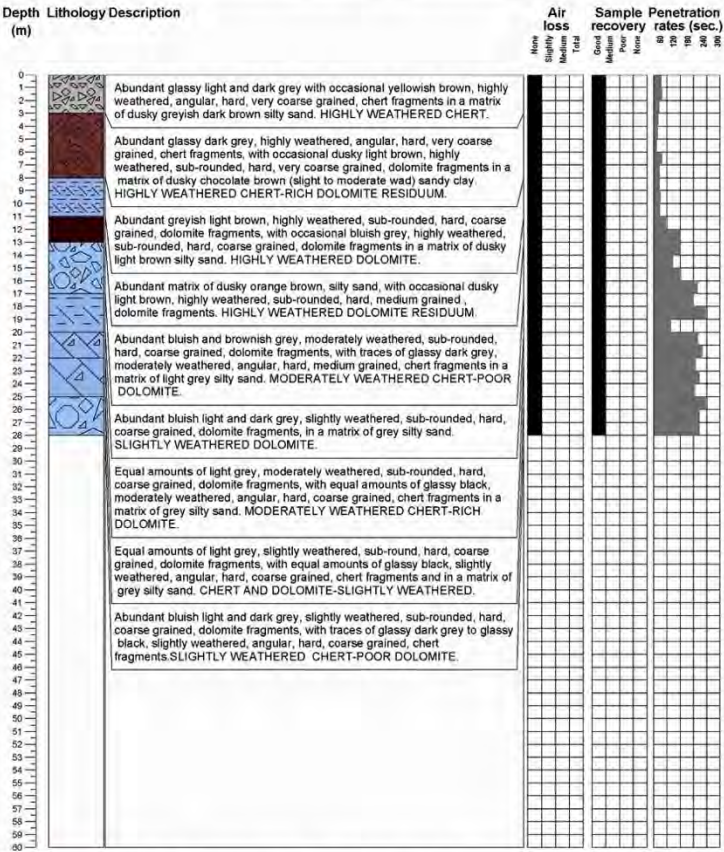


Notes: Drilling stopped at 54 mbl
 Water added at: 7-11, 15-18, 27-28, 29-30, 31-32, 35-37, 38-39, 43-46, 47-48, 49-54 m.
 Irregular hammer rates at: 5-6, 19-20, 23-24, 29-31, 38-39, 42-43, 45-46, 47-48 m.
 Borehole dry.
 Coordinate measured with hand-held GPS (WGS84)
 Elevation inferred from 5m contours (GIS)

PROJECT:

CLIENT:	LATITUDE:	BOREHOLE NO.:	KBH34
CONTRACTOR: Hennie Erwee Drilling	LONGITUDE:	DATE DRILLED:	2013/04/29
MACHINE TYPE: Super Rock 165mm / 1900kpa	ELEVATION: 1320 mamsl	DATE LOGGED:	2013/04/29
COMPRESSOR: 19 bar	ORIENTATION: Vertical	LOGGED BY:	WM & EH

Depth Lithology Description (m)

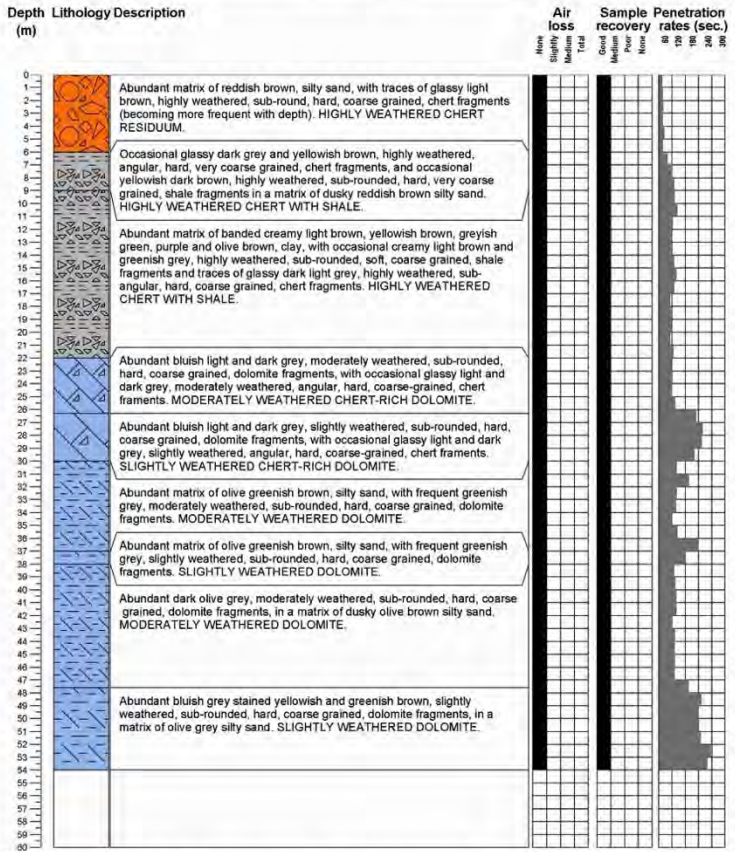


Notes: Drilling stopped at 28 mbl
 Water added at: 3-4, 5-7, 9-11, 13-15, 17-19, 20-22, 23-24 m.
 Irregular hammer rates at: 0-1, 4-6, 12-13, 15-16, 20-22 m.
 Borehole dry.
 Coordinate measured with hand-held GPS (WGS84)
 Elevation inferred from 5m contours (GIS)

PROJECT:

CLIENT:	LATITUDE:	BOREHOLE NO.:	KBH35
CONTRACTOR: Hennie Erwee Drilling	LONGITUDE:	DATE DRILLED:	2013/04/29
MACHINE TYPE: Super Rock 165mm / 1900kpa	ELEVATION: 1322 mamsl	DATE LOGGED:	2013/04/29
COMPRESSOR: 19 bar	ORIENTATION: Vertical	LOGGED BY:	WM & EH

Depth Lithology Description (m)

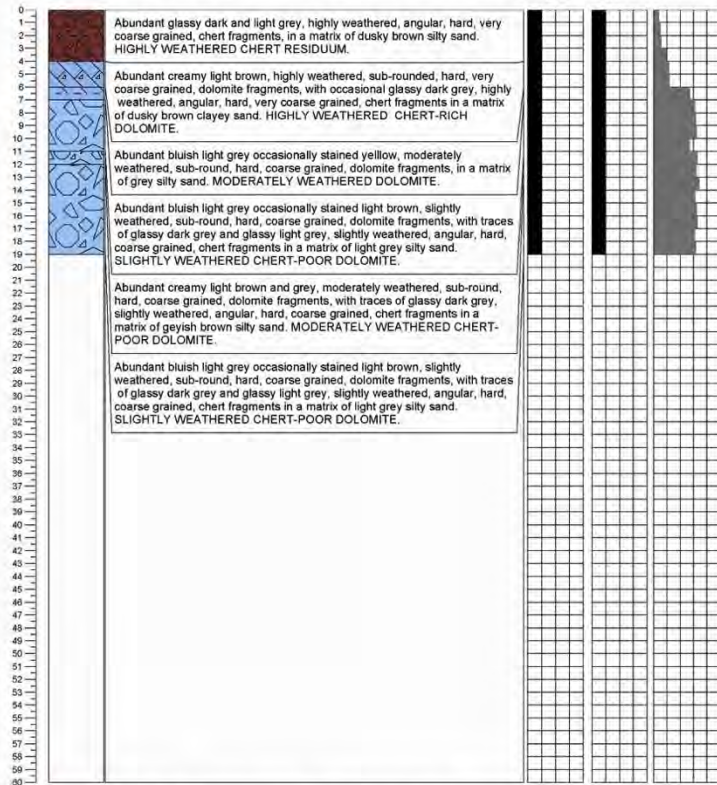


Notes: Drilling stopped at 54 mbl
 Water added at: 1-2, 3-4, 6-9, 11-12, 22-27, 30-32, 37-51, 53-54 m.
 Irregular hammer rates at: 13-14, 21-22, 26-27, 29-30, 32-33, 36-37, 47-48 m.
 Borehole dry.
 Coordinate measured with hand-held GPS (WGS84)
 Elevation inferred from 5m contours (GIS)

PROJECT:

CLIENT:	LATITUDE:	BOREHOLE NO.: KBH36	
CONTRACTOR: Hennie Erwe Drilling	LONGITUDE:	DATE DRILLED: 2013/04/29	
MACHINE TYPE: Super Rock 165mm / 1900kpa	ELEVATION: 1323 mamsl	DATE LOGGED: 2013/04/29	
COMPRESSOR: 19 bar	ORIENTATION: Vertical	LOGGED BY: WM & EH	

Depth Lithology Description
(m)

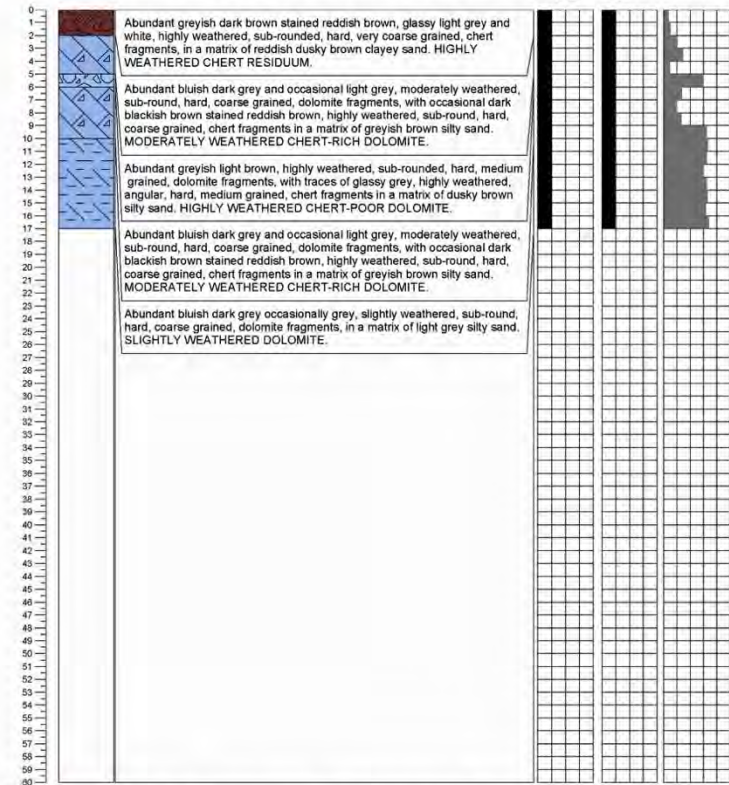


Notes: Drilling stopped at 19 mbgl
 Water added at: 1-8, 9-16, 17-19 m.
 Irregular hammer rates at: 3-4, 6-7, 9-11 m.
 Borehole dry.
 Coordinate measured with hand-held GPS (WGS84)
 Elevation inferred from 5m contours (GIS)

PROJECT:

CLIENT:	LATITUDE:	BOREHOLE NO.: KBH37	
CONTRACTOR: Hennie Erwe Drilling	LONGITUDE:	DATE DRILLED: 2013/04/29	
MACHINE TYPE: Super Rock 165mm / 1900kpa	ELEVATION: 1324 mamsl	DATE LOGGED: 2013/04/29	
COMPRESSOR: 19 bar	ORIENTATION: Vertical	LOGGED BY: WM & EH	

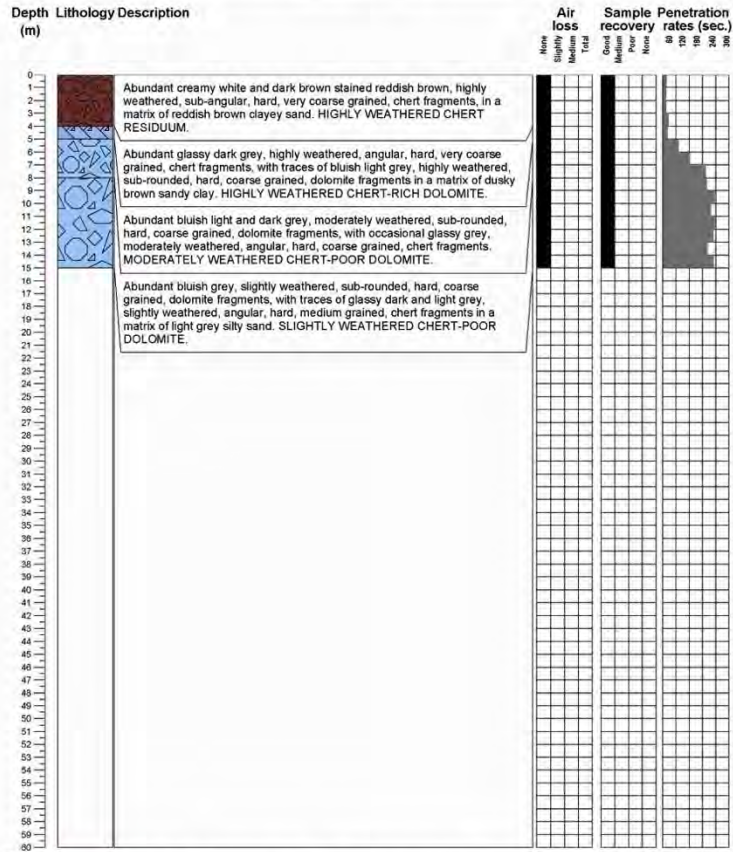
Depth Lithology Description
(m)



Notes: Drilling stopped at 17 mbgl
 Water added at: 3-6 m.
 Irregular hammer rates at: 0-1, 3-4, 5-7 m.
 Borehole dry.
 Coordinate measured with hand-held GPS (WGS84)
 Elevation inferred from 5m contours (GIS)

PROJECT:

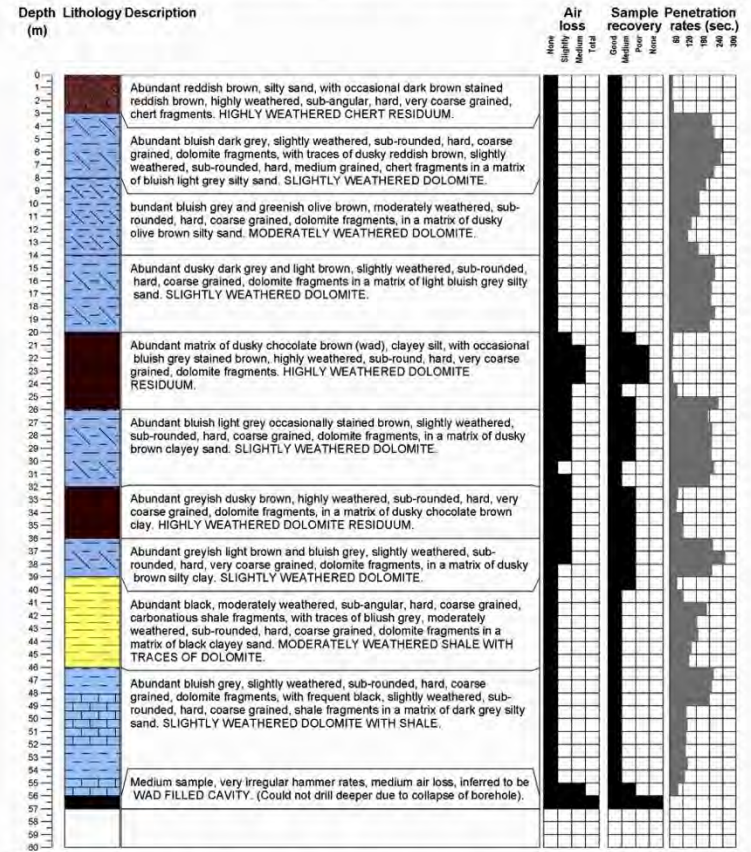
CLIENT:	LATITUDE:	BOREHOLE NO.:	KBH38
CONTRACTOR: Hennie Erwee Drilling	LONGITUDE:	DATE DRILLED:	2013/04/30
MACHINE TYPE: Super Rock 165mm / 1900kpa	ELEVATION: 1325 mamsl	DATE LOGGED:	2013/04/30
COMPRESSOR: 19 bar	ORIENTATION: Vertical	LOGGED BY:	WM & EH



Notes:
 Drilling stopped at 15 mblg
 Water added at: 2-5, 6-7 m.
 Irregular hammer rates at: 0-4, 5-7 m.
 Borehole dry.
 Coordinate measured with hand-held GPS (WGS84)
 Elevation inferred from 5m contours (GIS)

PROJECT:

CLIENT:	LATITUDE:	BOREHOLE NO.:	KBH39
CONTRACTOR: Hennie Erwee Drilling	LONGITUDE:	DATE DRILLED:	2013/04/30
MACHINE TYPE: Super Rock 165mm / 1900kpa	ELEVATION: 1327 mamsl	DATE LOGGED:	2013/04/30
COMPRESSOR: 19 bar	ORIENTATION: Vertical	LOGGED BY:	WM & EH

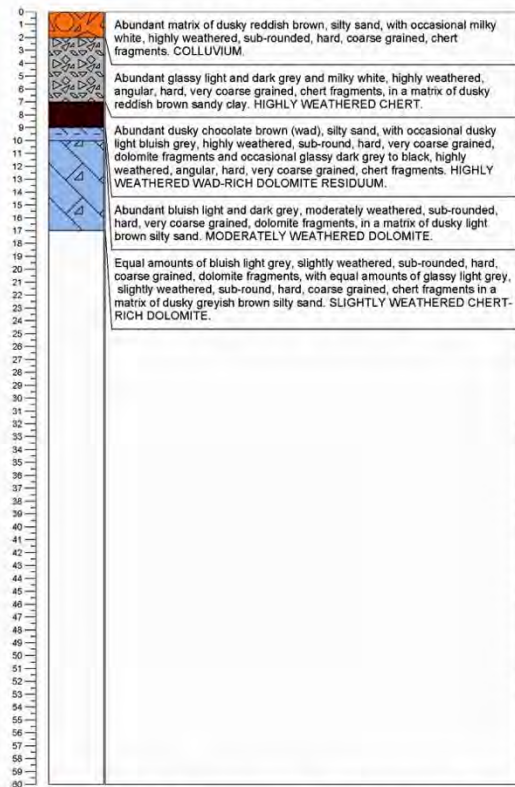


Notes:
 Drilling stopped at 57 mblg
 Water added t 0-1, 5-10, 12-13, 19-27, 28-29, 30-38, 55-56 m.
 Irregular hammer rates at: 0-3, 6-9, 10-12, 19-27, 31-35, 40-41, 44-45, 55-56 m.
 Borehole dry.
 Coordinate measured with hand-held GPS (WGS84)
 Elevation inferred from 5m contours (GIS)

PROJECT:

CLIENT:	LATITUDE:	BOREHOLE NO.:	KBH40
CONTRACTOR:	Hennie Erwee Drilling	DATE DRILLED:	2013/04/30
MACHINE TYPE:	Super Rock 165mm / 1900kpa	ELEVATION:	1323 mamsl
COMPRESSOR:	19 bar	ORIENTATION:	Vertical
		LOGGED BY:	WM & EH

Depth Lithology Description
(m)



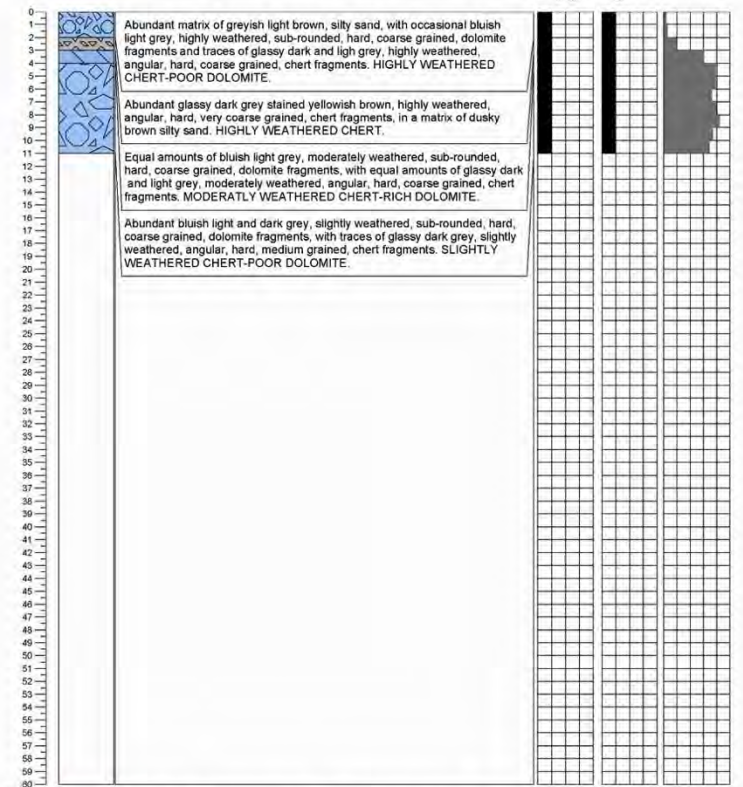
Air loss		Sample Penetration	
None	Total	recovery	rates (sec.)
Slightly	Medium	Good	Poor
Medium	None	None	None
		60	120
		120	180
		180	240
		240	300

Notes: Drilling stopped at 17 mbgl
Water added at: 0-4, 6-7, 8-9, 13-15 m.
Irregular hammer rates at: 0-9 m.
Borehole dry.
Coordinate measured with hand-held GPS (WGS84)
Elevation inferred from 5m contours (GIS)

PROJECT:

CLIENT:	LATITUDE:	BOREHOLE NO.:	KBH41
CONTRACTOR:	Hennie Erwee Drilling	DATE DRILLED:	2013/04/30
MACHINE TYPE:	Super Rock 165mm / 1900kpa	ELEVATION:	1322 mamsl
COMPRESSOR:	19 bar	ORIENTATION:	Vertical
		LOGGED BY:	WM & EH

Depth Lithology Description
(m)



Air loss		Sample Penetration	
None	Total	recovery	rates (sec.)
Slightly	Medium	Good	Poor
Medium	None	None	None
		60	120
		120	180
		180	240
		240	300

Notes: Drilling stopped at 11 mbgl
Water added at: 1-3, 4-8, 7-9 m.
Irregular hammer rates at: 0-9 m.
Borehole dry.
Coordinate measured with hand-held GPS (WGS84)
Elevation inferred from 5m contours (GIS)

Annexure 6: Interpreted magnetic geophysical data

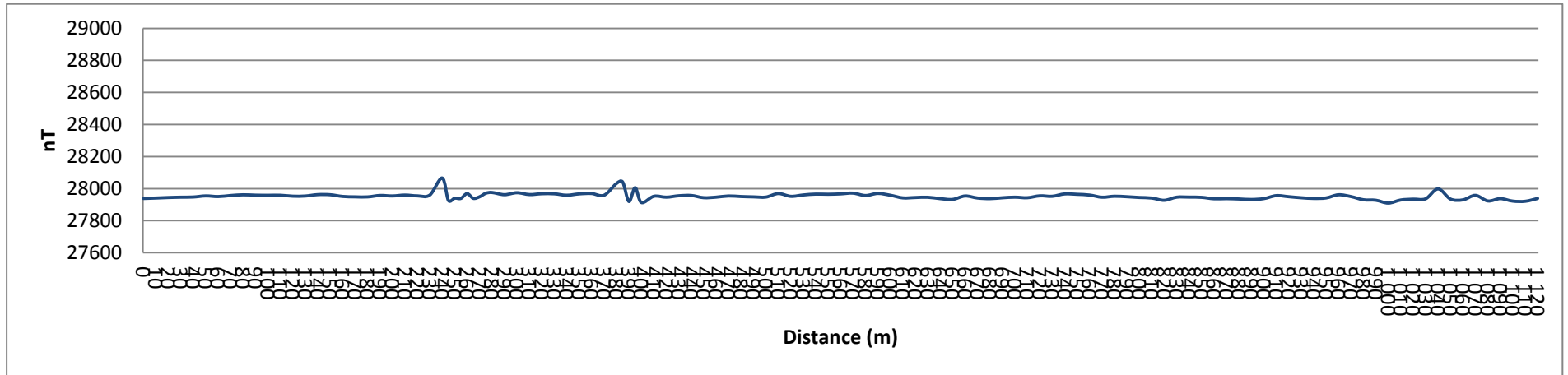


Figure 6-18: Magnetic geophysical traverse line 1

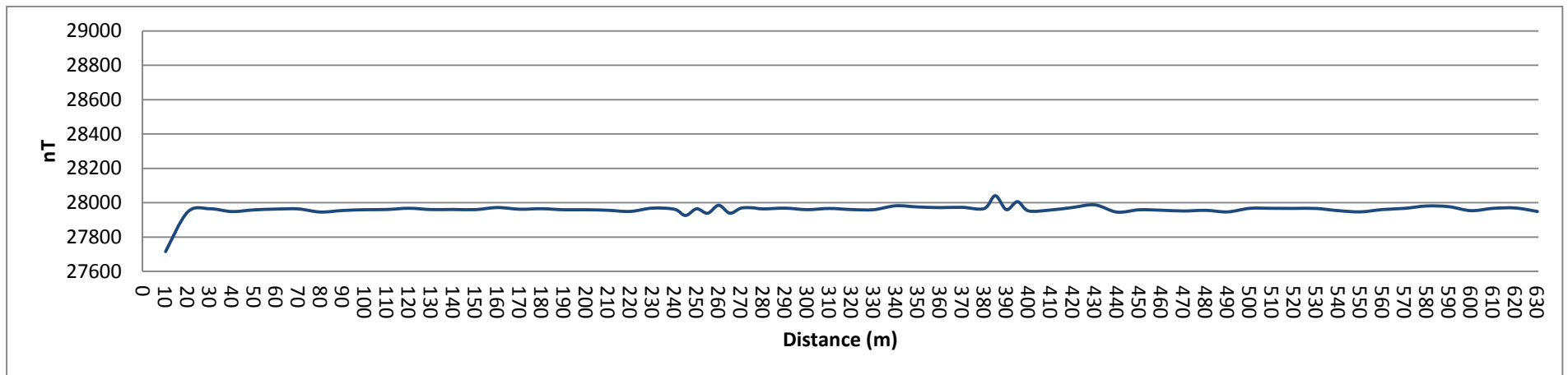


Figure 6-19: Magnetic geophysical traverse line 2

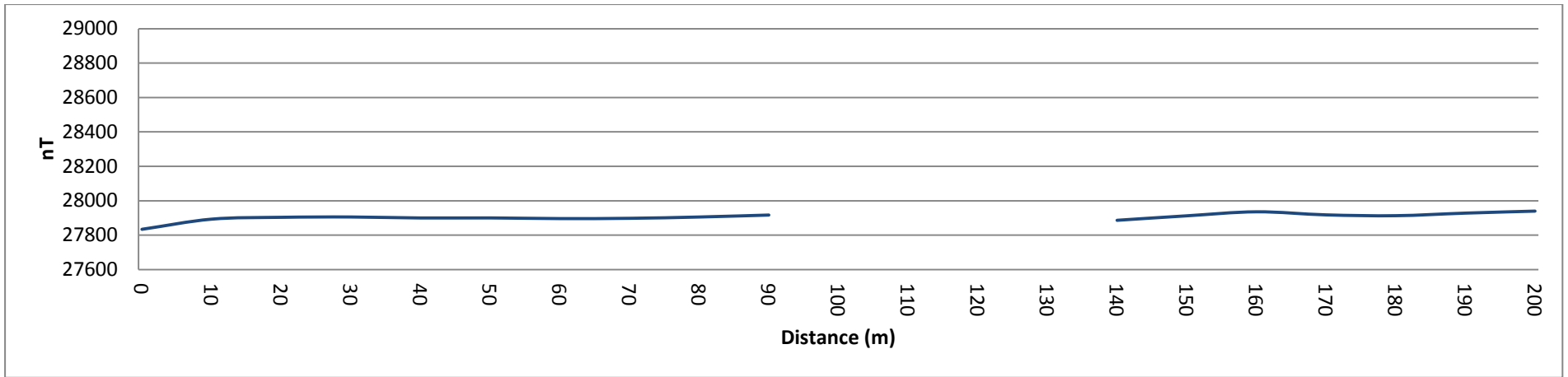


Figure 6-20: Magnetic geophysical traverse line 3

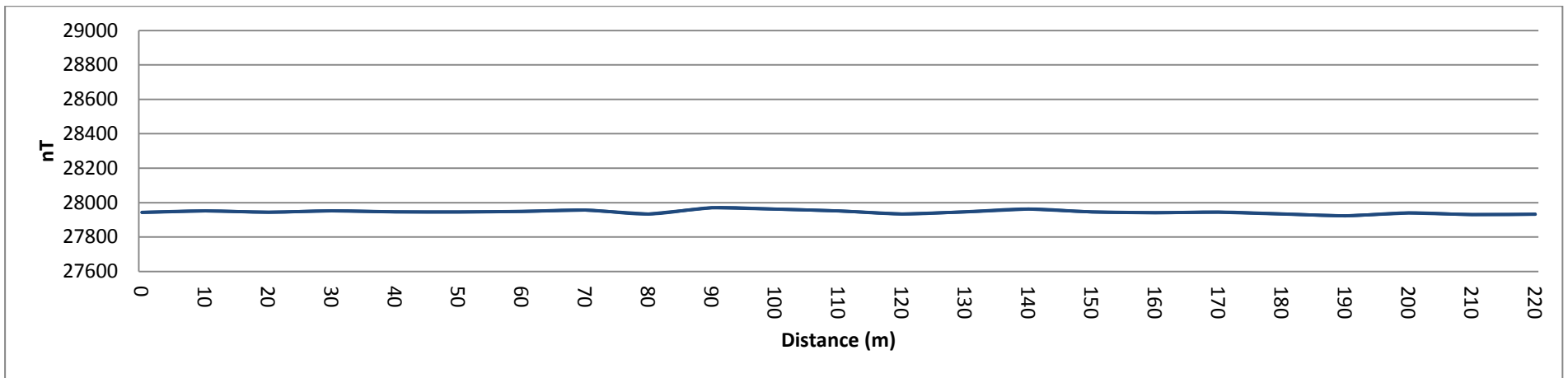


Figure 6-21: Magnetic geophysical traverse line 4

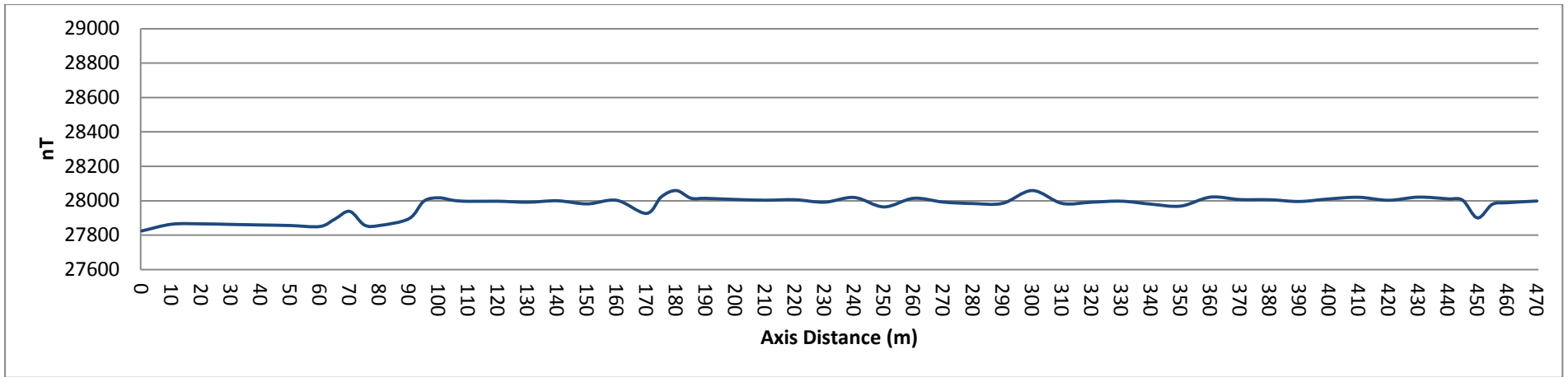


Figure 6-22: Magnetic geophysical traverse line 5

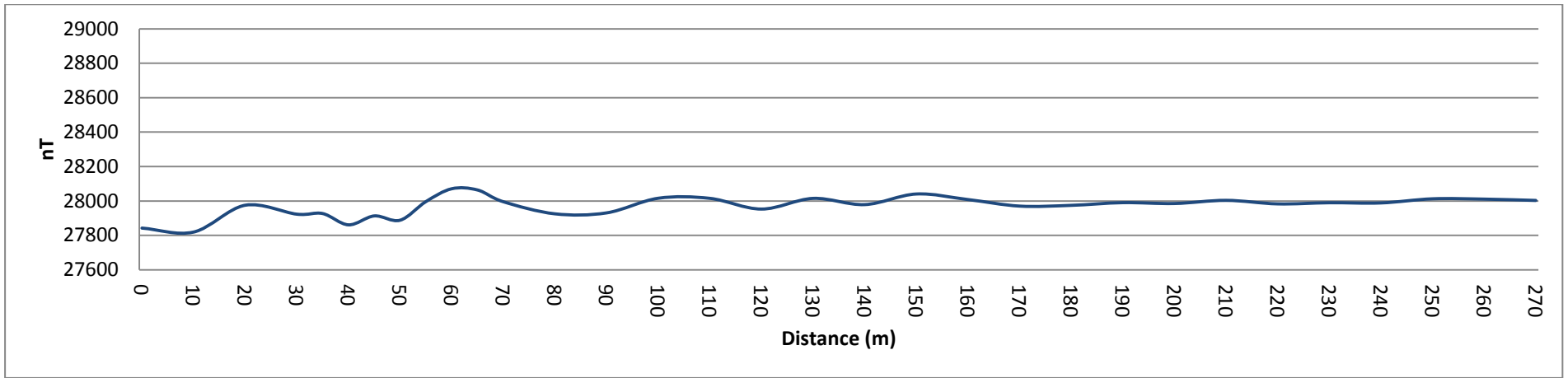


Figure 6-23: Magnetic geophysical traverse line 6

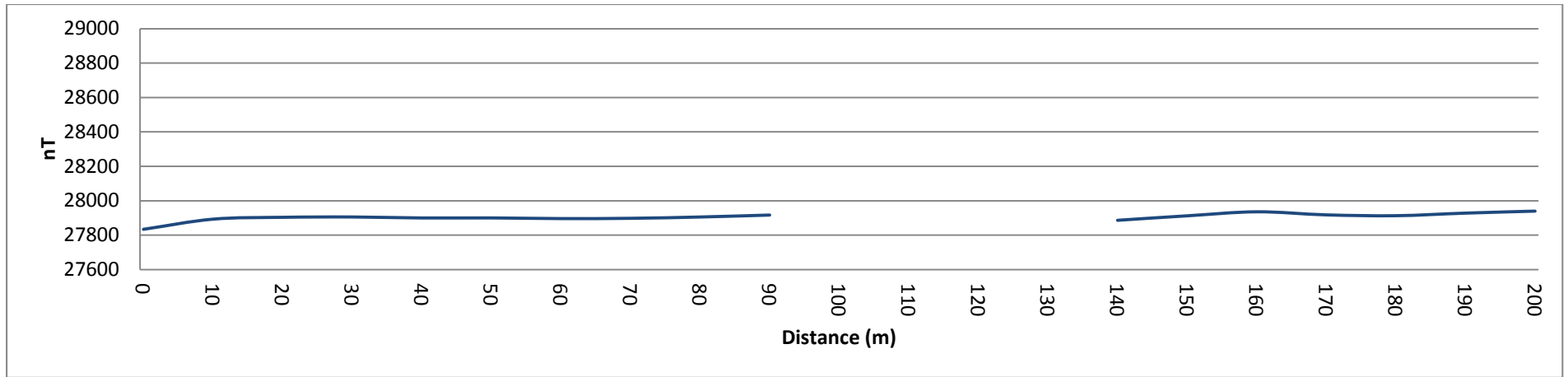


Figure 6-24: Magnetic geophysical traverse line 7

Annexure 7: Detailed determinations of the various angles of draw for the different lithologies

Table 6-5: Detailed determination of angles of draw

Lithology:		ALLUVIUM / COLLUVIUM	COMPLETELY WEATHERED (RESIDUAL) SHALE	SHALE		CHERT		DOLOMITE BEDROCK
Effective weathering:		Soil	Soil	Highly Weathered	Moderately Weathered	Residuum	Highly Weathered	Highly Weathered (No Chert)
Lithostratigraphical descriptions	Size	Predominantly abundant clayey matrix with transported gravel and cobbles	Abundant matrix of sandy silt, very little fragments	Predominantly abundant matrix with scattered highly weathered fragments (soft)	Massif shale with localized intact boulders expected	Chert rubble (generally highly weathered) with scattered chert cobbles and boulders. Matrix mostly clayey sand (in some instances abundant matrix).	Abundant angular to sub-rounded gravel/cobbles/boulders in a silty/clayey sandy matrix. Occasional shale lenses (HW).	Small boulders / highly fissured bedrock with in filled cavities / grykes
	Possible Shape	Irregular: rounded - angular (transported material)	Homogenously weathered	Possible boulders with localized more and localized less weathered zones / pockets	Generally layered massif	Rounded to angular loose boulders in a soil matrix.	Rounded (gravel) to angular (chips off boulders). Boulders expected to be rounded/sub-rounded along weathering planes	Highly variable - small boulders (no chert) with infillings in joints / grykes.
	Layering	-	Varved shale with different colored layers	Bedded with altering layers (varved). No prominent difference in consolidation within effective weathering zone between alternating layers.	Banded (varved)	No prominent layering, generally scattered rubble / cobbles and boulders	No prominent layering, generally scattered rubble / cobbles and boulders. Some layering observed within individual boulders (harder / softer alterations between black and grey chert).	No internal layering; differentially weathered.
	Cohesion None, slight, mod, good, excellent	None - slight (granular material) to good	None - slight	None - slight (granular)	-	Slight, with interlocking angular fragments (pseudo-structure).	Not deemed cohesive. Pseudo structure due to interlocking angular fragments - dependent on fragment size.	-
	Sorting/grading	Poorly-well sorted (soil > gravel)	Well sorted (predominantly matrix)	Poorly sorted	Well Sorted (shale only)	Poorly sorted (fragments in a matrix of vica versa)	Poorly sorted (fragments of different sizes in a matrix).	Poorly sorted - boulders & gravel within a matrix.
	Density	Unconsolidated - Moderately consolidated clayey material	Unconsolidated	Low density. More consolidated than CW shale (soil-like)	Moderate density with localized less dense pockets. Consolidated.	Predominantly unconsolidated.	Generally unconsolidated with larger boulders and debree.	Low
	Possible pockets	Yes - topography dependent: Mostly adjacent drainage channels	Yes - structural geological correlations (extent and faulting)	Pockets of completely weathered shale (soil-like)	Highly weathered pockets	Yes.	Yes.	In filled cavities, chert & dolomite residuum, wad, some shale lenses.
	Internal Movement	Yes - heaving expected	Some expected	Some possible internal movement along fractured areas expected	None expected	Moderate internal movement expected (especially adjacent or along angular fragments)	Internal movement expected (especially adjacent or along angular fragments).	Yes.

	Expected Permeability (with disregard of fractures & joints; generally impermeable, low, med, high, very high)	None - slight (granular material) to generally impermeable (cohesive)	Medium (poorly granular)	Low (bedrock but with some CW pockets)	Low (Bedrock)	Medium (depending on matrix, voids along angular fragments)	Medium (depending on matrix, voids along angular fragments)	High due to weathered nature
	Groundwater table fluctuation	Project area dewatered - slightly permeable for surface water	Project area dewatered - moderately permeable for surface water	Project area dewatered (effect of re-watering may cause mobilization)	Project Area Dewatered (effect of re-watering may cause mobilization)	Project area dewatered (effect of re-watering may cause mobilization)	Project Area Dewatered (effect of re-watering may cause mobilization)	Project Area Dewatered (effect of re-watering may cause mobilization)
Geotechnical descriptions	Hammer rate	Mostly regular, some irregular hammer rates	Mostly regular rates	Regular	Regular	Mostly regular with very occasional irregular hammer rates (but not very irregular)	Some irregular hammer rates recorded, mostly regular.	Irregular and very irregular hammer rates.
	Air loss	-	-	-	-	No air-loss recorded	Some air-loss recorded (only slight). Generally no air loss.	Air loss - total in some instances.
	Sample Recovery	Generally good	Good	Good	Good	Good	Generally good.	Poor - Good.
	Penetration rate	15 - 30 sec / m	< 45 sec / m	< 60 sec / m	> 60 sec / m	15 - 30 sec / m (< 15 sec / m in some cases)	Mostly 15 - 45 sec / m, but n=15 >> n=45.	10 - 60 sec / m (average ± 30 sec / m)
	Wad	-	-	-	-	No wad.	Mostly no wad, traces of wad in some cases.	Contains some wad
Evaluation	Mobilization Potential:	High	High	Moderate	Low	High	High	High
	Effective angle:	75°	80°	80°	85°	70°	75°	70°
	Motivation:	Unconsolidated cohesive matrix with scattered fragments	Unconsolidated non-cohesive matrix	Abundant matrix but more intact / soft rock than CW shale. Non-cohesive.	Intact with higher penetration rates, no irregular hammer rates (i.e. softer less consolidated material / transition zones)	No air loss recorded, unconsolidated material (irregular hammer rates) with rapid penetration rates. Generally non-cohesive.	Predominant difference between Residuum and HW chert = weathering colour. Penetration rates also rapid. Some instances of slight air loss. Unconsolidated.	Irregular hammer rates & air loss. Low penetration rates, more homogenously weathered, not as abrupt transitions from harder - softer (possibly due to chert bands).

Table 6-6: Detailed determination of angles of draw (cont.)

Lithology: Effective weathering:		DOLOMITE BEDROCK				DOLOMITE RESIDUUM		
		Highly Weathered (Chert Poor)	Highly Weathered (Chert Rich)	Moderately Weathered	Slightly Weathered	WAD	Chert-poor	Chert-rich
Lithostratigraphical descriptions	Size	Small boulders / highly fissured bedrock with in filled cavities / grykes. Contains chert rubble / some chert inclusions in bedrock.	Small boulders / highly fissured bedrock with in filled cavities / grykes. Localized broken chert bands.	Massif, occasional fractures.	Massif, generally not fractures.	Solely silt / clay	Dolomite residuum (i.e. wad and traces of dolomite in some instances) with small chert fragments/traces	Dolomite residuum (i.e. wad and traces of dolomite in some instances) with more abundant chert fragments
	Possible Shape	Highly variable - small boulders (some chert rubble and gravel) with infillings in joints / grykes.	Highly variable - small boulders with brittle chert bands with infillings in joints / grykes.	Massif Intact. Some instances inclusions in HW Dolomite (possibly as boulders/floaters).	Massif Intact.	Soil-like	Blocks and fragments (floaters) - matrix supported	Blocks and fragments (floaters) - clast supported
	Layering	Contains chert rubble; generally no chert layers, deemed more scattered inclusions / infillings.	Chert bands within dolomite boulders, more weathered above/below chert bands, bands expected to be brittle and broken in some instances.	Chert-rich dolomite expected to have continuous bands. Chert-poor dolomite expected to have thinner chert bands or chert boulders/inclusions.	Occasional chert bands (chert-rich dolomite).	-	Traces of chert layers	More abundant chert layers
	Cohesion None, slight, mod, good, excellent	-	-	-	-	Slight	Cohesionless	Cohesionless
	Sorting/grading	Poorly sorted - boulders & gravel within a matrix.	Poorly sorted - boulders & gravel within a matrix. Better sorting than Dolomite with less dolomite.	Massif, generally chert-poor (i.e. boulders and chert gravel - boulders).	-	Poorly sorted	Gap-graded (matrix > fragments)	Well graded (boulders - fine soils)
	Density	Low	Low, especially along chert bands	Generally moderate density (medium - hard rock), expected lower density along chert bands.	-	Very low	Low	Low
	Possible pockets	In filled cavities, chert & dolomite residuum, wad, some shale lenses.	In filled cavities, chert & dolomite residuum, wad, some shale lenses.	In some instances contains unconsolidated pockets / HW chert poor dolomite. Interlayered softer zones (possibly above/below more consolidated chert bands. Contains shale lenses.	Predominantly consolidated, possible fractures/cavernous areas expected due to inherent nature. Contains shale lenses in some instances.	Contains scattered boulders / chert bands. Wad filled-cavities	Cavity infillings	Cavity infillings
	Internal Movement	Yes.	Yes.	Some internal movement expected due to less consolidated pockets/possible grykes & fractures.	-	Yes.	High	Moderate with pockets of high potential

	Expected Permeability (with disregard of fractures & joints; generally impermeable, low, med, high, very high)	High due to weathered nature	High due to weathered nature, preferred water flow along chert bands	Low - Medium	Low	High	High	High
	Groundwater table fluctuation	Project Area Dewatered (effect of re-watering may cause mobilization)	Project Area Dewatered (effect of re-watering may cause mobilization)	Project Area Dewatered (effect of re-watering may cause mobilization)	Project Area Dewatered (effect of re-watering may cause mobilization)	Project Area Dewatered (effect of re-watering may cause mobilization)	Project Area Dewatered (effect of re-watering may cause mobilization)	Project Area Dewatered (effect of re-watering may cause mobilization)
Geotechnical descriptions	Hammer rate	Irregular and very irregular hammer rates.	Irregular and very irregular hammer rates.	Some irregular hammer rates recorded, mostly regular.	Mostly regular, some irregular rates at transition zones from SW-HW/MW	Mostly very irregular.	Very irregular hammer rates recorded	Very irregular hammer rates recorded
	Air loss	Slight to no air loss	Medium to no air loss	Slight air loss recorded very occasionally, predominantly no air loss.	-	Total.	Moderate	Slight
	Sample Recovery	Poor to Good	Poor - Good.	Good.	Good	-	-	-
	Penetration rate	10 - 60 sec / m (average ± 30 sec / m)	10 - 60 sec / m (average ± 30 sec / m)	60 - 180 sec / m, ave ± 80 sec / m	> 3 mins / m. Chert Rich Dolomite > Chert Poor Dolomite > Dolomite	> 10 sec / m	10 - 30 sec / m. (average ± 15 sec.)	10 - 30 sec / m. (average ± 20 - 30 sec)
	Wad	Contains some wad	Contains some wad	-	-	Solely	Contains more wad as chert-rich dolomite residuum, but not solely wad.	Not as prominent, contains some wad.
Evaluation	Mobilization Potential:	High	High	Moderate	Low	High	High	High
	Effective angle:	70°	75°	80°	90°	55°	60°	60°
	Motivation:		More potential mobilization & weathering along chert bands expected, and subsequently larger potential sinkhole formation.	Some shale inclusions, mostly chert poor dolomite. Contains some less consolidated pockets (possibly grykes or ascribed to inherent nature of bedrock).	Intact, no AL/SL/IR HR. Penetration rates > 3 mins / m.	Very low density, highly mobilizable, air loss, sample loss, extremely low penetration rates.	Highly mobilisable, moderate air loss,	Chert bands / blocks renders pseudo structure. Still highly mobilisable.

Annexure 8: Detailed per-borehole hazard characterization

Table 6-7: Detailed inherent hazard characterisation per drilled borehole

Borehole Number	Susceptibility for formation					Maximum possible feature Size	Static water Level	IHC Rating					Final IHC Rating	Gravity Anomaly	Nature of overlying material						General comment	
	WI		GWLD		WI in the event of GWLD			WI		GWLD		WI in the event of GWLD			Nature of blanketing layer	Nature of overburden		Nature of bedrock morphology				
	Sh	Sb	Sh	Sb				Sh	Sb	Sh	Sb											
KHB 01	M-H	M	L	L	M-H	4,3	M	Dry	5	3	1	1	5	5(Sh)/3(Sb)//1 DWS: 5//	High Plateau	-	No substantial blanketing layer	0 - 6.5	Colluvium, HW Chert Residuuum	6.5 - 14	SW CP Dolomite	Shallow dolomite bedrock, gravity high, possibly highly mobilisable material over bedrock
KHB 02	H	H	L	L	H	26,9	VL	Dry	8	8	1	1	8	8//1 DWS: 8//	Gradient into prominent E-W Low Through	-	No substantial blanketing layer	0 - 44	HW Chert, Residuuum & Dolomite with cavities/wad	44 - 49	SW Dolomite	Gradient into gravity low, deep weathered profile with cavities / WAD filled cavities
KHB 03	M	M-H	L	L	M	12,5	L	Dry	4	6	1	1	6	4(Sh)/6(Sb)//1 DWS: 6//	High Plateau	-	No substantial blanketing layer	0 - 23	Colluvium, HW Chert & Dol / Residuuum	23 - 30	SW Dolomite / SW CP Dolomite	2-m buffering layer at 8-10 mbgl. 6-m more competent dolomite before SW Dolomite (15-21 mbgl)
KHB 04	H	M-H	L	L	H	9,1	L	Dry	7	6	1	1	7	7(Sh)/6(Sb)//1 DWS: 7//	High gradient into prominent E-W Low Through	-	No substantial blanketing layer	0 - 18	Colluvium, HW Chert Residuuum, HW Dolomite with WAD	18 - 30	SW CP Dolomite	Gravity high gradient, deeper weathered profile with WAD (11-15 mbgl). Some AL and VI HR.
KHB 05	L-M	L-M	L	L	L-M	2,7	M	Dry	5	2	1	1	5	5(Sh)/2(Sb)//1 DWS: 5//	High gradient into NW-SE Low Through/Structure	-	No substantial blanketing layer	0 - 5	Colluvium, HW Chert Residuuum grading into more competent Dolomite	5 - 13	SW CP Dolomite	Shallow dolomite bedrock, gravity high, possibly highly mobilisable material over bedrock
KHB 06	L-M	L-M	L	L	L-M	6,0	L	Dry	4	3	1	1	4	4(Sh)/3(Sb)//1 DWS: 4//	High	-	No substantial blanketing layer	0 - 9	HW Chert grading into residuum and HW dolomite	9 - 17	SW CP Dolomite	Relatively shallow bedrock, gravity high with 4 meters overburden grading into more competent bedrock
KHB 07	M	M	L	L	M	10,7	L	Dry	4	3	1	1	4	4(Sh)/3(Sb)//1 DWS: 4//	Plateau	-	No substantial blanketing layer	0 - 17	HW Chert Residuuum with interlayered HW/SW dolomite bands	17 - 25	SW CP Dolomite	Gravity plateau with interlayered harder and softer dolomite. No Dolomite Residuuum.
KHB 08	L-M	L-M	L	L	L-M	3,4	M	Dry	5	2	1	1	5	5(Sh)/2(Sb)//1 DWS: 5//	Plateau	-	No substantial blanketing layer	0 - 10	Colloivium directly into HW Dolomite becoming more competent with depth.	10 - 18	SW CP Dolomite / SW Dolomite	Shallow Dolomite in Gravity plateau with shallow overburden and MW dolomite bands in SW dolomite. No Dolomite Residuuum.

KHB 09	L-M	L-M	L	L	L-M	4,1	M	Dry	5	2	1	1	5	5(Sh)/2(Sb)//1 DWS: 5//	Plateau	-	No substantial blanketing layer	0 - 6	HW Chert directly into HW Dolomite becoming more competent with depth.	15 - 21	SW CP Dolomite	Shallow Dolomite in Gravity plateau with shallow overburden and MW dolomite bands in SW dolomite. No Dolomite Residuum. SW Dolomite from 6-14 mbgl. Then 15-21 mbgl.
KHB 10	H	H	L	L	H	36,3	VL	Dry	8	8	1	1	8	8//1 DWS: 8//	Low/Gradient in SW-NE Through	-	No substantial blanketing layer	0 - 47	HW Chert Residuum grading into WAD and alternating bands of HW/MW Dolomite	47 - 53	SW CP Dolomite	SW-NE Gravity Through (Gradient Low) with deeper profile and some AL/SL/VI HR.
KHB 11	L-M	L-M	L	L	L-M	5,9	L	Dry	3	2	1	1	3	3(Sh)/2(Sb)//1 DWS: 3//	Plateau	-	No substantial blanketing layer	0 - 13	Shallow Colluvium/HW Chert grading into generally competent (still MW) Dolomite.	12 - 21	SW CP Dolomite	Gravity plateau with generally more competent Dolomite from 5-13 mbgl, grading into SW Dolomite. Can also be classified as Shallow Dolomite Bedrock
KHB 12	L-M	L-M	L	L	L-M	9,9	L	Dry	3	2	1	1	3	3(Sh)/2(Sb)//1 DWS: 3//	Plateau	-	No substantial blanketing layer	0 - 14	Chert Residuum grading into HW Dolomite and CP Dolomite Residuum. Some IR HR, No AL/SL.	23 - 29	SW CP/CR Dolomite	Gravity plateau, competent dolomite bedrock (8 m) from 14-22 mbgl, and from 23-29 mbgl.
KHB 13	L-M	L-M	L	L	L-M	4,1	M	Dry	5	2	1	1	5	5(Sh)/2(Sb)//1 DWS: 5//	Plateau	-	No substantial blanketing layer	0 - 11	HW CR/CP Dolomite directly into SW dolomite with bands of MW Dolomite	11 - 19	SW CP Dolomite	Gravity plateau with generally more competent Dolomite from 6-11 mbgl, grading into SW CP Dolomite from 11-19 mbgl.
KHB 14	L-M	L-M	L	L	L-M	4,7	M	Dry	2	2	1	1	2	2//1 DWS: 2//	Plateau	-	No substantial blanketing layer	0 - 19	Chert Residuum directly into MW CR Dolomite and SW CR Dolomite (alternating bangs of MW/SW)	19- 25	SW CP Dolomite	Gravity plateau with interlayered harder and softer dolomite. No Dolomite Residuum. Can also be classified as Shallow Dolomite Bedrock
KHB 15	L	L	L	L	L	2,7	M	Dry	5	1	1	1	5	5(Sh)/1(Sb)//1 DWS: 5//	Plateau	-	No substantial blanketing layer	0 - 4	Colluvium, HW Chert Residuum	4 - 13	SW CR Dolomite	Shallow Dolomite in Gravity plateau with shallow overburden.

KHB 16	M	M	L	L	M	5,3	L	Dry	4	3	1	1	4	4(Sh)/3(Sb)//1 DWS: 4//	High	-	No substantial blanketing layer	0 - 9	CR Dolomite Residuum, HW Chert, WAD (No AL/SL, some IR HR).	9 - 17	SW CP/SW Dolomite	Relatively shallow dolomite in gravity high. No air loss/sample loss. Overburden is Dolomite residuum, Chert and WAD gradiging into competent dolomite bedrock. Can be seen as shallow dolomite?
KHB 17	H	H	L	L	H	24,3	VL	Dry	8	8	1	1	8	8//1 DWS: 8//	Gradient into prominent E-W Low Through	-	No substantial blanketing layer	0 - 35	Chert/Dolomite Residuum with WAD, harder chert/dolomite bands with depth (AL, SL, VI HR).	35 - 41	SW Dolomite	Gradient into gravity low, deep weathered profile with prominent Dolomite Residuum Horisons (air loss, sample loss and very irregular hammer rates).
KHB 18	H	H	L	L	H	24,2	VL	Dry	8	8	1	1	8	8//1 DWS: 8//	Gradient into prominent E-W Low Through	-	No substantial blanketing layer	0 - 35	Chert/Dolomite Residuum with WAD, harder chert/dolomite bands with depth (AL, SL, VI HR).	35 - 41	SW Dolomite	Gradient into gravity low, deep weathered profile with prominent Dolomite Residuum Horisons (air loss, sample loss and very irregular hammer rates).
KHB 19	M	M	L	L	M	20,4	VL	Dry	4	4	1	1	4	4//1 DWS: 4//	Shallow Gradient into prominent E-W Low Through	-	No substantial blanketing layer	0 - 36	Colluvium/CR Dolomite Residuum grading into HW Dolomite. Deeper = MW/SW Dolomite alretnating layers	36 - 42	SW Dolomite	Gradient into gravity low, deep weathered profile (23-36 mbgl = alternating layers of MW/SW Dolomite).
KHB 20	L-M	L-M	L	L	L-M	8,8	L	Dry	3	2	1	1	3	3(Sh)/2(Sb)//1 DWS: 3//	Gradient into southern Low	-	No substantial blanketing layer	0 - 17	Colloivium, HW Chert with Shale grading into HW Dolomite. No AL/SL, some IR HR.	17 - 23	SW CP Dolomite	Gradient into prominent gravity low (southern portion of site) with no AL/SL. Directly into HRD.
KHB 21	L	L	L	L	L	16,9	VL	Dry	2	2	1	1	2	2//1 DWS: 2//	Steep Gradient Low	0 - 18	Varved Karoo shale with localised chert.	18 - 49	HW Dolomite and Shale grading into SW Dolomite with localised softer bands in SW Dolomite	49 - 55	SW Dolomite with SW Shale	Prominent steep gradient gravity Low, with interleyered Shale. No AL/SL/VI HR & 18m blanketing layer.

KHB 22	M	M	L	L	M	6,8	L	Dry	4	4	1	1	4	4//1 DWS: 4//	Gradient in SE-NW Through	-	No substantial blanketing layer	0 - 13	Colluvium, HW Chert & Dolomite Residuum (Slight AL / some IR HR).	17 - 23	SW CR Dolomite	Relatively shallow dolomite in steep gravity gradient with some AL and IR HR. Prominent CR Dol Res and Chert Res.
KHB 23	H	H	L	L	H	34,5	VL	Dry	8	8	1	1	8	8//1 DWS: 8//	Low/Gradient in SE-NW Through	-	No substantial blanketing layer	0 - 45	HW Chert / Dolomite and Residuum with WAD/Wad-Filled Cavities/Cavities (Total AL/SL/VI HR/No Hammer).	45 - 51	SW Dolomite	Low in prominent Through. Total AL and SL with cavity and WAD (6m from 23mbgl.)
KHB 24	M-H	H	L	L	H	29,9	VL	Dry	6	8	1	1	8	6(Sh)/8(Sb)//1 DWS: 8//	Low in E-W Through	-	No substantial blanketing layer	0 - 45	HW Chert / Dolomite and Residuum with WAD/Wad-Filled Cavities (Some AL/SL/VI HR). Localised harder bands.	45 - 54	SW CR Dolomite	Low in prominent E-W through with thick weathered material (some AL/SL/IR HR). Profile as a whole alternating hard/soft from 17-45 mbgl.
KHB 25	L-M	M	L	L	M	24,5	VL	Dry	3	4	1	1	4	3(Sh)/4(Sb)//1 DWS: 4//	Plateau within E-W Through (pinnacle?)	-	No substantial blanketing layer	0 - 55	HW Chert/Shale grading into HW/MW Dolomite. Alternating Hard and Softer bands in dolomite from 29-55 mbgl. No AL/SL, some IR HR.	55 - 60	SW Dolomite	Thin gravity plateau in E-W through. 4m Shallow dolomite from 29mbgl with alternating layered of MW/SW Dolomite to 55 mbgl. No AL/SL. Profile as a whole from 29mbgl = hard soft alternating layers
KHB 27	H	M-H	L	L	H	7,9	L	Dry	6	4	1	1	6	6(Sh)/4(Sb)//1 DWS: 6//	Gradient in SE-NW Through	-	No substantial blanketing layer	0 - 20	HW Chert / Dolomite and Residuum grading into more competent Dolomite with depth (from 18mbgl). AL/SL/VI HR (WAD).	20 - 26	SW CP Dolomite	Some buffering at 4-7mbgl (could be floater), gradient into prominent Through towards west. AL/SL/VI HR.
KHB 28	H	M-H	L	L	H	32,3	VL	Dry	8	8	1	1	8	8//1 DWS: 8//	Low in SE-NW Through	-	No substantial blanketing layer	0 - 60	MW/HW Dolomite with Cavity and WAD at depth (>40 mbgl).	-	Not encountered at 60 mbgl. Drilling stopped after collapsing hole at depth.	Deeply weathered profile. Cavity and WAD at depth. In prominent SE-NW Through (Low). No SW Dolomite encountered
KHB 29	M-H	M-H	L	L	M-H	23,1	VL	Dry	6	6	1	1	6	6//1 DWS: 6//	Low in SE-NW Through	-	No substantial blanketing layer	0 - 35	Chert Residuum, HW Dolomite (AL/SL/VI HR). Localised harder bands in HW dolomite.	35 - 41	SW Dolomite	HW Profile to 35 mbgl. In prominent SE-NW Through (Gravity not as prominently Low). Localised harder bands in profile.

KHB 30	L-M	M-H	L	L	M-H	29,0	VL	Dry	3	6	1	1	6	3(Sh)/6(Sb)//1 DWS: 6//	Plateau into N-S Through	-	No substantial blanketing layer	0 - 60	HW Chert Residuuum grading into alternating layers of HW/MW and SW Dolomite. No AL/SL. Frequent IR HR at transitions zones.	-	Not encountered	Profile as a whole: alternating layered of harder and softer/more weathered dolomite. Layered increments approximately every 5 meters. No AL/SL, IR HR.
KHB 31	M	M	L	L	M	11,9	L	Dry	4	4	1	1	4	4//1 DWS: 4//	Low in SE-NW Through	-	No substantial blanketing layer	0 - 26	Alternating HW/SW Dolomite (IR/VI HR, AL/SL).	26 - 32	SW CP Dolomite	Alternating Hard and Soft Dolomite. 4m buffer from 1mbgl. Located in prominent SE- NW Through.
KHB 32	H	H	L	L	H	36,1	VL	Dry	8	8	1	1	8	8//1 DWS: 8//	Low in SE-NW Through	-	No substantial blanketing layer	0 - 60	HW Chert/Dolomite Residuuum with Localised MW/Harder Dolomite at depth. Shallow Cavity (16- 19 mbgl) with AL/SL/VI HR/No Hammer.	-	Not encountered at 60 mbgl. Drilling stopped after collapsing hole at depth.	In prominent SE- NW Through (Low), AL/SL/VI HR/No Hammer. Shallow Cavity. No SW Dolomite up untill 60mbgl.
KHB 33	M-H	M	L	L	M-H	30,0	VL	Dry	6	4	1	1	6	6(Sh)/4(Sb)//1 DWS: 6//	Low in E-W Through	-	No substantial blanketing layer	0 - 48	HW Chert Residuuum / HW Dolomite grading into CR/CP Residuuum. Dolomite becomes gradualt more competent with depth (from 32-48 mbgl). Some IR HR/ Slight AL.	48 - 54	SW CP/CR Dolomite	Low in prominent E-W through with thick weathered material (some AL/SL/IR HR). Profile as a whole at depth alternating hard/soft from 32-48 mbgl.
KHB 34	M	M	L	L	M	13,6	L	Dry	4	4	1	1	4	4//1 DWS: 4//	Gradient into prominent E-W Low Through	-	No substantial blanketing layer	0 - 20	HW Chert/CR Dolomite Residuuum (No AL/SL, Some IR HR). Becomes more competent/alternating hard and soft Dolomite with depth (13-20mbgl).	20 - 28	SW CP/CR Dolomite	Gradient into E- W Through. No AL/SL. Alternating hard/soft dolomite from 13mbgl.
KHB 35	L-M	L-M	L	L	L-M	19,9	VL	Dry	3	3	1	1	3	3//1 DWS: 3//	Steep Gradient Low	-	No substantial blanketing layer	0 - 48	Chert Residuuum, HW Shale&Chert, Alternating MW/SW Dolomite (No AL/SL, Some IR HR).	48 - 54	SW Dolomite	Prominent steep gradient gravity Low, with interlayered Shale in upper horisons in Chert. Interlayered harder/softer in Dolomite (MW/SW). No AL/SL/VI HR & 18m blanketing layer.
KHB 36	L-M	L-M	L	L	L-M	4,7	M	Dry	5	2	1	1	5	5(Sh)/2(Sb)//1 DWS: 5//	Plateau	-	No substantial blanketing layer	0 - 12	Chert Residuuum into HW/SW Dolomite, Alternating layers of Harder and Softer in Dolomite. No AL/SL. Some IR HR at transitions zones.	12 - 19	SW CP Dolomite	SW Dolomite at 7-11mbgl. Alternating harder/softer Dolomite (MW/SW). No dolomite Residuuum.

KHB 37	L-M	L-M	L	L	L-M	4,7	M	Dry	5	2	1	1	5	5(Sh)/2(Sb)//1 DWS: 5//	Plateau	-	No substantial blanketing layer	0 - 9	Chert Residuuum directly into MW/HW Dolomite. No AL/SL. Some IR HR.	9 - 17	SW Dolomite	Shallow Dolomite in Gravity plateau with shallow overburden and HW dolomite bands in MW dolomite. No Dolomite Residuuum.
KHB 38	L-M	L-M	L	L	L-M	4,5	M	Dry	5	2	1	1	5	5(Sh)/2(Sb)//1 DWS: 5//	Plateau	-	No substantial blanketing layer	0 - 7	Chert Residuuum directly into HW&MW Dolomite. Some IR HR. No AL/SL.	7 - 15	SW CP Dolomite	Shallow Dolomite in Gravity plateau with shallow overburden.
KHB 39	L-M	L-M	L	L	M	19,5	VL	Dry	5	4	1	1	5	5(Sh)/4(Sb)//1 DWS: 5//	Plateau	-	No substantial blanketing layer	0 - 56	Chert Residuuum directly into SW Dolomite: more than 6m competent dolomite bands (3-8, 14-20, 26-32, 36-39, 46-49) with CP Dolomite Residuuum in between and Cavity at 56m+ (total AL/SL/VI HR).	-	Alternating layers of SW Dolomite (3mbgl for 5m, 14mbgl for 6m, 26mbgl for 7m). Cavity at EOH.	Gravity plateau with alternating hard/softer Dolomite layers. Interlayered CP Dolomite Residuuum. Cavity at depth, but substantial SW Dolomite Buffering above. Scenario deemed Shallow dolomite with interlayered highly weathered pockets in bedrock.
KHB 40	M	M	L	L	M	4,1	M	Dry	5	3	1	1	5	5(Sh)/3(Sb)//1 DWS: 5//	Plateau	-	No substantial blanketing layer	0 - 10	Colluvium, HW Chert, WAD (No AL/SL, frequent IR HR).	10 - 17	SW CR Dolomite	Gravity plateau adjacent prominent E-W Through and southern Karoo Low. IR HR and Dolomite residuum above shallow bedrock.
KHB 41	L-M	L-M	L	L	L-M	2,3	M	Dry	5	2	1	1	5	5(Sh)/2(Sb)//1 DWS: 5//	Plateau	-	No substantial blanketing layer	0 - 4	HW/MW Dolomite	4 - 11	SW CP Dolomite	Shallow Dolomite in Gravity plateau with shallow overburden.

L = Low. M = Medium. H = High. WI = Water ingress. GWLD = Ground water level drawdown. Sh = Sinkhole. Sb = Subsidence. IHC = Inherent Hazard Class. DWS = Dewatered scenario. CW = Completely weathered. HW = Highly weathered. MW = Moderately weathered. SW = Slightly weathered. CP = Chert-Poor. CR = Chert-Rich. AL = Air Loss. IR HR = Irregular hammer rate. WI HR = Very irregular hammer rates. SL = Sample loss.